MycoKeys 95: 1–13 (2023)
doi: 10.3897/mycokeys.95.97062
https://mycokeys.pensoft.net

RESEARCH ARTICLE

A peer-reviewed open-access journal
MycoKeys
Launched to accelerate biodiversity research

Acremonium capsici and *A. guizhouense*, two new members of *Acremonium* (Hypocreales, Sordariomycetes) isolated from the rhizosphere soil of *Capsicum annuum*

Shuo-Qiu Tong[1], Lei Peng[2], Yong-Jun Wu[1]

1 *College of Life Sciences, Institute of Agro-bioengineering, Guizhou University, Guiyang 550025, China*
2 *Tea Academy, Guizhou University, Guiyang 550025, China*

Corresponding author: Yong-Jun Wu (wyjbio@163.com)

Academic editor: Huzefa Raja | Received 2 November 2022 | Accepted 12 December 2022 | Published 4 January 2023

Citation: Tong S-Q, Peng L, Wu Y-J (2023) *Acremonium capsici* and *A. guizhouense*, two new members of *Acremonium* (Hypocreales, Sordariomycetes) isolated from the rhizosphere soil of *Capsicum annuum*. MycoKeys 95: 1–13. https://doi.org/10.3897/mycokeys.95.97062

Abstract

Two new species, *Acremonium capsici* and *A. guizhouense*, isolated from the rhizosphere soil of *Capsicum annuum*, are described and illustrated. Two-locus DNA sequences based on phylogeny, in combination with the morphology of the asexual morph, were used to characterize these species. In the phylogenetic tree, both new species clustered into a monophyletic clade with strong support, distinct from other previously known species of *Acremonium*. The new species differed from their allied species in their morphology.

Keywords

filamentous fungi, morphology, new species, phylogeny, taxonomy

Introduction

Capsicum annuum L. is a globally grown and consumed spice crop that is rich in vitamins. *C. annuum* originated from the tropical and subtropical regions of Central and South America. It was introduced into China at the end of the Ming Dynasty, and has a long history of cultivation in China. According to the Food and Agriculture Organization of the United Nations, global *C. annuum* production reached approximately 36.1 million ton in 2020, with China producing the most in the world.

Link (1809) erected the genus *Acremonium*, whose members are geographically widespread and involve many substrates (Yang et al. 2019). As described by Gams (1971), the main diagnostic criteria of the genus *Acremonium* are conidiophores simple or verticillate; phialides narrow, solitary, generally cylindrical and gradually tapered towards the tips; conidia unicellular, hyaline to light-pigmented, spherical to cylindrical, arranged in slimy heads or unconnected chains or both; chlamydospores and sclerotia present or absent. The genus *Acremonium* is similar to some genera – *Sarocladium* W. Gams & D. Hawksw., *Brunneomyces* Giraldo, Gené & Guarro, and *Chordomyces* Bilanenko, M.L. Georgieva & Grum-Grzhimaylo etc. (Giraldo et al. 2015, 2017), including some of the simplest morphologies of all filamentous anamorphic fungi (Summerbell et al. 2011), so the morphological delimitation between them is challenging (Yang et al. 2019). Recent phylogenetic studies have documented that the genus *Acremonium* is polyphyletic, including sexual and nomenclaturally complex asexual morphs (Summerbell et al. 2011; Giraldo et al. 2012). To date, *Acremonium* has 219 records in the Index Fungorum (http://www.indexfungorum.org/Names/Names.asp, retrieval on Dec. 2022). However, many *Acremonium* taxa have been reported, but there are no trustworthy classification systems and little sequence data are available in GenBank for multigene analyses (Park et al. 2017). In the future, the classification of *Acremonium* will become clearer with the increase of molecular data.

In this study, seven strains of *Acremonium* were isolated in the process of investigating the rhizosphere fungal diversity of cultivated *Capsicum annuum* in Guizhou Province, southwest China, based on a culturable method. Identification of these strains in combination with morphological characteristics and phylogenetic analysis showed that these strains belong to two previously undescribed species of *Acremonium*. The new species differed from their allied species in their morphology.

Materials and methods

Fungal isolation and morphology

Capsicum annuum plants were cultivated in farmlands located in Guiyang, Guizhou Province, China (26°45'75"N, 106°64'87"E). One composite rhizosphere soil sample was taken from five randomly selected *C. annuum* plants. The roots were shaken vigorously to separate soil that is not tightly attached to the roots, and the remaining soil attached to the region 2–3 mm from the plant root was collected as the rhizosphere soil sample (Smalla et al. 2001). Fungi were isolated and purified using a dilution plate method as follows: 2 g samples were weighed with glass beads in a conical flask containing 20 mL sterile water, mixed evenly using eddy shock for 10 min, diluted to 1:10,000, and cultured on Martin's medium supplemented with chloramphenicol and cycloheximide.

The purified isolates were transferred to potato dextrose agar (PDA), oatmeal agar (OA), malt extract agar (MEA), and corn meal agar (CMA) at 25 °C in darkness for 14 days to examine the macroscopic and morphological characteristics of the colonies. Photomicrographs of the diagnostic structures were obtained using an OLYMPUS

BX53 microscope equipped with differential interference contrast optics, an OLYMPUS DP73 high-definition color camera, and cellSens software v.1.18. Both dry and living cultures were deposited at the Institute of Agro-bioengineering, Guizhou University.

DNA extraction, PCR amplification, and sequencing

Total DNA was extracted from each of the new isolates using the BioTeke Fungus Genomic DNA Extraction kit (DP2032, BioTeke, Beijing, China) according to the manufacturer's instructions. According to Li et al. (2022), the internal transcribed spacers (ITS), the 28S nrRNA locus (LSU), translation elongation factor 1-alpha gene region (*TEF 1*-α), RNA polymerase II second largest subunit gene (*RPB2*), and small subunit rDNA (SSU) were amplified and sequenced using ITS1/ITS4 (White et al. 1990), LROR/LR7 (Vilgalys and Hester 1990), EF1-983F/EF1-2218R (Rehner and Buckley 2005), fRPB2-5f/fRPB2-7cR (Liu et al. 1999), and NS1/NS4 (White et al. 1990) primers, respectively. All new sequences were submitted to GenBank (Table 1).

Phylogenetic analyses

In this study, we utilized sequence data mainly from recent publications (Yang et al. 2019; Li et al. 2022) and the sequenced new isolates (Table 1). According to Li et al. (2022) and Yang et al. (2019), *Pestalotiopsis spathulata* (CBS 356.86) and *P. hawaiiensis* (CBS 114491) were chosen as the outgroup taxa. The sequences were aligned using MAFFT v7.037 (Katoh and Standley 2013) and adjusted using MEGA 6.06 (Tamura et al. 2013). The aligned sequences of LSU and ITS were concatenated using PhyloSuite v1.16 (Zhang et al. 2020).

The best-fit substitution model was selected using the corrected Akaike information criterion, in ModelFinder (Kalyaanamoorthy et al. 2017). The maximum likelihood (ML) and Bayesian inference (BI) methods were used in the analysis. The ML analysis was implemented in IQ-TREE v1.6.11 (Nguyen et al. 2015) with 10,000 bootstrap tests, using the ultrafast algorithm (Minh et al. 2013). For the BI, MrBayes v3.2 (Ronquist et al. 2012) was used and Markov chain Monte Carlo simulations were run for 5,000,000 generations with a sampling frequency of every 500 generations and a burn-in of 25%. The above analyses were carried out in PhyloSuite v1.16 (Zhang et al. 2020).

Results

Phylogenetic analyses

Ninety-five isolates (including the seven with new sequence data) were included in our dataset (Table 1), which comprised 976 positions (including gaps), of which 377 were phylogenetically informative (122 of LSU and 255 of ITS). For Maximum-likelihood analyses, IQ-TREE's ModelFinder under the corrected Akaike information

Table 1. Strains included in the present study.

Species	Strains	LSU	ITS	SSU	*TEF 1-α*	*RPB2*
Acremonium alternatum	CBS 407.66 T	HQ231988	HE798150			
Acremonium alternatum	CBS 831.97	HQ231989				
Acremonium arthrinii	MFLU 18-1225 T	MN036334		MN036335	MN038169	
Acremonium behniae	CBS 146824 T	MW175400	MW175360			
Acremonium biseptum	CBS 750.69 T	HQ231998				
Acremonium blochii	CBS 993.69	HQ232002	HE608636			
Acremonium borodinense	CBS 101148 T	HQ232003	HE608635			
Acremonium brachypenium	CBS 866.73 T	HQ232004	AB540570			
Acremonium camptosporum	CBS 756.69 T	HQ232008		HQ232186		
Acremonium cavaraeanum	CBS 101149 T	HF680202	HF680220			
Acremonium cavaraeanum	CBS 111656	HF680203	HF680221			
Acremonium cavaraeanum	CBS 758.69	HQ232012	HF680222			
Acremonium cerealis	CBS 207.65	HQ232013				
Acremonium cerealis	CBS 215.69	HQ232014				
Acremonium chiangraiense	MFLUCC 14-0397 T	MN648329	MN648324			
Acremonium chrysogenum	CBS 144.62 T	HQ232017		HQ232187		
Acremonium chrysogenum	CBS 401.65	MH870276	MH858636			
Acremonium citrinum	CBS 384.96 T	HF680217	HF680236			
Acremonium curvum	CGMCC 3.20954 T	ON041050	ON041034	ON876754	ON494579	ON494583
Acremonium dimorphosporum	CBS 139050 T	LN810506	LN810515			
Acremonium exiguum	CBS 587.73 T	HQ232035				
Acremonium exuviarum	UAMH 9995 T	HQ232036	AY882946			
Acremonium felinum	CBS 147.81 T	AB540488	AB540562			
Acremonium flavum	CBS 596.70 T	HQ232037		HQ232191		
Acremonium flavum	CBS 316.72	MH872204	MH860487			
Acremonium fuci	CBS 112868 T		AY632653			
Acremonium fuci	CBS 113889		AY632652			
Acremonium fusidioides	CBS 109069	HF680204	HF680223			
Acremonium fusidioides	CBS 991.69	HF680211	HF680230			
Acremonium fusidioides	CBS 840.68 T	HQ232039	FN706542			
Acremonium globosisporum	CGMCC 3.20955 T	ON041051	ON041035	ON876755	ON494580	ON494584
Acremonium globosisporum	GZUIFR 22.037	ON041052	ON041036	ON876756	ON494581	ON494585
Acremonium globosisporum	GZUIFR 22.038	ON041053	ON041037	ON876757	ON494582	ON494586
Acremonium hansfordii	CBS 390.73	HQ232043	AB540578			
Acremonium hennebertii	CBS 768.69 T	HQ232044	HF680238			
Acremonium inflatum	CBS 212.69 T	HQ232050				
Acremonium mali	ACCC 39305 T	MF993114	MF987658			
Acremonium moniliforme	CBS 139051 T	LN810507	LN810516			
Acremonium moniliforme	FMR 10363	LN810508	LN810517			
Acremonium parvum	CBS 381.70A	HQ231986	HF680219			
Acremonium persicinum	CBS 310.59 T	HQ232077				
Acremonium persicinum	CBS 101694	HQ232085				
Acremonium pinkertoniae	CBS 157.70 T	HQ232089		HQ232202		
Acremonium polychroma	CBS 181.27 T	HQ232091	AB540567			
Acremonium potronii	CBS 189.70	HQ232094				
Acremonium pseudozeylanicum	CBS 560.73 T	HQ232101				
Acremonium pteridii	CBS 782.69 T	HQ232102				
Acremonium pteridii	CBS 784.69	HQ232103				
Acremonium sclerotigenum	CBS 124.42 T	HQ232126	FN706552	HQ232209		
Acremonium sclerotigenum	A101	KC987215	KC987139	KC987177	KC998961	
Acremonium sclerotigenum	A130	KC987242	KC987166	KC987204	KC998988	
Acremonium sp.	E102	KC987248	KC987172	KC987210	KC998994	KC999030
Acremonium spinosum	CBS 136.33 T	HQ232137	HE608637	HQ232210		

Species	Strains	LSU	ITS	SSU	*TEF 1-α*	*RPB2*
Acremonium stroudii	CBS 138820 T		KM225291			
Acremonium tumulicola	CBS 127532 T	AB540478	AB540552			
Acremonium variecolor	CBS 130360 T	HE608651	HE608647			
Acremonium variecolor	CBS 130361	HE608652	HE608648			
Acremonium verruculosum	CBS 989.69 T	HQ232150				
Acremonium capsici	**SQT01 T**	**OP740978**	**OP703286**	**OP750190**	**OP757287**	**OP730522**
Acremonium capsici	**SQT02**	**OP740979**	**OP703287**	**OP750191**	**OP757288**	**OP730523**
Acremonium capsici	**SQT03**	**OP740980**	**OP703288**	**OP750192**	**OP757289**	**OP730524**
Acremonium guizhouense	**SQT04 T**	**OP740981**	**OP703289**	**OP750193**	**OP757290**	**OP730525**
Acremonium guizhouense	**SQT05**	**OP740982**	**OP703290**	**OP750194**	**OP757291**	**OP730526**
Acremonium guizhouense	**SQT06**	**OP740983**	**OP703291**	**OP750195**	**OP757292**	**OP730527**
Acremonium guizhouense	**SQT07**	**OP740984**	**OP703292**	**OP750196**	**OP757293**	**OP730528**
Bryocentria brongniartii	M139	EU940105		EU940052		
Bryocentria brongniartii	M190	EU940125		EU940052		
Bryocentria metzgeriae	M140	EU940106				
Bulbithecium hyalosporum	CBS 318.91 T	AF096187	HE608634			
Cephalosporium purpurascens	CBS 149.62 T	HQ232071				
Cosmospora lavitskiae	CBS 530.68 T	HQ231997				
Emericellopsis alkalina	CBS 127350 T	KC987247	KC987171	KC987209	KC998993	KC999029
Emericellopsis terricola	CBS 120.40 T	U57082	U57676	U44112		
Gliomastix roseogrisea	CBS 134.56 T	HQ232121				
Hapsidospora irregularis	ATCC 22087 T	AF096192		AF096177		
Kiflimonium curvulum	CBS 430.66 T	HQ232026	HE608638	HQ232188		
Lanatonectria flavolanata	CBS 230.31	HQ232157				
Leucosphaerina arxii	CBS 737.84 T	HE608662	HE608640			
Nigrosabulum globosum	ATCC 22102 T	AF096195				
Paracremonium contagium	CBS 110348 T	HQ232118	KM231831		KM231966	
Parasarocladium breve	CBS 150.62 T	HQ232005				
Parasarocladium radiatum	CBS 142.62 T	HQ232104		HQ232205		
Pestalotiopsis hawaiiensis	CBS 114491 T	KM116239	KM199339		KM199514	
Pestalotiopsis spathulata	CBS 356.86 T	KM116236	KM199338		KM199513	
Pseudoacremonium sacchari	CBS 137990 T	KJ869201	KJ869144			
Sarcopodium vanillae	CBS 100582	HQ232174	KM231780		KM231911	
Sarocladium bacillisporum	CBS 425.67 T	HQ231992	HE608639	HQ232179		
Sarocladium bactrocephalum	CBS 749.69 T	HQ231994	HG965006	HQ232180		
Sarocladium strictum	CBS 346.70 T	HQ232141	AY214439	HQ232211		
Sarocladium terricola	CBS 243.59 T	HQ232046		HQ232196		
Selinia pulchra	AR 2812	GQ505992	HM484859		HM484841	
Trichothecium crotocinigenum	CBS 129.64 T	HQ232018	AJ621773			
Trichothecium indicum	CBS 123.78T	AF096194		AF096179		
Trichothecium roseum	DAOM 208997	U69891		U69892		
Trichothecium sympodiale	ATCC 36477	U69889		U69890		

Notes: "T" stands for Ex-type strains. New isolates are in bold and blue.

criterion (AICc) proposed a TN+F+I+G4 for LSU, GTR+F+I+G4 for ITS. For Bayesian analysis, IQ-TREE's ModelFinder under the AICc proposed a GTR+F+G4 for LSU, GTR+F+I+G4 for ITS. The results show that the isolates SQT01, SQT02, and SQT03 clustered in a single clade with high support (ML BS 100/BI pp 1), and were closely related to *Acremonium variecolor* (Fig. 1). The isolates SQT04, SQT05, SQT06, and SQT07 also clustered in a single clade with high support (100/0.98), and were closely related to *A. persicinum* and *A. verruculosum* (Fig. 1).

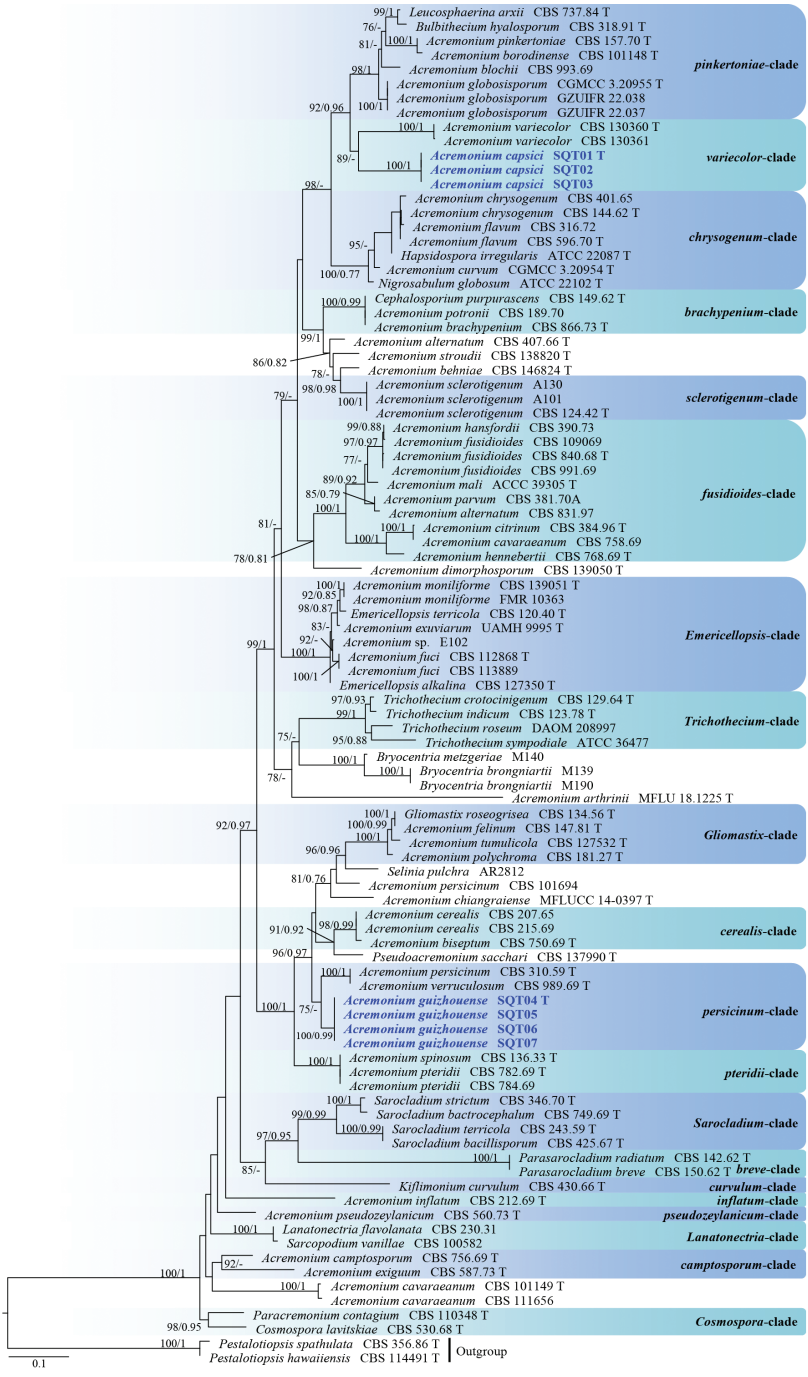

Figure 1. Phylogram generated from maximum likelihood analysis based on LSU + ITS sequence data. Bootstrap support values of maximum likelihood higher than 75% and Bayesian posterior probabilities greater than 0.75 are given above each branch. The new collection is highlighted in blue bold. Clades are identified using clade nomenclature formally defined by Summerbell et al. (2011), and Yang et al. (2019). Ex-type strains are indicated by "T".

Taxonomy

***Acremonium capsici* S.Q. Tong & Y.J. Wu, sp. nov.**
MycoBank No: 846330
Fig. 2

Etymology. Referring to the type strain isolated from the rhizosphere soil of *Capsicum annuum*.

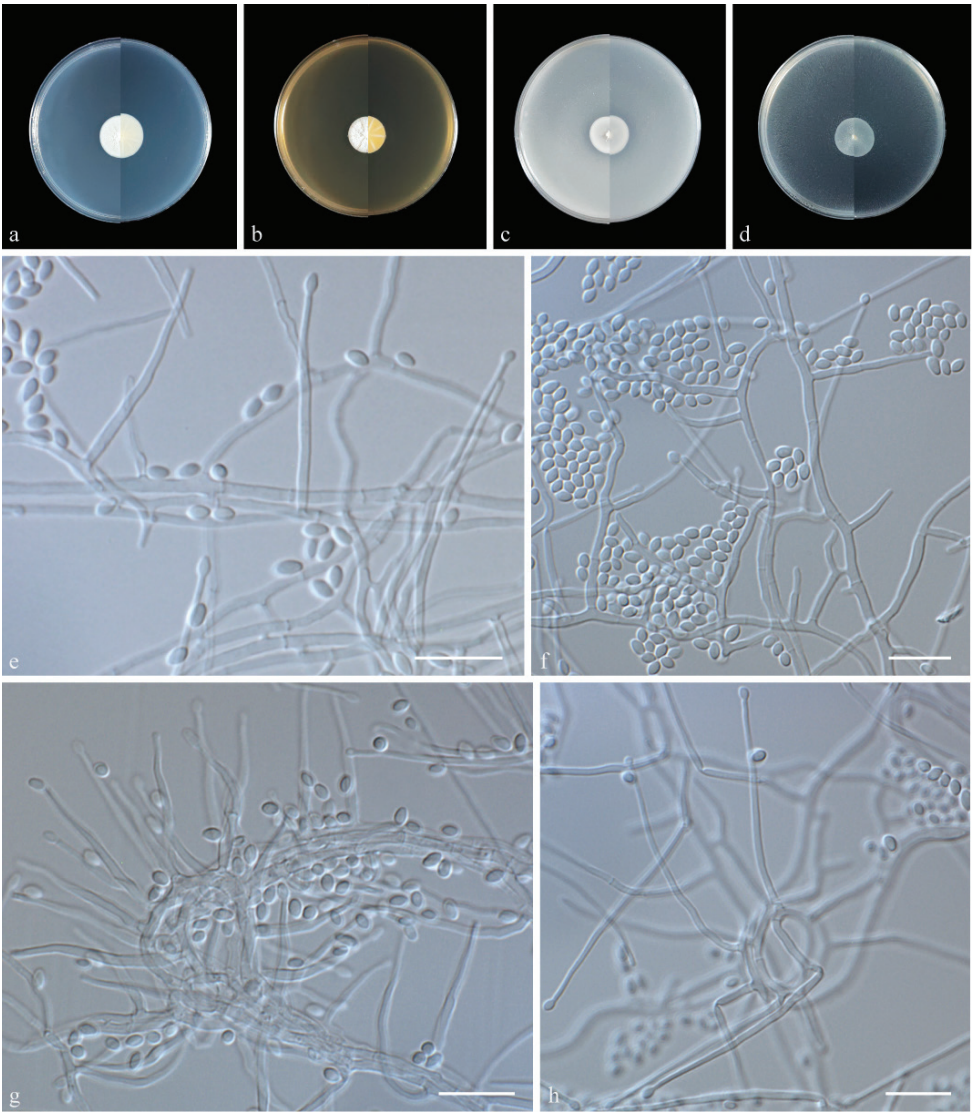

Figure 2. Morphology of *Acremonium capsici* sp. nov. **a–d** colony on PDA, MEA, OA, and CMA after 14 days at 25 °C (upper surface and lower surface) **e** phialides **f** conidia **g** phialides arising from ropes of hyphae **h** phialides arising from hyphal coils. Scale bars: 10 μm (**e–h**).

Type. Guiyang City, Guizhou Province, China 26°45'75"N, 106°64'87"E, isolated from the rhizosphere soil of *Capsicum annuum*, August 2022, Shuo-Qiu Tong (dried holotype culture SQT H-01, ex-holotype culture SQT01). GenBank: ITS = OP703286; LSU = OP740978; SSU = OP750190; *TEF 1*-α = OP757287; *RPB2* = OP730522.

Description. Culture characteristics (14 days at 25 °C) – Colonies on PDA 20–21 mm diam, white, hairy, flat, radially striated, with a regular edge; reverse white. Colonies on MEA 18–19 mm in diameter, white, floccose, radially striated, with a regular edge; reverse white. Colonies on OA 18–19 mm in diameter, pale white, flat, with regular edge; reverse pale white. Colonies on CMA 18–19 mm in diameter, pale white, felty, with regular edge; reverse pale white. ***Hyphae*** hyaline, smooth, septate, branched, 1.0–2.5 μm wide. ***Phialides*** straight to flexuous, hyaline, smooth, arising from superficial hyphae, from hyphal strands or from hyphal coils, 20–42 μm (n = 50) long, 1–2 μm (n = 50) wide at the base. ***Conidia*** arranged in slimy heads, one-celled, ovoid to ellipsoidal, fusiform, 2.0–3.5 × 1.5–2.0 μm (n = 50), hyaline, smooth, or rough. ***Chlamydospores*** and teleomorph were not observed.

Additional specimens examined. Guiyang City, Guizhou Province, China 26°45'75"N, 106°64'87"E, isolated from the rhizosphere soil of *Capsicum annuum*, August 2022, Shuo-Qiu Tong, SQT02, *ibid.*, SQT03. GenBank: ITS = OP703287–OP703288; LSU = OP740979–OP740980; SSU = OP750191–OP750192; *TEF 1*-α = OP757288–OP757289; *RPB2* = OP730523–OP730524.

Known distribution. Guiyang City, Guizhou Province, China.

Notes. In a phylogenetic tree based on LSU + ITS sequences, *Acremonium capsici* forms a separate clade sister to *A. variecolor* in *Acremonium sensu lato* (Bionectriaceae). In a comparison of LSU and ITS nucleotides, *A. capsici* (Type strain SQT01) has 93% and 83% similarity, in LSU (459/492 bp, one gap) and ITS (388/468 bp, 16 gaps), which is different from *A. variecolor* (CBS 130360). They are distinguished by the appearance of colonies on OA, MEA, and PDA: colonies of *A. capsici* grow slowly (less than 25 mm), and are white, while colonies of *A. variecolor* grow faster (more than 40 mm), and are white to yellowish (Giraldo et al. 2012). In addition, *A. capsici* bear simple phialides, while *conidiophores* of *A. variecolor* are mostly branched, bearing whorls of two to five phialides (Giraldo et al. 2012). *A. variecolor* produces sessile conidia, which is not seen in *A. capsici* (Giraldo et al. 2012).

Acremonium guizhouense **S.Q. Tong & Y.J. Wu, sp. nov.**
MycoBank No: 846331
Fig. 3

Etymology. Referring to the country where this fungus was first isolated.

Type. Guiyang City, Guizhou Province, China 26°45'75"N, 106°64'87"E, isolated from the rhizosphere soil of *Capsicum annuum*, August 2022, Shuo-Qiu Tong (dried holotype culture SQT H04, ex-holotype culture SQT04). GenBank: ITS = OP703289; LSU = OP740981; SSU = OP750193; *TEF 1*-α = OP757290; *RPB2* = OP730525.

Description. Culture characteristics (14 days at 25 °C) – Colonies on PDA 16–19 mm in diameter, yellowish white to grayish yellow, flat, zonate, with regular edge; reverse brownish orange. Colonies on MEA 9–13 mm in diameter, yellowish white to white, compact, convex with papillate surface, margin dentate, aerial mycelia extremely sparse; reverse yellowish white to umber. Colonies on OA 14–16 mm in diameter, pale, felty, with regular edge; reverse pale white. Colonies on CMA 16–14 mm in diameter, pale white, felty, with regular edge; reverse pale white. ***Hyphae*** hyaline, smooth, septate,

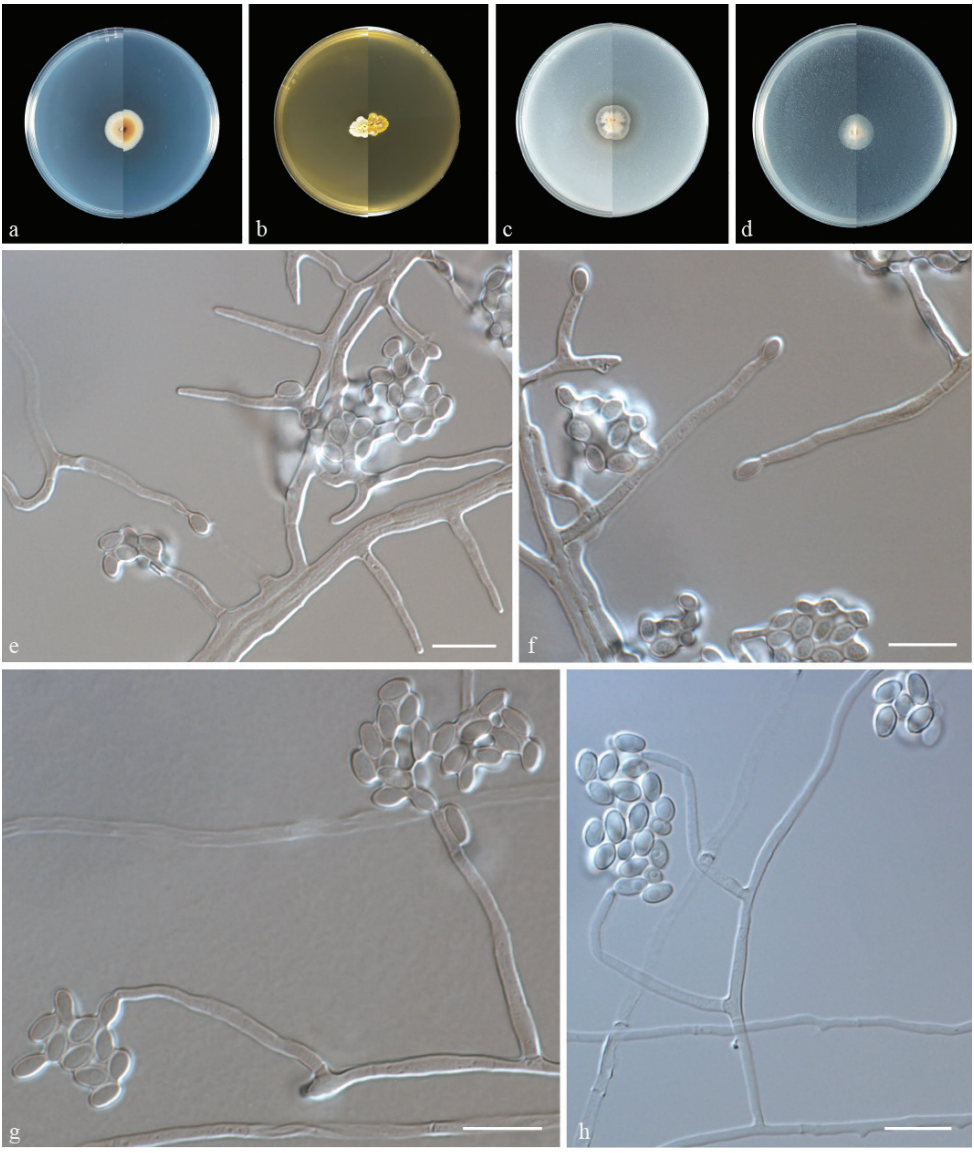

Figure 3. Morphology of *Acremonium guizhouense* sp. nov. **a–d** colony on PDA, MEA, OA, and CMA after 14 days at 25 °C (upper surface and lower surface) **e, f** phialides and conidia **g, h** conidia are held together in slimy heads. Scale bars: 10 μm (**e–h**).

branched, 1.0–3.0 μm wide. ***Phialides*** straight to flexuous, hyaline, smooth, arising from hyphae, 15.5–33.5 μm (n = 50) long, 1.5–2.5 μm (n = 50) wide at the base. ***Conidia*** gathered in slimy heads, one-celled, ovoid to ellipsoidal, 2.5–3.0 × 3.5–5.0 μm (n = 50), hyaline, smooth or rough. ***Chlamydospores*** and teleomorph not observed.

Additional specimens examined. Guiyang City, Guizhou Province, China 26°45'75"N, 106°64'87"E, isolated from the rhizosphere soil of *Capsicum annuum*, August 2022, Shuo-Qiu Tong, SQT05 = SQT06, *ibid.*, SQT07. GenBank: ITS = OP703290–OP703292; LSU = OP740982–OP740984; SSU = OP750194–OP750196; *TEF 1-α* = OP757291–OP757293; *RPB2* = OP730526–OP730528.

Known distribution. Guiyang City, Guizhou Province, China.

Notes. Phylogenetic and morphological data (Figs 1, 3) support our isolates SQT04–SQT07 as new species of *Acremonium*. *A. guizhouense* is phylogenetically closely related to *A. verruculosum* and *A. persicinum*. However, they can be distinguished by their sequence similarity (97% similarity, 10 base pairs (bp) differences and two gaps in 497 bp of LSU in *A. verruculosum* CBS 989.69; 98% similarity, 12 base pairs (bp) differences, and four gaps in 809 bp of LSU in *A. persicinum* CBS310.59). Since *A. verruculosum* and *A. persicinum* lack ITS sequences, it was not possible to compare *A. guizhouense* with them. Morphologically, the conidia of *A. verruculosum* are long ellipsoidal to cylindrical, rather than ovoid to ellipsoidal in *A. guizhouense* (Gams 1971). *A. verruculosum*, on the other hand, has larger conidia than *A. guizhouense* (5.6–6.0 × 2.3–2.5 μm vs. 2.5–3.0 × 3.5–5.0 μm) (Gams 1971). Furthermore, conidia of *A. verruculosum* are catenulate, fusiform, pyriform to ellipsoidal rather than arranged as slimy heads, ovoid to ellipsoidal in *A. guizhouense* (Gams 1971). The conidia of *A. guizhouense*, on the other hand, are smaller than that of *A. persicinum* (2.5–3.0 × 3.5–5.0 μm vs. 3.2–4.8 × 1.2–3.0 μm) (Gams 1971).

Discussion

Traditionally, a polyphasic approach based on morphology, physiology, biochemistry, or reactions to chemical tests, has been used to differentiate species (Senanayake et al. 2020). Currently, many new fungal taxa have been reported based on DNA sequences. Phylogenetic analysis is becoming increasingly important in reporting new taxa of fungi, and has gradually become a mandatory component. However, many previously published fungal taxa lack DNA molecular data, and even specimens have been lost (Zhang et al. 2022). Thus, there are still many undetermined, questionable, or misidentified taxa that warrant taxonomic investigations (Summerbell et al. 2018). Since most species of the genus *Acremonium* have only LSU and ITS sequences Li et al. (2022), we used only ribosomal sequences (LSU + ITS) for phylogenetic analysis, while the sequencing of other loci was aimed at establishing a database for future studies.

Members of the genus *Acremonium* are geographically widespread and ecologically diverse, and seem to colonize all types of substrates, including endophytes, epiphytes, saprophytes, human and plant pathogens, lichens, insects, or arthropods taxa (Yang et

al. 2019). In addition, *Acremonium* species have various functions, such as biological control (Shang et al. 2018), enhancing drought tolerance of grasses, and promoting nectar production of beans (Jaber and Vidal 2009), as well as improving plant resistance to plant pathogens (Kasselaki et al. 2006). In the present study, all the isolates were obtained from the rhizosphere soils of *Capsicum annuum*. Therefore, more studies are necessary to further confirm their relationship with their host plant *Capsicum annuum*.

In summary, seven isolates of *Acremonium* were obtained from the rhizosphere soils of *Capsicum annuum*. Morphological characteristics in combination with two-locus (LSU + ITS) phylogenetic analysis were used for delimitation. Therefore, two new species of *Acremonium capsici* (three isolates) and *Acremonium guizhouense* (four isolates) are introduced. This study contributes to our understanding of the rhizosphere microbial population of *Capsicum annuum* and also of *Acremonium* species.

Acknowledgements

This study was financially supported by Guizhou Provincial Science and Technology Projects (Qian Ke He Zhi Cheng-ZK[2022] General 172, and ZK[2021] General 262), and Guizhou Provincial Institutions of higher learning Engineering Center Projects (Qian Jiao He KY[2021]006). We appreciate Charlesworth for English-language editing of the whole manuscript.

References

Gams W (1971) *Cephalosporium*-artige Schimmelpilze (Hyphomycetes). G. Fischer, Stuttgart.

Giraldo A, Gené J, Cano J, de Hoog S, Guarro J (2012) Two new species of *Acremonium* from Spanish soils. Mycologia 104(6): 1456–1465. https://doi.org/10.3852/11-402

Giraldo A, Gené J, Sutton DA, Madrid H, de Hoog GS, Cano J, Decock C, Crous PW, Guarro J (2015) Phylogeny of *Sarocladium* (Hypocreales). Persoonia 34(1): 10–24. https://doi.org/10.3767/003158515X685364

Giraldo A, Gené J, Sutton DA, Wiederhold N, Guarro J (2017) New acremonium-like species in the Bionectriaceae and Plectosphaerellaceae. Mycological Progress 16(4): 349–368. https://doi.org/10.1007/s11557-017-1271-7

Jaber LR, Vidal S (2009) Interactions between an endophytic fungus, aphids, and extrafloral nectaries: Do endophytes induce extrafloral-mediated defences in *Vicia faba*? Functional Ecology 23(4): 707–714. https://doi.org/10.1111/j.1365-2435.2009.01554.x

Kalyaanamoorthy S, Minh BQ, Wong TK, von Haeseler A, Jermiin LS (2017) ModelFinder: Fast model selection for accurate phylogenetic estimates. Nature Methods 14(6): 587–589. https://doi.org/10.1038/nmeth.4285

Kasselaki AM, Shaw MW, Malathrakis NE, Haralambous J (2006) Control of *Leveillula taurica* in tomato by *Acremonium alternatum* is by induction of resistance, not hyperparasitism. European Journal of Plant Pathology 115(2): 263–267. https://doi.org/10.1007/s10658-006-9010-y

Katoh K, Standley DM (2013) MAFFT multiple sequence alignment software version 7: Improvements in performance and usability. Molecular Biology and Evolution 30(4): 772–780. https://doi.org/10.1093/molbev/mst010

Li X, Zhang ZY, Ren YL, Chen WH, Liang JD, Pan JM, Huang JZ, Liang ZQ, Han YF (2022) Morphological characteristics and phylogenetic evidence reveal two new species of *Acremonium* (Hypocreales, Sordariomycetes). MycoKeys 91: 85–96. https://doi.org/10.3897/mycokeys.91.86257

Link HF (1809) Observationes in ordines plantarum naturales: Dissertatio I. Magazin. der Gesellschaft Naturforschenden Freunde Berlin 3: 3–42.

Liu YJ, Whelen S, Hall BD (1999) Phylogenetic relationships among Ascomycetes: Evidence from an RNA polymerse II subunit. Molecular Biology and Evolution 16(12): 1799–1808. https://doi.org/10.1093/oxfordjournals.molbev.a026092

Minh Q, Nguyen M, von Haeseler AA (2013) Ultrafast approximation for phylogenetic bootstrap. Molecular Biology and Evolution 30(5): 1188–1195. https://doi.org/10.1093/molbev/mst024

Nguyen LT, Schmidt HA, von Haeseler A, Minh BQ (2015) IQ-TREE: A fast and effective stochastic algorithm for estimating maximum-likelihood phylogenies. Molecular Biology and Evolution 32(1): 268–274. https://doi.org/10.1093/molbev/msu300

Park SW, Nguyen TTT, Lee HB (2017) Characterization of two species of *Acremonium* (unrecorded in Korea) from soil samples: *A. variecolor* and *A. persicinum*. Mycobiology 45(4): 353–361. https://doi.org/10.5941/MYCO.2017.45.4.353

Rehner SA, Buckley E (2005) A *Beauveria* phylogeny inferred from nuclear ITS and EF1-α sequences: Evidence for cryptic diversification and links to *Cordyceps* teleomorphs. Mycologia 97(1): 84–98. https://doi.org/10.3852/mycologia.97.1.84

Ronquist F, Teslenko M, van der Mark P, Ayres DL, Darling A, Höhna S, Larget B, Liu L, Suchard MA, Huelsenbeck JP (2012) MrBayes 3.2: Efficient Bayesian phylogenetic inference and model choice across a large model space. Systematic Biology 61(3): 539–542. https://doi.org/10.1093/sysbio/sys029

Senanayake IC, Rathnayaka AR, Marasinghe DS, Calabon MS, Gentekaki E, Lee HB, Hurdeal VG, Pem D, Dissanayake LS, Wijesinghe SN, Bundhun D, Nguyen TT, Goonasekara ID, Abeywickrama PD, Bhunjun CS, Jayawardena RS, Wanasinghe DN, Jeewon R, Bhat DJ, Xiang MM (2020) Morphological approaches in studying fungi: Collection, examination, isolation, sporulation and preservation. Mycosphere: Journal of Fungal Biology 11(1): 2678–2754. https://doi.org/10.5943/mycosphere/11/1/20

Shang SQ, Chen YN, Bai YL (2018) The pathogenicity of entomopathogenic fungus *Acremonium hansfordii* to two-spotted spider mite, *Tetranychus urticae* and predatory mite *Neoseiulus barkeri*. Systematic and Applied Acarology 23(11): 2173–2183. https://doi.org/10.11158/saa.23.11.10

Smalla K, Wieland G, Buchner A, Zock A, Parzy J, Kaiser S, Roskot N, Heuer H, Berg G (2001) Bulk and rhizosphere soil bacterial communities studied by denaturing gradient gel electrophoresis: Plant-dependent enrichment and seasonal shifts revealed. Applied and Environmental Microbiology 67(10): 4742–4751. https://doi.org/10.1128/AEM.67.10.4742-4751.2001

Summerbell RC, Gueidan C, Schroers H-J, de Hoog GS, Starink M, Rosete YA, Guarro J, Scott JA (2011) *Acremonium* phylogenetic overview and revision of *Gliomastix*, *Sarocladium*, and *Trichothecium*. Studies in Mycology 68: 139–162. https://doi.org/10.3114/sim.2011.68.06

Summerbell RC, Gueidan C, Guarro J, Eskalen A, Crous PW, Gupta AK, Gené J, Cano-Lira JF, van Iperen A, Starink M, Scott JA (2018) The protean *Acremonium*. *A. sclerotigenum/egyptiacum*: Revision, food contaminant, and human disease. Microorganisms 6(3): 88. https://doi.org/10.3390/microorganisms6030088

Tamura K, Stecher G, Peterson D, Filipski A, Kumar S (2013) MEGA6: Molecular evolutionary genetics analysis version 6.0. Molecular Biology and Evolution 30(12): 2725–2729. https://doi.org/10.1093/molbev/mst197

Vilgalys R, Hester M (1990) Rapid genetic identification and mapping of enzymatically amplified ribosomal DNA from several Cryptococcus species. Journal of Bacteriology 172(8): 4238–4246. https://doi.org/10.1128/jb.172.8.4238-4246.1990

White TJ, Bruns T, Lee S, Taylor J (1990) Amplification and direct sequencing of fungal ribosomal RNA genes for phylogenetics. In: Innis MA, Gelfand DH, Sninsky JJ, White TJ (Eds) PCR protocols: a guide to methods and applications, Academic Press, San Diego, California, 315–322. https://doi.org/10.1016/B978-0-12-372180-8.50042-1

Yang CL, Xu XL, Jeewon R, Boonmee S, Liu YG, Hyde KD (2019) *Acremonium arthrinii* sp. nov., a mycopathogenic fungus on *Arthrinium yunnanum*. Phytotaxa 420: 283–299. https://doi.org/10.11646/phytotaxa.420.4.4

Zhang D, Gao FL, Jakovlić I, Zou H, Zhang J, Li WX, Wang GT (2020) PhyloSuite: An integrated and scalable desktop platform for streamlined molecular sequence data management and evolutionary phylogenetics studies. Molecular Ecology Resources 20(1): 348–355. https://doi.org/10.1111/1755-0998.13096

Zhang ZY, Ren YL, Chen WH, Liang JD, Han YF, Liang ZQ (2022) New taxonomic framework for Arthrodermataceae: A comprehensive analysis based on their phylogenetic reconstruction, divergence time estimation, phylogenetic split network, and phylogeography. Antonie van Leeuwenhoek 115(11): 1319–1333. https://doi.org/10.1007/s10482-022-01774-0

MycoKeys 95: 15–25 (2023)
doi: 10.3897/mycokeys.95.98384
https://mycokeys.pensoft.net

RESEARCH ARTICLE

A peer-reviewed open-access journal
MycoKeys
Launched to accelerate biodiversity research

Phaeotubakia lithocarpicola gen. et sp. nov. (Tubakiaceae, Diaporthales) from leaf spots in China

Ning Jiang[1], Ya-Quan Zhu[1], Han Xue[1], Chun-Gen Piao[1], Yong Li[1]

1 *Key Laboratory of Biodiversity Conservation of National Forestry and Grassland Administration, Ecology and Nature Conservation Institute, Chinese Academy of Forestry, Beijing 100091, China*

Corresponding author: Yong Li (lylx@caf.ac.cn)

Academic editor: Jennifer Luangsa-ard | Received 6 December 2022 | Accepted 3 January 2023 | Published 9 January 2023

Citation: Jiang N, Zhu Y-Q, Xue H, Piao C-G, Li Y (2023) *Phaeotubakia lithocarpicola* gen. et sp. nov. (Tubakiaceae, Diaporthales) from leaf spots in China. MycoKeys 95: 15–25. https://doi.org/10.3897/mycokeys.95.98384

Abstract

Tubakiaceae represents a distinct lineage of Diaporthales, including its type genus *Tubakia* and nine additional known genera. Tubakiaceous species are commonly known as endophytes in leaves and twigs of many tree species, but can also be plant pathogens causing conspicuous leaf symptoms. In the present study, isolates were obtained from diseased leaves of *Lithocarpus glaber* collected in Guangdong Province, China. The identification was conducted based on morphology and phylogeny of combined loci of 28S nrRNA gene (LSU), internal transcribed spacer regions and intervening 5.8S nrRNA gene (ITS) of the nrDNA operon, translation elongation factor 1-alpha (*tef1*) and beta tubulin (*tub2*). As a result, a distinct clade in Tubakiaceae was revealed named *Phaeotubakia lithocarpicola* **gen. et sp. nov.**, which was distinguished from the other tubakiaceous taxa by its dark brown conidiogenous cells and conidia.

Keywords

Ascomycota, morphology, new genus, phylogeny, plant disease, taxonomy, Tubakiaceae

Introduction

The fungal order Diaporthales contains members usually inhabiting plant tissues as pathogens, endophytes and saprophytes (Rossman et al. 2007; Senanayake et al. 2017, 2018; Fan et al. 2018; Jiang et al. 2021a; Udayanga et al. 2021). Tubakiaceae was proposed as a diaporthalean family based on its type genus *Tubakia*, and the other seven genera, namely *Apiognomonioides*, *Involutiscutellula*, *Oblongisporothyrium*, *Paratubakia*, *Racheliella*, *Saprothyrium* and *Sphaerosporithyrium* (Braun et al. 2018). Subsequently,

Ellipsoidisporodochium and *Obovoideisporodochium* were added to this family based on morphological and phylogenetical evidence (Zhang et al. 2021; Liu et al. 2022). Hence, ten genera have been accepted in Tubakiaceae before the present study.

Species of Tubakiaceae are usually characterized by forming pycnothyria composed of convex scutella with radiating threads of cells fixed to the substratum by a central columella, mostly surrounded by a sheath of small fertile cells that give rise to one-celled, phialidic conidiogenous cells (Harrington et al. 2012; Braun et al. 2018). However, some species also form crustose or pustulate pycnidioid conidiomata, for example, *Tubakia californica* is known to only have crustose pycnidioid conidiomata during its lifecycle (Braun et al. 2018). Moreover, conidia of tubakiaceous species are globose, subglobose, ellipsoid, broad ellipsoid-obovoid to subcylindrical or somewhat irregular in shape, aseptate, hyaline, subhyaline to pigmented (Braun et al. 2018; Zhang et al. 2021). Conidia of *Apiognomonioides*, *Ellipsoidisporodochium*, *Oblongisporothyrium*, *Obovoideisporodochium* and *Saprothyrium* species are known to be hyaline (Braun et al. 2018; Zhang et al. 2021; Liu et al. 2022). Conidia of *Involutiscutellula*, *Paratubakia* and *Sphaerosporithyrium* species are hyaline to slightly pigmented (Braun et al. 2018), while conidia of *Racheliella* and *Tubakia* species are hyaline to pigmented (Braun et al. 2014, 2018; Zhu et al. 2022).

Tubakiaceae species are known to be endophytes in leaves and twigs of many tree species, but can also cause conspicuous symptoms on host leaves as plant pathogens (Harrington et al. 2012; Braun et al. 2018; Zhu et al. 2022). Nearly all tubakiaceous species are reported from Fagaceae, such as species of *Castanea*, *Castanopsis*, *Fagus*, *Lithocarpus* and *Quercus* (Braun et al. 2018; Morales-Rodríguez et al. 2021). In addition, these fungi are also discovered from the other plant families, i.e., Altingiaceae, Anacardiaceae, Nyssaceae, Oleaceae, Rosaceae, Sapindaceae and Ulmaceae (Braun et al. 2018; Liu et al. 2022).

The aim of the present study is to identify two isolates obtained from diseased leaves of *Lithocarpus glaber* from Guangdong Province by morphological characters and phylogeny based on combined loci of 28S nrRNA gene (LSU), internal transcribed spacer regions and intervening 5.8S nrRNA gene (ITS) of the nrDNA operon, translation elongation factor 1-alpha (*tef1*) and beta tubulin (*tub2*).

Materials and methods

Sample collection, fungal isolation and morphology

Diseased leaves of *Lithocarpus glaber* were collected from Guangdong Province, China. The leaf samples were packed in paper bags and transferred to the laboratory for isolation. The leaves were firstly surface-sterilized for 2 min in 75% ethanol, 4 min in 1.25% sodium hypochlorite, and 1 min in 75% ethanol, then rinsed for 2 min in distilled water and blotted on dry sterile filter paper. Then diseased tissues were cut into 0.5 cm × 0.5 cm pieces using a double-edge blade, and transferred onto the surface of potato dextrose agar (PDA, 200 g potatoes, 20 g dextrose, 20 g agar per L), and incubated at 25 °C to obtain cultures. The hyphal tips were then transferred to clean plates of PDA, malt extract agar (MEA, 30 g malt extract, 5 g mycological peptone, 15 g agar per L) and synthetic low nutrient agar

(SNA, 1 g KN2PO4, 1 g KNO3, 0.5 g MgSO4-7H2O, 0.5 g KCl, 0.2 g glucose, 0.5 g gucrose per L) under a dissecting stereomicroscope with sterile needles. The cultures were deposited in China Forestry Culture Collection Center (CFCC, http://cfcc.caf.ac.cn/; accessed on 6 December 2022), and the specimens in the herbarium of the Chinese Academy of Forestry (CAF, http://museum.caf.ac.cn/; accessed on 6 December 2022).

Morphology of the new taxa was studied based on conidiomata formed on PDA plates under a dissecting microscope (M205 C, Leica, Wetzlar, Germany). The conidiogenous cells and conidia were immersed in tap water, then the microscopic photographs were captured with an Axio Imager 2 microscope (Zeiss, Oberkochen, Germany) equipped with an Axiocam 506 color camera, using differential interference contrast (DIC) illumination. More than 50 conidia were randomly selected for measurement. Culture characters were recorded from PDA, MEA and SNA after 10 days at 25 °C in the dark.

DNA extraction, PCR amplification and phylogenetic analyses

The fungal genomic DNA was extracted from mycelia grown on PDA palates after 10 days following the method in Doyle and Doyle (1990). Four partial loci, ITS and LSU regions, *tef1* and *tub2* genes were amplified by the following primer pairs: ITS1 and ITS4 for ITS (White et al. 1990), LR0R and LR5 for LSU (Vilgalys and Hester 1990), EF1-688F and EF2 for *tef1* (Carbone and Kohn 1999), and Bt2a and Bt2b for *tub2* (Glass and Donaldson 1995).

The polymerase chain reaction (PCR) conditions were set as follows: an initial denaturation step of 5 min at 94 °C, followed by 35 cycles of 30 s at 94 °C, 50 s at 48 °C (ITS and LSU) or 54 °C (*tef1* and *tub2*), and 1 min at 72 °C, and a final elongation step of 10 min at 72 °C. PCR products were assayed via electrophoresis in 2% agarose gels. DNA sequencing was performed using an ABI PRISM 3730XL DNA Analyser with a BigDye Terminator Kit v.3.1 (Invitrogen, Waltham, MA, USA) at the Shanghai Invitrogen Biological Technology Company Limited (Beijing, China).

The sequences obtained in the current study were assembled using SeqMan v. 7.1.0, and reference sequences were retrieved from the website of the National Center for Biotechnology Information (NCBI, https://www.ncbi.nlm.nih.gov; accessed on 15 October 2022), based on sequences from Braun et al. (2018) and Zhang et al. (2021). The sequences were aligned using MAFFT v. 7 and corrected manually using MEGA v. 7.0.21 (Katoh et al. 2019).

The phylogenetic analyses of combined matrixes of ITS-LSU-*tef1*-*rpb2* were performed using maximum parsimony (MP), maximum likelihood (ML) and Bayesian inference (BI) methods. MP analysis was run using a heuristic search option of 1000 search replicates with random-additions of sequences with a tree bisection and reconnection (TBR) algorithm in PAUP v. 4.0b10 (Swofford 2003). Maxtrees were set to 5 000, branches of zero length were collapsed and all equally parsimonious trees were saved. Other calculated parsimony scores were tree length (TL), consistency index (CI), retention index (RI) and rescaled consistency (RC). ML was implemented on the CIPRES Science Gateway portal (https://www.phylo.org) using RAxML-HPC BlackBox 8.2.10 (Miller et al. 2010; Stamatakis 2014), employing a GTR-GAMMA substitution model

with 1000 bootstrap replicates. Bayesian inference was performed using a Markov Chain Monte Carlo (MCMC) algorithm in MrBayes v. 3.0 (Ronquist and Huelsenbeck 2003). Two MCMC chains, starting from random trees for 1000000 generations and trees, were sampled every 100th generation, resulting in a total of 10000 trees. The first 25% of trees were discarded as burn-in of each analysis. Branches with significant Bayesian Posterior Probabilities (BPP > 0.9) were estimated in the remaining 7500 trees. Phylogenetic trees were viewed with FigTree v. 1.4.2 and processed by Adobe Illustrator CS5. The nucleotide sequence data of the new taxa were deposited in GenBank, and the GenBank accession numbers of all accessions included in the phylogenetic analyses are listed in Table 1.

Table 1. Isolates and GenBank accession numbers used in the phylogenetic analyses.

Species	Isolate[a]	Host	Location	GenBank accession number			
				ITS	LSU	*tef1*	*tub2*
Apiognomonioides supraseptata	CBS 632.92*	*Quercus glauca*	Japan	MG976447	MG976448	NA	NA
Ellipsoidisporodochium photiniae	SAUCC 210421*	*Photinia serratifolia*	China	OK175559	OK189532	OK206440	OK206442
Ellipsoidisporodochium photiniae	SAUCC 210423	*Photinia serratifolia*	China	OK175560	OK189533	OK206441	OK206443
Involutiscutellula rubra	CBS 192.71*	*Quercus phillyraeoides*	Japan	MG591899	MG591993	MG592086	MG592180
Involutiscutellula rubra	MUCC2303	*Quercus phillyraeoides*	Japan	MG591900	MG591994	MG592087	MG592181
Involutiscutellula rubra	MUCC2305	*Quercus phillyraeoides*	Japan	MG591902	MG591996	MG592089	MG592182
Melanconis groenlandica	CBS 116540*	*Betula nana*	Greenland	KU878552	KU878553	KU878554	KU878555
Oblongisporothyrium castanopsidis	CBS 124732	*Castanopsis cuspidata*	Japan	MG591849	MG591942	MG592037	MG592131
Oblongisporothyrium castanopsidis	CBS 189.71*	*Castanopsis cuspidata*	Japan	MG591850	MG591943	MG592038	MG592132
Obovoideisporodochium lithocarpi	SAUCC 0748*	*Lithocarpus fohaiensis*	China	MW820279	MW821346	MZ996876	MZ962157
Paratubakia subglobosa	CBS 124733	*Quercus glauca*	Japan	MG591913	MG592008	MG592102	MG592194
Paratubakia subglobosa	CBS 193.71*	*Quercus glauca*	Japan	MG591914	MG592009	MG592103	MG592195
Paratubakia subglobosoides	MUCC2293*	*Quercus glauca*	Japan	MG591915	MG592010	MG592104	MG592196
Phaeotubakia lithocarpicola	**CFCC 54422***	***Lithocarpus glaber***	**China**	**OP951017**	**OP951015**	**OQ127584**	**OQ127586**
Phaeotubakia lithocarpicola	**RK7CX**	***Lithocarpus glaber***	**China**	**OP951018**	**OP951016**	**OQ127585**	**OQ127587**
Racheliella wingfieldiana	CBS 143669*	*Syzigium guineense*	South Africa	MG591911	MG592006	MG592100	MG592192
Saprothyrium thailandense	MFLUCC 12-0303*	Decaying leaf	Thailand	MF190163	MF190110	NA	NA
Sphaerosporithyrium mexicanum	CPC 31361	*Quercus eduardi*	Mexico	MG591894	MG591988	MG592081	MG592175
Sphaerosporithyrium mexicanum	CPC 32258	*Quercus eduardi*	Mexico	MG591895	MG591989	MG592082	MG592176
Sphaerosporithyrium mexicanum	CPC 33021*	*Quercus eduardi*	Mexico	MG591896	MG591990	MG592083	MG592177
Tubakia americana	CBS 129014	*Quercus macrocarpa*	USA	MG591873	MG591966	MG592058	MG592152
Tubakia californica	CPC 31496	*Quercus agrifolia*	USA	MG591829	MG591922	MG592017	MG592111
Tubakia californica	CPC 31499	*Quercus wislizeni*	USA	MG591832	MG591925	MG592020	MG592114
Tubakia dryina	CBS 112097*	*Quercus robur*	Italy	MG591851	MG591944	MG592039	MG592133
Tubakia dryina	CBS 114912	*Quercus* sp.	Netherlands	MG591853	MG591946	MG592041	MG592135
Tubakia dryina	CBS 129016	*Quercus alba*	USA	MG591870	MG591963	MG592056	MG592150
Tubakia dryinoides	CBS 329.75	*Quercus* sp.	France	MG591874	MG591967	MG592059	MG592153
Tubakia dryinoides	CBS 190.71	*Castanea crenata*	Japan	MG591876	MG591968	MG592061	MG592155
Tubakia hallii	CBS 129013*	*Quercus stellata*	USA	MG591880	MG591972	MG592065	MG592159
Tubakia hallii	CBS 129015	*Quercus stellata*	USA	MG591881	MG591973	MG592066	MG592160
Tubakia japonica	CBS 191.71	*Castanea crenata*	Japan	MG591885	MG591977	MG592070	MG592164
Tubakia liquidambaris	CBS 139744	*Liquidambar styraciflua*	USA	MG605068	MG605077	MG603578	NA
Tubakia melnikiana	CPC 32249	*Quercus canbyi*	Mexico	MG591889	MG591983	MG592076	MG592170
Tubakia oblongispora	MUCC2295*	*Quercus serrata*	Japan	MG591897	MG591991	MG592084	MG592178
Tubakia paradryinoides	MUCC2294*	*Quercus acutissima*	Japan	MG591898	MG591992	MG592085	MG592179

Note: NA, not applicable. Ex-type strains are marked with *, and strains from the present study are in black bold.

[a] CBS: Westerdijk Fungal Biodiversity Institute, Utrecht, the Netherlands; CFCC: China Forestry Culture Collection Center, Beijing, China; CPC: Culture collection of P. W. Crous, housed at CBS; MFLUCC: Mae Fah Luang University Culture Collection, Thailand; MUCC: Lab. of Plant Pathology, Mie University, Japan; SAUCC: Shandong Agricultural University Culture Collection, China.

Results

Phylogenetic analyses

The alignment based on the sequence dataset (ITS, LSU, *tef1* and *tub2*) included 35 ingroup taxa, comprising 2736 characters in the aligned matrix. Of these, 1721 characters were constant, 206 variable characters were parsimony-uninformative and 809 characters were parsimony informative. The MP analysis resulted in two equally most parsimonious trees (TL = 2708, CI = 0.615, RI = 0.804, RC = 0.385) and the first tree is shown in Fig. 1. The topologies resulting from MP, ML and BI analyses of the concatenated dataset were congruent. Isolates from the present study formed an individual clade in Tubakiaceae representing a new genus and species named *Phaeotubakia lithocarpicola*.

Taxonomy

Phaeotubakia **Ning Jiang, gen. nov.**
MycoBank No: MB846813

Etymology. Named derived from *phaeo* (= pigmented) and its morphological similarity to *Tubakia*.

Type species. *Phaeotubakia lithocarpicola* Y.Q. Zhu & Ning Jiang.

Description. Sexual morph: Unknown. Asexual morph in vitro: Conidiomata sporodochial, slimy, black, semi-submerged. Conidiophores reduced to conidiogenous cells. Conidiogenous cells brown, smooth, guttulate, cylindrical to ampulliform, attenuate towards apex, phialidic. Conidia blastic, subglobose, broad ellipsoid to ellipsoid, seldom irregular, brown to dark brown, walls smooth, becoming thicker with age, base rounded or with truncate basal hilum.

Notes. *Phaeotubakia* is proposed as the eleventh genus of Tubakiaceae based on morphological features and phylogeny of combined ITS, LSU, *tef1* and *tub2* loci (Fig. 1). *Phaeotubakia* is distinguished from *Apiognomonioides*, *Ellipsoidisporodochium*, *Involutiscutellula*, *Oblongisporothyrium*, *Obovoideisporodochium*, *Paratubakia*, *Racheliella*, *Saprothyrium* and *Sphaerosporithyrium* by having brown to dark brown conidia (Braun et al. 2018; Zhang et al. 2021). Several species of *Tubakia* are known to have brown conidia, which is similar to *Phaeotubakia lithocarpicola* (Braun et al. 2018; Zhu et al. 2022). However, they are phylogenetically distinct (Fig. 1).

Phaeotubakia lithocarpicola **Y.Q. Zhu & Ning Jiang, sp. nov.**
MycoBank No: MB846814
Fig. 2

Etymology. Named after the host genus, *Lithocarpus*.

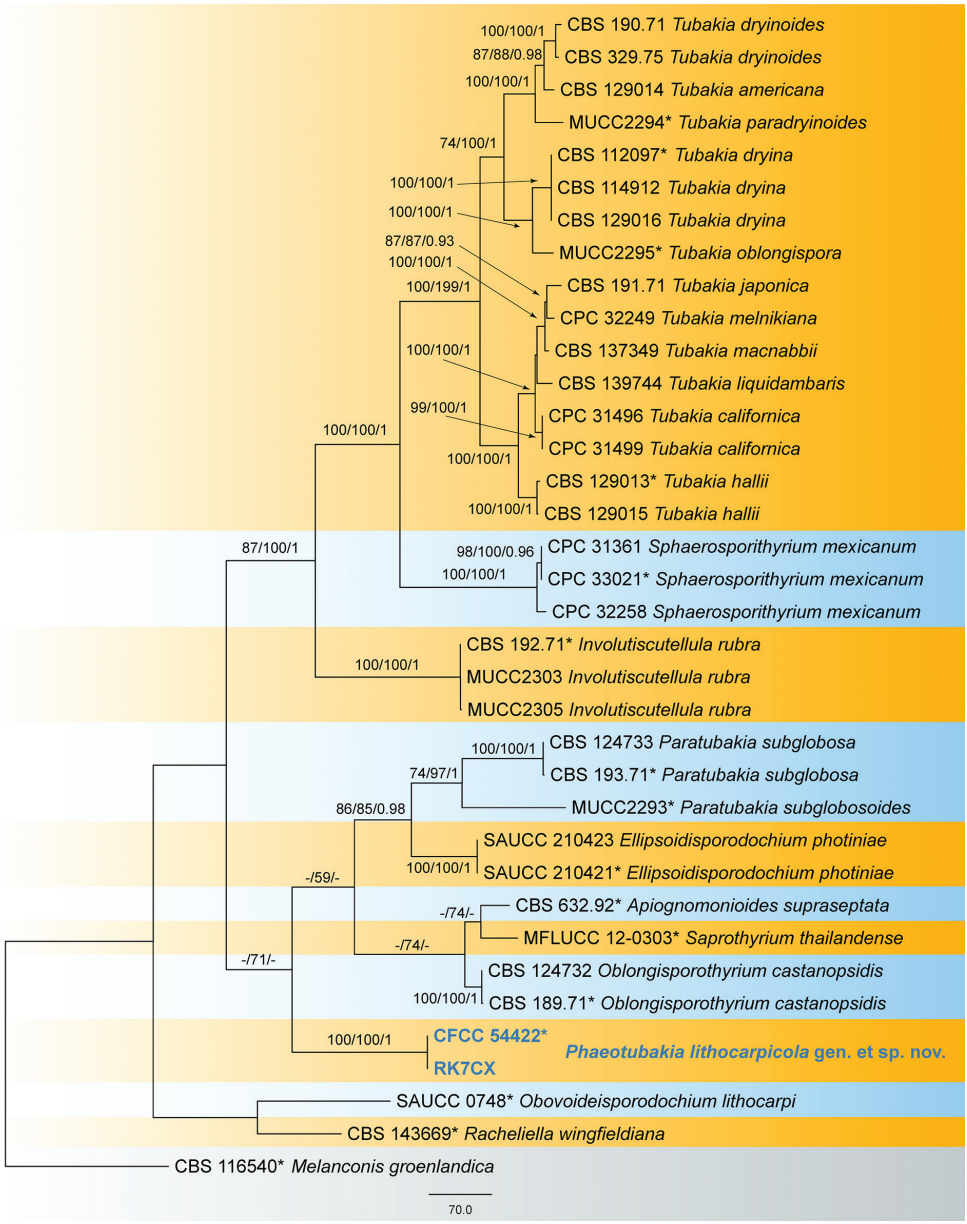

Figure 1. Phylogram of Tubakiaceae based on combined ITS, LSU, *tef1* and *tub2* loci. Numbers above the branches indicate maximum parsimony bootstrap (MP BP ≥ 50%), ML bootstrap values (ML-BS ≥ 50%) and Bayesian Posterior Probabilities (BPP ≥ 0.9). The tree is rooted with *Melanconis groenlandica* (CBS 116540). Ex-type strains are marked with *, and strains from the present study are marked in bold blue.

Description. From leaf spots, circular to subcircular, margin distinct, brown to fuscous. Sexual morph: Unknown. Asexual morph in vitro: Conidiomata sporodochial, appeared after 10 days on PDA surface, slimy, black, semi-submerged, 50–350 µm diam.

Conidiophores reduced to conidiogenous cells. Conidiogenous cells brown, smooth, guttulate, cylindrical to ampulliform, attenuate towards apex, phialidic, 6–15.5 × 3.5–5 µm. Conidia blastic, subglobose, broad ellipsoid to ellipsoid, seldom irregular, brown to dark brown, walls smooth, becoming thicker with age, base rounded or with truncate basal hilum, (13.5–)14–16.5(–18) × (5.5–)7–8.5(–9) µm (n = 50), L/W = 1.7–3.2.

Culture characters. Colonies on PDA flat, spreading, with flocculent aerial mycelium, white to pale luteous, with age forming concentric zones, reaching a 90 mm diameter and forming abundant black conidiomata after 10 days at 25 °C; on MEA flat, spreading, with flocculent aerial mycelium and crenate edge, pale luteous to pale grey, reaching a 45 mm diameter after 10 days at 25 °C; on SNA flat, spreading, with flocculent aerial mycelium forming concentric rings and entire edge, pale luteous, reaching a 60 mm diameter after 10 days at 25 °C.

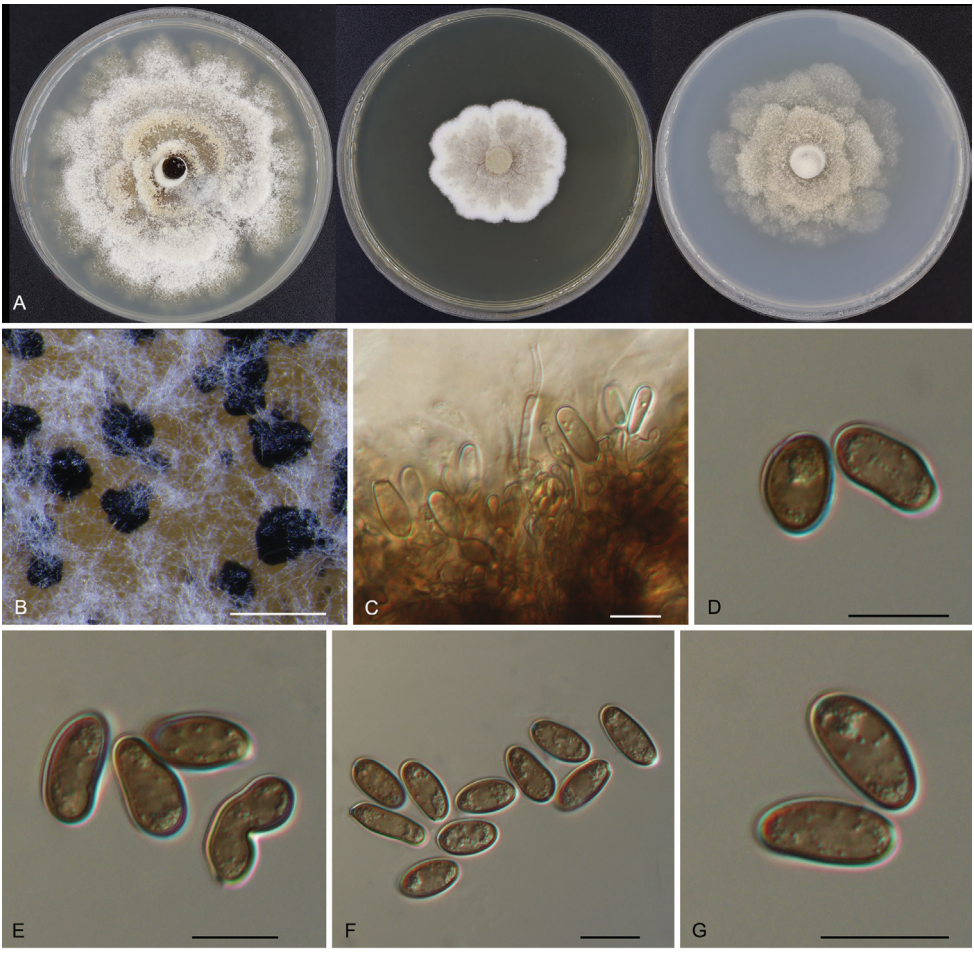

Figure 2. Morphology of *Phaeotubakia lithocarpicola* (CFCC 54452) **A** colonies on PDA, MEA and SNA after 10 days at 25 °C **B** conidiomata formed on PDA **C** conidiogenous cells giving rise to conidia **D–G** conidia. Scale bars: 200 µm (**B**); 10 µm (**C–G**).

Specimens examined. China, Guangdong Province, Qingyuan City, Yangshan County, Guangdong Nanling Nature Reserve, on diseased leaves of *Lithocarpus glaber*, 4 December 2019, Yong Li (holotype CAF 800071; ex-holotype culture CFCC 54422). Guangdong Province, Qingyuan City, Yangshan County, Guangdong Nanling Nature Reserve, on diseased leaves of *Lithocarpus glaber*, 3 December 2019, Danran Bian (culture RK7CX).

Notes. *Phaeotubakia lithocarpicola* is the sole species within the newly proposed genus, which is associated with leaf spot disease of *Lithocarpus glaber*. Two tubakiaceous species were reported from the host genus *Lithocarpus* before the present study, viz. *Obovoideisporodochium lithocarpi* from *Lithocarpus fohaiensis* in China and *Tubakia californica* from *Lithocarpus densiflorus* in the USA (Braun et al. 2018; Zhang et al. 2021). *Phaeotubakia lithocarpicola* represents the third tubakiaceous species discovered from the host genus *Lithocarpus*. However, *P. lithocarpicola* differs from *O. lithocarpi* and *T. californica* by brown conidiogenous cells and brown to dark brown conidia (Braun et al. 2018; Zhang et al. 2021).

Discussion

Diaporthales is a well-resolved fungal order based on evidence of both morphology and phylogeny (Senanayake et al. 2017, 2018; Fan et al. 2018; Jiang et al. 2020). *Tubakia* was placed in Melanconiellaceae of Diaporthales (Senanayake et al. 2017), and subsequently transferred to the newly established family of its own Tubakiaceae (Braun et al. 2018). Meanwhile, some species were removed from *Tubakia*, and seven new genera were proposed based on these species (Braun et al. 2018). Soon after, *Ellipsoidisporodochium* and *Obovoideisporodochium* were added to Tubakiaceae (Zhang et al. 2021; Liu et al. 2022). In the present study, the eleventh genus *Phaeotubakia* is proposed to be included in this family.

Members of Tubakiaceae are quite similar in morphology, but phylogenetically distinct (Braun et al. 2018; Senanayake et al. 2018; Zhang et al. 2021). The sexual morph of Tubakiaceae is not prominent, hence genera and species are distinguished mainly based on their asexual morphology and molecular data.

The newly proposed genus and species *Phaeotubakia lithocarpicola* in the present study produce brown to dark brown conidia on the PDA plates, which is morphologically different from the other tubakiaceous taxa, but similar to *Melanconis*-like taxa of Diaporthales (Voglmayr et al. 2012, 2017; Jiang et al. 2021b). Four families of Diaporthales are known to contain *Melanconis*-like genera and species, namely Juglanconidaceae, Melanconidaceae, Melanconiellaceae and Pseudomelanconidaceae (Jiang et al. 2018; Fan et al. 2018; Senanayake et al. 2018). Hence, traditional morphological identification of diaporthalean fungi is insufficient.

The center of genetic diversity of *Tubakia* appears to be in East Asia, e.g. China and Japan, where Fagaceae hosts are the most common hosts (Harrington and McNew 2018). *Obovoideisporodochium lithocarpi* and several new *Tubakia* species (*T. cyclobalanopsidis*

and *T. quercicola*) recently discovered from trees of Fagaceae (Zhang et al. 2021; Zhu et al. 2022), and *Phaeotubakia lithocarpicola* proposed in the present study support this phenomenon well. More taxa of Tubakiaceae may be revealed by more investigations of fungal diversity on Fagaceae in the future.

Acknowledgements

This research was funded by the National Microbial Resource Center of the Ministry of Science and Technology of the People's Republic of China (NMRC-2021-7).

References

Braun U, Bien S, Hantsch L, Heuchert B (2014) *Tubakia chinensis* sp. nov. and a key to the species of the genus *Tubakia*. Schlechtendalia (Halle) 28: 23–28. https://doi.org/10.25673/90134

Braun U, Nakashima C, Crous PW, Groenewald JZ, Moreno-Rico O, Rooney-Latham S, Blomquist CL, Haas J, Marmolejo J (2018) Phylogeny and taxonomy of the genus *Tubakia* s. lat. Fungal Systematics and Evolution 1(1): 41–99. https://doi.org/10.3114/fuse.2018.01.04

Carbone I, Kohn LM (1999) A method for designing primer sets for speciation studies in filamentous ascomycetes. Mycologia 3(3): 553–556. https://doi.org/10.1080/00275514.1999.12061051

Doyle JJ, Doyle JL (1990) Isolation of plant DNA from fresh tissue. Focus (San Francisco, Calif.) 12: 13–15.

Fan XL, Bezerra JDP, Tian CM, Crous PW (2018) Families and genera of diaporthalean fungi associated with canker and dieback of tree hosts. Persoonia 40(1): 119–134. https://doi.org/10.3767/persoonia.2018.40.05

Glass NL, Donaldson GC (1995) Development of primer sets designed for use with the PCR to amplify conserved genes from filamentous ascomycetes. Applied and Environmental Microbiology 61(4): 1323–1330. https://doi.org/10.1128/aem.61.4.1323-1330.1995

Harrington TC, McNew DL (2018) A re-evaluation of *Tubakia*, including three new species on *Quercus* and six new combinations. Antonie van Leeuwenhoek 111(7): 1003–1022. https://doi.org/10.1007/s10482-017-1001-9

Harrington TC, McNew D, Yun HY (2012) Bur oak blight, a new disease on *Quercus macrocarpa* caused by *Tubakia iowensis* sp. nov. Mycologia 104(1): 79–92. https://doi.org/10.3852/11-112

Jiang N, Li J, Piao CG, Guo MW, Tian CM (2018) Identification and characterization of chestnut branch-inhabiting melanocratic fungi in China. Mycosphere : Journal of Fungal Biology 9(6): 1268–1289. https://doi.org/10.5943/mycosphere/9/6/14

Jiang N, Fan X, Tian C, Crous PW (2020) Reevaluating Cryphonectriaceae and allied families in Diaporthales. Mycologia 112(2): 267–292. https://doi.org/10.1080/00275514.2019.1698925

Jiang N, Voglmayr H, Piao CG, Li Y (2021a) Two new species of *Diaporthe* (Diaporthaceae, Diaporthales) associated with tree cankers in the Netherlands. MycoKeys 85: 31–56. https://doi.org/10.3897/mycokeys.85.73107

Jiang N, Yang Q, Fan XL, Tian CM (2021b) *Micromelanconis kaihuiae* gen. et sp. nov., a new diaporthalean fungus from Chinese chestnut branches in southern China. MycoKeys 79: 1–16. https://doi.org/10.3897/mycokeys.79.65221

Katoh K, Rozewicki J, Yamada KD (2019) MAFFT online service: Multiple sequence alignment, interactive sequence choice and visualization. Briefings in Bioinformatics 20(4): 1160–1166. https://doi.org/10.1093/bib/bbx108

Liu SB, Zhang ZX, Liu RY, Mu TC, Zhang XG, Li Z, Xia JW (2022) Morphological and molecular identification of *Ellipsoidisporodochium* gen. nov. (Tubakiaceae, Diaporthales) in Hainan Province, China. Phytotaxa 552(4): 259–266. https://doi.org/10.11646/phytotaxa.552.4.3

Miller MA, Pfeiffer W, Schwartz T (2010) Creating the CIPRES Science Gateway for Inference of Large Phylogenetic Trees. Institute of Electrical and Electronics Engineers: New Orleans, LA, USA. https://doi.org/10.1109/GCE.2010.5676129

Morales-Rodríguez C, Bastianelli G, Aleandri M, Doğmuş-Lehtijärvi HT, Oskay F, Vannini A (2021) Revealing novel interactions between oak and *Tubakia* species: Evidence of the efficacy of the sentinel arboreta strategy. Biological Invasions 23(12): 3749–3765. https://doi.org/10.1007/s10530-021-02614-4

Ronquist F, Huelsenbeck JP (2003) MrBayes 3: Bayesian phylogenetic inference under mixed models. Bioinformatics (Oxford, England) 19(12): 1572–1574. https://doi.org/10.1093/bioinformatics/btg180

Rossman AY, Farr DF, Castlebury LA (2007) A review of the phylogeny and biology of the Diaporthales. Mycoscience 48(3): 135–144. https://doi.org/10.1007/S10267-007-0347-7

Senanayake IC, Crous PW, Groenewald JZ, Maharachchikumbura SSN, Jeewon R, Phillips AJL, Bhat DJ, Perera RH, Li QR, Li WJ, Tangthirasunun N, Norphanphoun C, Karunarathna SC, Camporesi E, Manawasighe IS, Al-Sadi AM, Hyde KD (2017) Families of Diaporthales based on morphological and phylogenetic evidence. Studies in Mycology 86(1): 217–296. https://doi.org/10.1016/j.simyco.2017.07.003

Senanayake IC, Jeewon R, Chomnunti P, Wanasinghe DN, Norphanphoun C, Karunarathna A, Pem D, Perera RH, Camporesi E, McKenzie EHC, Hyde KD, Karunarathna SC (2018) Taxonomic circumscription of Diaporthales based on multigene phylogeny and morphology. Fungal Diversity 93(1): 241–443. https://doi.org/10.1007/s13225-018-0410-z

Stamatakis A (2014) RAxML version 8: A tool for phylogenetic analysis and post-analysis of large phylogenies. Bioinformatics (Oxford, England) 30(9): 1312–1313. https://doi.org/10.1093/bioinformatics/btu033

Swofford DL 2003. PAUP*: Phylogenetic analysis using parsimony (* and other methods). Version 4.0b10. Sunderland, England.

Udayanga D, Miriyagalla SD, Manamgoda DS, Lewers KS, Gardiennet A, Castlebury LA (2021) Molecular reassessment of diaporthalean fungi associated with strawberry, including the leaf blight fungus, *Paraphomopsis obscurans* gen. et comb. nov. (Melanconiellaceae). IMA Fungus 12(1): 1–21. https://doi.org/10.1186/s43008-021-00069-9

Vilgalys R, Hester M (1990) Rapid genetic identification and mapping of enzymatically amplified ribosomal DNA from several *Cryptococcus* species. Journal of Bacteriology 172(8): 4238–4246. https://doi.org/10.1128/jb.172.8.4238-4246.1990

Voglmayr H, Rossman AY, Castlebury LA, Jaklitsch WM (2012) Multigene phylogeny and taxonomy of the genus *Melanconiella* (Diaporthales). Fungal Diversity 57(1): 1–44. https://doi.org/10.1007/s13225-012-0175-8

Voglmayr H, Castlebury LA, Jaklitsch WM (2017) *Juglanconis* gen. nov. on *Juglandaceae*, and the new family Juglanconidaceae (Diaporthales). Persoonia 38(1): 136–155. https://doi.org/10.3767/003158517X694768

White TJ, Bruns T, Lee S, Taylor J (1990) Amplification and direct sequencing of fungal ribosomal RNA genes for phylogenetics. PCR Protocols: A Guide to Methods and Applications 18: 315–322. https://doi.org/10.1016/B978-0-12-372180-8.50042-1

Zhang ZX, Mu TC, Liu SB, Liu RY, Zhang XG, Xia JW (2021) Morphological and phylogenetic analyses reveal a new genus and two new species of Tubakiaceae from China. MycoKeys 84: 185–201. https://doi.org/10.3897/mycokeys.84.73940

Zhu YQ, Jiang N, Dou ZP, Xue H, Piao CG, Li Y (2022) Additions to the knowledge of *Tubakia* (Tubakiaceae, Diaporthales) in China. Journal of Fungi (Basel, Switzerland) 8(11): 1143. https://doi.org/10.3390/jof8111143

MycoKeys 95: 27–45 (2023)
doi: 10.3897/mycokeys.95.96400
https://mycokeys.pensoft.net

RESEARCH ARTICLE

A peer-reviewed open-access journal
MycoKeys
Launched to accelerate biodiversity research

Morphological and phylogenetic analyses reveal two new species and a new record of *Apiospora* (Amphisphaeriales, Apiosporaceae) in China

Rongyu Liu[1,2], Duhua Li[2], Zhaoxue Zhang[2], Shubin Liu[2], Xinye Liu[1], Yixin Wang[1], Heng Zhao[3], Xiaoyong Liu[1], Xiuguo Zhang[1,2], Jiwen Xia[2], Yujiao Wang[1]

1 *College of Life Sciences, Shandong Normal University, Jinan, 250358, China* **2** *Shandong Provincial Key Laboratory for Biology of Vegetable Diseases and Insect Pests, College of Plant Protection, Shandong Agricultural University, Taian, 271018, China* **3** *Institute of Microbiology, School of Ecology and Nature Conservation, Beijing Forestry University, Beijing, 100083, China*

Corresponding authors: Jiwen Xia (xiajiwen1@126.com); Yujiao Wang (18354285903@163.com)

Academic editor: Xinlei Fan | Received 17 October 2022 | Accepted 3 January 2023 | Published 27 January 2023

Citation: Liu R, Li D, Zhang Z, Liu S, Liu X, Wang Y, Zhao H, Liu X, Zhang X, Xia J, Wang Y (2023) Morphological and phylogenetic analyses reveal two new species and a new record of *Apiospora* (Amphisphaeriales, Apiosporaceae) in China. MycoKeys 95: 27–45. https://doi.org/10.3897/mycokeys.95.96400

Abstract

The genus *Apiospora* includes endophytes, pathogens and saprobes, with a wide host range and geographic distribution. In this paper, six *Apiospora* strains isolated from diseased and healthy tissues of bamboo leaves from Hainan and Shandong provinces in China were classified using a multi-locus phylogeny based on a combined dataset of ITS, LSU, *tef1* and *tub2*, in conjunction with morphological characters, host association and ecological distribution. Two new species, *Apiospora dongyingensis* and *A. hainanensis*, and a new record of *A. pseudosinensis* in China, are described based on their distinct phylogenetic relationships and morphological analyses. Illustrations and descriptions of the three taxa are provided, along with comparisons with closely related taxa in the genus.

Keywords

Apiospora dongyingensis, *Apiospora hainanensis*, Ascomycota, bamboo, taxonomy

Introduction

Apiospora Sacc., the type genus of Apiosporaceae K.D. Hyde, J. Fröhl., Joanne E. Taylor & M.E. Barr, was introduced by Saccardo with *A. montagnei* Sacc. as the type species (Saccardo 1875). The sexual morphs of *Apiospora* are characterized by multi-locular perithecial stromata with hyaline ascospores surrounded by a thick gelatinous sheath (Dai et al. 2016, 2017; Pintos and Alvarado 2021). The asexual morphs of *Apiospora* are characterized by their basauxic conidiogenesis, and globose to subglobose conidia, which are usually lenticular or obovoid in the side view, and pale brown to brown in color (Kunze 1817; Hyde et al. 1998; Dai et al. 2016). Most species of *Apiospora* are quite similar to each other in morphology, thus it is difficult to distinguish them without molecular phylogenetic data.

Until the studies of Pintos and Alvarado (2021) and Jiang et al. (2022a), the closely related genera *Apiospora*, *Arthrinium* Kunze and *Neoarthrinium* Ning Jiang were considered a single taxon because of their similar morphological characteristics, especially the basauxic conidiogenesis. However, the conidia of *Apiospora* and *Neoarthrinium* are more or less rounded in the face view and lenticular in the side view, whereas the conidia of *Arthrinium* are variously shaped (angular, curved, fusiform, globose, polygonal, navicular). In addition, the conidiophores of several *Arthrinium* and *Neoarthrinium* species have thick blackish septa, which are rarely observed in *Apiospora* (Pintos and Alvarado 2021; Tian et al. 2021; Jiang et al. 2022a). *Apiospora* species have a worldwide distribution and can be found on various hosts, while *Arthrinium* species are rarely found in tropical and subtropical habitats and commonly occur on Cyperaceae Juss. and Juncaceae Juss. (Ramos et al. 2010; Dai et al. 2017; Wang et al. 2018; Hyde et al. 2020; Pintos and Alvarado 2021; Tian et al. 2021). Four *Neoarthrinium* species have been discovered on four hosts from three distantly related host plant families in China, Colombia and Great Britain (Jiang et al. 2022a). Most *Apiospora* species are associated with plants as endophytes, pathogens or saprobes (Agut and Calvo 2004; Dai et al. 2016, 2017; Tian et al. 2021). Some species are economically important plant pathogens, for example, *A. arundinis* causes bamboo brown culm streak, chestnut leaf spot and barley kernel blight (Martínez-Cano et al. 1992; Chen et al. 2014; Jiang et al. 2021), while *A. sacchari* causes damping-off of durum wheat (Mavragani et al. 2007). Some species have also been isolated from lichens, air, soil, seaweeds and animal tissues, and a few species are human pathogens which can cause cutaneous infections (Tian et al. 2021).

The aim of this study was to explore the diversity of *Apiospora* species in symptomatic and asymptomatic bamboo leaves collected in Hainan and Shandong provinces (China). We describe two newly discovered species, *Apiospora dongyingensis* and *A. hainanensis*, and a new record of *A. pseudosinensis* in China based on phylogenetic data and morphology.

Materials and methods

Isolation and morphological studies

The samples were collected at the Diaoluoshan National Nature Reserve, Hainan Province, and the Dongying Botanical Garden, Shandong Province (China). The strains of *Apiospora* were isolated from single spores and fungal tissue obtained from diseased and healthy bamboo leaves following the methods described by Chomnunti et al. (2014). Sampled spores were suspended in sterile distilled water, spread onto potato dextrose agar (PDA) plates, and incubated for one day at 25 °C. After germination, the spores were transferred to a new PDA plate to obtain a pure culture. Additionally, about 25 mm^2 tissue fragments were taken from the margin of leaf lesions and their surface sterilized by consecutive immersions in a 75% ethanol solution for 60 s, 5% sodium hypochlorite solution for 30 s, and then rinsed in sterile distilled water for 60 s (Mu et al. 2021). The surface sterilized plant tissue was dried with sterilized paper and moved on the PDA plates. All the PDA plates were incubated at 25 °C for 3–4 days in darkness, and then hyphae were picked out of the periphery of the colonies and grown on new PDA plates (Jiang et al. 2022b).

After 7 days of incubation, the morphological characters of the colonies were recorded on PDA with a digital camera (Canon G7X). Morphological descriptions were based on cultures sporulating on water agar (WA). The size of the conidiogenous cells and conidia were shown as minimum-maximum. Color notations were done using the color charts of Rayner (1970). The micro-morphological characters of the colonies were studied using a stereomicroscope (Olympus SZX10) and a microscope (Olympus BX53), both fitted with high-definition color digital cameras. Grown cultures of *Apiospora* were stored in 10% sterilized glycerin and sterile water at 4 °C for further studies in the future. All specimens were deposited in the Herbarium of the Department of Plant Pathology, Shandong Agricultural University (**HSAUP**). Living cultures were deposited in the Shandong Agricultural University Culture Collection (**SAUCC**). Taxonomic information on the new taxa was submitted to MycoBank (http://www.mycobank.org).

DNA extraction and amplification

Genomic DNA was extracted from fungal mycelia grown on PDA, using a modified cetyltrimethylammonium bromide (CTAB) protocol as described in Guo et al. (2000). DNA sequences of four different loci were obtained, including the nrDNA internal transcribed spacer regions 1 and 2 with the intervening 5.8S subunit (ITS), a partial sequence of the large subunit nrDNA subunit (LSU), a partial sequence of the translation elongation factor 1-alpha gene (*tef1*), and a partial sequence of the beta-tubulin gene (*tub2*). They were all amplified with the primer pairs and polymerase chain reaction (PCR) program listed in Table 1.

PCR was performed using an Eppendorf Master Thermocycler (Hamburg, Germany). Amplification reactions contained 12.5 μL 2× Taq Plus Master Mix II (Vazyme, Nanjing, China), 1 μL of each forward and reverse primers (10 μM) (Tsingke, Qingdao, China), 1 μL of template genomic DNA, and distilled deionized water to a total volume of 25 μL. The PCR products were visualized on 1% agarose electrophoresis gels. Bi-directional sequencing was conducted by the Tsingke Company Limited (Qingdao, China). Consensus sequences were obtained using MEGA 7.0 (Kumar et al. 2016). All sequences generated in this study were deposited in GenBank (Table 2).

Table 1. Gene regions and respective primer pairs used in the study.

Locus	PCR primers	PCR: thermal cycles: (Annealing temperature in bold)	Reference
ITS	ITS5/ITS4	(94 °C: 30 s, **55 °C**: 30 s, 72 °C: 45 s) × 29 cycles	White et al. 1990
LSU	LR0R/LR5	(94 °C: 30 s, **48 °C**: 50 s, 72 °C: 1 min 30 s) × 35 cycles	Vilgalys and Hester 1990; Cubeta et al. 1991
tef1	EF1-728F/EF2	(95 °C: 30 s, **51 °C**: 30 s, 72 °C: 1 min) × 35 cycles	O'Donnell et al. 1998; Carbone and Kohn 1999
tub2	Bt-2a/Bt-2b	(95 °C: 30 s, **56 °C**: 30 s, 72 °C: 1 min) × 35 cycles	Glass and Donaldson 1995

Table 2. Isolates and GenBank accession numbers used in the phylogenetic analyses.

Species	Isolate/Strain	Host/Substrate	Origin	GenBank accession numbers			
				ITS	LSU	*tef1*	*tub2*
Apiospora acutiapica	KUMCC 20-0210 (Type)	*Bambusa bambos*	China	MT946343	MT946339	MT947360	MT947366
A. agari	KUC21333 (Type)	*Agarum cribrosum*	Korea	MH498520	MH498440	MH544663	MH498478
A. aquatica	S-642 (Type)	Submerged wood	China	MK828608	MK835806	NA	NA
A. arctoscopi	KUC21331 (Type)	Egg of *Arctoscopus japonicus*	Korea	MH498529	MH498449	MN868918	MH498487
A. arundinis	CBS 124788	Living leaves of *Fagus sylvatica*	Switzerland	KF144885	KF144929	KF145017	KF144975
A. aurea	CBS 244.83 (Type)	Air	Spain	AB220251	KF144935	KF145023	KF144981
A. balearica	CBS 145129 (Type)	Undetermined Poaceae	Spain	MK014869	MK014836	MK017946	MK017975
A. biserialis	CGMCC 3.20135 (Type)	Bamboo	China	MW481708	MW478885	MW522938	MW522955
A. camelliae-sinensis	LC5007 (Type)	*Camellia sinensis*	China	KY494704	KY494780	KY705103	KY705173
A. chiangraiense	MFLUCC21-0053 (Type)	Dead culms of bamboo	Thailand	MZ542520	MZ542524	NA	MZ546409
A. chromolaenae	MFLUCC 17-1505 (Type)	*Chromolaena odorata*	Thailand	MT214342	MT214436	NA	NA
A. cordylines	GUCC 10027 (Type)	Leaves of *Cordyline fruticosa*	China	MT040106	NA	MT040127	MT040148
A. cyclobalanopsidis	CGMCC 3.20136 (Type)	*Cyclobalanopsidis glauca*	China	MW481713	MW478892	MW522945	MW522962
A. descalsii	CBS 145130 (Type)	*Ampelodesmos mauritanicus*	Spain	MK014870	MK014837	MK017947	MK017976
A. dichotomanthi	LC4950 (Type)	*Dichotomanthus tristaniaecarpa*	China	KY494697	KY494773	KY705096	KY705167
A. dongyingensis	**SAUCC 0302 (Type)**	**Leaf of bamboo**	**China**	**OP563375**	**OP572424**	**OP573264**	**OP573270**
	SAUCC 0303	**Leaf of bamboo**	**China**	**OP563374**	**OP572423**	**OP573263**	**OP573269**
A. esporlensis	CBS 145136 (Type)	*Phyllostachys aurea*	Spain	MK014878	MK014845	MK017954	MK017983
A. euphorbiae	IMI 285638b	*Bambusa* sp.	Bangladesh	AB220241	AB220335	NA	AB220288
A. fermenti	KUC21289 (Type)	Seaweed	Korea	MF615226	MF615213	MH544667	MF615231

Species	Isolate/Strain	Host/Substrate	Origin	GenBank accession numbers			
				ITS	LSU	*tef1*	*tub2*
A. gaoyouensis	CFCC 52301 (Type)	*Phragmites australis*	China	MH197124	NA	MH236793	MH236789
A. garethjonesii	JHB004 (Type)	Culms of dead bamboo	China	KY356086	KY356091	NA	NA
A. gelatinosa	HKAS 111962 (Type)	Culms of dead bamboo	China	MW481706	MW478888	MW522941	MW522958
A. guiyangensis	HKAS 102403 (Type)	Dead culms of Poaceae	China	MW240647	MW240577	MW759535	MW775604
A. guizhouensis	LC5322 (Type)	Air in karst cave	China	KY494709	KY494785	KY705108	KY705178
A. hainanensis	**SAUCC 1681 (Type)**	**Leaf of bamboo**	**China**	**OP563373**	**OP572422**	**OP573262**	**OP573268**
	SAUCC 1682	**Leaf of bamboo**	**China**	**OP563372**	**OP572421**	**OP573261**	**OP573267**
A. hispanica	IMI 326877 (Type)	Maritime sand	Spain	AB220242	AB220336	NA	AB220289
A. hydei	CBS 114990 (Type)	Culms of *Bambusa tuldoides*	China	KF144890	KF144936	KF145024	KF144982
A. hyphopodii	MFLUCC 15-0003 (Type)	Dead culms of bamboo	Thailand	KR069110	NA	NA	NA
A. hysterina	ICPM 6889 (Type)	Bamboo	New Zealand	MK014874	MK014841	MK017951	MK017980
A. iberica	AP10118 (Type)	*Arundo donax*	Portugal	MK014879	MK014846	MK017955	MK017984
A. intestini	CBS 135835 (Type)	Gut of grasshopper	India	KR011352	KR149063	KR011351	KR011350
A. italica	CBS 145138 (Type)	*Arundo donax*	Italy	MK014880	MK014847	MK017956	MK017985
A. jatrophae	CBS 134262 (Type)	*Jatropha podagrica*	India	JQ246355	NA	NA	NA
A. jiangxiensis	LC4577 (Type)	*Maesa* sp.	China	KY494693	KY494769	KY705092	KY705163
A. kogelbergensis	CBS 113333 (Type)	Dead culms of *Restionaceae*	South Africa	KF144892	KF144938	KF145026	KF144984
A. koreana	KUC21332 (Type)	Egg of *Arctoscopus japonicus*	Korea	MH498524	MH498444	MH544664	MH498482
A. locuta-pollinis	LC11683 (Type)	*Brassica campestris*	China	MF939595	NA	MF939616	MF939622
A. longistroma	MFLUCC 11-0481 (Type)	Culms of decaying bamboo	Thailand	KU940141	KU863129	NA	NA
A. malaysiana	CBS 102053 (Type)	*Macaranga hullettii* stem colonised by ants	Malaysia	KF144896	KF144942	KF145030	KF144988
A. marianiae	AP18219 (Type)	Dead stems of *Phleum pratense*	Spain	ON692406	ON692422	ON677180	ON677186
A. marii	CBS 497.90 (Type)	Atmosphere, pharmaceutical excipients, home dust and beach sands	Spain	MH873913	KF144947	KF145035	KF144993
A. marina	KUC21328 (Type)	Seaweed	Korea	MH498538	MH498458	MH544669	MH498496
A. mediterranea	IMI 326875 (Type)	Air	Spain	AB220243	AB220337	NA	AB220290
A. minutispora	17E-042 (Type)	Soil	South Korea	LC517882	NA	LC518889	LC518888
A. montagnei	AP301120 (Epitype)	*Arundo micrantha*	Spain	ON692408	ON692424	ON677182	ON677188
	AP19421	*Arundo micrantha*	Spain	ON692418	ON692425	ON677183	ON677189
	CPC 18900	Culms of *Phragmites australis*	Italy	KF144909	KF144956	KF145043	KF145001
A. mori	MFLU 18-2514 (Type)	Dead leaves of *Morus australis*	China	MW114313	MW114393	NA	NA
A. multiloculata	MFLUCC 21-0023 (Type)	Dead culms of *Bambusae*	Thailand	OL873137	OL873138	NA	OL874718
A. mytilomorpha	DAOM 214595 (Type)	Dead blades of *Andropogon* sp.	India	KY494685	NA	NA	NA
A. neobambusae	LC7106 (Type)	Leaf of bamboo	China	KY494718	KY494794	KY806204	KY705186
A. neochinense	CFCC 53036 (Type)	*Fargesia qinlingensis*	China	MK819291	NA	MK818545	MK818547
A. neogarethjonesii	HKAS 102408 (Type)	Dead culms of *Bambusae*	China	MK070897	MK070898	NA	NA
A. neosubglobosa	JHB007 (Type)	Bamboo	China	KY356090	KY356095	NA	NA

Species	Isolate/Strain	Host/Substrate	Origin	GenBank accession numbers			
				ITS	LSU	*tef1*	*tub2*
A. obovata	LC4940 (Type)	*Lithocarpus* sp.	China	KY494696	KY494772	KY705095	KY705166
A. ovata	CBS 115042 (Type)	*Arundinaria hindsii*	China	KF144903	KF144950	KF145037	KF144995
A. paraphaeosperma	MFLUCC13-0644 (Type)	Dead clumps of *Bambusa* sp.	Thailand	KX822128	KX822124	NA	NA
A. phyllostachydis	MFLUCC 18-1101 (Type)	*Phyllostachys heteroclada*	China	MK351842	MH368077	MK340918	MK291949
A. piptatheri	CBS 145149 (Type)	*Piptatherum miliaceum*	Spain	MK014893	MK014860	MK017969	NA
A. pseudomarii	GUCC 10228 (Type)	Leaves of *Aristolochia debilis*	China	MT040124	NA	MT040145	MT040166
A. pseudoparenchymatica	LC7234 (Type)	Leaf of bamboo	China	KY494743	KY494819	KY705139	KY705211
A. pseudorasikravindrae	KUMCC 20-0208 (Type)	*Bambusa dolichoclada*	China	MT946344	NA	MT947361	MT947367
A. pseudosinensis	CPC 21546 (Type)	Leaf of bamboo	Netherlands	KF144910	KF144957	KF145044	MN868936
A. pseudosinensis	**SAUCC 0221**	**Leaf of bamboo**	**China**	**OP563377**	**OP572426**	**OP573266**	**OP573272**
	SAUCC 0222	**Leaf of bamboo**	**China**	**OP563376**	**OP572425**	**OP573265**	**OP573271**
A. pseudospegazzinii	CBS 102052 (Type)	*Macaranga hullettii* stem colonized by ants	Malaysia	KF144911	KF144958	KF145045	KF145002
A. pterosperma	CPC 20193 (Type)	*Lepidosperma gladiatum*	Australia	KF144913	KF144960	KF145046	KF145004
A. pusillisperma	KUC21321 (Type)	Seaweed	Korea	MH498533	MH498453	MN868930	MH498491
A. qinlingensis	CFCC 52303 (Type)	*Fargesia qinlingensis*	China	MH197120	NA	MH236795	MH236791
A. rasikravindrae	LC5449	Soil in karst cave	China	KY494713	KY494789	KY705112	KY705182
A. sacchari	CBS 212.30	*Phragmites australis*	UK	KF144916	KF144962	KF145047	KF145005
A. saccharicola	CBS191.73	Air	Netherlands	KF144920	KF144966	KF145051	KF145009
A. sargassi	KUC21228 (Type)	*Sargassum fulvellum*	Korea	KT207746	KT207696	MH544677	KT207644
A. sasae	CBS 146808 (Type)	Dead culms of *Sasa veitchii*	Netherlands	MW883402	MW883797	MW890104	MW890120
A. septata	CGMCC 3.20134 (Type)	Bamboo	China	MW481711	MW478890	MW522943	MW522960
A. serenensis	IMI 326869 (Type)	Food, pharmaceutical excipients, atmosphere and home dust	Spain	AB220250	AB220344	NA	AB220297
A. setariae	CFCC 54041 (Type)	Decaying culms of *Setaria viridis*	China	MT492004	NA	NA	NA
A. sichuanensis	HKAS 107008 (Type)	Dead culms of Poaceae	China	MW240648	MW240578	MW759536	MW775605
A. sorghi	URM 93000 (Type)	*Sorghum bicolor*	Brazil	MK371706	NA	NA	MK348526
A. sphaerosperma	CBS114314	Leaf of *Hordeum vulgare*	Iran	KF144904	KF144951	KF145038	KF144996
A. stipae	CBS 146804 (Type)	Dead culm of *Stipa gigantea*	Spain	MW883403	MW883798	MW890082	MW890121
A. subglobosa	MFLUCC 11-0397 (Type)	Dead bamboo culms	Thailand	KR069112	KR069113	NA	NA
A. subrosea	LC7292 (Type)	Leaf of bamboo	China	KY494752	KY494828	KY705148	KY705220
A. thailandica	LC5630	Rotten wood	China	KY494714	KF144970	KY705113	KY806200
A. vietnamensis	IMI 99670 (Type)	*Citrus sinensis*	Vietnam	KX986096	KX986111	NA	KY019466
A. xenocordella	CBS 478.86 (Type)	Soil from roadway	Zimbabwe	KF144925	KF144970	KF145055	KF145013
A. yunnana	MFLUCC 15-0002 (Type)	Decaying bamboo culms	China	KU940147	KU863135	NA	NA
Arthrinium caricicola	CBS 145127	*Carex ericetorum*	China	MK014871	MK014838	MK017948	MK017977

Notes: Strains in this study are marked in bold. NA = not available.

Phylogenetic analyses

Newly generated ITS, LSU, *tef1* and *tub2* sequences from the six strains studied were aligned with all reference sequences of *Apiospora* and related species available in GenBank using the MAFFT v.7.11 online software (http://mafft.cbrc.jp/alignment/server/, Katoh et al. 2019) with the default settings, manually correcting the resulting alignment where necessary. Maximum likelihood (ML) and Bayesian inference (BI) phylogenetic analyses were conducted individually on each locus (ITS, LSU, *tef1* and *tub2*) and on a combined dataset including all of them. The best-fitting evolutionary model of each partition was determined using MrModeltest v. 2.3 (Nylander 2004). ML and BI were run on the CIPRES Science Gateway portal (https://www.phylo.org/) using RaxML-HPC2 on XSEDE (8.2.12) (Miller et al. 2012; Stamatakis 2014) and MrBayes on XSEDE (3.2.7a), respectively (Huelsenbeck and Ronquist 2001; Ronquist and Huelsenbeck 2003; Ronquist et al. 2012). For ML analyses the default parameters were used, while BI was carried out using a Markov chain Monte Carlo (MCMC) algorithm. BI analyses included four MCMC chains and were run for 5,000,000 generations until the average standard deviation of split frequencies was below 0.01 with trees saved every 1000 generations. The burn-in fraction was set to 0.25 and posterior probabilities (PP) were determined from the remaining trees. The resulting 50% majority-rule tree was plotted using FigTree v. 1.4.4 (http://tree.bio.ed.ac.uk/software/figtree) and edited with Adobe Illustrator CS6.0.

Results

Phylogenetic analyses

Among the six strains of *Apiospora* isolated from the samples studied, two new species were discovered, and another one found for the first time in China after the combined analysis of ITS, LSU, *tef1* and *tub2* DNA sequences from 89 isolates of *Apiospora* plus *Arthrinium caricicola* Kunze & J.C. Schmidt (CBS 145127) as the outgroup taxon.

A total of 2241 characters including gaps were compared in the phylogenetic analysis, viz. ITS: 1–706, LSU: 707–1513, *tef1*: 1514–1932, *tub2*: 1933–2241. Of these characters, 1436 were constant, 271 were variable and parsimony-uninformative, and 534 were parsimony-informative. For the BI and ML analyses, the substitution model GTR+I+G was selected for all partitions.

The BI analysis reached the established convergence after 3935000 generations, resulting in 39351 sampled trees, of which 29514 trees were used to calculate the posterior probabilities. The ML tree topology agreed with that obtained from the BI analysis, and therefore, only one tree (the ML) is presented (Fig. 1). The four strains (SAUCC 0302, SAUCC 0303, SAUCC 1681 and SAUCC 1682) studied in the present work represent two independent clades, interpreted as newly discovered independent species. These are described below and accommodated under the new names *Apiospora dongyingensis* and

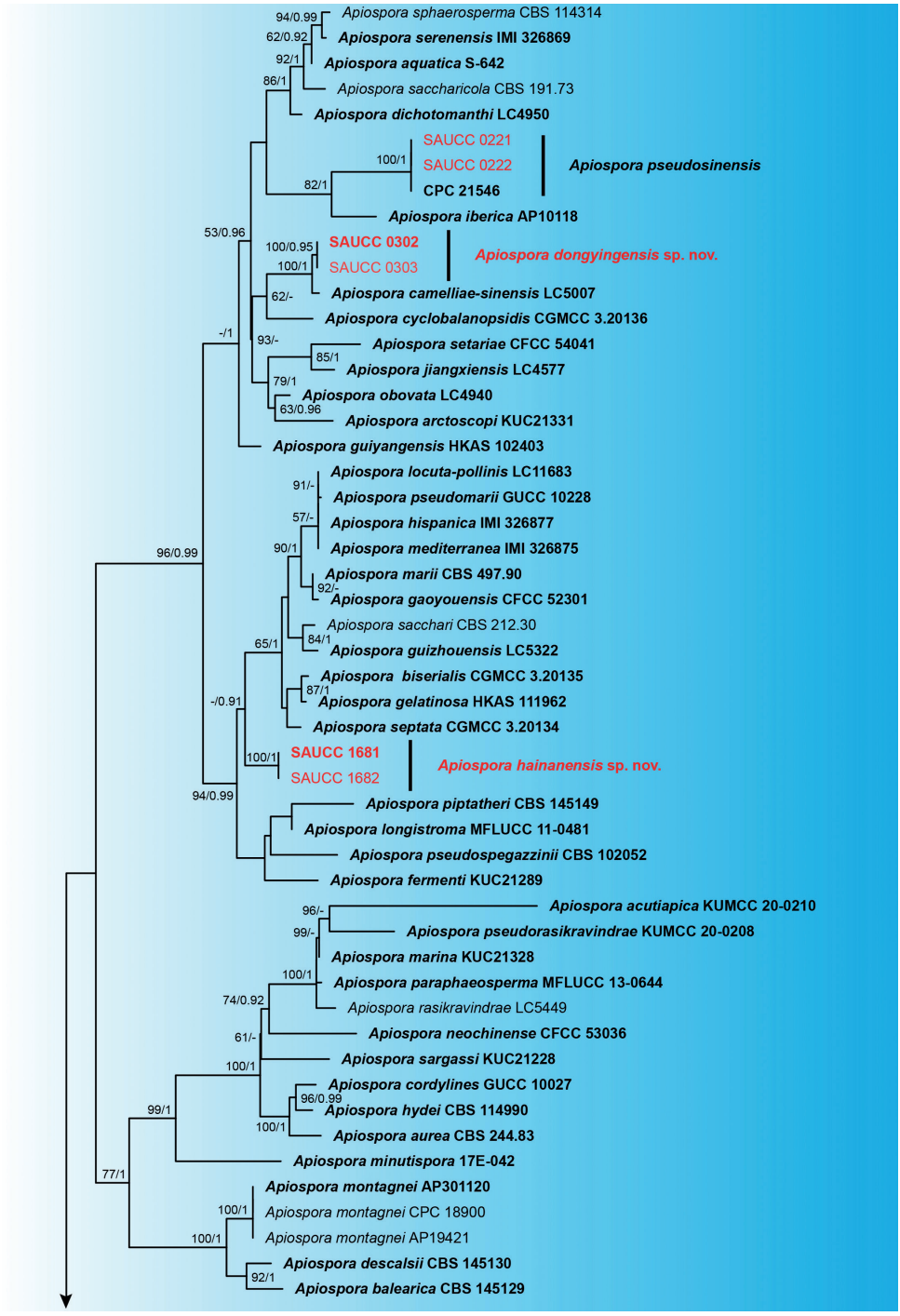

Figure 1. Phylogram of *Apiospora* based on combined ITS, LSU, *tef1* and *tub2* genes. ML bootstrap support values (MLBS ≥ 50%) and Bayesian posterior probability (BYPP ≥ 0.90) are shown as first and second position above nodes, respectively. Strains from this study are shown in red, ex-type or ex-epitype cultures are indicated in bold face. Some branches were shortened according to the indicated mulipliers.

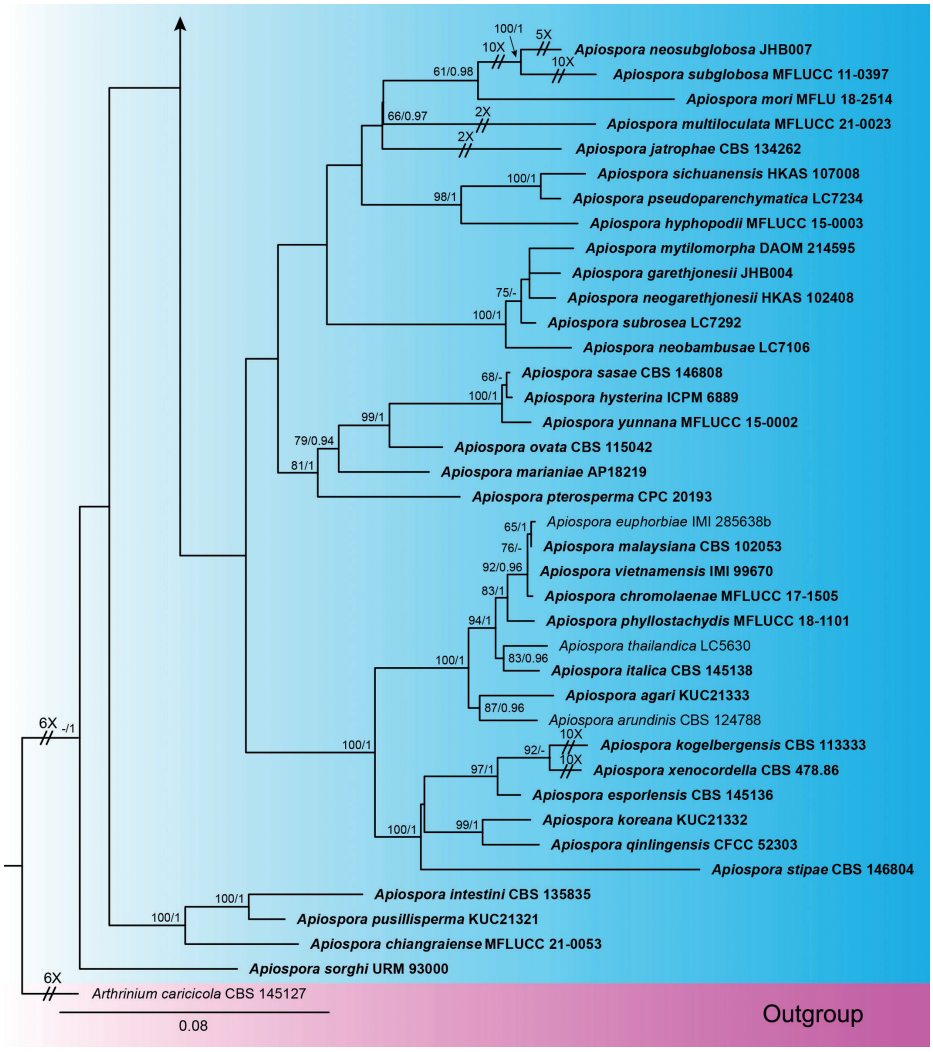

Figure 1. Continued.

A. hainanensis. Another two strains (SAUCC 0221 and SAUCC 0222) clustered with *A. pseudosinensis* (CPC 21546) with full support (MLBS: 100% and BYPP: 1), and are therefore considered no different from this species.

Taxonomy

Apiospora dongyingensis **R.Y. Liu, J.W. Xia & X.G. Zhang, sp. nov.**
MycoBank No: 846065
Fig. 2

Etymology. Named after Dongying City (China) where the type was collected.

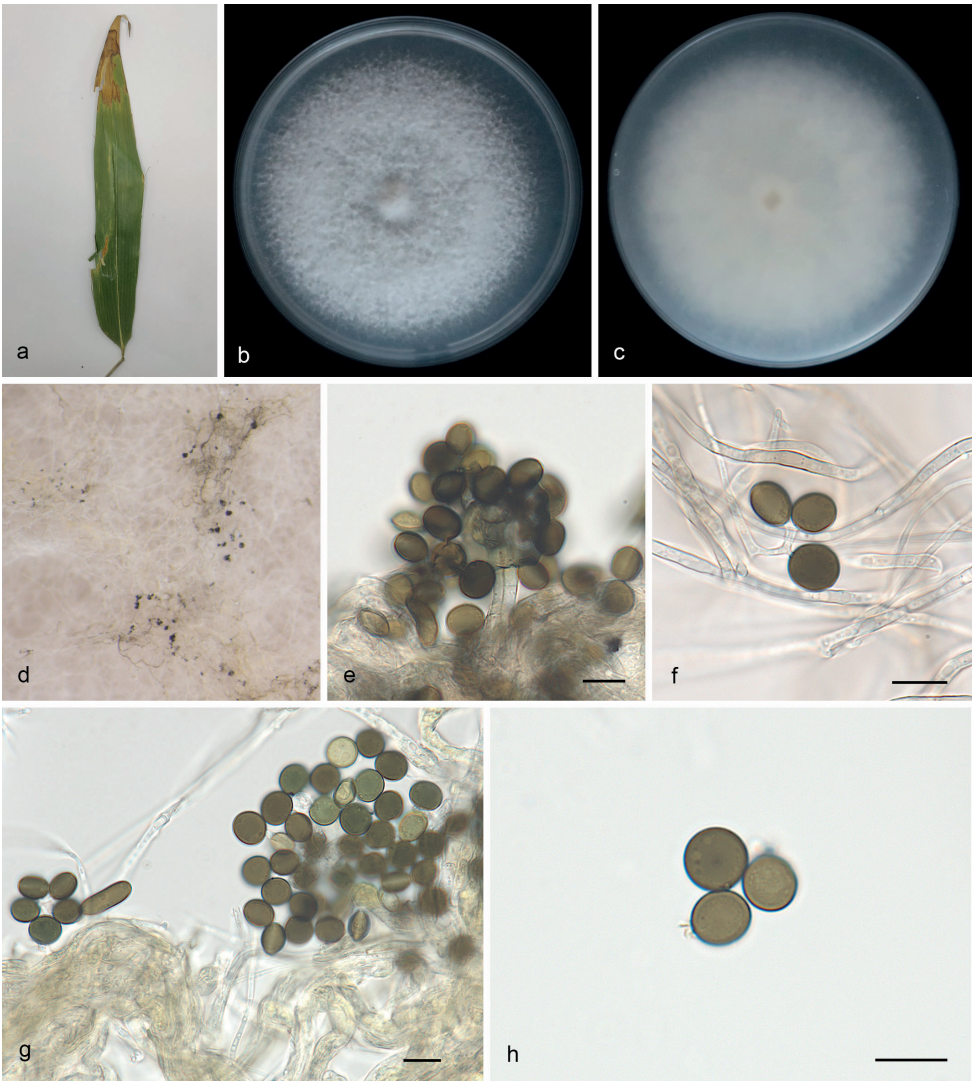

Figure 2. *Apiospora dongyingensis* (SAUCC 0302, ex-holotype culture) **a** leaf of host plant **b, c** surface (**b**) and reverse (**c**) sides of colony after incubation for 7 days on PDA **d** conidiomata formed in culture **e, f** conidiogenous cells and conidia **g, h** conidia. Scale bars: 10 μm (**e–h**).

Type. China, Shandong Province: Dongying Botanical Garden, on diseased leaves of bamboo, 13 July 2022, R.Y. Liu, holotype HSAUP 0302, ex-type living culture SAUCC 0302.

Description. ***Asexual morph*:** On WA, hyphae 1.3–3.6 μm diam., hyaline, branched, septate. Conidiophores cylindrical, septate, verrucose, flexuous, sometimes reduced to conidiogenous cells. Conidiogenous cells globose to subglobose, erect, blastic, aggregated in clusters on hyphae, hyaline to pale brown, smooth, branched, 8.2–13.9 × 4.2–8.2 μm, mean ± SD: 9.6 ± 1.6 × 6.7 ± 1.1 μm (n = 40). Conidia

globose, subglobose to lenticular, with a longitudinal germ slit, occasionally elongated to ellipsoidal, brown to dark brown, smooth to finely roughened, 8.0–16.5 × 5.5–9.0 μm, mean ± SD: 9.4 ± 1.9 × 7.3 ± 1.0 μm, L/W = 1.3–1.9 (n = 40). ***Sexual morph*:** Undetermined.

Culture characteristics. Colonies on PDA flat with entire margin, aerial mycelium white to gray, floccose cottony; surface and reverse gray in the center and grayish margin. PDA attaining 78.5–86.5 mm in diameter after 7 days at 25 °C, growth rate 11.0–12.5 mm/day.

Additional specimen examined. China, Shandong Province: Dongying Botanical Garden, on diseased leaves of bamboo, 13 July 2022, R.Y. Liu, paratype HSAUP 0303, ex-paratype living culture SAUCC 0303.

Notes. *Apiospora dongyingensis* is closely related but phylogenetically distinct from *A. camelliae-sinensis* (M. Wang, F. Liu & L. Cai) Pintos & P. Alvarado and *A. cyclobalanopsidis* (Y. Feng & Jian K. Liu) X.G. Tian & Tibpromma (Fig. 1). *A. dongyingensis* differs from *A. camelliae-sinensis* by 18 nucleotides (13/518 in ITS, 2/804 in LSU, 2/374 in *tef1* and 1/265 in *tub2*) and *A. cyclobalanopsidis* by 58 nucleotides (17/518 in ITS, 4/799 in LSU, 26/377 in *tef1* and 11/266 in *tub2*). Morphologically, it differs from *A. camelliae-sinensis* and *A. cyclobalanopsidis* in its conidia (globose, subglobose to lenticular, 8.0–16.5 × 5.5–9.0 μm in *A. dongyingensis* vs. globose to subglobose, 9.0–13.5 × 7.0–12.0 μm in *A. camelliae-sinensis* and surface view globose to ellipsoid, 8–12 μm long and side view lenticular, 10–14 μm long in *A. cyclobalanopsidis*; Wang et al. 2018; Feng et al. 2021; Pintos and Alvarado 2021; Tian et al. 2021).

***Apiospora hainanensis* R.Y. Liu, J.W. Xia & X.G. Zhang, sp. nov.**
MycoBank No: 846066
Fig. 3

Etymology. Named after Hainan Province (China) where the type was collected.

Type. China, Hainan Province: Diaoluoshan National Nature Reserve, on diseased leaves of bamboo, 23 June 2021, R.Y. Liu, holotype HSAUP 1681, ex-type living culture SAUCC 1681.

Description. *Asexual morph*: On WA, hyphae 1.2–3.4 μm diam., hyaline, branched, septate. Conidiophores cylindrical, septate, verrucose, flexuous, sometimes reduced to conidiogenous cells. Conidiogenous cells globose to subglobose, erect, blastic, aggregated in clusters on hyphae, hyaline to pale brown, smooth, branched, 6.4–8.8 × 5.2–7.1 μm, mean ± SD: 7.9 ± 1.1 × 6.1 ± 0.9 μm (n = 40). Conidia globose, subglobose to lenticular, with a longitudinal germ slit, occasionally elongated to ellipsoidal, brown to dark brown, smooth to finely roughened, 5.5–8.5 × 5.0–7.5 μm, mean ± SD: 6.8 ± 0.9 × 6.7 ± 0.7 μm, L/W = 1.0–1.1 (n = 40). ***Sexual morph*:** Undetermined.

Culture characteristics. Colonies on PDA flat with entire margin, aerial mycelium white to grey, floccose cottony; reverse white to pale honey colored. PDA attaining 77.5–85.5 mm in diameter after 7 days at 25 °C, growth rate 10.5–12.5 mm/day.

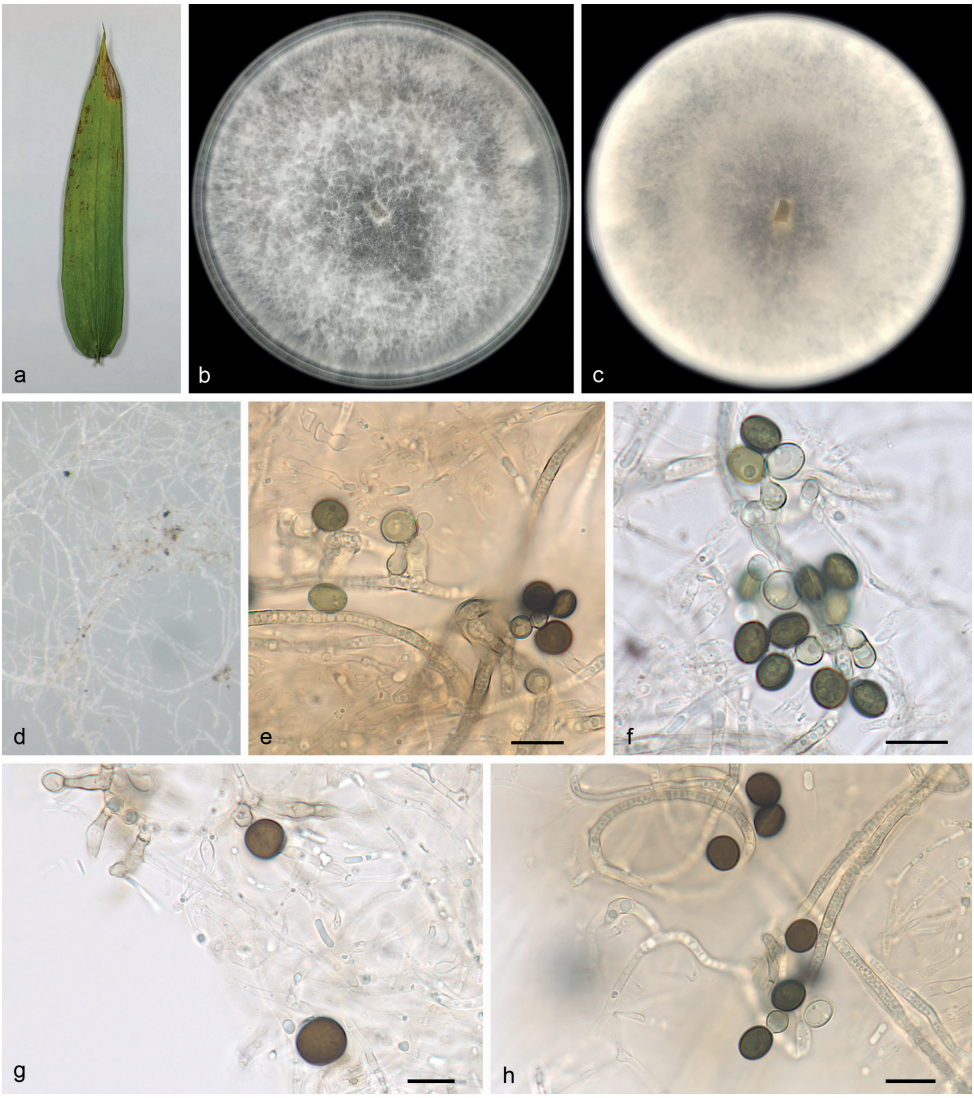

Figure 3. *Apiospora hainanensis* (SAUCC 1681, ex-holotype culture) **a** leaf of host plant **b, c** surface (**b**) and reverse (**c**) sides of colony after incubation for 7 days on PDA **d** conidiomata formed in culture **e, f** conidiogenous cells and conidia **g, h** conidia. Scale bars: 10 μm (**e–h**).

Additional specimen examined. China, Hainan Province: Diaoluoshan National Nature Reserve, on diseased leaves of bamboo, 23 June 2021, R.Y. Liu, paratype HSAUP 1682, ex-paratype living culture SAUCC 1682.

Notes. The two strains (SAUCC 1681 and SAUCC 1682) of *A. hainanensis* clustered together with significant support in an isolated branch basal to *A. sacchari* and related species of the phaeospermum clade (Pintos and Alvarado 2022; Fig. 1). Other species in a more or less similar phylogenetic position include *A. septata* (Y. Feng & Jian K. Liu) X.G. Tian & Tibpromma, *A. piptatheri* (Pintos & P. Alvarado)

Pintos & P. Alvarado, *A. longistroma* (D.Q. Dai & K.D. Hyde) Pintos & P. Alvarado, *A. pseudospegazzinii* (Crous) Pintos & Alvarado and *A. fermenti* (S.L. Kwon, S. Jang & J.J. Kim) S.L. Kwon & J.J. Kim. Morphologically, it differs from *A. septata*, *A. piptatheri*, *A. longistroma*, *A. pseudospegazzinii* and *A. fermenti* in its conidia (globose, subglobose to lenticular, 5.5–8.5 × 5.0–7.5 μm in *A. hainanensis* vs. surface view globose to ellipsoid, 8–13 μm long and side view lenticular, 8–14 μm long in *A. septata*, globose to ellipsoidal, 6–8 × 3–5 μm in *A. piptatheri*, asexual morph undetermined in *A. longistroma*, surface view globose, 7–9 μm diam. and side view lenticular, 5–6 μm diam. in *A. pseudospegazzinii*, surface view globose to elongate ellipsoid, 7.5–9 × 7–9 μm and side view lenticular, 6–7 μm diam. in *A. fermenti*; Crous and Groenewald 2013; Dai et al. 2016; Pintos et al. 2019; Feng et al. 2021; Kwon et al. 2021, 2022; Pintos and Alvarado 2021; Tian et al. 2021).

Apiospora pseudosinensis **(Crous) Pintos & P. Alvarado, Fungal Systematics and Evolution 7: 207. (2021)**
Fig. 4

≡ *Arthrinium pseudosinense* Crous, in Crous & Groenewald, IMA Fungus 4(1): 148 (2013).

Description. ***Asexual morph*****:** On WA, hyphae 1.1–2.9 μm diam., hyaline, branched, septate. Conidiophores cylindrical, septate, verrucose, flexuous, sometimes reduced to conidiogenous cells. Conidiogenous cells globose to subglobose, erect, blastic, aggregated in clusters on hyphae, hyaline to pale brown, smooth, branched, 9.4–11.0 × 6.1–8.8 μm, mean ± SD: 10.4 ± 0.7 × 7.7 ± 1.1 μm (n = 40). Conidia globose, subglobose to lenticular, with a longitudinal germ slit, occasionally elongated to ellipsoidal, brown to dark brown, smooth to finely roughened, 7.5–11.5 × 7.0–9.5 μm, mean ± SD: 10.1 ± 1.3 × 8.3 ± 0.6 μm, L/W = 1.1–1.3 (n = 40). ***Sexual morph*****:** Undetermined.

Culture characteristics. Colonies on PDA flat with irregular margin, aerial mycelium white to pale yellow, floccose cottony; reverse pale yellow to yellow. PDA attaining 69.5–78.5 mm in diameter after 7 days at 25 °C, growth rate 9.5–11.5 mm/day.

Specimens examined. China, Shandong Province: Dongying Botanical Garden, on diseased leaves of bamboo, 15 July 2022, R.Y. Liu, HSAUP 0221, living culture SAUCC 0221; China, Hainan Province: Diaoluoshan National Nature Reserve, on diseased leaves of bamboo, 29 June 2021, R.Y. Liu, HSAUP 0022, living culture SAUCC 0022.

Notes. *Apiospora pseudosinensis* was originally described from bamboo leaves collected in the Utrecht Botanical Garden of the Netherlands (Crous and Groenewald 2013; Pintos and Alvarado 2021). In the present study, DNA sequences obtained from two strains (SAUCC 0221 and SAUCC 0222) collected also from bamboo leaves, were not significantly different from those of *A. pseudosinensis* (Fig. 1). Morphologically, our strains were similar to the original description (conidia 8–10 × 7–10 μm diam. in surface view, 7–8 μm diam. in side view). We therefore consider the newly found strains as *A. pseudosinensis* (Crous and Groenewald 2013; Pintos and Alvarado 2021).

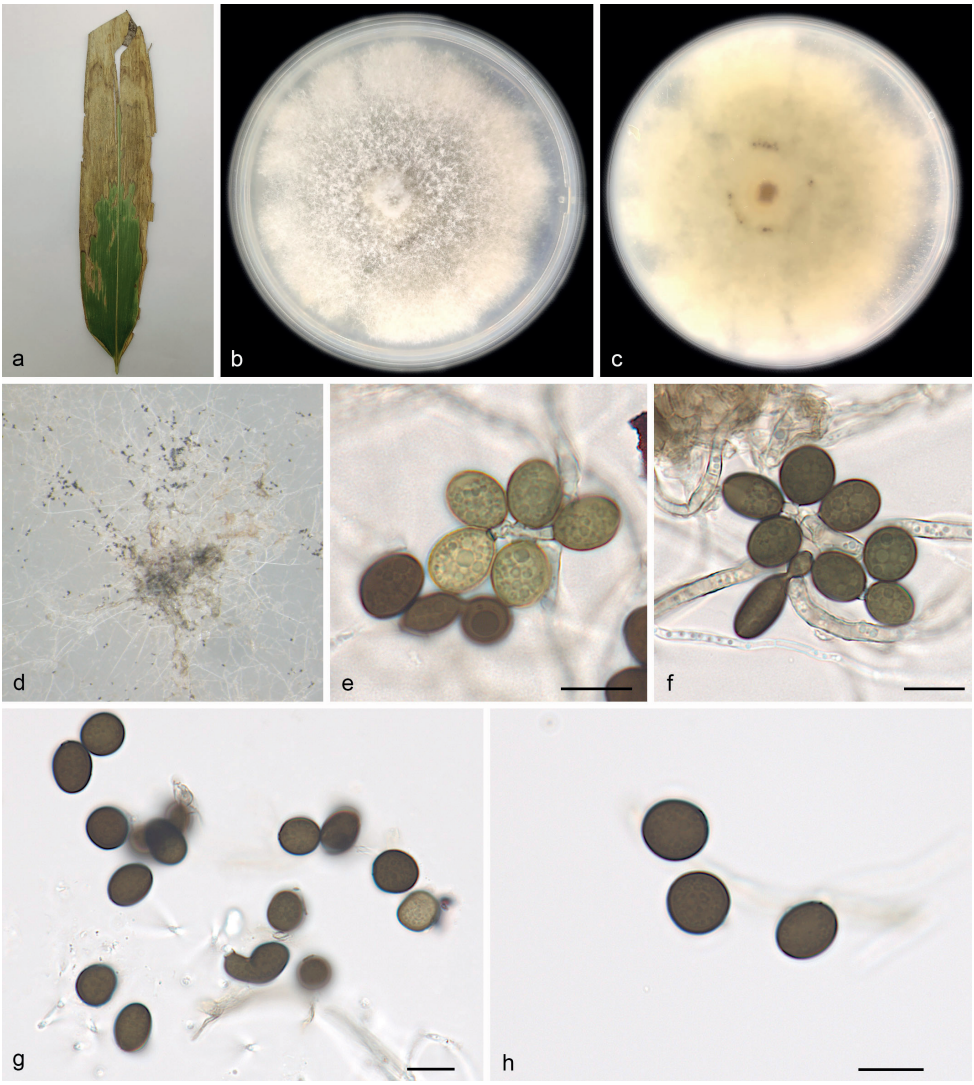

Figure 4. *Apiospora pseudosinensis* (SAUCC 0221) **a** leaf of host plant **b, c** surface (**b**) and reverse (**c**) sides of colony after incubation for 7 days on PDA **d** conidiomata formed in culture **e, f** conidiogenous cells and conidia **g, h** conidia. Scale bars: 10 μm (**e–h**).

Discussion

The family Apiosporaceae was proposed to accommodate genera with apiosporous hyaline ascospores and a basauxic, *Arthrinium*-like conidiogenesis (Hyde et al. 1998). Crous and Groenewald (2013) synonymized *Apiospora* with *Arthrinium* on the basis of the one fungus-one name policy (Hawksworth et al. 2011). Crous and Groenewald (2013) also resolved the genetic identity of multiple species of *Arthrinium*

(= *Apiospora*), analysing ex-type collections, and confirmed that most species occur in Poaceae (R.Br.) Barnh. hosts, although some were known from many other plant host families. However, with the aid of additional genetic data from the type species of *Arthrinium*, *Ar. caricicola*, *Apiospora* and *Arthrinium* were separated again as two distinct genera (Pintos and Alvarado 2021). *Arthrinium* species have variously shaped conidia and inhabit Cyperaceae and Juncaceae in temperate, cold or alpine habitats. Most *Apiospora* species have rounded/lenticular conidia and inhabit mainly Poaceae (and many other host plant families) in a wide range of habitats, including tropical and subtropical regions (Pintos and Alvarado 2021; Samarakoon et al. 2022). An epitype for the type species of *Apiospora*, *A. montagnei*, was recently proposed by Pintos and Alvarado (2022).

There are many *Apiospora* species found on bamboos across the world (Table 2). Bamboos (Poaceae) are distributed in tropical and subtropical to mild temperate regions, with the heaviest concentration and largest number of species in China. Due to their abundance and economic importance, it is of great significance to study and identify the fungi growing on bamboo (Feng et al. 2021). In the present study, two new species (*Apiospora dongyingensis* and *A. hainanensis*) are introduced, and another one (*A. pseudosinensis*) is reported for the first time in China. All of them were collected from bamboo leaves and described based on their phylogenetic data and morphological characters. The descriptions and molecular data for species of *Apiospora* represent an important resource for understanding the diversity of bamboo fungi.

Acknowledgements

This work was supported by the National Natural Science Foundation of China (no. 31900014, U2002203 and 31750001).

References

Agut M, Calvo MA (2004) In vitro conidial germination in *Arthrinium aureum* and *Arthrinium phaeospermum*. Mycopathologia 157(4): 363–367. https://doi.org/10.1023/B:MYCO.0000030432.08860.f3

Carbone I, Kohn LM (1999) A method for designing primer sets for speciation studies in filamentous ascomycetes. Mycologia 91(3): 553–556. https://doi.org/10.1080/00275514.1999.12061051

Chen K, Wu XQ, Huang MX, Han YY (2014) First report of brown culm streak of *Phyllostachys praecox* caused by *Arthrinium arundinis* in Nanjing, China. Plant Disease 98(9): e1274. https://doi.org/10.1094/PDIS-02-14-0165-PDN

Chomnunti P, Hongsanan S, Aguirre-Hudson B, Tian Q, Peršoh D, Dhami MK, Alias AS, Xu J, Liu X, Stadler M, Hyde KD (2014) The sooty moulds. Fungal Diversity 66(1): 1–36. https://doi.org/10.1007/s13225-014-0278-5

Crous PW, Groenewald JZ (2013) A phylogenetic re-evaluation of *Arthrinium*. IMA Fungus 4(1): 133–154. https://doi.org/10.5598/imafungus.2013.04.01.13

Cubeta MA, Echandi E, Abernethy T, Vilgalys R (1991) Characterization of anastomosis groups of binucleate *Rhizoctonia* species using restriction analysis of an amplified ribosomal RNA gene. Phytopathology 81(11): 1395–1400. https://doi.org/10.1094/Phyto-81-1395

Dai DQ, Jiang HB, Tang LZ, Bhat DJ (2016) Two new species of *Arthrinium* (Apiosporaceae, Xylariales) associated with bamboo from Yunnan, China. Mycosphere 7(9): 1332–1345. https://doi.org/10.5943/mycosphere/7/9/7

Dai DQ, Phookamsak R, Wijayawardene NN, Li WJ, Bhat DJ, Xu JC, Taylor JE, Hyde KD, Chukeatirote E (2017) Bambusicolous fungi. Fungal Diversity 82(1): 1–105. https://doi.org/10.1007/s13225-016-0367-8

Feng Y, Liu JK, Lin CG, Chen YY, Xiang MM, Liu ZY (2021) Additions to the Genus *Arthrinium* (Apiosporaceae) From Bamboos in China. Frontiers in Microbiology 12: e661281. https://doi.org/10.3389/fmicb.2021.661281

Glass NL, Donaldson GC (1995) Development of primer sets designed for use with the PCR to amplify conserved genes from filamentous ascomycetes. Applied and Environmental Microbiology 61(4): 1323–1330. https://doi.org/10.1128/aem.61.4.1323-1330.1995

Guo LD, Hyde KD, Liew ECY (2000) Identification of endophytic fungi from *Livistona chinensis* based on morphology and rDNA sequences. The New Phytologist 147(3): 617–630. https://doi.org/10.1046/j.1469-8137.2000.00716.x

Hawksworth DL, Crous PW, Redhead SA, Reynolds DR, Samson RA, Seifert KA, Taylor JW, Wingfield MJ, Abaci Ö, Aime C, Asan A, Bai F-Y, de Beer ZW, Begerow D, Berikten D, Boekhout T, Buchanan PK, Burgess T, Buzina W, Cai L, Cannon PF, Crane JL, Damm U, Daniel H-M, van Diepeningen AD, Druzhinina I, Dyer PS, Eberhardt U, Fell JW, Frisvad JC, Geiser DM, Geml J, Glienke C, Gräfenhan T, Groenewald JZ, Groenewald M, de Gruyter J, Guého-Kellermann E, Guo L-D, Hibbett DS, Hong S-B, de Hoog GS, Houbraken J, Huhndorf SM, Hyde KD, Ismail A, Johnston PR, Kadaifciler DG, Kirk PM, Kõljalg U, Kurtzman CP, Lagneau P-E, Lévesque CA, Liu X, Lombard L, Meyer W, Miller A, Minter DW, Najafzadeh MJ, Norvell L, Ozerskaya SM, Öziç R, Pennycook SR, Peterson SW, Pettersson OV, Quaedvlieg W, Robert VA, Ruibal C, Schnürer J, Schroers H-J, Shivas R, Slippers B, Spierenburg H, Takashima M, Taşkoin E, Thines M, Thrane U, Uztan AH, van Raak M, Varga J, Vasco A, Verkley G, Videira SIR, de Vries RP, Weir BS, Yilmaz N, Yurkov A, Zhang N (2011) The Amsterdam declaration on fungal nomenclature. IMA Fungus 2(1): 105–112. https://doi.org/10.5598/imafungus.2011.02.01.14

Huelsenbeck JP, Ronquist F (2001) MRBAYES: Bayesian inference of phylogeny. Bioinformatics 17(17): 754–755. https://doi.org/10.1093/bioinformatics/17.8.754

Hyde K, Fröhlich J, Taylor J (1998) Fungi from palms. XXXVI. Reflections on unitunicate ascomycetes with apiospores. Sydowia 50: 21–80.

Hyde K, Norphanphoun C, Maharachchikumbura S, Bhat D, Jones E, Bundhun D, Chen Y, Bao D, Boonmee S, Calabon M (2020) Refined families of Sordariomycetes. Mycosphere 11(1): 305–1059. https://doi.org/10.5943/mycosphere/11/1/7

Jiang N, Fan XL, Tian CM (2021) Identification and characterization of leaf-inhabiting fungi from *Castanea* plantations in China. Journal of Fungi 7(1): e64. https://doi.org/10.3390/jof7010064

Jiang N, Voglmayr H, Ma CY, Xue H, Piao CG, Li Y (2022a) A new *Arthrinium*-like genus of Amphisphaeriales in China. MycoKeys 92: 27–43. https://doi.org/10.3897/mycokeys.92.86521

Jiang N, Voglmayr H, Xue H, Piao CG, Li Y (2022b) Morphology and Phylogeny of *Pestalotiopsis* (Sporocadaceae, Amphisphaeriales) from Fagaceae Leaves in China. Microbiology Spectrum 10(6): 03272–22. https://doi.org/10.1128/spectrum.03272-22

Katoh K, Rozewicki J, Yamada KD (2019) MAFFT online service: Multiple sequence alignment,interactive sequence choice and visualization. Briefings in Bioinformatics 20(4): 1160–1166. https://doi.org/10.1093/bib/bbx108

Kumar S, Stecher G, Tamura K (2016) MEGA7: Molecular Evolutionary Genetics Analysis Version 7.0 for bigger datasets. Molecular Biology and Evolution 33(7): 1870–1874. https://doi.org/10.1093/molbev/msw054

Kunze G (1817) Zehn neue Pilzgattungen. Mykol (1): 1–18.

Kwon SL, Park MS, Jang S, Lee YM, Heo YM, Hong JH, Lee H, Jang Y, Park JH, Kim C, Kim GH, Lim YW, Kim JJ (2021) The genus *Arthrinium* (Ascomycota, Sordariomycetes, Apiosporaceae) from marine habitats from Korea, with eight new species. IMA Fungus 12(1): 1–26. https://doi.org/10.1186/s43008-021-00065-z

Kwon SL, Cho M, Lee YM, Kim C, Lee SM, Ahn BJ, Lee H, Kim JJ (2022) Two unrecorded *Apiospora* species isolated from marine substrates in Korea with eight new combinations (*A. piptatheri* and *A. rasikravindrae*). Mycobiology 50(1): 46–54. https://doi.org/10.1080/12298093.2022.2038857

Martínez-Cano C, Grey WE, Sands DC (1992) First report of *Arthrinium arundinis* causing kernel blight on barley. Plant Disease 76(10): e1077. https://doi.org/10.1094/PD-76-1077B

Mavragani DC, Abdellatif L, McConkey B, Hamel C, Vujanovic V (2007) First report of damping-off of durum wheat caused by *Arthrinium sacchari* in the semi-arid Saskatchewan fields. Plant Disease 91(4): e469. https://doi.org/10.1094/PDIS-91-4-0469A

Miller MA, Pfeiffer W, Schwartz T (2012) The CIPRES science gateway: enabling high-impact science for phylogenetics researchers with limited resources. Proceedings of the 1st Conference of the Extreme Science and Engineering Discovery Environment. Bridging from the extreme to the campus and beyond. Association for Computing Machinery 39: 1–8. https://doi.org/10.1145/2335755.2335836

Mu TC, Zhang ZX, Liu RY, Liu SB, Li Z, Zhang XG, Xia JW (2021) Morphological and molecular phylogenetic analyses reveal three species of *Colletotrichum* in Shandong province, China. MycoKeys 85: 57–71. https://doi.org/10.3897/mycokeys.85.75944

Nylander JAA (2004) MrModeltest v. 2. Program distributed by the author. Evolutionary Biology Centre, Uppsala University.

O'Donnell K, Kistler HC, Cigelnik E, Ploetz RC (1998) Multiple evolutionary origins of the fungus causing panama disease of banana: Concordant evidence from nuclear and mito-

chondrial gene genealogies. Proceedings of the National Academy of Sciences of the United States of America 95(5): 2044–2049. https://doi.org/10.1073/pnas.95.5.2044

Pintos Á, Alvarado P (2021) Phylogenetic delimitation of *Apiospora* and *Arthrinium*. Fungal Systematics and Evolution 7(1): 197–221. https://doi.org/10.3114/fuse.2021.07.10

Pintos Á, Alvarado P (2022) New studies on *Apiospora* (Amphisphaeriales, Apiosporaceae): Epitypification of *Sphaeria apiospora*, proposal of *Ap. marianiae* sp. nov. and description of the asexual morph of *Ap. sichuanensis*. MycoKeys 92: 63–78. https://doi.org/10.3897/mycokeys.92.87593

Pintos Á, Alvarado P, Planas J, Jarling R (2019) Six new species of *Arthrinium* from Europe and notes about *A. caricicola* and other species found in *Carex* spp. hosts. MycoKeys 49: 15–48. https://doi.org/10.3897/mycokeys.49.32115

Ramos HP, Braun GH, Pupo MT, Said S (2010) Antimicrobial activity from endophytic fungi *Arthrinium* state of *Apiospora montagnei* Sacc. and *Papulaspora immersa.* Brazilian Archives of Biology and Technology 53(3): 629–632. https://doi.org/10.1590/S1516-89132010000300017

Rayner RW (1970) A Mycological Colour Chart. CMI and British Mycological Society, Kew.

Ronquist F, Huelsenbeck JP (2003) MrBayes 3: Bayesian phylogenetic inference under mixed models. Bioinformatics 19(12): 1572–1574. https://doi.org/10.1093/bioinformatics/btg180

Ronquist F, Teslenko M, van der Mark P, Ayres DL, Darling A, Hohna S, Larget B, Liu L, Suchard MA, Huelsenbeck JP (2012) MrBayes 3.2: Efficient Bayesian phylogenetic inference and model choice across a large model space. Systematic Biology 61(3): 539–542. https://doi.org/10.1093/sysbio/sys029

Saccardo P (1875) Conspectus generum pyrenomycetum italicorum additis speciebus fungorum Venetorum novis vel criticis, systemate carpologico dispositorum. Atti della Società Veneto-Trentina di Scienze Naturali 4: 77–100.

Samarakoon MC, Hyde KD, Maharachchikumbura SS, Stadler M, Gareth Jones EB, Promputtha I, Suwannarach N, Camporesi E, Bulgakov TS, Liu JK (2022) Taxonomy, phylogeny, molecular dating and ancestral state reconstruction of Xylariomycetidae (Sordariomycetes). Fungal Diversity 112(1): 1–88. https://doi.org/10.1007/s13225-021-00495-5

Stamatakis A (2014) RAxML version 8: A tool for phylogenetic analysis and post-analysis of large phylogenies. Bioinformatics 30(9): 1312–1313. https://doi.org/10.1093/bioinformatics/btu033

Tian X, Karunarathna SC, Mapook A, Promputtha I, Xu J, Bao D, Tibpromma S (2021) One new species and two new host records of *Apiospora* from bamboo and maize in northern Thailand with thirteen new combinations. Life 11(10): e1071. https://doi.org/10.3390/life11101071

Vilgalys R, Hester M (1990) Rapid genetic identification and mapping of enzymatically amplified ribosomal DNA from several *Cryptococcus* species. Journal of Bacteriology 172(8): 4238–4246. https://doi.org/10.1128/jb.172.8.4238-4246.1990

Wang M, Tan XM, Liu F, Cai L (2018) Eight new *Arthrinium* species from China. MycoKeys 1: 1–24. https://doi.org/10.3897/mycokeys.39.27014

White TJ, Bruns T, Lee S, Taylor J (1990) Amplification and direct sequencing of fungal ribosomal RNA genes for phylogenetics. PCR Protocols: A Guide to Methods and Applications 18: 315–322. https://doi.org/10.1016/B978-0-12-372180-8.50042-1

Supplementary material 1

Morphological and phylogenetic analyses reveal two new species and a new record of *Apiospora* (Amphisphaeriales, Apiosporaceae) in China

Authors: Rongyu Liu, Duhua Li, Zhaoxue Zhang, Shubin Liu, Xinye Liu, Yixin Wang, Heng Zhao, Xiaoyong Liu, Xiuguo Zhang, Jiwen Xia, Yujiao Wang

Data type: phylogenetic

Explanation note: The combined ITS, LSU, *tef1* and *tub2* genes.

Link: https://doi.org/10.3897/mycokeys.95.96400.suppl1

MycoKeys 95: 47–60 (2023)
doi: 10.3897/mycokeys.95.97474
https://mycokeys.pensoft.net

RESEARCH ARTICLE

A peer-reviewed open-access journal
MycoKeys
Launched to accelerate biodiversity research

Additions to Thelebolales (Leotiomycetes, Ascomycota): *Pseudogeomyces lindneri* gen. et sp. nov. and *Pseudogymnoascus campensis* sp. nov.

Zhi-Yuan Zhang[1], Yan-Feng Han[2], Wan-Hao Chen[3], Gang Tao[1]

1 *College of Eco-Environmental Engineering, Guizhou Minzu University, Guiyang 550025, China* **2** *Institute of Fungus Resources, College of Life Sciences, Guizhou University, Guiyang 550025, China* **3** *Basic Medical School, Guizhou University of Traditional Chinese Medicine, Guiyang 550025, China*

Corresponding authors: Zhi-Yuan Zhang (zzymetac16@163.com), Gang Tao (ttg729@sina.com)

Academic editor: N. Wijayawardene | Received 12 November 2022 | Accepted 22 January 2023 | Published 6 February 2023

Citation: Zhang Z-Y, Han Y-F, Chen W-H, Tao G (2023) Additions to Thelebolales (Leotiomycetes, Ascomycota): *Pseudogeomyces lindneri* gen. et sp. nov. and *Pseudogymnoascus campensis* sp. nov. MycoKeys 95: 47–60. https://doi.org/10.3897/mycokeys.95.97474

Abstract

Thelebolales are globally distributed fungi with diverse ecological characteristics. The classification of Thelebolales remains controversial to date and this study introduces two new taxa, based on morphological and phylogenetic analyses. The results of phylogenetic analyses indicated that the new taxa formed distinct lineages with strong support that were separated from the other members of Thelebolales. The new taxa described herein did not form sexual structures. The phylogenetic relationships of the new taxa and the morphological differences between these taxa and the other species under Thelebolales are also discussed.

Keywords

Leotiomycetes, taxonomy, Thelebolales, two new taxa

Introduction

Eriksson and Winka (1997) established the class Leotiomycetes to accommodate the inoperculate discomycetes. Members of this class are ecologically diverse and include saprophytic fungi, endophytic fungi, plant and mammalian pathogens, aquatic and aerial fila-

mentous fungi, mycorrhizal fungi, fungal parasites, root symbionts and wood-rotting fungi, of which the lattermost group mostly includes saprophytic fungi that grow on various substrates (Ekanayaka et al. 2019; Johnston et al. 2019). The order Thelebolales comprises important members of Leotiomycetes due to their diverse functions and potential applications (Hassan et al. 2017; Batista et al. 2020). Thelebolales was established by Haeckel in 1894; however, the classification of this order remains controversial to date (Ekanayaka et al. 2019; Johnston et al. 2019; Batista et al. 2020; Quijada et al. 2022). According to Johnston et al. (2019) and Batista et al. (2020), Thelebolales comprises Pseudeurotiaceae and Thelebolaceae. However, Ekanayaka et al. (2019) reported that Pseudeurotiaceae was nested within Thelebolaceae; thus, the former was regarded as a synonym of the latter. Recently, the work of Quijada et al. (2022) showed that Thelebolaceae is monophyletic and valid, whereas Pseudeurotiaceae is polyphyletic and includes multiple clades and established the Holwayaceae (i.e. *Alatospora-Miniancora* clade, Ekanayaka et al. (2019)).

The genus *Pseudogymnoascus* was established by Raillo in 1929; however, a type strain was formally specified during the establishment of the genus. Several years later, Samson (1972) designated *Pseudogymnoascus roseus* Raillo the neotype of *Pseudogymnoascus*, as CBS 395.65 could still be cultivated. At present, the genus *Pseudogymnoascus* comprises 17 valid species (Zhang et al. 2020b; Villanueva et al. 2021; Zhang et al. 2021) belonging to 13 clades (Minnis and Lindner 2013). The genus *Pseudogymnoascus* comprises a diverse group of fungi that are widely distributed on Earth and are highly ecologically diverse.

In this study, two new taxa belonging to the order Thelebolales were isolated in a survey on fungi from urban soil samples in China. This study provides a description, illustrations and a phylogenetic tree for the two new species isolated herein.

Materials and methods

Fungal isolation and morphology

Soil samples were collected from Cengong County (27°16'98"N, 108°81'46"E) in Kaili City, Guizhou Province, China by Zhi-Yuan Zhang in June 2020. The soil samples were collected from a depth of 3–10 cm from the soil surface. The fungi were isolated using the dilution plate method (Li et al. 2022). Briefly, 2 g of each of the collected samples was suspended in 20 ml of sterile water in a 50 ml sterile conical flask. The conical flasks were thoroughly shaken using a Vortex vibration meter. The suspension was then diluted to a concentration of 10^{-4}. Then, 1 ml of the diluted sample was transferred to a sterile Petri dish, following which modified SDA medium (1 g dextrose, 20 g peptone, 20 g agar, and 1 litre ddH_2O) containing 50 mg/l penicillin and 50 mg/l streptomycin was added and mixed. The experiment was performed in three replicates. The plates were incubated at 25 °C for 1–2 weeks and single colonies were selected from the plates and inoculated on to new potato dextrose agar (**PDA**) plates.

The isolates of potentially new species were transferred to a new plate containing PDA, malt extract agar (**MEA**), oatmeal agar (**OA**) and corn meal agar (**CMA**) and incubated in the dark at 25 °C for 14 days. Photomicrographs of the diagnostic structures were prepared using an OLYMPUS BX53 microscope, equipped with differential interference contrast (**DIC**) optics, an OLYMPUS DP73 high-definition colour camera and cellSens software v.1.18. The dry and living cultures were deposited at the Institute of Fungus Resources, Guizhou University, Guiyang City, Guizhou, China (**GZUIFR**).

DNA extraction, PCR amplification and sequencing

The total DNA was extracted using 5% chelex-100 solution. The internal transcribed spacer (**ITS**), nuclear large subunit (**LSU**) rDNA, DNA replication licensing factor (*MCM7*), RNA polymerase II second largest subunit (*RPB2*) and the translation elongation factor EF-1α (*EF1A*) were amplified and sequenced according to the method described by Minnis and Lindner (2013). The sequences of the primers used for amplifying these loci are listed in Suppl. material 1: table S1. The novel sequences identified in this study were deposited in GenBank (Suppl. material 1: table S2).

Phylogenetic analyses

The ITS, LSU, *MCM7*, *RPB2* and *EF1A* sequences were retrieved from GenBank, based on previous studies by Zhang et al. (2020b, 2021) and Villanueva et al. (2021) (Suppl. material 1: table S2). The following two datasets were used in this study: (1) the ITS + LSU dataset was used for inferring the phylogenetic placement of the two novel taxa under the order Thelebolales and (2) the ITS + LSU + *MCM7* + *RPB2* + *EF1A* dataset was used for inferring the phylogenetic placement of the new species.

The TBtools software was used for simplifying the nomenclature and renaming (Chen et al. 2020). A single-locus dataset was aligned and edited using MAFFT v.7.037b (Katoh and Standley 2013) and MEGA v.6.06 (Tamura et al. 2013). The "Concatenate Sequence" function in PhyloSuite v1.16 (Zhang et al. 2020a) was used for concatenating each locus. The best-fit substitution model was selected using the corrected Akaike Information Criterion (AICc) in ModelFinder (Kalyaanamoorthy et al. 2017). The combined loci were analysed using the Bayesian Inference (BI) and Maximum Likelihood (ML) methods. The results of ML analysis were implemented in IQ-TREE v.1.6.11 (Nguyen et al. 2015) with 10^4 bootstrap (BS) tests, using the ultrafast algorithm (Minh et al. 2013). BI analysis was performed with MrBayes v.3.2 (Ronquist et al. 2012) and the Markov Chain Monte Carlo (MCMC) simulations were executed for 10^8 generations with a sampling frequency every 10^3 generations and a burn-in of 25%. All the aforementioned analyses were performed in PhyloSuite v.1.16 (Zhang et al. 2020a).

Results

Phylogenetic analyses

The concatenated alignment of ITS + LSU sequences primarily from the genera under the order Thelebolales comprised 1,209 nucleotides, including inserted gaps (ITS: 433 bp, LSU: 776 bp). The concatenated ITS + LSU + *MCM7* + *RPB2* + *EF1A* dataset from *Pseudogymnoascus* and its related taxa comprised 2,981 nucleotides, including inserted gaps (ITS: 430 bp, LSU: 790 bp, *MCM7*: 475 bp, *RPB2*: 525 bp and *EF1A*: 761 bp). The best-fit evolutionary models obtained by ML and BI analyses of each locus are listed in Suppl. material 1: table S3.

The clades formed by the genera in the first phylogenetic tree (Fig. 1) had a high support rate (*Pseudogymnoascus* (100% BS support [BS]/1 posterior probability [PP]), *Solomyces* (100% BS/1 PP), *Pseudogeomyces* (100% BS/1 PP), *Geomyces* (100% BS/1 PP), *Pseudeurotium* (100% BS/1 PP) and *Zongqia* (100% BS/1 PP)). The unidentified isolate, 12NJ10, formed a single clade (clade N; Minnis and Lindner (2013)) and was separated from the clades formed by the other genera. The new isolates identified in this study were divided into two genera, of which two isolates clustered under the genus *Pseudogymnoascus* and three isolates were clustered under the new genus, *Pseudogeomyces*.

The genera in the second phylogenetic tree (Fig. 2) clustered into monophyletic clades with high support value. The new isolates (ZY 22.003, ZY 22.004 and ZY 22.005) under the new genus, *Pseudogeomyces*, clustered together with the other unidentified four isolates (12NJ08, 17WV09, 23WI14 and 23WI08) in a well-supported clade (100% BS /1 PP) that was separated from the other clades under Thelebolales. The new isolates, ZY 22.001 and ZY 22.002, belonging to the new species, *Pseudogymnoascus campensis*, were clustered into a single clade with high support value (97% BS/0.96 PP) under the genus *Pseudogymnoascus*.

Taxonomy

Pseudogeomyces **Zhi.Y. Zhang & Y.F. Han, gen. nov.**
MycoBank No: 846356

Etymology. Referring to its similarity to *Geomyces*.

Geographical distribution. China and the USA.

Description. ***Saprobic*** on the soil. ***Sexual morph*****:** not observed. ***Asexual morph*****:** ***Hyphae*** branched, septate, smooth. ***Conidiophores*** solitary, rare branches, hyaline, smooth, arising from the erect or geniculated hyphae, usually bearing two to three branches at the tip. ***Conidia*** hyaline, rough, verrucosa, solitary, obovoid, globose to subglobose, borne on hyphae, short protrusions, side branches or in conidiophores separated by connective cells. ***Intercalary conidia*** hyaline, globose to subglobose, fusiform with both truncate. ***Chlamydospores*** not observed.

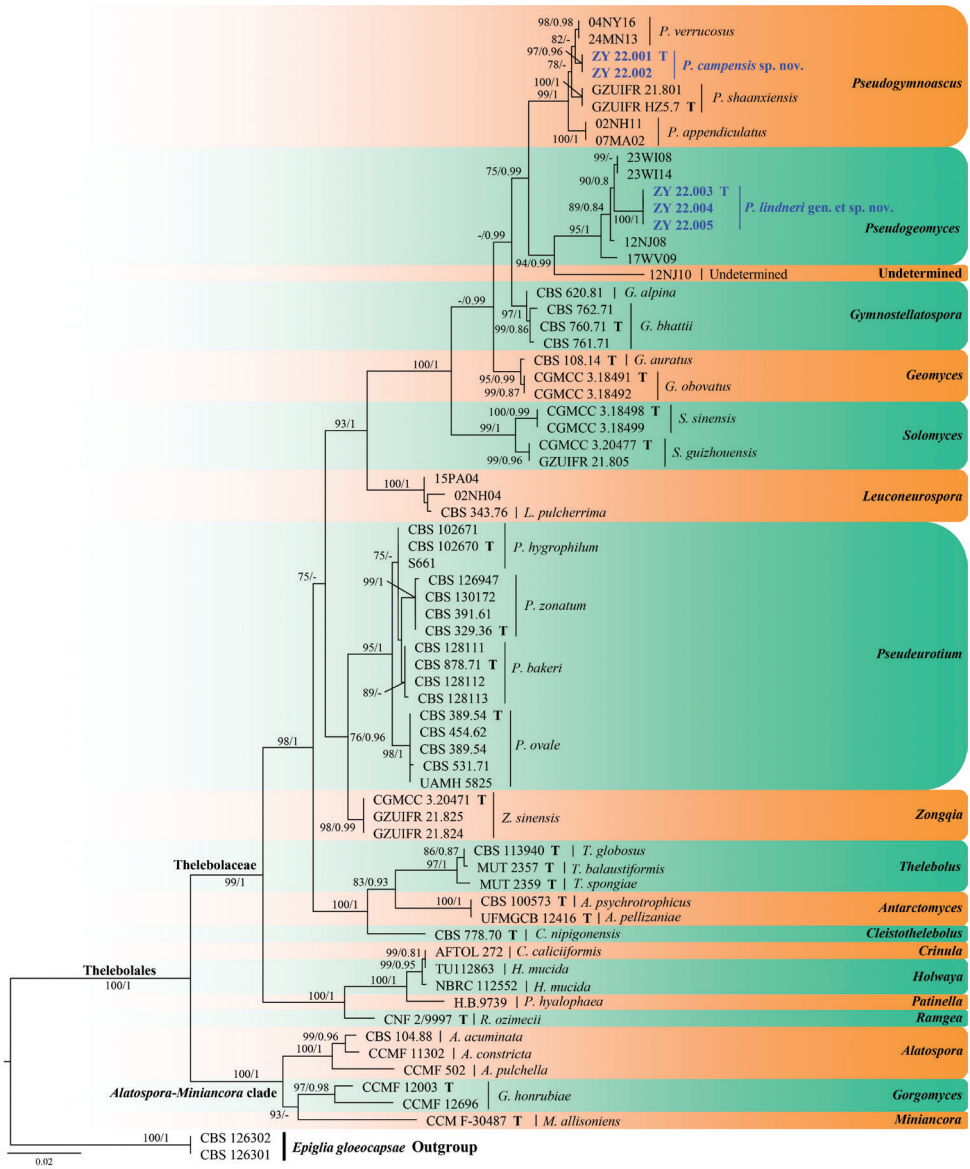

Figure 1. Phylogram generated from a Maximum Likelihood analysis of sequences of Thelebolales, based on ITS and LSU. ML bootstrap values (≥ 75%) and Bayesian posterior probability (≥ 0.75) are indicated along branches (BP/ML). The new taxa are highlighted in bold and blue and "T" indicate ex-type cultures.

Type species. *Pseudogeomyces lindneri* Zhi. Y. Zhang & Y. F. Han.

Notes. *Pseudogeomycesis* is introduced to accommodate *Pseudogeomycesis lindneri* obtained from urban soil in China and the four isolates (12NJ08, 17WV09, 23WI14 and 23WI08) obtained from bat hibernacular soil in New Jersey, West Virginia and Wisconsin, USA (Minnis and Lindner 2013). Unfortunately, these isolates have

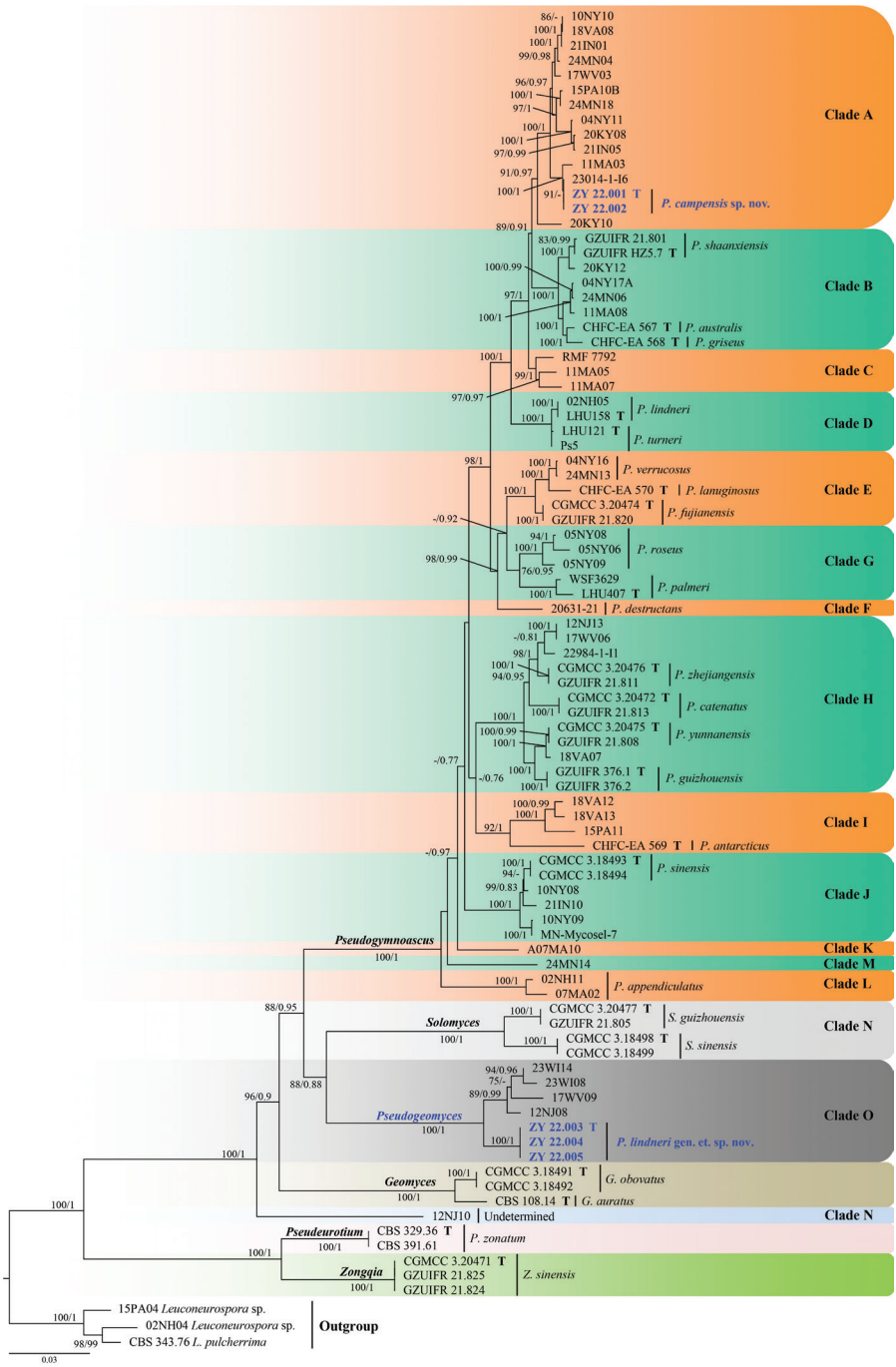

Figure 2. Phylogram generated from A Maximum Likelihood analysis of sequences of Thelebolaceae, based on ITS, LSU, *EF1A*, *RPB2* and *MCM7*. ML bootstrap values (≥ 75%) and Bayesian posterior probability (≥ 0.75) are indicated along branches (BP/ML). Clades are identified using clade nomenclature (A to O) formally defined by Minnis and Lindner (2013). The new taxa are highlighted in bold and blue and "T" indicate ex-type cultures.

not been identified to species to date. Currently, the order Thelebolales consists of 24 genera (Wijayawardene et al. 2017; Ekanayaka et al. 2019; Zhang et al. 2021). The results of phylogenetic analyses (Figs 1, 2) revealed that *Pseudogeomycesis* formed a distinct clade with high support value. However, *Ascophanus*, *Ascozonus*, *Caccobius*, *Coprobolus*, *Leptokalpion*, *Neelakesa* and *Pseudascozonus* are lacking sequence data (Ekanayaka et al. 2019; https://www.ncbi.nlm.nih.gov/, retrieval in Oct 2022); thus, these genera were not included in our phylogenetic analysis. Besides, these genera were reported without asexual morphs (Wijayawardene et al. 2017). Therefore, it was not possible to compare the morphological differences of the newly-established genus, *Pseudogeomycesis* (sexual stage not observed), with the aforementioned genera. However, members of these genera are saprobes (involving dung and wood), terrestrial and widely distributed (Wijayawardene et al. 2017). Of the remaining genera, *Pseudogeomyces* were similar to *Geomyces* and the asexual morphs of *Pseudogymnoascus*. However, *Pseudogeomyces* differed from *Geomyces* and *Pseudogymnoascus* with the presence of two to three irregular branches at the tip of the conidiophores (Kuehn 1958; Van Oorschot 1980).

Pseudogeomyces lindneri **Zhi. Y. Zhang & Y. F. Han, sp. nov.**
MycoBank No: 846365
Fig. 3

Etymology. Named after Daniel Lindner, for acknowledging his contributions to the modern taxonomy of *Pseudogymnoascus* and its related taxa.

Type. Kaili City, Guizhou Province, China 27°16'98"N, 108°81'46"E, isolated from the green belt soil, July 2022, Zhi-Yuan Zhang (holotype ZY H-22.003, ex-type ZY 22.003, *ibid.*, ZY 22.004).

Geographical distribution. Guizhou Province, China.

Description. Culture characteristics (14 days at 25 °C): ***Colonies*** on PDA 15–16 mm in diameter, white to pale pink, raised, fluffy, irregular, producing abundant caesious exudates; reverse: brown to cinnamon. ***Colonies*** on MEA 18–19 mm in diameter, off-white, felty, with radial grooves, nearly round, exudates and diffusible pigments absent; reverse: brown to cinnamon. ***Colonies*** on OA 25–26 mm in diameter, white, aerial mycelia sparse, flat, nearly round, exudates and diffusible pigments absent; reverse: white. ***Colonies*** on CMA 34–35 mm in diameter, white, aerial mycelia sparse, flat, nearly round, margin regular, exudates and diffusible pigments absent; reverse: white.

Hyphae hyaline, smooth, branched, septate, 1.0–2.0 µm in diameter. ***Conidiophores*** solitary, rare branches, hyaline, smooth, arising from erect or geniculated hyphae, sometimes reduced to conidiogenous cells, erect, usually bearing two to four conidiogenous cells at the tip. ***Conidia*** hyaline, rough, verrucosa, solitary, obovoid, globose to subglobose, 3.0–7.5 × 2.5–5.5 µm (av. 4.8 × 3.8, n = 50), borne on hyphae, short protrusions, side branches or in conidiophores separated by connective cells. ***Intercalary conidia*** hyaline, globose to subglobose, fusiform, with both

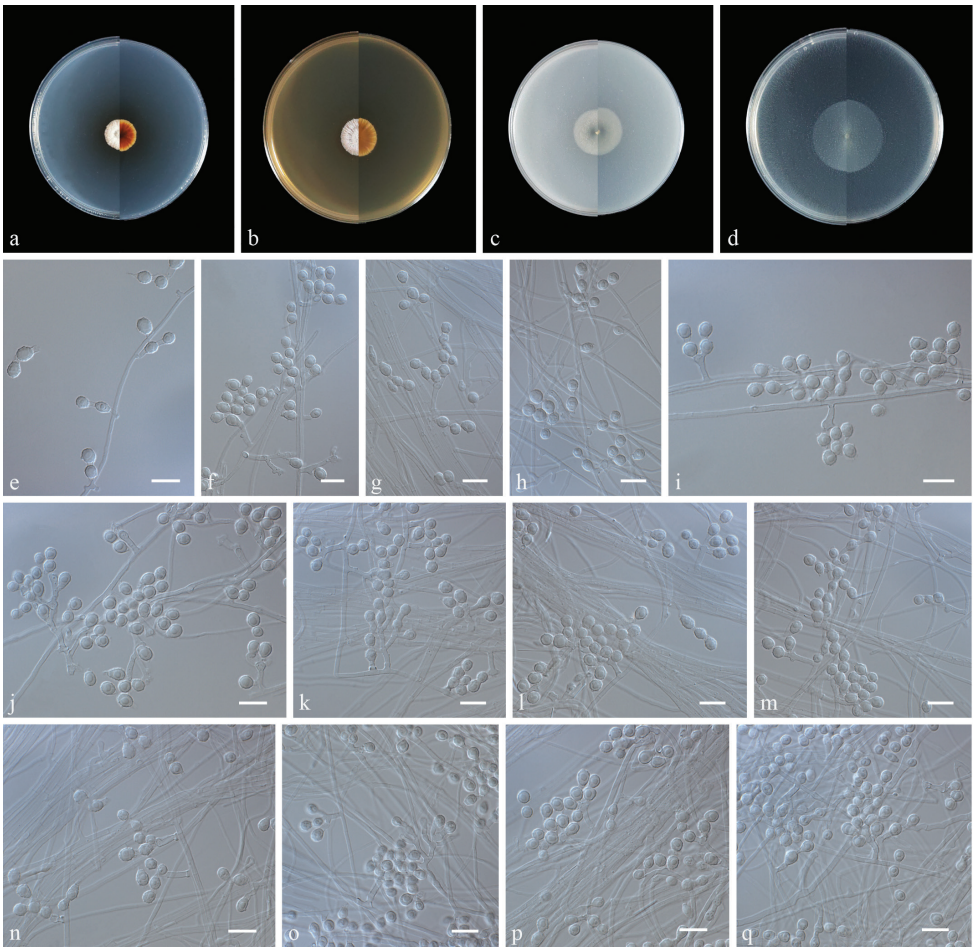

Figure 3. Morphology of *Pseudogeomyces lindneri* sp. nov. **a–d** colony on PDA, MEA, OA and CMA after 14 d at 25 °C (upper surface and lower surface) **e–q** Conidiophore, Conidia and Intercalary conidia. Scale bars: 10 mm (**a–d**); 10 μm (**e–q**).

truncate 3.5–6.5 × 3.0–4.5 μm (av. 4.9 × 4.0, n = 50). ***Chlamydospores*** not observed. ***Sexual morph*** undetermined.

Notes. Based on multi-locus phylogenetic analyses (Figs 1, 2) and morphological characteristics, *Pseudogeomyces lindneri* is proposed as the type species of *Pseudogeomyces*. The isolates ZY 22.003, ZY 22.004 and ZY 22.005 formed a single phylogenetic clade and were separated from the other four unidentified isolates (12NJ08, 17WV09, 23WI14 and 23WI08) under *Pseudogeomyces*. Morphologically, *Pseudoge. lindneri* differed from other taxa under the family Thelebolaceae in terms of the presence of two to four irregular branches at the tip of the conidiophores and that the conidia and intercalary conidia are generally connected by connective cells in a chain (Kuehn 1958; Van Oorschot 1980).

Pseudogymnoascus campensis **Zhi. Y. Zhang & Y. F. Han, sp. nov.**
MycoBank No: 846366
Fig. 4

Etymology. Refers to Guizhou Minzu University where this fungal type was isolated.

Type. Guizhou Minzu University, Guiyang City, Guizhou Province, China 26°37'57"N, 106°62'41"E. Colonies form on PDA as a contaminating fungus, July 2022, Zhi-Yuan Zhang (dried holotype ZY H-22.001, ex-type ZY 22.001, *ibid.*, ZY 22.002).

Geographical distribution. Guizhou Province, China.

Description. Culture characteristics (14 days at 25 °C): ***Colonies*** on PDA 20–21 mm in diameter, white to light green, fluffy, nearly round, margin regular, exudates and diffusible pigments absent; reverse: claret-red to white from centre to margin. ***Colonies*** on MEA 23–24 mm in diameter, white, elevated at the centre, velvety to floccose, margin regular, exudates and diffusible pigments absent; reverse: pale yellow to white. ***Colonies*** on OA 27–28 mm in diameter, white, flat, nearly round, margin regular, exudates absent, producing a diffusible faint white pigment; reverse: white. ***Colonies*** on CMA 32–38 mm in diameter, khaki to white, radially sectored by cracks, powdery, exudates and diffusible pigments absent; reverse: khaki.

Hyphae hyaline, smooth, branched, septate, 1.0–2.5 μm in diameter. Sometimes lateral hyphae end in barrel-, reniform- or pyriform-shaped chains with blunt-ended arthroconidia, sometimes bearing aleurioconidia, sessile or stalked. ***Conidiophores*** abundant, solitary, erect, arising in acute angles with the main axis, hyaline, smooth, usually bearing verticils of two to three branches arising from the stipe at an acute angle. ***Aleurioconidia*** pyriform or obovoid, with a broad truncated basal scar, 3.0–5.0 × 2.0–2.5 μm (av. 3.6 × 2.7, n = 50), in conidiophores separated by connective cells, smooth or rough. ***Intercalary conidia*** barrel, reniform, pyriform to elongated or irregular, with a broad truncated scar at the base or both ends, 3.5–5.5 × 2.0–3.0 μm (av. 4.0 × 2.6, n = 50), smooth or rough. ***Arthroconidia*** not observed. ***Sexual morph*** unknown.

Notes. Minnis and Lindner (2013) proposed multiple clades of *Pseudogymnoascus* and allies (clades A to O), based on phylogenetic analyses using North American isolates. In this study, *Pseudogymnoascus campensis* was placed in clade A (Fig. 1). Clade A harbours 13 isolates for which no morphological data are yet available and remain as unidentified species to date (Minnis and Lindner 2013; Leushkin et al. 2015). These isolates were obtained from bat hibernacular soil in the USA (Minnis and Lindner 2013). *Pseudogymnoascus campensis* (ZY 22.001 and ZY 22.002), 23014-1-I6 and 11MA03 formed an independent lineage with strong support (ML BS 100/PP 1, Fig. 1). The closest known species to *Pseudogy. campensis* are *Pseudogy. shaanxiensis*, *Pseudogy. australis* and *Pseudogy. griseus*, which are members of the neighbouring clade B (Zhang et al. 2020b, Villanueva et al. 2021). However, *Pseudogy. campensis* can be distinguished from *Pseudogy. shaanxiensis*, *Pseudogy. australis* and *Pseudogy. griseus* by the absence of exudates on PDA, MEA and CMA media and lack of arthroconidia (Zhang et al. 2020b; Villanueva et al. 2021).

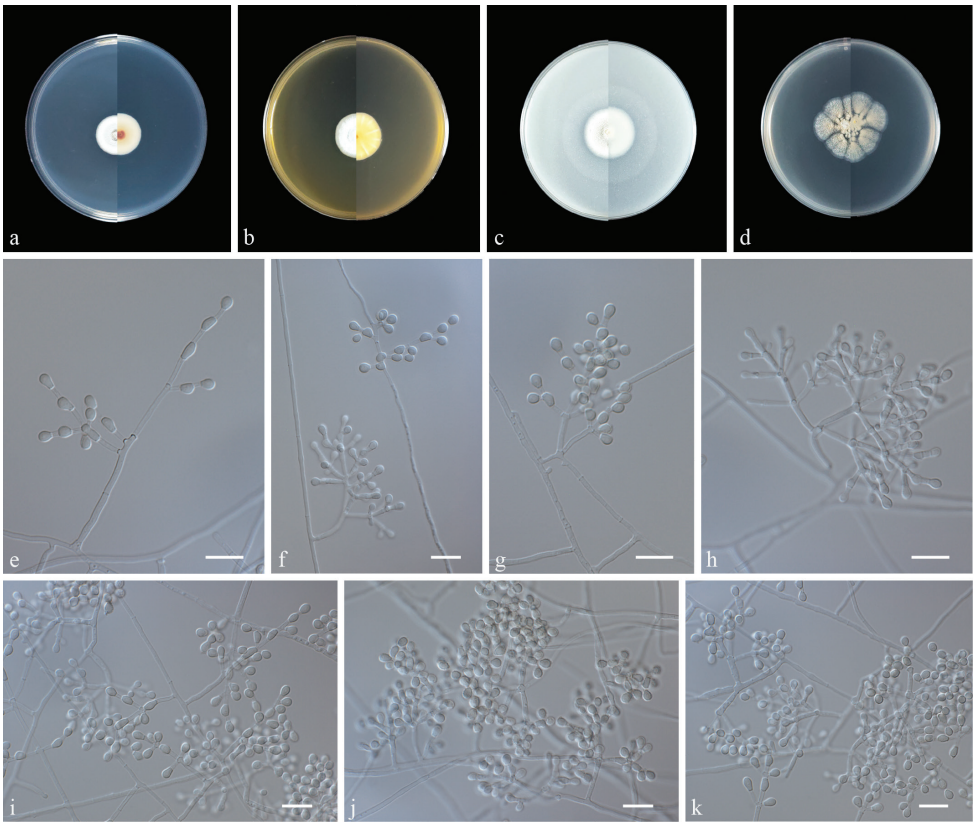

Figure 4. Morphology of *Pseudogymnoascus campensis* sp. nov. **a–d** colony on PDA, MEA, OA and CMA after 14 d at 25 °C (upper surface and lower surface) **e, f** fertile hyphae bearing arthroconidia and aleurioconidia **g–k** Conidiophore and Conidia. Scale bars: 10 μm (**e–k**).

Discussion

Previously, Minnis and Lindner (2013) performed a phylogenetic analysis, based on numerous multi-loci sequences of *Pseudogymnoascus* and its allies isolated from North American cave soils and obtained very robust results. However, many of the isolates obtained in the study were not identified as species. Based on their work, we subsequently defined *Pseudogymnoascus* and its allies isolated from China and reported two new genera and several new species (Zhang et al. 2020b, 2021). Similarly, Villanueva et al. (2021) identified four strains isolated from Antarctica, based on the above study and found that they were all previously undescribed species. In this study, one new genus and one new species are being proposed, based on the aforementioned study.

The classification of Thelebolales remains controversial to date (Ekanayaka et al. 2019; Johnston et al. 2019; Batista et al. 2020; Quijada et al. 2022). In contrast, however, the work of Ekanayaka et al. (2019) contained more genera in Thelebolales; therefore, we continued the phylogenetic analysis in Thelebolales, based on this study.

This study, based on ITS+LSU phylogenetic analyses, showed that Thelebolales consisted of Thelebolaceae and *Alatospora-Miniancora* clade (Fig. 1), which is consistent with Ekanayaka et al. (2019). Our proposed new genus *Pseudogeomyces* was nested in Thelebolaceae and is well supported (Fig. 1).

The ITS region is the most frequently used molecular marker in fungal classification studies, primarily due to its suitable variability. Additionally, Vu et al. (2019) demonstrated the high efficacy of ITS and LSU concatenation in discriminating filamentous fungal species. Numerous fungal ITS and LSU sequences are presently available in public databases (Zhang et al. 2022). Additionally, some fungal taxa, including the majority of genera under Thelebolales, have only ITS and/or LSU regions. Therefore, we only explored the position of the new genus, *Pseudogeomyces*, in Thelebolales, based on the phylogenetic analysis of ITS + LSU sequences.

In accordance with the most recent revision to the rules governing fungal nomenclature, presently referred to as the "International Code of Nomenclature for algae, fungi and plants", the system of dual nomenclature sanctioned by Article 59 has been modified to "One Fungus, One Name" (McNeill et al. 2012), where a single name is applied, regardless of the life stage considered. Most of the new taxa erected in recent years under *Pseudogymnoascus* and allies are based on asexual structures rather than sexual structures (Zhang et al. 2020b; Villanueva et al. 2021; Zhang et al. 2021). In this study, the new isolates were separately cultured in four media for observing the sexual structures, but the approach proved unsuccessful. The sexual structures of fungi appear when grown in nature rather than under laboratory conditions. Therefore, studying the production of sexual structures by these fungi under laboratory conditions is highly necessary.

Acknowledgements

This work was financially supported by the National Natural Science Foundation of China (no. 32060011, 31860520) and the National Key R&D Program of China (Grant 2019YFD1002003). We appreciate Charlesworth for English language editing to the whole manuscript.

References

Batista TM, Hilário HO, de Brito GAM, Moreira RG, Furtado C, De Menezes GCA, Rosa CA, Rosa LH, Franco GR (2020) Whole-genome sequencing of the endemic Antarctic fungus *Antarctomyces pellizariae* reveals an ice-binding protein, a scarce set of secondary metabolites gene clusters and provides insights on Thelebolales phylogeny. Genomics 112(5): 2915–2921. https://doi.org/10.1016/j.ygeno.2020.05.004

Chen CJ, Chen H, Zhang Y, Thomas HR, Frank MH, He YH, Xia R (2020) TBtools: An integrative toolkit developed for interactive analyses of big biological data. Molecular Plant 13(8): 1194–1202. https://doi.org/10.1016/j.molp.2020.06.009

Ekanayaka AH, Hyde KD, Gentekaki E, McKenzie EHC, Zhao Q, Bulgakov TS, Camporesi E (2019) Preliminary classification of Leotiomycetes. Mycosphere 10(1): 310–489. https://doi.org/10.5943/mycosphere/10/1/7

Eriksson OE, Winka K (1997) Supraordinal taxa of Ascomycota. Myconet 1: 1–16.

Hassan N, Rafiq M, Hayat M, Nadeem S, Shah AA, Hasan F (2017) Potential of psychrotrophic fungi isolated from Siachen glacier, Pakistan, to produce antimicrobial metabolites. Applied Ecology and Environmental Research 15(3): 1157–1171. https://doi.org/10.15666/aeer/1503_11571171

Johnston PR, Quijada L, Smith CA, Baral HO, Hosoya T, Baschien C, Pärtel K, Zhuang WY, Haelewaters D, Park D, Carl S, López-Giráldez F, Wang Z, Townsend JP (2019) A multigene phylogeny toward a new phylogenetic classification of Leotiomycetes. IMA Fungus 10(1): 1. https://doi.org/10.1186/s43008-019-0002-x

Kalyaanamoorthy S, Minh BQ, Wong TKF, von Haeseler A, Jermiin LS (2017) ModelFinder: Fast model selection for accurate phylogenetic estimates. Nature Methods 14(6): 587–589. https://doi.org/10.1038/nmeth.4285

Katoh K, Standley DM (2013) MAFFT multiple sequence alignment software version 7: Improvements in performance and usability. Molecular Biology and Evolution 30(4): 772–780. https://doi.org/10.1093/molbev/mst010

Kuehn HH (1958) A preliminary survey of the Gymnoascaceae. I. Mycologia 50(3): 417–439. https://doi.org/10.1080/00275514.1958.12024739

Leushkin EV, Logacheva MD, Penin AA, Sutormin RA, Gerasimov ES, Kochkina GA, Ivanushkina NE, Vasilenko OV, Kondrashov AS, Ozerskaya SM (2015) Comparative genome analysis of *Pseudogymnoascus* spp. reveals primarily clonal evolution with small genome fragments exchanged between lineages. BMC Genomics 16(1): 1. https://doi.org/10.1186/s12864-015-1570-9

Li X, Zhang ZY, Ren YL, Chen WH, Liang JD, Pan JM, Huang JZ, Liang ZQ, Han YF (2022) Morphological characteristics and phylogenetic evidence reveal two new species of *Acremonium* (Hypocreales, Sordariomycetes). MycoKeys 91: 85–96. https://doi.org/10.3897/mycokeys.91.86257

McNeill J, Buck WR, Demoulin V, Greuter W, Hawkworth DL, Herendeen PS, Knapp S, Marhold K, Prado J, Prud'homme van Reine WF, Smith GF, Wiersema JH, Turland NJ, International Botanical Congress (2012) International code of nomenclature for algae, fungi and plants (Melbourne code); adopted by the 18th International Botanical Congress, Melbourne, Australia, Jul 2011. Koenigstein, Germany: Koeltz Scientific Books.

Minh Q, Nguyen M, von Haeseler AA (2013) Ultrafast approximation for phylogenetic bootstrap. Molecular Biology and Evolution 30(5): 1188–1195. https://doi.org/10.1093/molbev/mst024

Minnis AM, Lindner DL (2013) Phylogenetic evaluation of *Geomyces* and allies reveals no close relatives of *Pseudogymnoascus destructans*, comb. nov., in bat hibernacula of eastern North America. Fungal Biology 117(9): 638–649. https://doi.org/10.1016/j.funbio.2013.07.001

Nguyen LT, Schmidt HA, von Haeseler A, Minh BQ (2015) IQ-TREE: A fast and effective stochastic algorithm for estimating maximum-likelihood phylogenies. Molecular Biology and Evolution 32(1): 268–274. https://doi.org/10.1093/molbev/msu300

Quijada L, Matočec N, Kušan I, Tanney JB, Johnston PR, Mešić A, Pfister DH (2022) Apothecial ancestry, evolution, and re-evolution in Thelebolales (Leotiomycetes, Fungi). Biology 11(4): 583. https://doi.org/10.3390/biology11040583

Ronquist F, Teslenko M, van der Mark P, Ayres DL, Darling A, Höhna S, Larget B, Liu L, Suchard MA, Huelsenbeck JP (2012) MrBayes 3.2: Efficient Bayesian phylogenetic inference and model choice across a large model space. Systematic Biology 61(3): 539–542. https://doi.org/10.1093/sysbio/sys029

Samson RA (1972) Notes on *Pseudogymnoascus*, *Gymnoascus* and related genera. Acta Botanica Neerlandica 21(5): 517–527. https://doi.org/10.1111/j.1438-8677.1972.tb00804.x

Tamura K, Stecher G, Peterson D, Filipski A, Kumar S (2013) MEGA6: Molecular evolutionary genetics analysis version 6.0. Molecular Biology and Evolution 30(12): 2725–2729. https://doi.org/10.1093/molbev/mst197

Van Oorschot CA (1980) A revision of *Chrysosporium* and allied genera. Studies in Mycology 20: 1–89.

Villanueva P, Vásquez G, Gil-Durán C, Oliva V, Díaz A, Henríquez M, Álvarez E, Laich F, Chávez R, Vaca I (2021) Description of the first four species of the genus Pseudogymnoascus from Antarctica. Frontiers in Microbiology 12: 713189. https://doi.org/10.3389/fmicb.2021.713189

Vu D, Groenewald M, de Vries M, Gehrmann T, Stielow B, Eberhardt U, Al-Hatmi A, Groenewald JZ, Cardinali G, Houbraken J, Boekhout T, Crous PW, Robert V, Verkley GJM (2019) Large-scale generation and analysis of filamentous fungal DNA barcodes boosts coverage for kingdom fungi and reveals thresholds for fungal species and higher taxon delimitation. Studies in Mycology 92(1): 135–154. https://doi.org/10.1016/j.simyco.2018.05.001

Wijayawardene NN, Hyde KD, Rajeshkumar KC, Hawksworth DL, Madrid H, Kirk PM, Braun U, Singh RV, Crous PW, Kukwa M, Lücking R, Kurtzman CP, Yurkov A, Haelewaters D, Aptroot A, Lumbsch HT, Timdal E, Ertz D, Etayo J, Phillips AJL, Groenewald JZ, Papizadeh M, Selbmann L, Dayarathne MC, Weerakoon G, Jones EBG, Suetrong S, Tian Q, Castañeda-Ruiz RF, Bahkali AH, Pang KL, Tanaka K, Dai DQ, Sakayaroj J, Hujslová M, Lombard L, Shenoy BD, Suija A, Maharachchikumbura SSN, Thambugala KM, Wanasinghe DN, Sharma BO, Gaikwad S, Pandit G, Zucconi L, Onofri S, Egidi E, Raja HA, Kodsueb R, Cáceres MES, Pérez-Ortega S, Fiuza PO, Monteiro JS, Vasilyeva LN, Shivas RG, Prieto M, Wedin M, Olariaga I, Lateef AA, Agrawal Y, Fazeli SAS, Amoozegar MA, Zhao GZ, Pfliegler WP, Sharma G, Oset M, Abdel-Wahab MA, Takamatsu S, Bensch K, de Silva NI, de Kesel A, Karunarathna A, Boonmee S, Pfister DH, Lu YZ, Luo ZL, Boonyuen N, Daranagama DA, Senanayake IC, Jayasiri SC, Samarakoon MC, Zeng XY, Doilom M, Quijada L, Rampadarath S, Heredia G, Dissanayake AJ, Jayawardana RS, Perera RH, Tang LZ, Phukhamsakda C, Hernández-Restrepo M, Ma X, Tibpromma S, Gusmao LFP, Weerahewa D, Karunarathna SC (2017) Notes for genera: Ascomycota. Fungal Diversity 86(1): 1–594. https://doi.org/10.1007/s13225-017-0386-0

Zhang D, Gao FL, Jakovlić I, Zou H, Zhang J, Li WX, Wang GT (2020a) PhyloSuite: An integrated and scalable desktop platform for streamlined molecular sequence data management and evolutionary phylogenetics studies. Molecular Ecology Resources 20(1): 348–355. https://doi.org/10.1111/1755-0998.13096

Zhang Z, Dong C, Chen W, Mou Q, Lu X, Han Y, Huang J, Liang Z (2020b) The enigmatic Thelebolaceae (Thelebolales, Leotiomycetes): One new genus *Solomyces* and five new species. Frontiers in Microbiology 11: 572596. https://doi.org/10.3389/fmicb.2020.572596

Zhang ZY, Shao QY, Li X, Chen WH, Liang JD, Han YF, Huang JZ, Liang ZQ (2021) Culturable fungi from urban soils in China I: Description of 10 new taxa. Microbiology Spectrum 9(2): e00867–e21. https://doi.org/10.1128/Spectrum.00867-21

Zhang Z, Chen W, Liang Z, Zhang L, Han Y, Huang J, Liang Z (2022) Revealing the non-overlapping characteristics between original centers and genetic diversity of *Purpureocillium lilacinum*. Fungal Ecology 60: 101179. https://doi.org/10.1016/j.funeco.2022.101179

Supplementary material 1

Sequences of primers used for the amplification of molecular markers in this study. GenBank accession numbers of the sequences used in this study. The best-fit evolutionary model in the phylogenetic analyses

Authors: Zhi-Yuan Zhang, Yan-Feng Han, Wan-Hao Chen, Gang Tao

Data type: table (word file)

Link: https://doi.org/10.3897/mycokeys.95.97474.suppl1

MycoKeys 95: 61–82 (2023)
doi: 10.3897/mycokeys.95.97156
https://mycokeys.pensoft.net

RESEARCH ARTICLE

A peer-reviewed open-access journal
MycoKeys
Launched to accelerate biodiversity research

Morphological and molecular analyses reveal two new species of *Termitomyces* (Agaricales, Lyophyllaceae) and morphological variability of *T. intermedius*

Song-Ming Tang[1,2,3], Santhiti Vadthanarat[2], Jun He[1], Bhavesh Raghoonundon[2], Feng-Ming Yu[2,4], Samantha C. Karunarathna[5], Shu-Hong Li[1], Olivier Raspé[2]

1 *Biotechnology and Germplasm Resources Institute, Yunnan Academy of Agricultural Sciences, Kunming 650205, China* **2** *School of Science, Mae Fah Luang University, Chiang Rai 57100, Thailand* **3** *College of Agriculture & Biological Sciences, Dali University, Dali 671003, Yunnan, China* **4** *Key Laboratory for Plant Diversity and Biogeography of East Asia, Kunming Institute of Botany, Chinese Academy of Sciences, Kunming 650201, China* **5** *Qujing Normal University, Qujing, Yunnan 655011, China*

Corresponding authors: Shu-Hong Li (shuhongfungi@126.com), Olivier Raspe (ojmraspe@gmail.com)

Academic editor: Rui-Lin Zhao | Received 4 November 2022 | Accepted 23 January 2023 | Published 8 February 2023

Citation: Tang S-M, Vadthanarat S, He J, Raghoonundon B, Yu F-M, Karunarathna SC, Li S-H, Raspé O (2023) Morphological and molecular analyses reveal two new species of *Termitomyces* (Agaricales, Lyophyllaceae) and morphological variability of *T. intermedius*. MycoKeys 95: 61–82. https://doi.org/10.3897/mycokeys.95.97156

Abstract

Two new species, *Termitomyces tigrinus* and *T. yunnanensis* are described based on specimens collected from southwestern China. *Termitomyces yunnanensis* is morphologically characterized by a conspicuously venose pileus surface that is grey, olive grey, light grey to greenish grey at center, light grey towards margin, and a cylindrical white stipe. *Termitomyces tigrinus* is morphologically characterized by a densely tomentose to tomentose-squamulose pileus showing alternating greyish white and dark grey zones, and a stipe that is bulbous at the base. The two new species are supported by phylogenetic analyses of combined nuclear rDNA internal transcribed spacer ITS1-5.8S-ITS2 rDNA (ITS), the mitochondrial rDNA small subunit (mrSSU) and the nuclear rDNA large subunit (nrLSU). The morphological variability of *T. intermedius*, including five specimens newly collected from Yunnan Province, China, is also discussed. The collections showed variability in colour of the stipe surface and in the shape of cheilocystidia when compared to the original description. Full descriptions of the two new species and of *T. intermedius*, as well as a taxonomic key to the 14 *Termitomyces* species reported from China are provided.

Keywords

2 new species, morphology, multi-gene phylogeny, taxonomy, tropical Asia, Yunnan

Introduction

Termitomyces R. Heim (1942a) was established based on the type species *T. striatus* (Beeli) R. Heim (Heim 1942a). *Termitomyces* species are characterized by their obligate symbiotic association with termites (Aanen et al. 2002). Most of species in this genus present a pseudorhiza connected to the termite nests, a usually conspicuous perforatorium (differentiated structure at the centre of the pileus, often in the form of a papilla or umbo), pinkish spore deposit, and smooth broadly ellipsoid to ellipsoid basidiospores (Mossebo et al. 2017; Izhar et al. 2020; Seelan et al. 2020; Usman and Khalid 2020). To date, 59 species of *Termitomyces* have been described worldwide (based on Index Fungorum, accessed on 17 January 2023), of which 14 are reported from China (Wei et al. 2004; Huang et al. 2017; Ye et al. 2019; Tang et al. 2020).

Termitomyces species were formerly placed in several different genera, including *Agaricus* (Berkeley 1847), *Armillaria* (Saccardo 1887), *Collybia* (Höhnel and Litschauer 1908), *Schulzeria* (Beeli 1927) and *Lepiota* (Beeli 1927). In 1942, *Termitomyces* was erected with the introduction of seven new species (Heim 1942b). Later, two genera viz. *Podabrella* and *Rajapa*, were segregated from *Termitomyces* by Singer (1945), but these two genera were not broadly accepted as independent (Heim 1977; Gómez 1994; Frøslev et al. 2003; He et al. 2019).

Termitomyces species are ecmically important and widely traded as food in the markets of tropical and subtropical areas (Parent and Thoen 1977; Mondal et al. 2004; Chandra et al. 2007; Ye et al. 2019). In India, *Termitomyces* species such as *T. microcarpus* (Berk. & Broome) R. Heim and *T. heimii* Natarajan have also been used for the treatment of diseases such as cold, fever, and fungal infections (Venkatachalapathi and Paulsamy 2016).

Recently, molecular phylogenetic approaches have increasingly been applied to investigate phylogenetic relationships among genera and species of Agaricales (Hofstetter et al. 2002). Through these studies, *Termitomyces* was strongly supported as a genus in Lyophyllaceae, with close relationship to the genera *Calocybe* Kühner, *Tephrocybe* Donk, and *Lyophyllum* P. Karst. (Bellanger et al 2015; He et al. 2019). *Sinotermitomyces* M. Zang, originally described in southwestern China (Zang 1981), was also proven to be a synonym of *Termitomyces* based on the study of type material (Wei et al. 2006).

For the past 70 years, a number of new *Termitomyces* species have been described based only on morphological characteristics. The lack of good illustrations and/or of detailed descriptions made the taxonomy of *Termitomyces* complicated, until the advent of molecular phylogeny. Mossebo et al. (2017) provided molecular markers (nrLSU and mrSSU), bringing more evidence for the classification of *Termitomyces* species. Since then, a series of new *Termitomyces* species have been described from Asia based on combined molecular and morphological data (Ye et al. 2019; Izhar et al. 2020; Seelan et al. 2020; Tang et al. 2020; Usman and Khalid 2020).

During investigations of *Termitomyces* across southwestern China and Thailand, several *Termitomyces* collections were made. Amongst them, two *Termitomyces* species

from Yunnan, China, are newly described herein. In addition to the morphological descriptions and illustrations, molecular phylogenetic analyses based on the ITS1-5.8S-ITS2, mrSSU and nrLSU supported the two new species.

Materials and methods

Studied specimens

Eleven specimens were collected from Southwestern China. Collection locations were subtropical broad-leaved forests in Yunnan Province, where the annual average temperature is 12–22 °C, and the elevation is 1,000–3,500 m (Xiwen and Walker 1986). Three additional specimens were obtained on loan from the Herbarium of Meise Botanic Garden, Belgium (**BR**).

Morphological studies

Descriptions of macro-morphological characteristics and habitats were obtained from the photographs and notes. Colour codes were based on Kornerup and Wanscher (1978). Once the macromorphological characteristics were noted, specimens were dried at 40 °C in a food dryer until no more moisture was left, and stored in sealed plastic bags. For microscopy study, dried mushroom materials were sectioned and mounted in 5% KOH solution and 1% Congo red. Microscopic characters such as basidia, basidiospores, and cystidia were observed and photographed using a light microscope (Nikon eclipse 80i) equipped. For microscopic characters' descriptions, 60–100 basidiospores, 20 basidia, and 10 cystidia were randomly measured, the abbreviations [x/y/z] denote x basidiospores measured from y basidiomata of z collections, (a–) b–c (–d) denote basidiospore dimensions, where the range b–c represents 95% of the measured values while "a", and "d" are extreme values, L_m and W_m, the average length and width are also given with their standard deviations; Q refers to the length/width ratio of individual basidiospore while Q_m refers to the average Q value ± standard deviation. Specimens of the two new *Termitomyces* species were deposited at the herbarium of the Kunming Institute of Botany, Chinese Academy of Sciences (KUN-HKAS) and Mae Fah Luang University herbarium (MFLU).

DNA extraction, PCR amplification and sequencing

Genomic DNA was extracted from dry specimens using Ezup Column Fungi Genomic DNA extraction Kit following the manufacturer's protocol. PCR amplification, PCR product purification, and sequencing. The primers used for nrLSU amplification were LR0R and LR5 (Vilgalys and Hester 1990). The mrSSU region was amplified with *Termitomyces* specific primer pairs viz. SSUFW105 and SSUREV475 (Aanen et al. 2002). The ITS gene region was amplified using the primers ITS1 or ITS5, and ITS4 (White et al. 1990).

Sequence alignment and phylogenetic analyses

A total of 29 newly generated sequences and 66 sequences from GenBank were used as ingroup and twelve sequences of *Lyophyllum shimeji* (Kawam.) Hongo, *L. decastes* (Fr.) Singer, *Asterophora lycoperdoides* (Bull.) Ditmar, and *A. parasitica* (Bull.) Singer retrieved from GenBank were used as outgroup (see Table 1). The outgroup taxa were selected based on the phylogeny in Hofstetter et al. (2014). The sequences were aligned with MAFFT version 7 (Katoh and Standley 2013) and checked in Bioedit version 7.0.5 (Hall 2007). The alignment was submitted to Figshare (10.6084/m9.figshare.20472915).

Phylogenies and node support were first inferred by Maximum Likelihood (ML) from the three single-gene alignments separately, using RAxML-HPC2 version 8.2.12 (Stamatakis 2014) with 1,000 rapid bootstraps, as implemented on the Cipres portal (Miller et al. 2010). Since no supported conflict (bootstrap support value (BS) ≥ 70%) was detected among the topologies, the three single-gene alignments were concatenated using SequenceMatrix (Vaidya et al. 2011). Partitioned Maximum Likelihood (ML) analysis was performed on the concatenated data set, as described above. For Bayesian Inference (BI), the best substitution model for each character set was determined with the program MrModeltest 2.3 (Nylander 2004) on Cipres. The selected models were GTR+I+G for nrLSU, GTR+G for mrSSU, GTR+G for ITS1+ITS2, and K80 for 5.8S. Bayesian analysis was performed using MrBayes version 3.2.7a (Ronquist et al. 2011) as implemented on the Cipres portal (Miller et al. 2010). Two runs of six chains each were conducted by setting generations to 50,000,000 and using the stoprul command with the stopval set to 0.01; trees were sampled every 200 generations. A clade was considered to be strongly supported if showing a BS ≥ 70% and a posterior probability (PP) ≥ 0.90.

Results

Phylogenetic analyses

The alignments of the nrLSU, mrSSU, 5.8S and ITS1+ITS2 sequences were 538, 354, 157, and 464 characters long after trimming, respectively. The combined data set had an aligned length of 1,516 characters, of which 946 characters were constant, 570 were variable but parsimony-uninformative, and 400 were parsimony-informative.

ML and BI analyses generated nearly identical tree topologies with little variation in statistical support. Thus, only the ML tree is displayed (Fig. 1). Phylogenetic data together with thorough morphological analysis (see below) showed that the two newly described taxa in this study are significantly different from other known *Termitomyces* species.

Table 1. Names, specimen vouchers, origin, and corresponding GenBank accession numbers of the sequences used in this study. New species are shaded in gray and newly generated sequences are in bold; "*" following a species name indicates that the specimen is the type of that species and "N/A" refers to the unavailability of data.

Taxon	Voucher specimen	Origin	GenBank accession no.			Reference
			ITS	mrSSU	nrLSU	
Termitomyces acriumbonatus	LAH36362	Pakistan	MT179687	N/A	MT179690	Usman et al. (2020)
*T. acriumbonatus**	LAH35345	Pakistan	MT179688	N/A	MT179689	Usman et al. (2020)
T. aurantiacus	DM 152E	Cameroon	N/A	KY809186	KY809234	Willis (2007)
T. aurantiacus	tgf 82	Tanzania	N/A	AY127852	AY127804	Mossebo et al. (2017)
*T. brunneopileatus**	DM392	Cameroon	N/A	KY809225	KY809273	Mossebo et al. (2017)
T. brunneopileatus	DM394	Cameroon	N/A	KY809197	KY809244	Mossebo et al. (2017)
T. bulborhizus	KM128338	China	N/A	KY809213	KY809261	Mossebo et al. (2017)
*T. floccosus**	MFLU 19–1312	Thailand	**MT683161**	MN701029	MN633305	Tang et al. (2020)
*T. fragilis**	HKAS 88912	China	KY214475	N/A	N/A	Ye et al. (2019)
T. fragilis	HKAS 88909	China	KY214476	N/A	N/A	Ye et al. (2019)
*T. gilvus**	BORH/FUMS-A03	Malaysia	N/A	MK478904	MK472701	Seelan et al. (2020)
T. globulus	DM770	Cameroon	N/A	KY809204	KY809252	Frøslev et al. (2003)
T. heimii	Muid.sn	N/A	N/A	AF357091	AF042586	Moncalvo et al. (2000)
T. intermedius	YO198	Japan	AB968241	N/A	N/A	Terashima et al. (2016)
T. intermedius	HKAS 117638	China	**ON557369**	**ON557367**	**ON556484**	**This study**
T. intermedius	HKAS 117639	China	**ON557370**	**ON557368**	**ON556485**	**This study**
T. le-testui	DM150G	Cameroon	N/A	KY809184	KY809231	Mossebo et al. (2017)
T. le-testui	KM128346	China	N/A	KY809215	KY809263	Mossebo et al. (2017)
T. mammiformis	DM25E	Cameroon	N/A	KY809182	KY809229	Mossebo et al. (2017)
T. mammiformis	DM25G	Cameroon	N/A	KY809183	KY809230	Mossebo et al. (2017)
T. mboudaeinus	DM223E	Cameroon	N/A	KY809189	KY809237	Mossebo et al. (2017)
T. medius f. *ochraceus*	DM602B	Cameroon	N/A	KY809198	KY809246	Mossebo et al. (2017)
T. radicatus	MRNo173	Thailand	LC068787	N/A	N/A	Ye et al. (2019)
T. robustus	KM142418	Tanzania	N/A	KY809217	KY809265	Mossebo et al. (2017)
T. robustus	DM436	Cameroon	N/A	KY809223	KY809271	Mossebo et al. (2017)
T. sagittiformis	KM109566	South Africa	N/A	KY809212	KY809260	Mossebo et al. (2017)
T. schimperi	DM24E	Cameroon	N/A	KY809181	KY809228	Mossebo et al. (2017)
*T. sheikhupurensis**	SKP124	Pakistan	MT192217	N/A	MT192228	Izhar et al. (2020)
T. sheikhupurensis	SKP224	Pakistan	MT192218	N/A	N/A	Izhar et al. (2020)
T. singidensis	tgf74	Tanzania	N/A	AY232687	AY232713	Frøslev et al. (2003)
T. striatus	KM142436	Malawi	N/A	KY809219	KY809267	Mossebo et al. (2017)
T. striatus	BR5020212704478V	Mali	**OP179298**	**OP179292**	**OP168082**	**This study**
T. striatus	BR5020168468769	Rwanda	**OP179297**	**OP179294**	**OP168081**	**This study**
T. striatus	BR5020169404421	Congo	**OP179299**	**OP179293**	**OP168080**	**This study**
T. striatus f. *bibasidiatus**	DM280B	Cameroon	N/A	KY809193	KY809241	Mossebo et al. (2017)
T. striatus f. *subclypeatus**	DM370B	Cameroon	N/A	KY809220	KY809268	Mossebo et al. (2017)
T. striatus f. *subclypeatus*	DM151C	Cameroon	N/A	KY809194	KY809242	Mossebo et al. (2017)
T. subumkowaan	DM260F	Cameroon	N/A	KY809190	KY809239	Mossebo et al. (2017)
*T. subumkowaan**	DM260B	Cameroon	N/A	KY809227	KY809275	Mossebo et al. (2017)
T. tigrinus*	**HKAS 107560**	**China**	**MT683156**	**MT683152**	**MT679729**	**This study**
T. tigrinus	**HKAS 107561**	**China**	**MT683157**	**MT683153**	**MT679730**	**This study**
T. umkowaan	HUH-SH5	Pakistan	KJ703245	N/A	N/A	Hussai et al. 2015
T. upsilocystidiatus T	MFLU 19–1289	China	**MT683160**	MN636642	MN636637	Tang et al. (2020)
T. yunnanensis*	**HKAS 124501**	**China**	**OP179295**	**OP179290**	**OP168083**	**This study**
T. yunnanensis	**HKAS 124502**	**China**	**OP179296**	**OP179291**	**OP168084**	**This study**
Outgroup						
Lyophyllum shimeji	Lc42	N/A	AF357060	AF357137	AF357078	Hofstetter et al. (2014)
L. decastes	JM87/16	N/A	AF357059	AF357136	AF042583	Hofstetter et al. (2014)
Asterophora lycoperdoides	CBS170.86	N/A	AF357037	AF357109	AF223190	Hofstetter et al. (2014)
A. parasitica	CBS683.82	N/A	AF357038	AF357110	AF223191	Hofstetter et al. (2014)

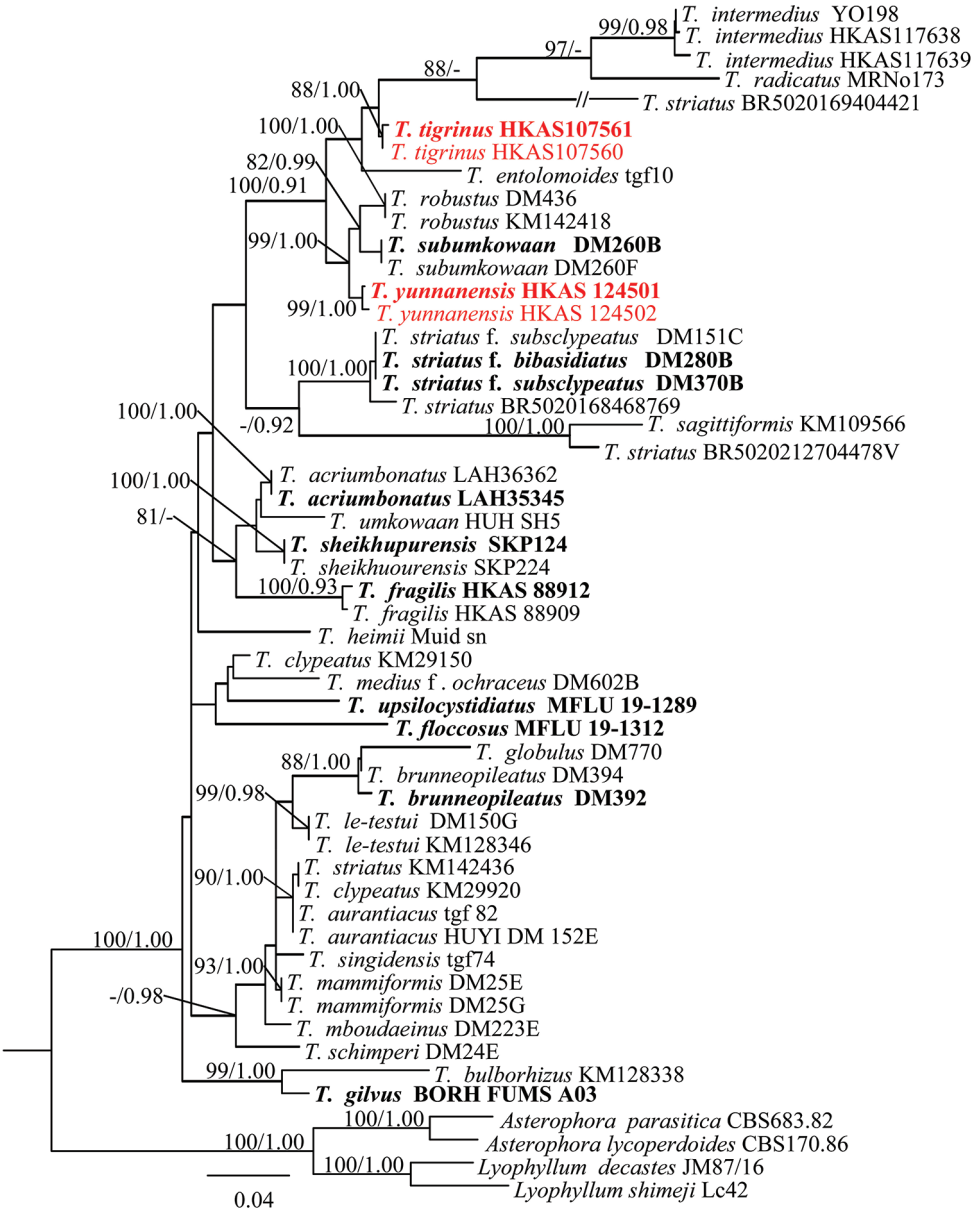

Figure 1. Strict consensus tree illustrating the phylogeny based on the combined nrLSU, mrSSU, 5.8S and ITS1+ITS2 data set. Maximum likelihood bootstrap proportions equal to or higher than 70%, and Bayesian posterior probabilities equal to or higher than 0.90 are indicated at nodes. The two *Asterophora* species and two *Lyophyllum* species were used as the outgroup. The two newly described species are in red. Holotype specimens are in bold.

Taxonomy

Termitomyces intermedius **Har. Takah. & Taneyama**
Figs 2, 3

Description. Basidiomata medium-sized. Pileus 4–11 cm in diam., broadly conical or convex when seen from aside, dark grey (1F1), unchanging, often rimose-squamulose in dry condition, squamules easily falling away; margin deflexed to inflexed, undate; perforatorium small and mucronate, dark grey (1F1); context white (1A1), 2–3 mm thick half-way to the margin, tough. Lamellae subventricose, 5–7 mm wide, subfree, crowded, white (1A1) when young, becoming to yellowish white (1A2) when mature; lamellulae in 1–2 tiers; lamellar edge eroded. Stipe central, 3–13 × 1.2–1.6 cm, cylindrical, sometime subbulbous (1.9–2.3 cm) at the base, pale grey (1B1) usually rimose in dry condition, smooth, sometimes irregularly pustulate bumps on the surface; context solid, white, fibrous. Annulus absent. Pseudorhiza terete, tapering downwards; surface pale grey (1B1), smooth; context solid, fibrous. Odour pleasant. Taste not distinctive.

Basidia 43–68 × 10–20 μm, av. 50 ± 8.3 × 14 ± 2.5 μm, clavate, thin-walled, 1-spored or 2-spored, (4-spored basidia not seen); sterigmata 1–2 μm long. Basidiospores [67/9/3] (9.0–) 10.3–14.1 (–14.9) × (5.3–) 5.8–8.9 (–10.2) μm, L_m × W_m = 11.9 ± 1.1 × 7.3 ± 0.9 μm, Q = 1.4–1.8 (–2.0), Q_m = 1.60 ± 0.18, broadly ellipsoid to ellipsoid, colorless, thin-walled, smooth. Hymenophoral trama regular, parallel, 150–230 μm wide, made up of thin-walled, fusiform to narrowly cylindrical hyphae elements 10–23 μm wide, filamentous hyphae abundant, 4–6 μm wide. Subhymenium 8–15 μm thick, with 1–2 layers of ovoid, subglobose, fusiform, ellipsoid or irregular cells, 5–7 × 3–5 μm. Pleurocystidia 40–136 (–169) × 19–34 μm, av. 95 ± 34.1 × 24 ± 9.9 μm, oblong, obovoid or ellipsoid, thin-walled. Lamellar edge heteromorphous, with abundant cheilocystidia. Cheilocystidia 52–114 × 20–29 μm, av. 78 ± 23.3 × 29 ± 8.4 μm, clavate to pyriform, narrowly lageniform, lageniform or broadly lageniform, thin-walled. Pileipellis 2-layered; suprapellis an ixocutis composed of cylindrical hyphae with obtuse apex, thin-walled, hyaline at places in KOH and terminal elements 16–73 × 3–6 μm, av. 46 ± 17.3 × 5 ± 0.9 μm; subpellis made up of inflated elements, 52–131 × 20–27 μm, av. 95 ± 24.8 × 24 ± 8.4 μm. Clamp connections not seen in any tissue.

Habitat and distribution. Basidiomata scattered to gregarious around termite underground nests; occurring in summer. Known from China and Japan.

Additional material examined. **China**. Yunnan Provinces: Kunming city, Shilin county, altitude 1,750 m, 12 July 2019, S.M. Tang 2019071204 (HKAS 117639); Baoshan city, Kejie village, altitude 1,680 m, 3 August 2019, Song-Ming Tang 2019080315 (HKAS 117640); Kejie village, altitude 1,599 m, 3 August 2020, Feng-Ming Yu 2019080321 (HKAS 117641); Dali city, altitude 1,890 m, 21 July 2020, Jun He 202072101 (HKAS 117643); Yuxi city, 1,708 m, 24 July 2020, Jun He 2020072422 (HKAS 117644).

Figure 2. Fresh basidiomata of *Termitomyces intermedius* (**a, b** HKAS 117640, **c** KHAS 117638, **d** HKAS 117644, e-HKAS 117643, f-HKAS 117639). Scale bars: 1 cm. Photographs by Song-Ming Tang.

Notes. *Termitomyces intermedius* was originally described from Japan (Terashima et al. 2016), subsequently, it was reported from China in Guangdong province (Huang et al. 2017). Comparison of our specimen (HKAS117638) with *T. intermedius*

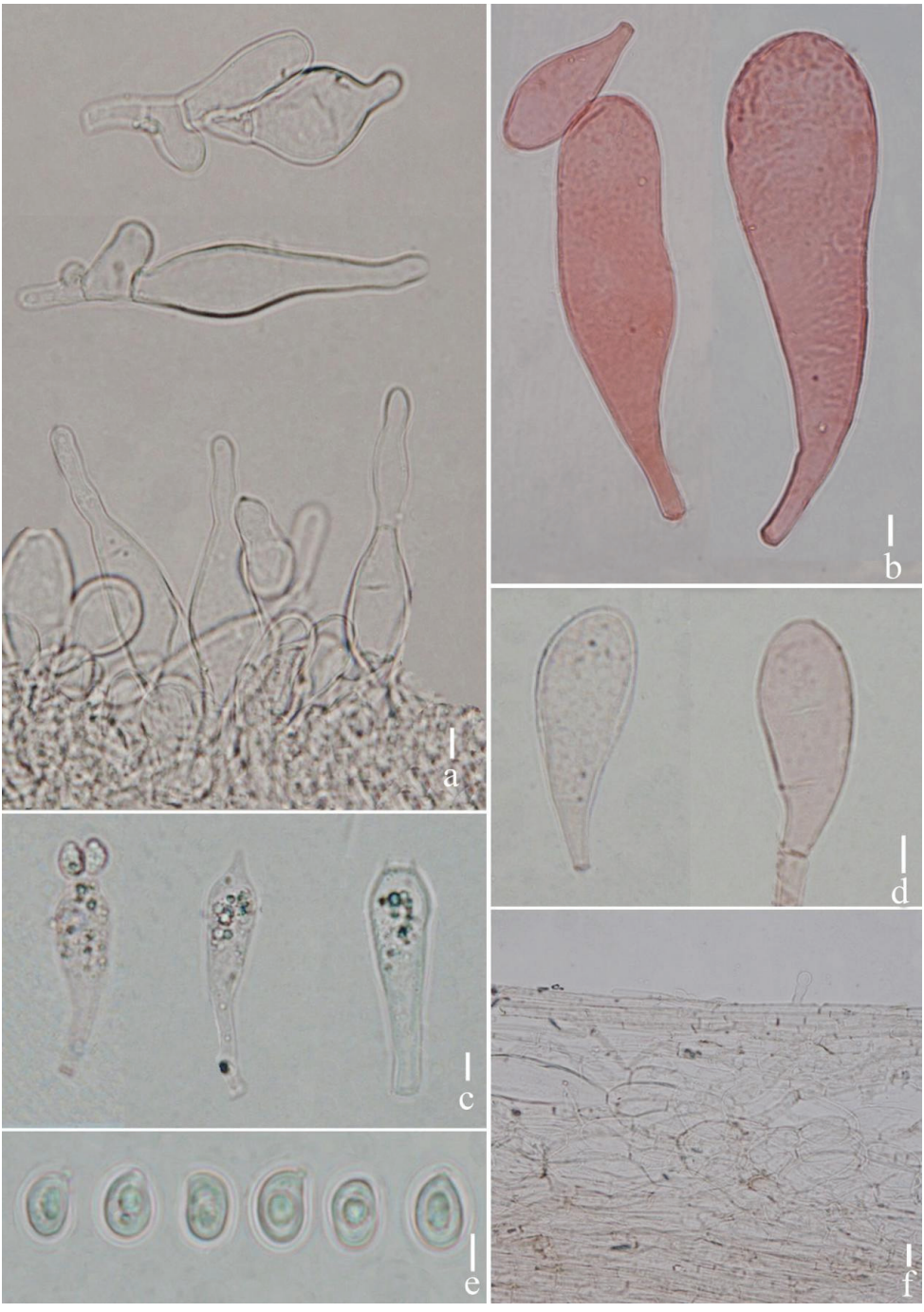

Figure 3. *Termitomyces intermedius* **a** cheilocystidia **b** large pleurocystidia **c** basidia **d** small pleurocystidia **e** basidiospores **f** pileipellis. Scale bars: 10 μm (**a–e**); 5 μm (**e**); 20 μm (**f**). Photographs by Song-Ming Tang.

(TNS-F-48178, Terashima et al. 2016) ITS sequences showed 0.65% difference (4/614 differences, including 3 gaps); nrLSU 100% similarity with GDGM46311 and GDGM46325 (Huang et al. 2017); *tef*1 100% similarity with FB-T1-04 (Kobayashi et al. 2021). Morphologically, our specimen HKAS117638 has narrowly lageniform, lageniform or broadly lageniform cheilocystidia, pileus and stipe surface often rimose-squamulose in dry condition, squamules easily falling away, stipe surface pale grey and sometime subbulbous at the base, while the original description mentioned that *T. intermedius* has broadly clavate to pyriform cheilocystidia and did not mention the pileus and stipe surface in dry condition, stipe white on the surface and cylindrical (Terashima et al. 2016). In *Termitomyces* species, cheilocystidia shape can be variable within the same species. In *T. aurantiacus* (R. Heim) R. Heim for example, cheilocystidia can be rostrate, with median constriction, or moniliform. In *T. mammiformis* R. Heim cheilocystidia can be ovoid, with a median constriction, or narrowly utriform. In *T. schimperi* cheilocystidia can be rostrate, oblong, narrowly utriform, or conical (Heim 1977).

Termitomyces tigrinus **S.M. Tang & Raspé, sp. nov.**
MycoBank No: 836040
Fig. 4

Etymology. The epithet "tigrinus" refers to the alternating greyish white and dark grey zones on the pileus.

Type material. ***Holotype*****.** **China**. Yunnan Province: Chuxiong County, Fuming, elev. 1,800 m, 16 July 2019, Song-Ming Tang (***Holotype*****:** HKAS 107560, ***isotype*****:** MFLU 22-0143).

Diagnosis. Differs from other *Termitomyces* species in having a regular alternating greyish white and dark grey zones on the pileus, and subclavate stipe.

Description. Basidiomata medium-sized. Pileus 7–9 cm in diam., convex to plano-convex, circular when seen from above, dark grey (1F1–2) at the centre, greyish white (1B1) to grey (1C1–1D1) towards margin, with regular alternating dark grey and greyish white zones, densely tomentose to tomentose-squamulose, hairs grey to drab, in dry conditions, often cracked into large or small scales; margin exceeding lamellae, undate; perforatorium small, as an acute papilla, dark grey (1C1). context 1–2 mm thick half-way to the margin, tough, white (1A1). Lamellae close, ventricose, 3–5 mm wide, adnexed, crowded, white (1A1) at first, then cream to greyish pink when mature; lamellar edge eroded; lamellulae in 1–2 tiers. Stipe 5–7 × 1–3.5 cm, central, subclavate, white (1A1) at the apex, greyish white (1B1) to grey (1C1–1D1) toward the base, smooth; context white (1A1), solid, fibrous. Annulus absent. Pseudorhiza terete, strongly tapering; surface grey (1D1–2) to dark grey (1F1–1F2), smooth; context solid, fibrous. Odour slightly fragrant. Taste not distinctive.

Basidia of two types conspicuously different by the apex of sterigmata being either acute or obtuse, first type rather abundant, clavate, sterigmata apex acute, mostly

4–spored sometimes 1–spored or 2–spored, 25–32 × 7–12 μm, av. 28 ± 2.4 × 11 ± 0.5 μm, sterigmata 1–3 μm long; the second type fewer in number, clavate, sterigmata apex obtuse, mostly 1–spored, 2–spored, sometimes 4–spored, 24–30 × 9–13 μm, av. 26 ± 2.2 × 12 ± 0.7 μm, sterigmata 2–4 μm long. Basidiospores [90/5/2] (6.1–) 7.2–9.6 (–10.1) × (3.3–) 5.2–7.3 (–7.9) μm, $L_m \times W_m$ = 8.1 ± 1.1 × 6.3 ± 0.8 μm, Q = (1.01–) 1.20–2.03 (–2.30), Q_m = 1.53 ± 0.20, broadly ellipsoid to ellipsoid, colourless, thin-walled, smooth. Hymenophoral trama regular, element parallel, 51–100 μm wide, made up of thin-walled, ellipsoid to clavate inflated hyphae 16–18 μm wide, filamentous hyphae abundant, 5–10 μm wide. Subhymenium 8–21 μm thick, with 1–2 layers of ovoid, subglobose, fusiform, ellipsoid or irregular cells, 8–11 × 3–6 μm. Pleurocystidia absent. Lamellar edge composed mostly of undifferentiated, basidiole-like cells. Cheilocystidia few, broadly clavate, 17–36 × 9–16 μm, av. 28 ± 2.0 × 14 ± 0.6 μm. Pileipellis 2-layered, suprapellis an ixocutis 22–51 × 5–7 μm av. 30 ± 5.7 × 6 ± 0.5 μm, cylindrical hyphae with obtuse apex, thin-walled, hyaline in KOH; subpellis made up of inflated elements, 31–81 × 7–14 μm, av. 58 ± 7.6 × 10 ± 0.8 μm. Clamp connections not seen in any tissues.

Habitat and distribution. Basidiomata scattered on soil with decaying litter under which termites have built their nest. Occurring in summer. So far only known from southwestern China.

Additional species examined. **China**. Yunnan Province, Chuxiong city, 20 July 2019, Jun He (HKAS 107561).

Notes. *Termitomyces tigrinus* is distinguished from other *Termitomyces* by densely tomentose to tomentose-squamulose pileus with regularly alternating greyish white and dark grey zones, and a small, dark grey perforatorium as an acute papilla, two conspicuously different types of basidia, broadly ellipsoid to ellipsoid basidiospores, clavate, thin-walled cheilocystidia that are rare (HKAS 107560), or absent (in HKAS 107561).

Morphologically, *T. tigrinus* is similar to *T. robustus* (Beeli) R. Heim in having grey to black stipe. However, *T. robustus* has a blunt perforatorium (Heim 1951), smaller basidia (20–25 × 7–8 μm) and basidiospores (7.0–8.0 × 5.0–5.5 μm) (Otieno 1969).

Termitomyces entolomoides R. Heim with *T. tigrinus* in having a tapering upwards stipe, dark grey pileus and greyish white to grey stipe. However, *T. entolomoides* has been originally described from Congo by Heim (1951), has a small basidioma (pileus 3–4 cm diam.), a grey pseudorhiza and relatively smaller basidiospores (6.2–6.6 × 4–4.2 μm; Heim 1951).

In our multi-locus phylogeny, *T. tigrinus* is closely related to *T. intermedius*, *T. radicatus* Natarajan and *T. striatus*. However, *T. intermedius* has a cylindrical stipe, and cheilocystidia clavate to pyriform, narrowly lageniform, lageniform or broadly lageniform (this study). *Termitomyces radicatus* has a pale orange pileus, dark brown perforatorium, relatively smaller pileus (1.5–3.5 cm), and cylindrical stipe (Pegler and Vanhaecke 1994). *Termitomyces striatus* has a white to ocher pileus, irregularity fibrous striate on the stipe surface, long pseudorhiza (30–100 cm), with squama of various sizes and shapes on the surface cheilocystidia and pleurocystidia pyriform,broadly clavate, cylindrical or ovoid, (20–45 × 11–22 μm; Heim 1977).

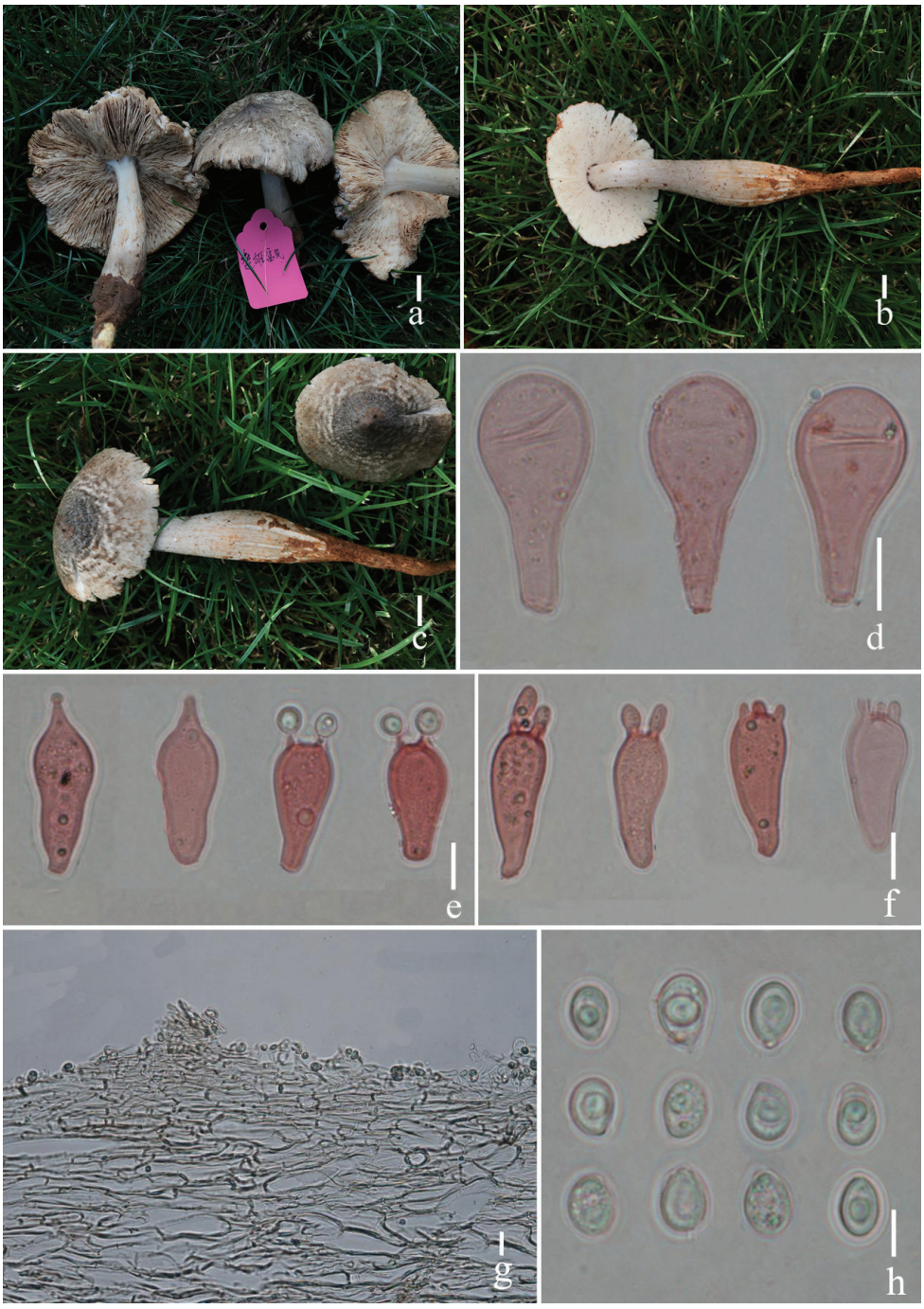

Figure 4. *Termitomyces tigrinus* **a–c** basidiomata (**a** HKAS 107560, **b, c** HKAS 107561) **d** cheilocystidia **e** basidia with acute sterigmata apex **f** basidia with obtuse sterigmata apex **g** pileipellis **h** basidiospores. Scale bars: 1 cm (**a–c**); 10 μm (**d–f**); 20 μm (**g**); 5 μm (**h**). Photographs by Song-Ming Tang.

Termitomyces yunnanensis **S.M. Tang & Raspé, sp. nov.**
MycoBank No: 845183
Figs 5, 6

Etymology. The epithet "yunnanensis" refers to the holotype coming from Yunnan province.

Type material. ***Holotype*****: China.** Yunnan province: Kunming city, Shilin county, 20 August 2020, elev. 1580 m, S.M. Tang (***Holotype*****:** HKAS124501, ***isotype*** MFLU 22-0144).

Diagnosis. Differs from other *Termitomyces* species in having a clearly conspicuously venose pileus surface, and an umbonate perforatorium.

Description. Basidiomata medium-sized. Pileus 4–8 cm in diam., at first convex becoming convexo-applanate to plano-concave or concave, medium grey (1E1), olive grey (1E2), light grey (1D1) to greenish grey (1D2) at center, light grey (1D1) towards margin, conspicuously venose surface; margin inflexed when young, becoming straight or reflexed when mature; perforatorium an umbo, ca. 7–9 mm, dark grey (1F1); context 2–4 mm thick half-way to the margin, tough, white (1A1). Lamellae subventricose, free to adnexed, crowded; lamellulae in 1–2 tiers, white (1A1), 3–5 mm wide; lamellar edge eroded. Stipe 3–4 × 1–2 cm, central, cylindrical, rarely subbulbous at the base, smooth; context solid, fibrous, white (1A1). Annulus absent. Pseudorhiza terete, tapering downwards, surface grey (1D1–2) to dark grey (1F1–1F2), smooth; context solid, fibrous.. Odour slightly fragrant. Taste not distinctive.

Basidia of two conspicuously different types by the sterigmata apex acute or obtuse, first type rather abundant, sterigmata apex acute, clavate, mostly 2–spored, sometimes 4–spored, 20–30 × 7–15 µm, av. 25 ± 2.4 × 11 ± 1.8 µm, sterigmata 1–4 µm long; the second type fewer in number, sterigmata obtuse, clavate, mostly 2–spored, sometimes 4–spored, 24–32 × 8–15 µm, av. 27 ± 2.2 × 10 ± 1.1 µm, sterigmata 2–3 (–5) µm long. Basidiospores [139/2/2] 6.5–10.2 (–11.1) × (3.9–) 4.5–8.2 (–9.1) µm, L_m × W_m = 8.6 ± 1.0 × 5.9 ± 0.8 µm, Q = 1.2–1.8, Q_m = 1.47 ± 0.16, broadly ellipsoid to ellipsoid, colorless, thin-walled, smooth. Hymenophoral trama regular, parallel, 150–200 µm wide, made up of thin-walled, ellipsoid to clavate inflated cells hyphae 20–28 µm wide, filamentous hyphae abundant, 3–6 µm wide. Subhymenium 10–20 µm thick, with 1–2 layers of ovoid, subglobose, fusiform, ellipsoid or irregular cells, 7–13 × 3–6 µm. Cheilocystidia 14–37 × 13–23 µm, av. 23 ± 9.1 × 18 ± 4.9 µm, ellipsoid, obovoid to broadly clavate, thin-walled. Pleurocystidia similar to cheilocystidia in shape, 33–50 × 19–32 µm, av. 37 ± 9.1 × 25 ± 5.8 µm. Lamellar edge heteromorphous, more in number of cheilocystidia. Pileipellis 2-layered, suprapellis an ixocutis, 9–39 × 3–5 µm av. 23 ± 8.1 × 4 ± 0.5 µm, cylindrical hyphae with obtuse apex, thin-walled, hyaline at places in KOH; subpellis made up of inflated elements, subcylindrical, 17–49 × 10–18 µm av. 34 ± 9.2 × 13 ± 2.4 µm. Clamp connections not seen in any tissues.

Habitat and distribution. Solitary above underground termite nests; basidiomata occurring in summer. Known from southwestern China.

Figure 5. Fresh basidiomata representative of *Termitomyces yunnanensis* **a, b** HKAS 124501 **c** HKAS 124502 **d** HKAS 124503 **e** HKAS 124517. Scale bars: 1 cm. Photographs by Song-Ming Tang.

Additional material examined. **China**. Yunnan Province: Kunming city, Shilin county, Banqiao town, 11 July 2019 alt. 1500 m, J. He (HKAS 124502); ibid, 11 July 2019, alt. 1350 m, S.M. Tang (KHAS 124503); Yuxi city, Eshan county, 7 August 2019, alt. 1480 m, S.M. Tang (HKAS 124517).

Notes. *Termitomyces yunnanensis* is distinguished from other *Termitomyces* species by its clearly striated pileus surface, medium grey, olive grey, light grey to greenish grey at center, light grey towards margin on the pileus surface; perforatorium dark grey and umbonate, thin-walled or thick-walled basidia, ellipsoid, obovoid to broadly clavate cheilocystidia and pleurocystidia.

According to our multi-locus phylogenetic analyses, *T. yunnanensis* was clustered together with *T. subumkowaan* Mossebo and *T. robustus*. However, *T. subumkowaan* has yellowish to brownish grey pileus, obtuse perforatorium concolorous with pileus,

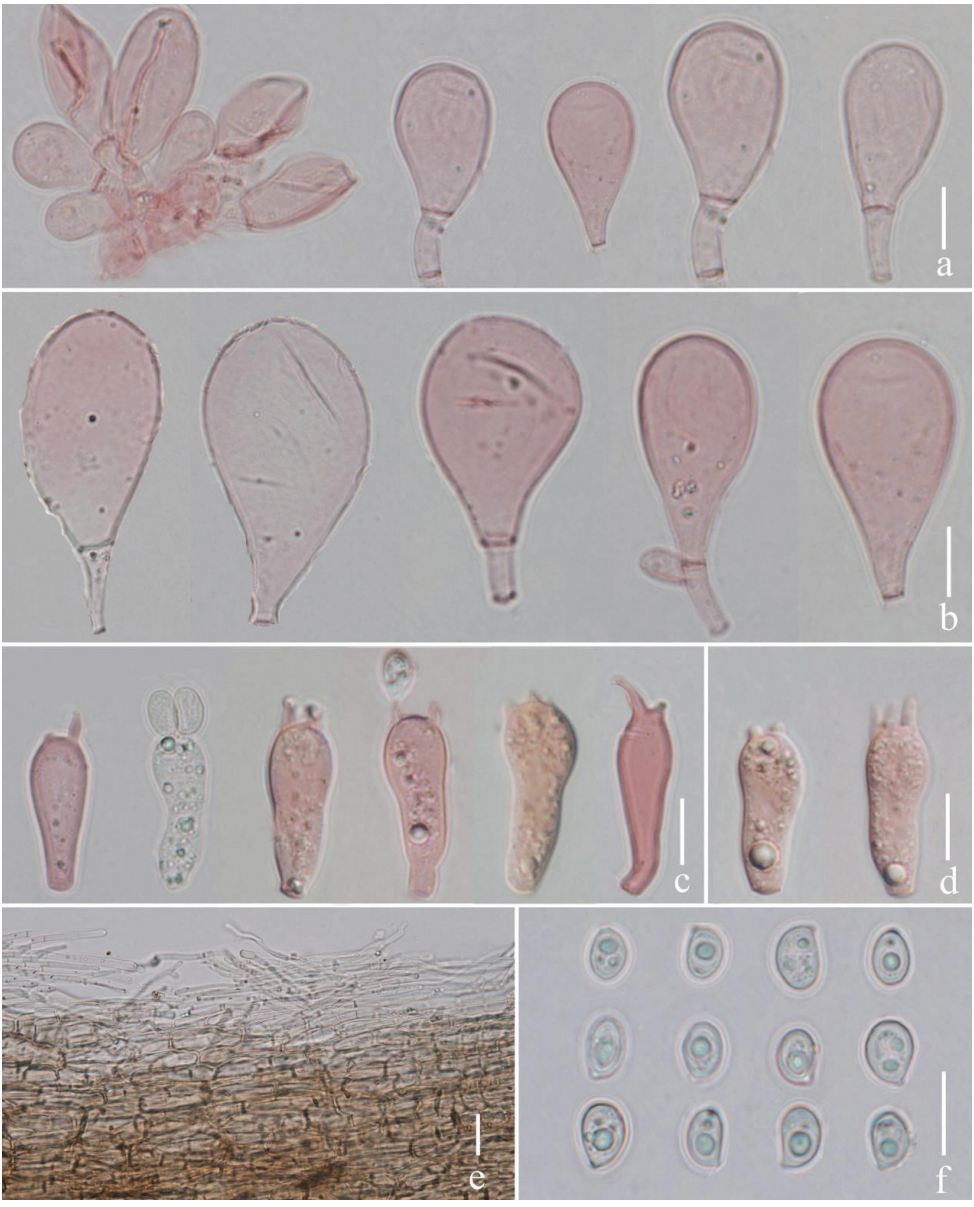

Figure 6. *Termitomyces yunnanensis* **a** lamellar edge and cheilocystidia **b** pleurocystidia **c** basidia with acute sterigmata apex **d** basidia with obtuse sterigmata apex **e** pileipellis **f** basidiospores. Scale bars: 10 μm (**a–d, f**); 20 μm (**e**). Photographs by Song-Ming Tang.

stipe cylindrical, bulbous at the base, and pleurocystidia extremely rare (Mossebo et al. 2002; Mossebo et al. 2017). *Termitomyces robustus* has bigger pileus (7–11 cm), pileus grey, often rimose-squamulose when dry, perforatorium concolorous with pileus, acute and bigger perforatorium (Sitotaw et al. 2015).

Morphologically, *T. medius* R. Heim & Grassé, *T. mammiformis*, *T. griseiumbo* and *T. striatus* are similar to *T. yunnanensis* in having a clearly striated pileus surface. However, *T. medius* has smaller pileus (2.2–2.9 cm), and acute perforatorium, reflexed pileus margin when mature, smaller basidiospores (6–8 × 4–4.8 μm) and basidia (17–20 × 7–7.5 μm), pleurocystidia (25–40 × 12–25 μm) narrowly utriform, ovoid to obovoid (Heim 1977). *Termitomyces mammiformis* has subconical scales on the pileus surface, and an annulus on the stipe (Heim 1977). *Termitomyces grisumbo* has ochraceous pileus, and relatively bigger pileus (12–15 cm), and smaller basidiospores (5.5–7 × 3.5–4.5 μm), pleurocystidia abundant and polymorphic, clavate to pyriform, with one or more transverse septa (Mossebo et al. 2002).

Termitomyces striatus originally described from Sierra Leone (Africa), has clear striae on the pileus, ring of scales on the pseudorhiza, and small basidiospores (6.5–7.7 × 4–5 μm) (Heim 1977). However, *T. striatus* was divided 10 formae (Mossebo et al. 2009), namely f. *annulatus*, f. *striatus*, f. *ochraceus*, f. *bibasidiatus*, f. *griseus*, f. *griseiumboides*, f. *subumbonatus*, f. *brunneus*, f. *pileatus* and f. *subclypeatus.* However, according to the phylogenetic analysis of nrLSU and mtSSU sequence in Mossebo et al. (2017), f. *striatus* (tgf99), f. *bibasidiatus* (DM280), f. *subumbonatus* (DM208) and f. *subclypeatus* (DM151, DM370) were in a different species-level clades, and should therefore be considered as different species. *Termitomyces* f. *bibasidiatus*, f. *subumbonatus*, f. *subclypeatus* were originally described from Cameroon (Africa) and these species are morphologically different from *T. yunnanensis.* *Termitomyces* f. *bibasidiatus* has relatively long pseudorhiza (20–60 cm), pale, reddish grey to brownish orange yellow pileus, and globose to ovoid pileipellis cells (Mossebo et al. 2017). An annulus is present in *Termitomyces* f. *subumbonatus* (Mossebo et al. 2002), but absent in *T. yunnanensis*. *Termitomyces* f. *subclypeatus* has whitish orange to pale orange pileus with a greyish yellow to brownish orange perforatorium (Mossebo et al. 2017).

Key to species of *Termitomyces* reported from China

To date, 14 *Termitomyces* species have been reported from China. However, the identification of some species, namely *T. aurantiacus*, *T. eurrhizus*, *T. entolomoides*, *T. globulus*, *T. mammiformis* and *T. tylerianus*, was based on morphology only. Further studies using DNA sequence analyses are required to confirm or inform the presence of those species in China.

1 Basidiomata small, with pileus diam. ≤ 4.5 cm when mature **2**
– Basidiomata medium to large, with pileus diam. > 4.5 cm when mature **5**
2 Pileus surface cream to whitish; pileus diam. 2.5–3.0 cm; perforatorium pointed, pseudorhiza long and slender, cheilocystidia and pleurocystidia absent, annulus present ..... ***T. tylerianus***
– Pileus surface brownish-gray, dirty white, grayish brown **3**
3 Pseudorhiza absent or present; pileus small, diam. 1.2–2.5 cm, dirty-white, soon split at the margin ..... ***T. microcarpus***
– Pseudorhiza present, pileus larger **4**

4 Pileus 2.0–4.5 cm diam., stipe white to cream, cylindrical, smooth ..... ***T. fragilis***
– Pileus 3.5–4.0 cm diam.; stipe pale grey, tapering upwards, floccules..... ***T. entolomoides***
5 Pileus white or greyish white..... **6**
– Pileus ochraceous-orange or yellowish-brown, grey to dark brown or dirty white..... **7**
6 Stipe surface smooth, perforatorium obtuse, gray to brownish gray..... ***T. heimii***
– Stipe surface squamulose, perforatorium mammiform, pale brown to dark brown ..... ***T. mammiformis***
7 Pileus ochraceous-orange or yellowish-brown..... **8**
– Pileus grey to dark brown or dirty white **9**
8 Perforatorium mucronate, pileus reddish-brown, 5–8 cm diam.; stipe white to whitish, cylindrical..... ***T. aurantiacus***
– Perforatorium non-differentiated, pileus reddish-brown to yellowish-brown, 15–20 cm diam., stipe white, smooth and tapering upwards..... ***T. globulus***
9 Annulus present; perforatorium strongly differentiated; stipe cylindrical, pseudorrhiza black and long..... ***T. eurrhizus***
– Annulus absent, pseudorrhiza white to pale yellow..... **10**
10 Stipe cylindrical **11**
– Stipe tapering upwards..... **12**
11 Pileus densely tomentose to tomentose-squamulose, regular greyish white and grey dark rimose-squamulose in dry condition..... ***T. intermedius***
– Pileus surface conspicuously venose, smooth..... ***T. yunnanensis***
12 Stipe surface with white to yellowish-brown floccules and tapering upwards, pileus 5–22 cm diam.; perforatorium broadly round or blunt..... ***T. bulborhizus***
– Stipe surface smooth **13**
13 Stipe grey, cheilocystidia few, broadly clavate, perforatorium acute, pileus dark grey, greyish white to grey, stipe greyish white to grey on the surface ..... ***T. tigrinus***
– Stipe white, cheilocystidia common mostly Y-shaped, perforatorium obtuse, pileus white to cream, stipe white on the surface..... ***T. upsilocystidiatus***

Discussion

In this study, we combined sequences of three non-translated loci (nrLSU, mrSSU and ITS) to carry out phylogenetic analyses of *Termitomyces* species in order to investigate the phylogenetic relationships between the two new species we described and other *Termitomyces* species.

Most *Termitomyces* species have uniform morphology, although some show extensive variability. In this study, five *T. intermedius* specimens were collected from Yunnan Province, China and showed differences in stipe surface colour and cheilocystidia shape when compared to the holotype of *T. intermedius* from Japan (Terashima et al. 2016). However, the latter, and our collections had identical DNA sequences

(see above notes), which indicates their conspecificity. *Termitomyces le-testui* (Pat.) R. Heim, *T. microcarpus* (Berk. & Broome) R. Heim, *T. striatus*, and *T. schimperi* were also reported to be morphologically variable, with multiple formae described (See Index Fungorum). However, some specimens identified as *T. striatus* (DM280, DM151, BR5020212704478V, BR5020168468769 and BR5020169404421), despite showing similar morphology, clustered in different species-level clades in our phylogeny. Because of this morphological variability in some *Termitomyces* species, species identification or delineation should not be based only on morphology. Molecular analyses are also necessary to resolve the relationship between *Termitomyces* species.

In China, *Termitomyces* species are considered as delicacies, widely collected and consumed by local people, usually stir-fried with chili, bacon and garlic. They are called "Jizongjun" in Chinese, which means the taste of chicken. *Termitomyces* species are considered nutritious (a good source of proteins, lipids, crude fibres and minerals) for a daily healthy diet (Kansci et al. 2003). *Termitomyces* are an important source of income for people from rural areas of China. *Termitomyces tigrinus*, *T. intermedius* and *T. yunnanensis* are commonly found in mushroom markets from July to September and often sold around 120–200 RMB/kg.

To date, 14 *Termitomyces* species have been reported in China (including the result in this study) namely *T. aurantiacus* (Yunnan and Gui zhou), *T. bulborhizus* (Sichuan and Yunnan), *T. eurrhizus* (Berk.) R. Heim (Yunnan, Henan, Guizhou, Tibet, Guangdong and Hainan), *T. entolomoides* R. Heim (Guangdong), *T. fragilis* L. Ye, Karun, J. C. Xu, K. D. Hyde & Mortimer (Yunnan), *T. globulus* R. Heim & Gooss.-Font. (Sichuan and Yunnan), *T. heimii* (Yunnan), *T. intermedius* Har. Takah. & Taneyama (Henan, Guangdong and Yunnan), *T. mammiformis* (Yunnan and Tibet), *T. microcarpus* (Yunnan, Sichuan and Guizhou), *T. tigrinus* (Yunnan), *T. tylerianus* Otieno (Yunnan and Guangdong), *T. upsilocystidiatus* (Yunnan), *T. yunnanensis* (Yunnan) (Wei et al. 2004; Huang et al. 2017; Ye et al. 2019; Tang et al. 2020). These species are mainly distributed in southern part of China.

Termitomyces tigrinus and *T. yunnanensis* are widely distributed in the subtropical broad-leaved forests of Dali, Yuxi, Baoshan, and Chuxiong in Yunnan, where the annual average temperature is 12–22 °C, and the elevation is between 1,000–3,500 m (Xiwen and Walker 1986). *Termitomyces* species form symbiotic relationships with termites in the subfamily Macrotermitinae, and their distribution thus depends on the presence of termites. In China, Yunnan, Guangxi and Hainan provinces have a tropical to subtropical climate suitable for termites, hence the abundance of *Termitomyces* species in those provinces.

Acknowledgements

This work was supported by grants from the National Natural Science Foundation of China to Shu-Hong Li (No. 32060006, 31160010, 31560009, and 31960391) and Yunnan Science and Technology Department and Technology Talents and Platform Program

"Yunnan Province Technology Innovation Talents Objects" (Project ID 2017HB084) and edible fungi industry system of China (CARS-20), and YCJ[2020]323. The authors appreciate the support given by Thesis Writing Grant of Mae Fah Luang University, Thailand, to S.-M. Tang. J. Degreef, A. Mukandera and the herbarium of Meise Botanic Garden, Belgium (BR) are also thanked for the loan of specimens.

References

Aanen DK, Eggleton P, Rouland-Lefèvre C, Guldberg-Frøslev T, Rosendahl S, Boomsma JJ (2002) The evolution of fungus-growing termites and their mutualistic fungal symbionts. Proceedings of the National Academy of Sciences of the United States of America 99(23): 14887–14892. https://doi.org/10.1073/pnas.222313099

Beeli M (1927) Contribution à l'étude de la flore mycologique du Congo. IV. Bulletin de la Société Royale de Botanique de Belgique 60(2): 75–87. https://doi.org/10.1080/00378941.1928.10836267

Bellanger JM, Moreau PA, Corriol G, Bidaud A, Chalange R, Dudova Z, Richard F (2015) Plunging hands into the mushroom jar: A phylogenetic framework for Lyophyllaceae (Agaricales, Basidiomycota). Genetica 143(2): 169–194. https://doi.org/10.1007/s10709-015-9823-8

Berkeley M (1847) Decades of fungi XII–XIV. Lond Journal of Botany 6: 312–326.

Chandra K, Ghosh K, Roy SK, Mondal S, Maiti D, Ojha AK, Das D, Mondal S, Islam SS (2007) A water soluble glucan isolated from an edible mushroom *Termitomyces microcarpus*. Carbohydrate Research 342(16): 2484–2489. https://doi.org/10.1016/j.carres.2007.07.013

Frøslev TG, Aanen DK, Laessøe T, Rosendahl S (2003) Phylogenetic relationships of *Termitomyces* and related taxa. Mycological Research 107(11): 1277–1286. https://doi.org/10.1017/S0953756203008670

Gómez LD (1994) Una nueva especie neotropical de *Termitomyces* (Agaricales: Termitomycetaceae). Revista de Biología Tropical 42(3): 439–441.

Hall T (2007) BioEdit v7. http://www.mbio.ncsu.edu/BioEdit/BioEdit.html

He MQ, Zhao RL, Hyde KD, Begerow D, Kemler M, Yurkov A, McKenzie EHC, Raspé O, Kakishima M, Sánchez-Ramírez S, Vellinga EC, Halling R, Papp V, Zmitrovich IV, Buyck B, Ertz D, Wijayawardene NN, Cui BK, Schoutteten N, Liu XZ, Li TH, Yao YJ, Zhu XY, Liu AQ, Li GJ, Zhang MZ, Ling ZL, Cao B, Antonín V, Boekhout T, Da Silva BDB, De Crop E, Decock C, Dima B, Dutta AK, Fell JW, Geml J, Ghobad-Nejhad M, Giachini AJ, Gibertoni TB, Gorjón SP, Haelewaters D, He SH, Hodkinson BP, Horak E, Hoshino T, Justo A, Lim YW, Menolli Jr N, Mešić A, Moncalvo JM, Mueller GM, Nagy LG, Nilsson RH, Noordeloos M, Nuytinck J, Orihara T, Ratchadawan C, Rajchenberg M, Silva-Filho AGS, Sulzbacher MA, Tkalčec Z, Valenzuela R, Verbeken A, Vizzini A, Wartchow F, Wei T-Z, Weiß M, Zhao C-L, Kirk PM (2019) Notes, outline and divergence times of Basidiomycota. Fungal Diversity 99(1): 105–367. https://doi.org/10.1007/s13225-019-00435-4

Heim R (1942a) Les champignons des termitières: Nouveaux aspects d'un problème de biologie et de systématique générales. La Revue Scientifique 80: 69–86.

Heim R (1942b) Nouvelles études descriptives sur les agarics termitophiles d'Afrique tropicale. Archives du Muséum National d'Histoire Naturelle 18: 107–166.

Heim R (1951) Les *Termitomyces* du Congo belge recueillis par Madame Goossens-Fontana. Bulletin du Jardin Botanique de l'Etat [Bruxelles] 21(3/4): 205–222. https://doi.org/10.2307/3666672

Heim R (1977) Termites et champignons. Les champignons termitophiles d'Afrique noire et d'Asie méridionale. Ed. Boubée, Paris, 205 pp.

Hofstetter V, Clémençon H, Vilgalys R, Moncalvo JM (2002) Phylogenetic analyses of the Lyophylleae (Agaricales, Basidiomycota) based on nuclear and mitochondrial rDNA sequences. Mycological Research 106(9): 1043–1059. https://doi.org/10.1017/S095375620200641X

Hofstetter V, Redhead SA, Kauff F, Moncalvo JM, Matheny PB, Vilgalys R (2014) Taxonomic revision and examination of ecological transitions of the Lyophyllaceae (Basidiomycota, Agaricales) based on a multigene phylogeny. Cryptogamie. Mycologie 35(4): 399–425. https://doi.org/10.7872/crym.v35.iss4.2014.399

Höhnel F, Litschauer V (1908) Fragmente zur Mykologie. V. Mitteilung (Nr. 169 bis 181). Sitzungsberichte der Kaiserlichen Akademie der Wissenschaften Math.-. Naturw. Klasse Abt. I 117: 985–1032.

Huang QJ, Zhang M, Zhou W (2017) *Termitomyces intermedius* a species distributed in the southern subtropical to temperate southern margin. Journal of Edible Fungi 24: 74–78. [in Chinese]

Hussain S, Afshan NS, Ahmad H, Khalid AN (2015) New report of edible mushroom, *Termitomyces umkowaan* from Pakistan. Sylwan 159(6): 185–197.

Izhar A, Khalid AN, Bashir H (2020) *Termitomyces sheikhupurensis* sp. nov. (Lyophyllaceae, Agaricales) from Pakistan, evidence from morphology and DNA sequences data. Turkish Journal of Botany 44(6): 694–704. https://doi.org/10.3906/bot-2003-51

Kansci G, Mossebo DC, Selatsa AB, Fotso M (2003) Nutrient content of some mushroom species of the genus *Termitomyces* consumed in Cameroon. Die Nahrung 47(3): 213–216. https://doi.org/10.1002/food.200390048

Katoh K, Standley DM (2013) MAFFT multiple sequence alignment software version 7: Improvements in performance and usability. Molecular Biology and Evolution 30(4): 772–780. https://doi.org/10.1093/molbev/mst010

Kobayashi Y, Katsuren M, Hojo M, Wada S, Terashima Y, Kawaguchi M, Shigenobu S (2021) Taxonomic revision of *Termitomyces* species found in Ryukyu Archipelago, Japan, based on phylogenetic analyses with three loci. Mycoscience 63(1): 33–38. https://doi.org/10.47371/mycosci.2021.11.001

Kornerup A, Wanscher JH (1978) Methuen handbook of colour, 3rd edn. Eyre Methuen, London, 252 pp.

Miller MA, Pfeiffer W, Schwartz T (2010) Creating the CIPRES Science Gateway for inference of large phylogenetic trees. 2010 Gateway Computing Environments Workshop (GCE), New Orleans, LA, USA, 2010, 1–8. https://doi.org/10.1109/GCE.2010.5676129

Moncalvo JM, Vilgalys R, Redhead SA, Johnson JE, James TY, Aime MC, Hofstetter V, Verduin SJ, Larsson E, Baroni TJ (2002) One hundred and seventeen clades of euagarics.

Molecular Phylogenetics and Evolution 23(3): 357–400. https://doi.org/10.1016/S1055-7903(02)00027-1

Mondal S, Chakraborty I, Pramanik M, Rout D, Islam SS (2004) Structural studies of water-soluble polysaccharides of an edible mushroom, *Termitomyces eurhizus*. A reinvestigation. Carbohydrate Research 339(6): 1135–1140. https://doi.org/10.1016/j.carres.2004.02.019

Mossebo DC, Amougou A, Atangana RE (2002) Contribution à l'étude du genre *Termitomyces* (Basidiomycètes) au Cameroun: Écologie et systématique. Bulletin de la Société Mycologique de France 118(3): 195–249.

Mossebo DC, Njouonkou AL, Piatek M, Kengni AB, Djamndo DM (2009) *Termitomyces striatus* f. *pileatus*, f. nov. and f. *brunneus* f. nov. from Cameroon with a key to central African species. Mycotaxon 107(1): 315–329. https://doi.org/10.5248/407.315

Mossebo DC, Essouman E, Machouart M, Gueidan C (2017) Phylogenetic relationships, taxonomic revision and new taxa of *Termitomyces* (Lyophyllaceae, Basidiomycota) inferred from combined nLSU and mtSSU rDNA sequences. Phytotaxa 321(1): 71–102. https://doi.org/10.11646/phytotaxa.321.1.3

Nylander JAA (2004) MrModeltest v. 2.2. [Program distributed by the author]. Uppsala University, Department of Systematic Zoology, Uppsala, Sweden.

Otieno NC (1969) Further contributions to a knowledge of termite fungi in East Africa: The genus *Termitomyces* Heim. Sydowia 22: 160–165.

Parent G, Thoen D (1977) Food value of edible mushrooms from Upper-Shaba region. Economic Botany 31(4): 436–445. https://doi.org/10.1007/BF02912557

Pegler DN, Vanhaecke M (1994) *Termitomyces* of Southeast Asia. Kew Bulletin 49(4): 717–736. https://doi.org/10.2307/4118066

Ronquist F, Huelsenbeck J, Teslenko M (2011) MrBayes version 3.2 manual: tutorials and model summaries. http://brahms.biology.rochester.edu/software.html

Saccardo P (1887) Sylloge Hymenomycetum, Vol. I. Agaricineae. Sylloge fungorum 5: 1–1146.

Seelan SJS, Yee CS, Fui FS, Dawood M, Tan YS (2020) New Species of *Termitomyces* (Lyophyllaceae, Basidiomycota) from Sabah (Northern Borneo), Malaysia. Mycobiology 48(2): 95–103. https://doi.org/10.1080/12298093.2020.1738743

Singer R (1945) New genera of fungi II. Lloydia 8: 139–144.

Sitotaw R, Mulat A, Abate D (2015) Morphological and molecular studies on *Termitomyces* species of Menge district, Asossa zone, Northwest Ethiopia. Science, Technology and Arts Research Journal 4(4): 49–57. https://doi.org/10.4314/star.v4i4.7

Stamatakis A (2014) RAxML version 8: A tool for phylogenetic analysis and post-analysis of large phylogenies. Bioinformatics 30(9): 1312–1313. https://doi.org/10.1093/bioinformatics/btu033

Tang SM, He MQ, Raspé O, Luo X, Zhang XL, Li YJ, Su KM, Li SH, Thongklang N, Hyde KD (2020) Two new species of *Termitomyces* (Agaricales, Lyophyllaceae) from China and Thailand. Phytotaxa 439(3): 231–242. https://doi.org/10.11646/phytotaxa.439.3.5

Terashima Y, Takahashi H, Taneyama Y (2016) The fungal flora in southwestern Japan: Agarics and boletes. Tokai University Press, Kanagawa, 324–355.

Usman M, Khalid AN (2020) *Termitomyces acriumbonatus* sp. nov. (Lyophyllaceae, Agaricales) from Pakistan. Phytotaxa 477(2): 217–228. https://doi.org/10.11646/phytotaxa.477.2.6

Vaidya G, Lohman DJ, Meier R (2011) SequenceMatrix: Concatenation software for the fast assembly of multi-gene datasets with character set and codon information. Cladistics 27(2): 171–180. https://doi.org/10.1111/j.1096-0031.2010.00329.x

Venkatachalapathi A, Paulsamy S (2016) Exploration of wild medicinal mushroom species in Walayar valley, the Southern Western Ghats of Coimbatore District Tamil Nadu. Mycosphere 7(2): 118–130. https://doi.org/10.5943/mycosphere/7/2/3

Vilgalys R, Hester M (1990) Rapid genetic identification and mapping of enzymatically amplified ribosomal DNA from several *Cryptococcus* species. Journal of Bacteriology 172(8): 4238–4246. https://doi.org/10.1128/jb.172.8.4238-4246.1990

Wei TZ, Yao YJ, Wang B, Pegler DN (2004) *Termitomyces bulborhizus* sp. nov. from China, with a key to allied species. Mycological Research 108(12): 1458–1462. https://doi.org/10.1017/S0953756204001042

Wei TZ, Tang BH, Yao YJ, Pegler DN (2006) A revision of *Sinotermitomyces*, a synonym of *Termitomyces* (Agaricales). Fungal Diversity 21: 225–237.

White TJ, Bruns T, Lee S JWT, Taylor J (1990) Amplification and direct sequencing of fungal ribosomal RNA genes for phylogenetics. In: Innis MA, Gelfand DH, Sninsky JJ, White TJ (Eds) PCR Protocols: a Guide to Methods and Applications. Academic Press, New York, 315–322. https://doi.org/10.1016/B978-0-12-372180-8.50042-1

Willis E (2007) The Taxonomic Identity of *Termitomyces aurantiacus* using the internal transcribed spacer regions 1 & 2 (ITS1 & ITS2) of the ribosomal DNA (rDNA). Doctoral dissertation, University of Putra, Malaysia.

Xiwen L, Walker D (1986) The plant geography of Yunnan Province, southwest China. Journal of Biogeography 13(5): 367–397. https://doi.org/10.2307/2844964

Ye L, Karunarathna SC, Li H, Xu J, Hyde KD, Mortimer PE (2019) A survey of *Termitomyces* (Lyophyllaceae, Agaricales), including a new species, from a subtropical forest in Xishuangbanna, China. Mycobiology 47(4): 391–400. https://doi.org/10.1080/12298093.2019.1682449

Zang M (1981) *Sinotermitomyces*, a new genus of Amanitaceae from Yunnan, China. Mycotaxon 13: 171–174.

MycoKeys 95: 83–100 (2023)
doi: 10.3897/mycokeys.95.98986
https://mycokeys.pensoft.net

RESEARCH ARTICLE

A peer-reviewed open-access journal
MycoKeys
Launched to accelerate biodiversity research

Two new species of *Astrothelium* from Sud Yungas in Bolivia and the first discovery of vegetative propagules in the family Trypetheliaceae (lichen-forming Dothideomycetes, Ascomycota)

Martin Kukwa[1], Pamela Rodriguez-Flakus[2], André Aptroot[3], Adam Flakus[2]

1 *Department of Plant Taxonomy and Nature Conservation, Faculty of Biology, University of Gdańsk, Wita Stwosza 59, PL-80-308 Gdańsk, Poland* **2** *W. Szafer Institute of Botany, Polish Academy of Sciences, Lubicz 46, PL-31-512 Kraków, Poland* **3** *Laboratório de Botânica / Liquenologia, Instituto de Biociências, Universidade Federal de Mato Grosso do Sul, Avenida Costa e Silva s/n, Bairro Universitário, CEP 79070-900, Campo Grande, Mato Grosso do Sul, Brazil*

Corresponding author: Pamela Rodriguez-Flakus (p.rodriguez@botany.pl)

Academic editor: T. Lumbsch | Received 19 December 2022 | Accepted 18 January 2023 | Published 8 February 2023

Citation: Kukwa M, Rodriguez-Flakus P, Aptroot A, Flakus A (2023) Two new species of *Astrothelium* from Sud Yungas in Bolivia and the first discovery of vegetative propagules in the family Trypetheliaceae (lichen-forming Dothideomycetes, Ascomycota). MycoKeys 95: 83–100. https://doi.org/10.3897/mycokeys.95.98986

Abstract

Two new species of *Astrothelium* are described from the Yungas forest in Bolivian Andes. *Astrothelium chulumanense* is characterised by pseudostromata concolorous with the thallus, perithecia immersed for the most part, with the upper portion elevated above the thallus and covered, except the tops, with orange pigment, apical and fused ostioles, the absence of lichexanthone (but thallus UV+ orange-yellow), clear hamathecium, 8-spored asci and amyloid, large, muriform ascospores with median septa. *Astrothelium isidiatum* is known only in a sterile state and produces isidia that develop in groups on areoles, but easily break off to reveal a medulla that resembles soralia. Both species, according to the two-locus phylogeny, belong to *Astrothelium* s.str. The production of isidia is reported from the genus *Astrothelium* and the family Trypetheliaceae for the first time.

Keywords

lichens, lichenised fungi, Neotropics, South America, taxonomy

Introduction

Trypetheliaceae Zenker is the core family of the order Trypetheliales Lücking, Aptroot & Sipman and comprises about 500 species and 19 genera (Lücking et al. 2017; Wijayawardene et al. 2022); however, according to Aptroot et al. (2016a), the species diversity is higher. It is predicted that the total number of species is close to 800, with the majority of unrecognised taxa to be found in the Neotropics (Aptroot et al. 2016a). Nevertheless, with about 500 species already known, Trypetheliaceae is one of the three, together with Graphidaceae Dumort. and Pyrenulaceae Rabenh., most speciose families of tropical crustose lichens (Aptroot et al. 2016a; Mendonça et al. 2020).

Species of Trypetheliaceae grow in various, mostly tropical and subtropical ecosystems in Africa, America, Asia and Australia and are important and common elements in the rain and dry forests and savannahs (Aptroot et al. 2016a). Despite that, only recently, the generic concept within the family has been revised and the importance of morphological and chemical characters evaluated using molecular approaches (Lücking et al. 2016a; Hongsanan et al. 2020). This resulted in the recognition of several new species (e.g. Aptroot and Cáceres (2016); Aptroot and Lücking (2016); Aptroot et al. (2016b, 2019, 2022); Flakus et al. (2016); Lücking et al. (2016b); Cáceres and Aptroot (2017); Aptroot and Weerakoon (2018); Hongsanan et al. (2020); Jiang et al. (2022)).

Within Trypetheliaceae, the genus *Astrothelium* Eschw. is the most speciose and comprises about 275 species (Lücking et al. 2017; Wijayawardene et al. 2022). It is characterised by the following features: corticate thallus, ascomata which can be simple, aggregated or forming pseudostromata (often differing in structure and colour) and are immersed to prominent, with apical or eccentric and simple or fused ostioles, hyphal and usually carbonised ascomatal wall (textura intricata), clear or inspersed with oil droplets hamathecium and distoseptate, hyaline, transversely septate or muriform ascospores (Aptroot and Lücking 2016). *Astrothelium*, as presently circumscribed, is paraphyletic and consists of two clades. However, as the relationships between those two clades and the *Aptrootia* Lücking & Sipman and *Architrypethelium* Aptroot, are not fully resolved and supported, the conservative solution was adopted here, with *Aptrootia* and *Architrypethelium* treated as separate genera and all other species retained in the large genus *Astrothelium* (Lücking et al. 2016a).

In Bolivia, 35 species of *Astrothelium* are known so far, of which 12 have been recently described (Flakus et al. 2016). In this paper, we describe two further species from a mountain forest in Sud Yungas in Bolivia, including the peculiar, sterile species with isidia. This is the first time that vegetative lichenised propagules have been reported from the genus and the family Trypetheliaceae. Both species are characterised morphologically, anatomically and chemically. Additionally, a comparison with similar species is provided. The placement of both novel species in *Astrothelium* was corroborated by molecular analyses.

Materials and methods

Taxon sampling and morphological studies

Our study was based on specimens freshly collected by the authors and deposited at KRAM, LPB and UGDA. Morphology and anatomy were examined using stereo- and compound microscopes (Nikon SMZ 800, Nikon Eclipse 80i DIC; Tokyo, Japan). Sections were prepared manually using a razor blade. Sections and squash mounts were examined in tap water, 10% potassium hydroxide (KOH) (K) or lactophenol cotton blue (LPCB; Sigma-Aldrich, catalogue no. 61335-100ML; St. Louis, Missouri, USA) and amyloid reactions of anatomical structures were tested using Lugol's solution (I) (Fluka no. 62650-1L-F) or with Lugol's solution preceded by a 10% KOH treatment (K/I). All photomicrographs showing anatomical characters were made using transmitted differential interference contrast (DIC) microscopy. All measurements were made in distilled water. Lichen substances were investigated by thin-layer chromatography (TLC) following the methods by Culberson and Kristinsson (1970) and Orange et al. (2001).

DNA extraction, PCR amplification and DNA sequencing

Freshly collected hymenia or thallus fragments were removed from the specimens and carefully cleaned in double-distilled water (ddH_2O) on a microscope slide under sterile conditions to remove any visible impurities using ultra-thin tweezers and a razor blade. Genomic DNA was extracted from a few ascomata or thallus pieces using the QIAamp DNA Investigator Kit (Qiagen, Hilden, Germany) following the manufacturer's instructions. We amplified both the mtDNA small subunit DNA (mtSSU) using primers pair mrSSU1 and mrSSU3R (Zoller et al. 1999) and nuc rDNA large subunit (nuLSU) with primers ITS1F, LROR, LR3 and LR5 (Vilgalys and Hester 1990; Rehner and Samuels 1994). Polymerase chain reactions (PCR) were performed in a volume of 25 µl comprising 1 µl of DNA template, 0.2 µl of AmpliTaq 360 DNA polymerase (Applied Biosystems, California, USA), 2.5 µl of 10× AmpliTaq 360 PCR Buffer, 2.5 µl 25mM $MgCl_2$, 1 µl of each primer (10 µM), 2 µl GeneAmp dNTPs (10 mM; Applied Biosystems, California, USA), 0.2 µl bovine serum albumin (BSA; New England Biolabs, Massachusetts, USA) and sterile distilled water was added to attain the final volume. PCR amplifications were performed using the thermocycling conditions of Rodriguez-Flakus and Printzen (2014). PCR products were visualised by running 3 µl of the PCR product on 1% agarose gels. PCR amplicons were purified using the ExoSAP method (EURx, Gdańsk, Poland) and sequenced by Macrogen (Amsterdam, the Netherlands). The newly-generated mtSSU and nuLSU sequences were checked, assembled and edited manually using Geneious Pro 8.0. (Biomatters, Auckland, New Zealand) and deposited in GenBank.

Phylogenetic analyses and taxon selection

All sequences generated were checked by BLAST (Altschul et al. 1990) to verify potential contaminations by an unrelated fungus. BLAST searches of both mtSSU and nuLSU rDNA sequences from both species revealed the highest similarity with members of *Astrothelium* (Trypetheliaceae, Dothideomycetes). Therefore, we aligned our sequences with the available sequences of the members of *Astrothelium* (Lücking et al. 2016a) (Table 1). Alignments were generated for each region using MAFFT (Katoh et al. 2005) as implemented on the GUIDANCE2 Web server (Penn et al. 2010). GUIDANCE2 assigns a confidence score to each ambiguous nucleotide site in the alignment and later removes regions of uncertain columns. We used the default cut-off score of 0.93 in all single gene alignments. The following analyses were performed in the CIPRES Scientific Gateway (Miller et al. 2010). Maximum Likelihood (ML) analyses were carried out in each single-locus alignment using IQ-TREE version 2.1.2 (Nguyen et al. 2015; Chernomor et al. 2016) to detect potential conflicts. We performed 1000 ultrafast bootstrap replicates to estimate branch support amongst the two loci which later were concatenated to a single alignment. The concatenated dataset was used as an input file for analysing the ML in our studies. In which, we performed 5000 replicates under the best-fitting substitution model determined by the ModelFinder Plus (MFP) as implemented in IQ-TREE (Kalyaanamoorthy et al. 2017). The selected model was GTR+F+I+G2 according to AICc in our partitioned per each locus dataset (gene partitioned -s and -m + MFP + MERGE). Bayesian Inference (BI) of the phylogenetic relationships was calculated using the Markov Chain Monte Carlo (MCMC) approach as implemented in MrBayes 3.2.6 on XSEDE (Ronquist et al. 2012) using the partitions and substitution models obtained. Two independent parallel runs were started each with four incrementally heated (0.15) chains. This MCMC was allowed to run for 40 million generations, sampling every 1000th tree and discarding the first 50% of the sampled tree as a burn-in factor. The resulting ML and BI phylogenetic trees were visualised in TreeView (Page 1996). The tree was rooted by using *Architrypethelium* and *Aptrootia* species as the outgroups.

Results and discussion

Two new sequences of each marker (mtSSU and nuLSU) from two new species of *Astrothelium* were generated for this study (Table 1). The final DNA alignment consisted of sequences obtained from 98 specimens and two markers with a total of 1128 characters, 487 distinct patterns, 288 parsimony-informative, 102 singleton sites and 738 constant sites. The ML phylogenetic tree is presented in Fig. 1.

Table 1. Voucher data and GenBank accession numbers for the sequences included in this study. Newly-generated sequences are shown in bold.

Taxon	Origin	Collector	Voucher	Herbarium	Isolate	GenBank accession numbers	
						mtSSU	nuLSU
Aptrootia elatior	New Zealand	Knight	O61815	OTA	MPN560B	KM453821	KM453754
Aptrootia robusta	Australia	Lumbsch	20012	F	MPN235B	KM453822	KM453755
Aptrootia terricola	Costa Rica	Lücking	17211	F	DNA1501	DQ328995	KM453756
Architrypethelium lauropaluanum	Peru	Nelsen	Cit1P	F	MPN48	KX215566	KX215605
Architrypethelium nitens	Panama	Lücking	27038	F	MPN257	KM453823	KM453757
Architrypethelium uberinum	Brazil	Nelsen	s.n.	F	MPN489	–	KM453758
Astrothelium aenascens 1	Thailand	Luangsuphabool	27887	RAMK	HRK93	LC128018	LC127403
Astrothelium aenascens 2	Thailand	Luangsuphabool	27888	RAMK	HRK98	LC128019	LC127404
Astrothelium aeneum	Panama	Lücking	27056	F	MPN302	–	KX215606
Astrothelium bicolor	USA	Nelsen	4002a	F	MPN139	GU327706	GU327728
Astrothelium carassense	Brazil	Lücking	31004	F	MPN438	KM453849	KM453784
Astrothelium cecidiogenum	Costa Rica	Lücking	s.n.	F	N/A	DQ328991	–
Astrothelium chulumanense	Bolivia	Flakus	29985	KRAM	14-31	**OQ275191**	**OQ281430**
Astrothelium cinereorosellum 2	Philippines	RivasPlata	2106	F	MPN199C	–	KX215610
Astrothelium cinereorosellum 1	Philippines	RivasPlata	2110	F	MPN191	KM453873	KM453809
Astrothelium cinnamomeum	Costa Rica	Lücking	15322b	DUKE	AFTOL110	AY584632	AY584652
Astrothelium crassum	Peru	Nelsen	s.n.	F	MPN98	GU327685	GU327710
Astrothelium aff. *crassum*	Brazil	Cáceres	6011	F	MPN335	KM453827	KM453761
Astrothelium croceum	Peru	Nelsen	211D	F	MPN55	KX215567	KX215611
Astrothelium degenerans 1	Costa Rica	Lücking	17502b	CR	DNA1496	DQ328987	–
Astrothelium degenerans 2	Panama	Lücking	27109	F	MPN267	KM453835	KM453770
Astrothelium diplocarpum 2	Nicaragua	Lücking	28529	F	MPN210	KM453846	KM453781
Astrothelium diplocarpum 1	USA	Nelsen	s.n.	F	MPN134	KX215568	–
Astrothelium endochryseum	Brazil	Lücking	31088	F	MPN436	KM453837	KM453772
Astrothelium erubescens	Peru	Nelsen	AnaG	F	MPN96	KX215569	KX215614
Astrothelium euthelium 1	Thailand	Lücking	24075	F	MPN226	–	KX215615
Astrothelium euthelium 2	Philippines	RivasPlata	1194B	F	MPN22B	–	KX215616
Astrothelium flavocoronatum 1	Thailand	Luangsuphabool	27890	RAMK	KY859	LC128014	LC127398
Astrothelium flavocoronatum 2	Thailand	Luangsuphabool	27889	RAMK	TSL63	AB759874	LC127397
Astrothelium floridanum 1	USA	Nelsen	4008	F	MPN132	GU327705	GU327727
Astrothelium floridanum 2	Panama	Lücking	27131a	F	MPN304	KM453876	KM453811
Astrothelium gigantosporum	Panama	Lücking	33037	F	MPN590	KM453851	KM453786
Astrothelium grossum 2	Panama	Lücking	27045	F	MPN259	KM453834	KM453769
Astrothelium grossum 1	Peru	Nelsen	4000a	F	MPN47	GU327689	GU327713
Astrothelium inspersoaeneum	Peru	Nelsen	Cit1K	F	MPN45	KX215571	–
Astrothelium isidiatum	Bolivia	Flakus	30000	KRAM	14-8	**OQ275190**	**OQ281431**
Astrothelium kunzei 1	Salvador	Lücking	28120	F	MPN201B	–	KX215624
Astrothelium kunzei 2	Salvador	Lücking	28137	F	MPN203B	–	KX215625
Astrothelium laevigatum	Brazil	Lücking	31010	F	MPN430	KX215572	–
Astrothelium laevithallinum	Brazil	Lücking	31061	F	MPN442	KM453836	KM453771
Astrothelium leucoconicum	Peru	Nelsen	4000c	F	MPN42	KM453830	KM453764
Astrothelium leucosessile 1	Panama	Lücking	27059	F	MPN258	KM453828	KM453762
Astrothelium leucosessile 2	Brazil	Cáceres	11201	F	MPN713	KM453869	KM453805
Astrothelium macrocarpum 1	Panama	Lücking	27077	F	MPN260	KM453829	KM453763
Astrothelium macrocarpum 2	Thailand	n/a	27892	RAMK	UBN37	LC128015	LC127400
Astrothelium macrocarpum 3	Thailand	n/a	27894	RAMK	UBN43	LC128016	LC127399
Astrothelium macrostiolatum	Thailand	Luangsuphabool	27895	RAMK	PHL84	LC128022	LC127407
Astrothelium megaspermum 2	Gabon	Ertz	9725	BR	AFTOL2094	GU561847	FJ267702

Taxon	Origin	Collector	Voucher	Herbarium	Isolate	GenBank accession numbers	
						mtSSU	nuLSU
Astrothelium megaspermum 3	USA	Nelsen	s.n.	F	MPN138	KX215574	KX215632
Astrothelium megaspermum 1	Thailand	Nelsen	s.n.	F	MPN32B	KX215576	–
Astrothelium meristosporum 2	Philippines	RivasPlata	2128	F	MPN198	–	KX215634
Astrothelium meristosporum 1	Philippines	RivasPlata	2108	F	MPN189	KM453850	KM453785
Astrothelium neglectum 1	Thailand	Luangsuphabool	27898	RAMK	TAK8	LC128025	LC127410
Astrothelium neglectum 2	Thailand	Luangsuphabool	27896	RAMK	TAK12	LC128026	LC127411
Astrothelium neglectum 3	Thailand	Luangsuphabool	27897	RAMK	TAK17	LC128027	LC127412
Astrothelium neogalbineum 1	Brazil	Cáceres	11100	F	MPN711	KM453877	KM453812
Astrothelium neogalbineum 2	Peru	Nelsen	Cit1T	F	MPN51	KX215577	KX215635
Astrothelium neoinspersum 2	Peru	Nelsen	AnaJ	F	MPN61C	–	KX215636
Astrothelium neoinspersum 1	Peru	Nelsen	s.n.	F	MPN62	KM453866	KM453802
Astrothelium neovariolosum 1	Thailand	Luangsuphabool	27899	RAMK	KY777	LC128023	LC127408
Astrothelium neovariolosum 2	Thailand	Luangsuphabool	27900	RAMK	KY848	LC128024	LC127409
Astrothelium nicaraguense 1	Nicaragua	Lücking	28503	F	MPN205	–	KX215637
Astrothelium nicaraguense 2	Nicaragua	Lücking	28551	F	MPN213	–	KX215639
Astrothelium nitidiusculum 2	Fiji	Lumbsch	20547i	F	MPN768	–	KX215640
Astrothelium nitidiusculum 1	Brazil	Cáceres	11297	F	MPN704	KM453868	KM453804
Astrothelium norisianum	Peru	Nelsen	4000d	F	MPN52C	KM453848	KM453783
Astrothelium aff. *norisianum*	Peru	Nelsen	Cit1B	F	MPN23B	KX215578	KX215607
Astrothelium aff. *obscurum*	Philippines	RivasPlata	2175	F	MPN194	–	KX215608
Astrothelium obtectum	Brazil	Lücking	31242	F	MPN422	KM453832	KM453767
Astrothelium perspersum	Gabon	Ertz	9716	BR	AFTOL2099	GU561848	FJ267701
Astrothelium phlyctaena 1	USA	Nelsen	4167	F	MPN373	–	KX215641
Astrothelium phlyctaena 2	USA	Nelsen	4149	F	MPN386	–	KX215644
Astrothelium pulcherrimum	Panama	Lücking	27046	F	MPN313	KM453879	KM453814
Astrothelium pupula	Colombia	Lücking	26305	F	MPN224	KM453880	KM453815
Astrothelium purpurascens	Peru	Nelsen	s.n.	F	MPN53C	KM453847	KM453782
Astrothelium robustum 1	Costa Rica	Mercado	586	F	MPN754	KM453826	KM453760
Astrothelium robustum 2	Nicaragua	Lücking	28519	F	MPN209	–	KX215645
Astrothelium robustum 3	Nicaragua	Lücking	28547	F	MPN212	–	KX215646
Astrothelium rufescens 1	Brazil	Nelsen	B1	F	MPN143	–	KX215650
Astrothelium rufescens 2	Argentina	Lücking	30511	CTES	MPN346	–	KX215652
Astrothelium sanguinarium 1	Brazil	Cañez	3133	CGMS	MPN765	KM453853	KM453788
Astrothelium sanguinarium 2	Brazil	Cañez	3135	CGMS	MPN766	KX215579	KX215653
Astrothelium sanguinarium 3	Brazil	Cañez	3137a	CGMS	MPN767	KX215580	KX215654
Astrothelium scoria	Panama	Lücking	27181	F	MPN310	–	KX215655
Astrothelium scorizum	Brazil	Lücking	29814	F	MPN336	KM453872	KM453808
Astrothelium aff. *sepultum 2*	Costa Rica	Lücking	21027	F	MPN229	–	KX215609
Astrothelium aff. *sepultum 1*	Peru	Nelsen	4001a	F	MPN63C	GU327690	GU327714
Astrothelium siamense 1	Thailand	Luangsuphabool	27901	RAMK	KRB105	LC128020	LC127405
Astrothelium siamense 2	Thailand	Luangsuphabool	27902	RAMK	KRB139	LC128021	LC127406
Astrothelium subcatervarium	Peru	Nelsen	4009a	F	MPN97	GU327707	GU327729
Astrothelium subendochryseum	Salvador	Lücking	28121	F	MPN202B	–	KX215659
Astrothelium subinterjectum	Brazil	Nelsen	B15	F	MPN157	KX215583	KX215660
Astrothelium subscoria 1	Nicaragua	Lücking	28640	F	MPN217	KM453878	KM453813
Astrothelium subscoria 2	Bolivia	Lücking	29010	F	MPN325	KX215584	KX215661
Astrothelium tuberculosum	Costa Rica	Lücking	16306a	F	DNA1504	DQ329008	–
Astrothelium variolosum 1	Peru	Nelsen	s.n.	F	MPN43	KM453833	KM453768
Astrothelium variolosum 2	Peru	Nelsen	Cit1F	F	MPN41	KX215585	KX215662

The phylogenetic reconstruction shows that all *Astrothelium* species form a well-supported clade divided into two subclades, of which the smaller and well-supported (six species) refers to the clade labelled as *Astothelium* s.lat. by Lücking et al. (2016a) and the larger one refers to *Astrothelium* s.str., but is poorly supported (Fig. 1). Our results differ from those received by Lücking et al. (2016a) as all species of *Astrothelium*, although still divided into two groups, form one clade, with *Aptrootia* and *Architrypethelium* forming the sister clade. However, our analyses were restricted only to *Astrothelium* and two related genera, *Aptrootia* and *Architrypethelium*.

Astrothelium chulumanense and *A. isidiatum* are placed in the larger clade defined by Lücking et al. (2016a) as *Astrothelium* s.str. *Astrothelium chulumanense* forms a strongly-supported clade together with *A. robustum* Müll. Arg.; however, the relationship of this two-species clade with other species within *Astrothelium* s.str. is not well resolved (Fig. 1). *Astrothelium isidiatum* is grouped with *A. laevigatum* Müll. Arg., but the support is weak (Fig. 1). In addition, the relationships of this two-species clade within *Astrothelium* s.str. are not supported.

The most surprising finding is the presence of isidia in one of the new species, *Astrothelium isidiatum*. This is the first case when vegetative lichenised diaspores are reported in Trypetheliaceae. Moreover, the new species is sterile and lichen taxa being sterile, but reproducing by isidia or other similar propagules consisting of mycobiont and photobiont, are known in several other groups of lichenised fungi. In extreme cases even entire lineages evolved into permanently asexually reproducing genera, like *Botryolepraria* Canals et al., *Lepraria* Ach. and others (Canals et al. 1997; Ekman and Tønsberg 2002; Kukwa and Pérez-Ortega 2010; Hodkinson and Lendemer 2013; Lendemer and Hodkinson 2013; Guzow-Krzemińska et al. 2019). In some genera, sterile taxa producing vegetative diaspores prevail, like in *Herpothallon* Tobler (Aptroot et al. 2009), but in others, they are rarer, for example, in *Ochrolechia* A. Massal. (Kukwa 2011). It seems that, in groups of perithecioid lichens, they are much rarer than in apothecioid lichens (e.g. Diederich and Ertz (2020); Orange and Chhetri (2022)). *Astrothelium isidiatum* is the first species of the Trypetheliaceae, as mentioned above, reproducing by lichenised propagules. However, it is highly possible that more such taxa can be discovered in poorly-explored areas, like Bolivian and other South American ecosystems, but such sterile lichens cause difficulties in placing them properly in higher taxa without molecular approaches; therefore, they can be easily omitted in taxonomic revisions. Additionally, they may have more inconspicuous thalli compared to fertile species (thallus areoles of *A. isidiatum* were found dispersed amongst other lichens) and can be easily overlooked.

The two new species of *Astrothelium*, as well as some of these recently described taxa within Trypetheliaceae from Bolivia by Flakus et al. (2016), may be potentially endemic to some areas in this country. With tens of thousands of samples collected by our team across all major ecosystems in Bolivia over almost 20 years, single or only very few records of each new species have been found (Flakus et al. 2016), which may suggest their restricted distribution. This situation can be similar to the genus *Sticta*

Figure 1. Phylogenetic placement of the two new species of *Astrothelium* within Trypetheliaceae inferred from ML analyses of combined mtSSU and nuLSU rDNA dataset. *Aptrootia* and *Architrypethelium* species were used as the outgroups. Bold branches represent either bootstrap values ≥ 70 and/or Bayesian posterior probabilities ≥ 0.95.

(Schreb.) Ach. in which several species are confined only to some regions (Moncada et al. 2014, 2018, 2020; Dal Forno et al. 2018; Simon et al. 2018; Mercado-Díaz et al. 2020; Ossowska et al. 2022).

Taxonomy

Astrothelium chulumanense **Flakus, Kukwa & Aptroot, sp. nov.**
MycoBank No: 847215
Fig. 2

Diagnosis. Characterised by pseudostromata not differing in colour from the thallus, perithecia immersed for the most part in thallus, with the upper part elevated above the thallus and covered, except the tops, with orange pigment, apical and fused ostioles, the absence of lichexanthone, clear hamathecium, 8-spored asci and amyloid, large (125–167 × 27–35 µm), muriform ascospores with a thickened median septum.

Type. Bolivia. Dept. La Paz; Prov. Sud Yungas, Pataloa, near estación biológica Santiago de Chirca, near Chulumani, 16°23'57.16"S, 67°34'33.96"W, elev. 2271 m, Yungas montane forest, corticolous, 22 Jan 2020, A. Flakus 29985 & P. Rodriguez-Flakus (holotype KRAM-L 73244, isotypes LPB, UGDA).

Description. Thallus corticate, with corticiform layer 10–20 µm thick, uneven, folded to bumpy, somewhat shiny, continuous, ca. 0.1mm thick, greenish, surrounded by a dark prothallus, not inducing swellings of the host bark, covering areas ≤ 8 cm diam. Pseudostromata with a surface similar to the thallus, distinctly raised above the thallus, hemispherical to wart-shaped, ca. 1.5–3 mm in diam. and 0.5–1.5 mm high, the same colour like thallus with black to orange-black apical spot, inside containing bark tissue. Ascomata perithecia, pyriform to hemispherical, aggregated, 0.6–1 mm diam., emerging from beneath the upper periderm layers of the bark and surrounded by bark tissues in outside part, immersed in most parts in regular in outline pseudostromata, upper part elevated above the thallus and covered, except the tops, with orange pigment. Ostioles apical, centrally fused to form a shared channel leading to various chambers. Wall fully carbonised, not differentiated into excipulum and involucrellum, thicker, ≤ ca. 100 µm wide in the upper part and thinner, up to ca. 20 µm wide, near the base. Ostioles apical, fused, black. Hamathecium clear, composed of thin and anastomosing paraphysoids, 1.5–2.5 µm wide. Asci 8-spored, 350–470 × 56–60 µm. Ascospores distoseptate, hyaline, I+ violet, densely muriform, with a gelatinous layer in younger stages, with a distinct thickened median septum, sometimes breaking into two parts in the septa, narrowly ellipsoid, 125–167 × 27–35 µm, ends rounded, lumina diamond-shaped.

Chemistry. Thallus surface UV+ orange-yellow, K–, C–, KC–, thallus medulla K–; pseudostromata surface UV+ orange-yellow, K–, inner part of pseudostromata K–, visible part of perithecia K+ red. Trace of unidentified substance detected in the thallus by thin layer chromatography; pigment on the top of perithecia.

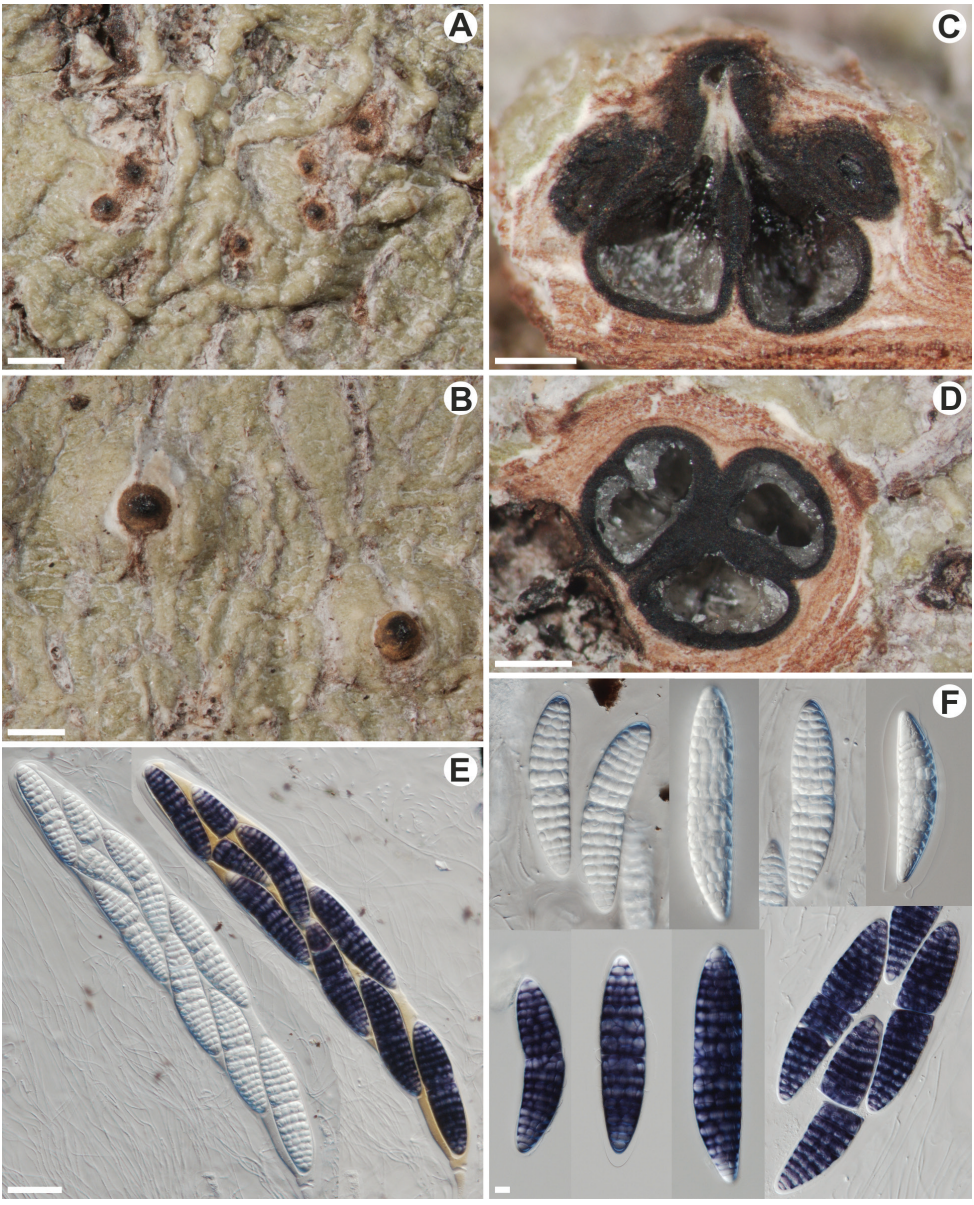

Figure 2. *Astrothelium chulumanense* (holotype) **A, B** thallus and ascomata **C** vertical cross section through pseudostromata **D** horizontal cross section through pseudostromata **E** asci (violet ascospores in Lugol's solution) **F** ascospores (violet in Lugol's solution). Scale bars: 1000 µm (**A, B**); 500 µm (**C, D**); 50 µm (**E**); 10 µm (**F**).

Etymology. The species is named after its locus classicus located near Chulumani town in Bolivia.

Distribution and habitat. So far, the species is known only from the type locality in Yungas forest in Bolivia.

Notes. *Astrothelium chulumanense* can be distinguished by pseudostromata not differing in colour from the thallus, the orange-yellow reaction in UV (perhaps due to the presence of an unknown substance), the absence of lichexanthone, perithecia immersed for the most part in the thallus, but with upper part elevated above the thallus and covered, except the tops, with orange pigment, apical and fused ostioles, clear hamathecium, 8-spored asci and amyloid, large, muriform ascospores with median septa. The new species is phylogenetically related and externally similar to *A. robustum*. Both species have also ascomata with fused ostioles; however, ascospores in *A. robustum* are (3–)5–7(–9)-septate and I negative. Furthermore, the species does not produce secondary metabolites (Aptroot and Lücking 2016; Aptroot 2021).

Only four *Astrothelium* species have clear hamathecium, 8-spored asci and large, muriform ascospores, which react I+ violet. *Astrothelium amylosporum* Flakus & Aptroot has pseudostromata not covered by thallus and lacks pigments, whereas *A. palaeoexostemmatis* Sipman & Aptroot lacks pigments, has smaller ascospores (85–100 × 20–24 µm) and ascomata are almost completely covered by the thallus and do not form distinct pseudostromata. *Astrothelium sanguinarium* (Malme) Aptroot & Lücking differs in the shape of pseudostromata, the pigment is red (isohypocrellin), reacts K+ yellow-green and is present internally within pseudostromata. *Astrothelium sanguineoxanthum* Aptroot has smaller (up to 86 µm long) ascospores, whitish pseudostromata and produces lichexanthone and isohypocrellin (internal in pseudostromata) (Aptroot and Lücking 2016; Aptroot et al. 2016b, 2019; Flakus et al. 2016; Aptroot 2021).

Several other species of the genus have pseudostromata or aggregated ascomata often with fused ostioles, clear hymenium, large (at least some over 80 µm long) and muriform, but I negative ascospores and 8-spored asci. They differ significantly in other characters (for the key to all species, see Aptroot (2021)). In *A. alboverrucum* (Makhija & Patw.) Aptroot & Lücking, ascomata are solitary to diffusely pseudostromatic, prominent, with whitish surrounding the black ostiolar area (Aptroot and Lücking 2016). *Astrothelium carassense* Lücking, M. P. Nelsen & Marcelli differs in perithecia completely immersed in pseudostromata, which are covered with orange pigment (Lücking et al. 2016b). *Astrothelium chapadense* (Malme) Aptroot & Lücking differs in dark brown pseudostromata, up to 100 µm long ascospores and the lack of secondary metabolites (Aptroot and Lücking 2016). *Astrothelium confluens* (Müll. Arg.) Aptroot & Lücking has ascomata completely covered by the thallus and ascospores measuring ca. 130 × 20 µm (Aptroot and Lücking 2016). *Astrothelium defossum* (Müll. Arg.) Aptroot & Lücking has joined ascomata, which are dispersed to confluent or diffusely pseudostromatic with lichexanthone on the surface (Aptroot and Lücking 2016). *Astrothelium elixii* Flakus & Aptroot develops white pruinose pseudostromata and produces lichexanthone and isohypocrellin (internal in pseudostromata) (Flakus et al. 2016). *Astrothelium flavoduplex* Aptroot & M. Cáceres differs from the new species by the presence of lichexanthone, oval to irregular or reticulate in outline pseudostromata, which are yellow to brownish and contain up to 50 ascomata with no fused ostioles (Aptroot and Cáceres 2016). *Astrothelium flavomurisporum* Aptroot & M. Cáceres has aggregated ascomata (but without pseudostroma) covered with the thallus, lumina of ascospores with yellow oil and lacks secondary metabolites (Aptroot and Cáceres

2016). *Astrothelium megeustomum* Aptroot & Fraga Jr produces ascomata mostly immersed in the bark tissue below pseudostromata, up to 125 µm long ascospores and lichexanthone around ostiolar region (Aptroot et al. 2016b). *Astrothelium mesoduplex* Aptroot & M. Cáceres has ascomata immersed in superficially yellow to orange, pale yellow inside pseudostromata and shorter, up to 100 µm long ascospores (Aptroot and Cáceres 2016). *Astrothelium octosporoides* Aptroot & Lücking differs in solitary or a few grouped ascomata covered by the thallus and the lack of secondary metabolites (Aptroot and Lücking 2016). *Astrothelium purpurascens* (Müll. Arg.) Aptroot & Lücking develops ascomata with fused ostioles covered with the thallus, produces isohypocrellin and has mostly shorter ascospores (100–130 µm) (Aptroot and Lücking 2016). *Astrothelium variabile* Flakus & Aptroot has aggregated ascomata in well-delimited and white pseudostromata, not fused ostioles, lacks pigments and produces lichexanthone (Flakus et al. 2016). *Astrothelium xanthosuperbum* Aptroot & M. Cáceres differs in black, raised above the thallus pseudostromata, which are usually in lines, the lack of pigments and the production of lichexanthone (Aptroot and Cáceres 2016).

Astrothelium isidiatum **Kukwa, Flakus & Rodr. Flakus, sp. nov.**
MycoBank No: 847216
Fig. 3

Diagnosis. The new species differs from all known species of the genus by developing groups of isidia on the surface of areoles, which break off to reveal a medulla that resembles soralia.

Type. Bolivia. Dept. La Paz; Prov. Sud Yungas, near Reserva Ecológica de Apa Apa, Sanani near Chulumani, 16°20'39.70"S, 67°29'54.32"W, elev. 2423 m, Yungas montane forest, corticolous, 23 Jan 2020, A. Flakus 30000 & P. Rodriguez-Flakus (KRAM-L 73245 holotype; LPB, UGDA isotypes).

Description. Thallus endosubstratal to episubstratal and then grey-green, shiny, folded in non-areolate parts, with areoles, isidiate. Areoles tuberculate, sometimes with cylindrical outgrowth developing at the lateral parts of areoles (Fig. 3C), constricted at the base (especially when young) or not, rounded to elongate and up to 1.2 mm wide. Isidia mostly cylindrical, globose when young, simple, rarely branched, constricted at the base or not, developing on areoles, up to 0.5 mm long and 0.2 mm wide, often shed from areoles and then exposing the yellow medulla of areoles, which then resemble soralia; sometimes elongated isidia-like outgrowth developing directly from the endosubstratal thallus present (Fig. 3D). Cortex up to 30–50 µm in width, of two layers, lower part prosoplectenchymatous and visible mostly in young areoles and upper part gelatinous. Photobiont layer up to 35 µm wide. Medulla whitish (only in young areoles) to yellow, densely filled with rhomboid or irregular crystals (crystals not dissolving in K), crystals 4–35 × 3–12 µm. The upper layer of areoles with shed isidia pseudoparenchymatous. Ascomata and pycnidia unknown.

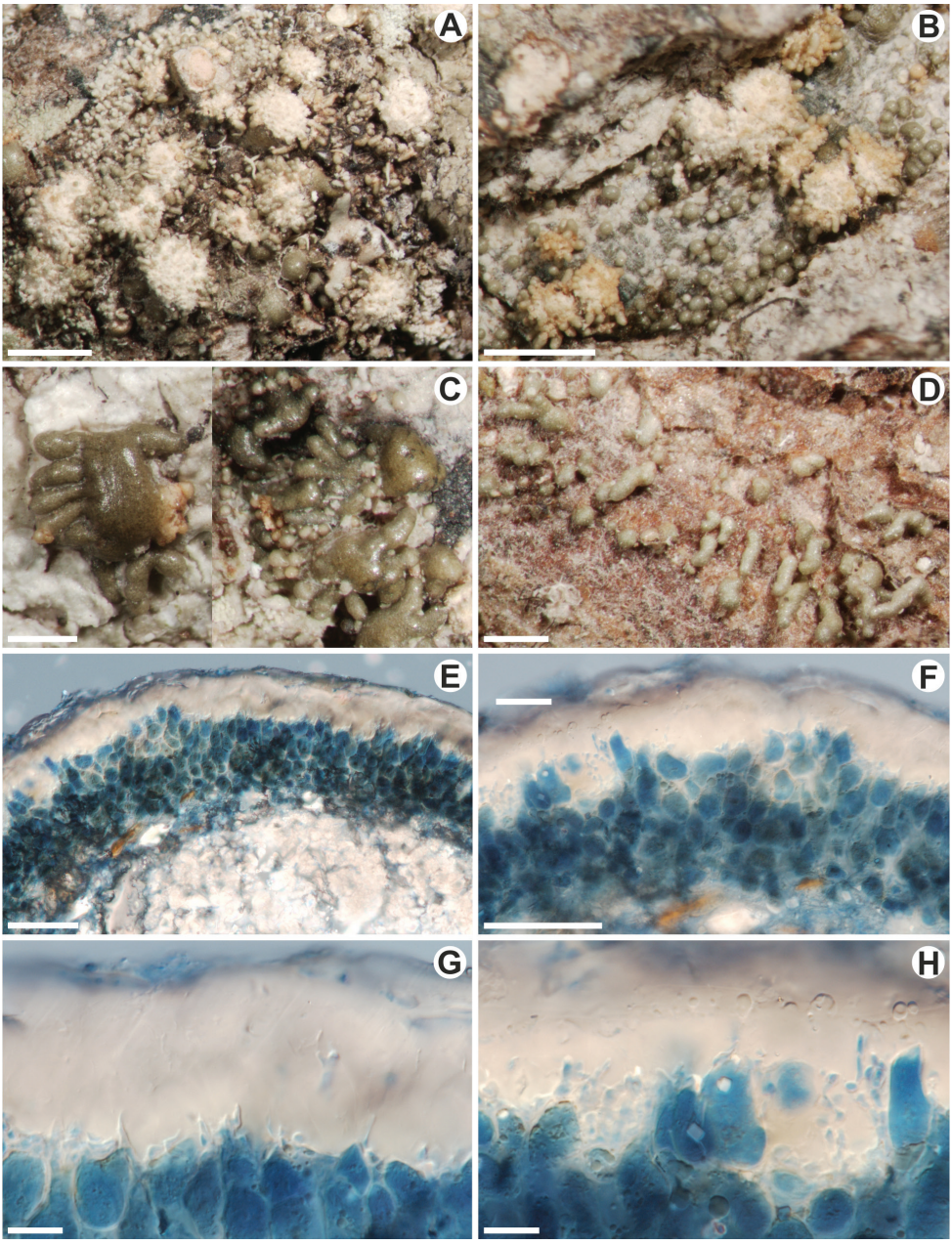

Figure 3. *Astrothelium isidiatum* (type collection) **A–D** thallus morphology **A, B** isidia developing in groups on areoles which are partly shed exposing the medulla of the areoles **C** isidia-like outgrows developing on lateral parts of areoles **D** isidia-like outgrowths developing directly from the endosubstratal parts of the thallus **E, F** a vertical cross-section through thallus with crystals present in the medulla (**E**) (in LPCB) **G, H** vertical cross-section through cortical layer (in LPCB). Scale bars: 1000 µm (**A, B**); 500 µm (**C, D**); 50 µm (**E, F**); 10 µm (**G, H**).

Chemistry. Thallus surface UV–, K–, C–, KC–; medulla with yellow pigment, K+ yellow going into solution, C+ yellow-orange; upper parts of areoles with shed isidia with patches of orange pigment reacting K+ purple. Unidentified substances (probably some of them are anthraquinones) in trace to minor amounts detected by thin layer chromatography.

Etymology. The name refers to the production of isidia, which are unique in the genus.

Distribution and habitat. So far, the species is known only from the type locality in the Yungas forest in Bolivia.

Notes. This is a very characteristic species with areoles filled with crystals, cylindrical isidia developing on the areoles and usually yellow thallus medulla. The ascomata were not found in the studied material. It differs from all species of *Astrothelium* and Trypetheliaceae in the presence of isidia.

Some species of Trypetheliaceae, for example, *Architrypethelium lauropaluanum* Lücking, M. P. Nelsen & Marcelli, *Astrothelium komposchii* Aptroot or *A. puiggarii* (Müll. Arg.) Aptroot & Lücking (Aptroot and Lücking 2016; Aptroot et al. 2016c; Lücking et al. 2016b), develop thalli with areoles resembling isidia which somehow are similar to these of *A. isidiatum* (Fig. 3C, D). However, *A. isidiatum* differs by developing cylindrical and often constricted at the base isidia which are covering the entire areoles (Fig. 3A, B). The isidia are easily broken and shed from areoles revealing the medulla of areoles that then resemble soralia.

We are not aware of any other similar species in other groups, which remind us of the unique taxon described here.

Acknowledgements

We would like to thank Robert Lücking for his constructive comments on the manuscript, members of Herbario Nacional de Bolivia, Instituto de Ecología, Universidad Mayor de San Andrés La Paz, for their generous cooperation and, in particular, our friend Silvia C. Gallegos for her invaluable assistance during the fieldwork. This research received support from the National Science Centre (project no 2015/17/B/NZ8/02441: Hidden genetic diversity in sterile crustose lichens in the Neotropical forests – an innovative case study in Bolivia, a hotspot of biodiversity) and statutory funds from the W. Szafer Institute of Botany, Polish Academy of Sciences, Krakow, Poland.

References

Altschul SF, Gish W, Miller W, Myers EW, Lipman DJ (1990) Basic local alignment search tool. Journal of Molecular Biology 215(3): 403–410. https://doi.org/10.1016/S0022-2836(05)80360-2

Aptroot A (2021) World key to the species of Pyrenulaceae and Trypetheliaceae. Archive For Lichenology 29: 1–91.

Aptroot A, Cáceres MES (2016) New Trypetheliaceae from the Amazon basin in Rondônia (Brazil), the centre of diversity of the genus *Astrothelium*. Lichenologist 48(6): 693–712. https://doi.org/10.1017/S0024282915000584

Aptroot A, Lücking R (2016) A revisionary synopsis of the Trypetheliaceae (Ascomycota: Trypetheliales). Lichenologist 48(6): 763–982. https://doi.org/10.1017/S0024282916000487

Aptroot A, Weerakoon G (2018) Three new species and ten new records of Trypetheliaceae (Ascomycota) from Sri Lanka. Cryptogamie. Mycologie 39(3): 373–378. https://doi.org/10.7872/crym/v39.iss3.2018.373

Aptroot A, Thor G, Lücking R, Elix JA, Chaves JL (2009) The lichen genus *Herpothallon* reinstated. Bibliotheca Lichenologica 99: 19–66.

Aptroot A, Cáceres MES, Johnston MK, Lücking R (2016a) How diverse is the lichenized fungal family Trypetheliaceae (Ascomycota: Dothideomycetes)? A quantitative prediction of global species richness. Lichenologist 48(6): 983–1011. https://doi.org/10.1017/S0024282916000463

Aptroot A, Mendonça CO, Andrade DS, Silva JR, Martins SMA, Gumboski E, Fraga CAV, Cáceres MES (2016b) New Trypetheliaceae from northern and southern Atlantic rainforests in Brazil. Lichenologist 48(6): 713–725. https://doi.org/10.1017/S0024282916000037

Aptroot A, Ertz D, Etayo Salazar J, Gueidan C, Mercado Diaz J, Schumm F, Weerakoon G (2016c) Forty-six new species of Trypetheliaceae from the tropics. Lichenologist 48(6): 609–638. https://doi.org/10.1017/S002428291600013X

Aptroot A, Sipman HJM, Barreto FMO, Nunes AD, Cáceres MES (2019) Ten new species and 34 new country records of Trypetheliaceae. Lichenologist 51(1): 27–43. https://doi.org/10.1017/S002428291800052X

Aptroot A, de Souza MF, dos Santos LA, Junior IO, Barbosa BMC, Cáceres MES (2022) New species of lichenized fungi from Brazil, with a record report of 492 species in a small area of the Amazon Forest. The Bryologist 125(3): 433–465. https://doi.org/10.1639/0007-2745-125.3.433

Cáceres MES, Aptroot A (2017) Lichens from the Brazilian Amazon, with special reference to the genus *Astrothelium*. The Bryologist 120(2): 165–181. https://doi.org/10.1639/0007-2745-120.2.165

Canals A, Hernández-Mariné M, Gómez-Bolea A, Llimona X (1997) *Botryolepraria*, a new monotypic genus segregated from *Lepraria*. Lichenologist 29(4): 339–345. https://doi.org/10.1006/lich.1997.0081

Chernomor O, von Haeseler A, Quang Minh B (2016) Terrace Aware Data Structure for Phylogenomic Inference from Supermatrices. Systematic Biology 65(6): 997–1008. https://doi.org/10.1093/sysbio/syw037

Culberson CF, Kristinsson H (1970) A standardized method for the identification of lichen products. Journal of Chromatography A 46: 85–93. https://doi.org/10.1016/S0021-9673(00)83967-9

Dal Forno M, Moncada B, Lücking R (2018) *Sticta aongstroemii*, a newly recognized species in the *S. damicornis* morphodeme (Lobariaceae) potentially endemic to the Atlantic Forest in Brazil. Lichenologist 50(6): 691–696. https://doi.org/10.1017/S0024282918000403

Diederich P, Ertz D (2020) First checklist of lichens and lichenicolous fungi from Mauritius, with phylogenetic analyses and descriptions of new taxa. Plant and Fungal Systematics 65(1): 13–75. https://doi.org/10.35535/pfsyst-2020-0003

Ekman S, Tønsberg T (2002) Most species of *Lepraria* and *Leproloma* form a monophyletic group closely related to Stereocaulon. Mycological Research 106(11): 1262–1276. https://doi.org/10.1017/S0953756202006718

Flakus A, Kukwa M, Aptroot A (2016) Trypetheliaceae of Bolivia: An updated checklist with descriptions of twenty-four new species. Lichenologist 48(6): 661–692. https://doi.org/10.1017/S0024282915000559

Guzow-Krzemińska B, Jabłońska A, Flakus A, Rodriguez-Flakus P, Kosecka M, Kukwa M (2019) Phylogenetic placement of *Lepraria cryptovouauxii* sp. nov. (Lecanorales, Lecanoromycetes, Ascomycota) with notes on other *Lepraria* species from South America. MycoKeys 53: 1–22. https://doi.org/10.3897/mycokeys.53.33508

Hodkinson BP, Lendemer JC (2013) Next-generation sequencing reveals sterile crustose lichen phylogeny. Mycosphere 4(6): 1028–1039. https://doi.org/10.5943/mycosphere/4/6/1

Hongsanan S, Hyde KD, Phookamsak R, Wanasinghe DN, McKenzie EHC, Sarma VV, Lücking R, Boonmee S, Bhat JD, Liu N-G, Tennakoon DS, Pem D, Karunarathna A, Jiang S-H, Jones GEB, Phillips AJL, Manawasinghe IS, Tibpromma S, Jayasiri SC, Sandamali D, Jayawardena RS, Wijayawardene NN, Ekanayaka AH, Jeewon R, Lu Y-Z, Phukhamsakda C, Dissanayake AJ, Zeng X-Y, Luo Z-L, Tian Q, Thambugala KM, Dai D, Samarakoon MC, Chethana KWT, Ertz D, Doilom M, Liu J-K, Pérez-Ortega S, Suija A, Senwanna C, Wijesinghe SN, Niranjan M, Zhang S-N, Ariyawansa HA, Jiang H-B, Zhang J-F, Norphanphoun C, de Silva NI, Thiyagaraja V, Zhang H, Bezerra JDP, Miranda-González R, Aptroot A, Kashiwadani H, Harishchandra D, Sérusiaux E, Abeywickrama PD, Bao D-F, Devadatha B, Wu H-X, Moon KH, Gueidan C, Schumm F, Bundhun D, Mapook A, Monkai J, Bhunjun CS, Chomnunti P, Suetrong S, Chaiwan N, Dayarathne MC, Yang J, Rathnayaka AR, Xu JC, Zheng J, Liu G, Feng Y, Xie N (2020) Refined families of Dothideomycetes: Orders and families incertae sedis in Dothideomycetes. Fungal Diversity 105(1): 17–318. https://doi.org/10.1007/s13225-020-00462-6

Jiang S-H, Zhang C, Xue X-D, Aptroot A, Wei J-C, Wei X-L (2022) Morphological and phylogenetic characterizations reveal five new species of *Astrothelium* (Trypetheliales, Ascomycota) from China. Journal of Fungi 8(10): 994. https://doi.org/10.3390/jof8100994

Kalyaanamoorthy S, Minh BQ, Wong TKF, Von Haeseler A, Jermiin LS (2017) ModelFinder: fast model selection for accurate phylogenetic estimates. Nature Methods 14(6): 587–589. https://doi.org/10.1038/nmeth.4285

Katoh K, Kuma K, Toh H, Miyata T (2005) MAFFT version 5: Improvement in accuracy of multiple sequence alignment. Nucleic Acids Research 33(2): 511–518. https://doi.org/10.1093/nar/gki198

Kukwa M (2011) The lichen genus *Ochrolechia* in Europe. Fundacja Rozwoju Uniwersytetu Gdańskiego, Gdańsk, 309 pp.

Kukwa M, Pérez-Ortega S (2010) A second species of *Botryolepraria* from the Neotropics and the phylogenetic placement of the genus within Ascomycota. Mycological Progress 9(3): 345–351. https://doi.org/10.1007/s11557-009-0642-0

Lendemer JC, Hodkinson BP (2013) A radical shift in the taxonomy of *Lepraria* s.l.: Molecular and morphological studies shed new light on the evolution of asexuality and lichen growth form diversification. Mycologia 105(4): 994–1018. https://doi.org/10.3852/12-338

Lücking R, Nelsen MP, Aptroot A, Klee RB, Bawingan PA, Benatti MN, Binh NQ, Bungartz F, Caceres MES, Canez LS, Chaves J-L, Ertz D, Esquivel RE, Ferraro LI, Grijalva A, Gueidan C, Hernandez JE, Knight A, Lumbsch HT, Marcelli MP, Mercado-Diaz JA, Moncada B, Morales EA, Naksuwankul K, Orozco T, Parnmen S, Rivas Plata E, Salazar-Allen N, Spielmann AA, Ventura N (2016a) A phylogenetic framework for reassessing generic concepts and species delimitation in the lichenized family Trypetheliaceae (Ascomycota: Dothideomycetes). Lichenologist 48(6): 739–762. https://doi.org/10.1017/S0024282916000505

Lücking R, Nelsen MP, Aptroot A, Benatti MN, Binh NQ, Gueidan C, Gutiérrez MC, Jungbluth P, Lumbsch HT, Marcelli MP, Moncada B, Naksuwankul K, Orozco T, Salazar-Allen N, Upreti DK (2016b) A pot-pourri of new species of Trypetheliaceae resulting from molecular phylogenetic studies. Lichenologist 48(6): 639–660. https://doi.org/10.1017/S0024282916000475

Lücking R, Hodkinson BP, Leavitt SD (2017) [(2016)] The 2016 classification of lichenized fungi in the Ascomycota and Basidiomycota – Approaching one thousand genera. The Bryologist 119(4): 361–416. https://doi.org/10.1639/0007-2745-119.4.361

Mendonça CO, Aptroot A, Lücking R, Cáceres MES (2020) Global species richness prediction for Pyrenulaceae (Ascomycota: Pyrenulales), the last of the "big three" most speciose tropical microlichen families. Biodiversity and Conservation 29(3): 1059–1079. https://doi.org/10.1007/s10531-019-01925-2

Mercado-Díaz JA, Lücking R, Moncada B, Widhelm TJ, Lumbsch HT (2020) Elucidating species richness in lichen fungi: The genus *Sticta* (Ascomycota: Peltigeraceae) in Puerto Rico. Taxon 69(5): 851–891. https://doi.org/10.1002/tax.12320

Miller MA, Pfeiffer W, Schwartz T (2010) Creating the CIPRES Science Gateway for inference of large phylogenetic trees. Proceedings of the Gateway Computing Environments Workshop (GCE). 14 Nov. 2010. New Orleans Convention Center, New Orleans, LA, 1–8. https://doi.org/10.1109/GCE.2010.5676129

Moncada B, Lücking R, Suárez A (2014) Molecular phylogeny of the genus *Sticta* (lichenized Ascomycota: Lobariaceae) in Colombia. Fungal Diversity 64(1): 205–231. https://doi.org/10.1007/s13225-013-0230-0

Moncada B, Mercado-Díaz JA, Lücking R (2018) The identity of *Sticta damicornis* (Ascomycota: Lobariaceae): a presumably widespread taxon is a Caribbean endemic. Lichenologist 50(5): 591–597. https://doi.org/10.1017/S0024282918000373

Moncada B, Lücking R, Lumbsch HT (2020) Rewriting the evolutionary history of the lichen genus *Sticta* (Ascomycota: Peltigeraceae subfam. Lobarioideae) in the Hawaiian islands. Plant and Fungal Systematics 65(1): 95–119. https://doi.org/10.35535/pfsyst-2020-0005

Nguyen L-T, Schmidt HA, Von Haeseler A, Minh BQ (2014) IQ-TREE: a fast and effective stochastic algorithm for estimating maximum-likelihood phylogenies. Molecular Biology and Evolution 32: 268–274. https://doi.org/10.1093/molbev/msu300

Orange A, Chhetri SG (2022) Verrucariaceae from Nepal. Lichenologist 54(3–4): 139–174. https://doi.org/10.1017/S0024282922000160

Orange A, James PW, White FJ (2001) Microchemical Methods for the Identification of Lichens. British Lichen Society, London, 101 pp.

Ossowska E, Moncada B, Kukwa M, Flakus A, Rodriguez-Flakus P, Olszewska S, Lücking R (2022) New species of *Sticta* (lichenised Ascomycota, lobarioid Peltigeraceae) from Bolivia suggest a high level of endemism in the Central Andes. MycoKeys 92: 131–160. https://doi.org/10.3897/mycokeys.92.89960

Page RDM (1996) Tree View: An application to display phylogenetic trees on personal computers. Bioinformatics 12(4): 357–358. https://doi.org/10.1093/bioinformatics/12.4.357

Penn O, Privman E, Ashkenazy H, Landan G. Graur D, Pupko T (2010) GUIDANCE: a web server for assessing alignment confidence scores. Nucleic Acids Research 38(Web Server): W23–W28. https://doi.org/10.1093/nar/gkq443

Rehner SA, Samuels GJ (1994) Taxonomy and phylogeny of *Gliocladium* analysed from nuclear large subunit ribosomal DNA sequences. Mycological Research 98(6): 625–634. https://doi.org/10.1016/S0953-7562(09)80409-7

Rodriguez-Flakus P, Printzen C (2014) *Palicella*, a new genus of lichenized fungi and its phylogenetic position within Lecanoraceae. The Lichenologist 46(4): 535–552. https://doi.org/10.1017/S0024282914000127

Ronquist F, Teslenko M, van der Mark P, Ayres DL, Darling A, Höhna S, Larget B, Liu L, Suchard MA, Huelsenbeck JP (2012) MrBayes 3.2: Efficient Bayesian Phylogenetic Inference and Model Choice Across a Large Model Space. Systematic Biology 61(3): 539–542. https://doi.org/10.1093/sysbio/sys029

Simon A, Goffinet B, Magain N, Sérusiaux E (2018) High diversity, high insular endemism and recent origin in the lichen genus *Sticta* (lichenized Ascomycota, Peltigerales) in Madagascar and the Mascarenes. Molecular Phylogenetics and Evolution 122: 15–28. https://doi.org/10.1016/j.ympev.2018.01.012

Vilgalys R, Hester M (1990) Rapid genetic identification and mapping of enzymatically amplified ribosomal DNA from several Cryptococcus species. Journal of Bacteriology 172(8): 4238–4246. https://doi.org/10.1128/jb.172.8.4238-4246.1990

Wijayawardene NN, Hyde KD, Dai DQ, Sánchez-García M, Goto BT, Saxena RK, Erdoğdu M, Selçuk F, Rajeshkumar KC, Aptroot A, Błaszkowski J, Boonyuen N, da Silva GA, de Souza FA, Dong W, Ertz D, Haelewaters D, Jones EBG, Karunarathna SC, Kirk PM, Kukwa M, Kumla J, Leontyev DV, Lumbsch HT, Maharachchikumbura SSN, Marguno F, Martínez-Rodríguez P, Mešić A, Monteiro JS, Oehl F, Pawłowska J, Pem D, Pfliegler WP, Phillips AJL, Pošta A, He MQ, Li JX, Raza M, Sruthi OP, Suetrong S, Suwannarach N, Tedersoo L, Thiyagaraja V, Tibpromma S, Tkalčec Z, Tokarev YS, Wanasinghe DN, Wijesundara DSA, Wimalaseana SDMK, Madrid H, Zhang GQ, Gao Y, Sánchez-Castro I, Tang LZ, Stadler M, Yurkov A, Thines M (2022) Outline of Fungi and fungus-like taxa – 2021. Mycosphere 13(1): 53–453. https://doi.org/10.5943/mycosphere/13/1/2

Zoller S, Scheidegger C, Sperisen C (1999) PCR primers for the amplification of mitochondrial small subunit ribosomal DNA of lichen-forming ascomycetes. Lichenologist 31(5): 511–516. https://doi.org/10.1006/lich.1999.0220

MycoKeys 95: 101–129 (2023)
doi: 10.3897/mycokeys.95.97601
https://mycokeys.pensoft.net

RESEARCH ARTICLE

A peer-reviewed open-access journal
MycoKeys
Launched to accelerate biodiversity research

Chaenothecopsis (Mycocaliciales, Ascomycota) from exudates of endemic New Zealand Podocarpaceae

Christina Beimforde[1], Alexander R. Schmidt[1], Hanna Tuovila[2], Uwe Kaulfuss[3], Juliane Germer[1], William G. Lee[4,5], Jouko Rikkinen[2,6]

1 *Department of Geobiology, University of Göttingen, Goldschmidtstraße 3, 37077, Göttingen, Germany* **2** *Finnish Museum of Natural History, University of Helsinki, P.O. Box 7, 00014, Helsinki, Finland* **3** *Johann-Friedrich-Blumenbach Institute of Zoology and Anthropology, University of Göttingen, Untere Karspüle 2, 37073, Göttingen, Germany* **4** *Landcare Research, Private Bag 1930, Dunedin 9016, New Zealand* **5** *School of Biological Sciences, University of Auckland, Private Bag 9209, Auckland 1142, New Zealand* **6** *Organismal and Evolutionary Biology Research Programme, Faculty of Biological and Environmental Sciences, University of Helsinki, P.O. Box 65, 00014, Helsinki, Finland*

Corresponding author: Christina Beimforde (christina.beimforde@uni-goettingen.de)

Academic editor: G. Rambold | Received 15 November 2022 | Accepted 26 January 2023 | Published 16 February 2023

Citation: Beimforde C, Schmidt AR, Tuovila H, Kaulfuss U, Germer J, Lee WG, Rikkinen J (2023) *Chaenothecopsis* (Mycocaliciales, Ascomycota) from exudates of endemic New Zealand Podocarpaceae. MycoKeys 95: 101–129. https://doi.org/10.3897/mycokeys.95.97601

Abstract

The order Mycocaliciales (Ascomycota) comprises fungal species with diverse, often highly specialized substrate ecologies. Particularly within the genus *Chaenothecopsis*, many species exclusively occur on fresh and solidified resins or other exudates of vascular plants. In New Zealand, the only previously known species growing on plant exudate is *Chaenothecopsis schefflerae*, found on several endemic angiosperms in the family Araliaceae. Here we describe three new species; *Chaenothecopsis matai* Rikkinen, Beimforde, Tuovila & A.R. Schmidt, *C. nodosa* Beimforde, Tuovila, Rikkinen & A.R. Schmidt, and *C. novae-zelandiae* Rikkinen, Beimforde, Tuovila & A.R. Schmidt, all growing on exudates of endemic New Zealand conifers of the Podocarpaceae family, particularly on *Prumnopitys taxifolia*. Phylogenetic analyses based on ribosomal DNA regions (ITS and LSU) grouped them into a distinct, monophyletic clade. This, as well as the restricted host range, suggests that all three taxa are endemic to New Zealand. Copious insect frass between the ascomata contain ascospores or show an early stage of ascomata development, indicating that the fungi are spread by insects. The three new species represent the first evidence of *Chaenothecopsis* from any Podocarpaceae species and the first from any gymnosperm exudates in New Zealand.

Keywords

Chaenothecopsis, Mycocaliciales, New Zealand, *Phyllocladus*, plant exudate, Podocarpaceae, *Prumnopitys*, resinicolous fungi

Introduction

The order Mycocaliciales Tibell & Wedin represents an isolated lineage of non-lichenized ascomycetes with sessile or pin-like ascomata (Tibell and Wedin 2000). Species of this lineage are currently assigned to two families and five genera of which *Chaenothecopsis* Vain. represents the largest genus. However, generic delimitations within the Mycocaliciales are in need of revision, since molecular studies show that the currently established genera are not monophyletic (e.g. Tibell and Vinuesa 2005; Tuovila 2013).

The substrate ecology of mycocalicoid species currently assigned to *Chaenothecopsis* is particularly diverse. There are many highly specialized species that have adapted to utilize specific substrates of certain tree species (Tibell 1987; Tuovila 2013) or to live in association with lichens or green algae (Titov 2006). Within *Chaenothecopsis* a number of species occur exclusively on fresh and recently solidified exudates of diverse gymnosperms and angiosperms, with most of them exhibiting a high level of host specificity (e.g. Tibell and Titov 1995; Tuovila et al. 2013). Most resinicolous *Chaenothecopsis* species are known from terpenoid conifer resins of temperate boreal forests of the Northern Hemisphere including species of *Abies* Mill., *Larix* Mill., *Picea* A.Dietr., *Pinus* L. and *Tsuga* Carrière (e.g. Titov and Tibell 1993; Tibell and Titov 1995; Rikkinen 1999, 2003; Tuovila et al. 2011b). Only two species have so far been reported from conifers of warm temperate forests in Asia (*Cunninghamia* R.Br.; Tuovila et al. 2013) and an araucarian conifer from New Caledonia (*Agathis* Salisb.; Rikkinen et al. 2014). Additional *Chaenothecopsis* species, all belonging to a distinct, monophyletic group, grow on angiosperm exudates of host trees in the Sapindales Juss. ex Bercht. & J. Presl., including Anacardiaceae R.Br. (*Khaya* A.Juss. and *Rhus* L.; Tuovila et al. 2011a) and Simaroubaceae DC. (*Ailanthus* Desf.; Tuovila et al. 2014), as well as the Apiales Nakai (*Kalopanax* Miq. (Tuovila et al. 2014), *Pseudopanax* K.Koch (Beimforde et al. 2017), and *Schefflera* J.R.Forst. & G.Forst. (Samuels and Buchanan 1983)). Of the mycocalicioid fungi so far known from New Zealand, most species of *Chaenothecopsis* are believed to be more or less cosmopolitan and live as saprophytes on the lignum of local conifers or angiosperms (Tibell 1987). Only one New Zealand species, *Chaenothecopsis schefflerae* (Samuels & D.E. Buchanan) Tibell, is known from plant exudates so far. It occurs exclusively on angiosperm exudates produced by different species of endemic Araliaceae Juss. (*Schefflera*, *Pseudopanax*; Samuels and Buchanan 1983; Beimforde et al. 2017).

Several fossils in Paleogene amber demonstrate that the ascoma morphology and resinicolous ecology of conifer-associated taxa have remained unchanged for tens of millions of years (Rikkinen and Poinar 2000; Tuovila et al. 2013; Rikkinen et al. 2018; Rikkinen and Schmidt 2018), but the evolutionary origin of the resinicolous ecology within the Mycocaliciales is still unclear. Molecular phylogenetic analyses indicate that the resinicolous ecology on conifer resin predates fungi occupying angiosperm exudate. *Chaenothecopsis* species from angiosperm exudates are grouped in a well-supported monophyletic group, suggesting a single origin of this ecological mode, whereas species

on conifer resin are scattered throughout the genus, suggesting a longer evolutionary history (e.g. Rikkinen et al. 2014; Tuovila et al. 2014; Beimforde et al. 2017).

Here we describe three new *Chaenothecopsis* species that grow mainly on exudates of *Prumnopitys taxifolia* (Banks & Sol. ex D. Don) de Laub. (Podocarpaceae Endl.), an endemic New Zealand gymnosperm also known as black pine or Mataī. The morphology of each species is examined using light and scanning electron microscopy (SEM) and their phylogenetic relationships are elucidated based on ribosomal DNA data of the internal transcribed spacer region (ITS) and the large ribosomal subunit (nucLSU). The new species are described as *Chaenothecopsis matai*, *C. nodosa* and *C. novae-zelandiae*. They represent the first *Chaenothecopsis* species from any species of the conifer family Podocarpaceae and the first report of *Chaenothecopsis* species associated with gymnosperm exudate from New Zealand.

Methods

Biological material

Chaenothecopsis specimens were collected from *Prumnopitys taxifolia* (Podocarpaceae) growing in different localities in the North and South Islands of New Zealand (Fig. 1, Suppl. material 1). Specimens were also collected on exudates of *Phyllocladus trichomanoides* D. Don (Podocarpaceae) from the North Island. Type specimens are deposited in the New Zealand Fungarium (PDD), Landcare Research in Auckland (Suppl. material 1).

Light microscopy and scanning electron microscopy

Morphological features (Figs 2–10) of the fungal specimens were studied and imaged using a Carl Zeiss StereoDiscovery V8 dissection microscope, a Leica DMLS microscope and a Carl Zeiss AxioScope A1 compound microscope equipped with Canon EOS 5D digital cameras. Ascomatal details were studied under 40- to 100-fold magnification, sometimes with an additional 1.6-fold magnification. Spores and inner ascomatal structures were analyzed and imaged on a microscope slide in water using Differential Interference Contrast (DIC) illumination. Some diagnostic structures, such as paraphyses and stipe hyphae, were observed by utilizing potassium hydroxide (KOH).

Light-microscopical images of ascomata on *Prumnopitys* Phil. exudates were obtained from 40–60 focal planes by using incident and transmitted light simultaneously. Individual images of focal planes were digitally stacked using the software package HeliconFocus 7.0 (Helicon Soft Limited, Kharkiv, Ukraine).

For scanning electron microscopy (Figs 3, 6, 9, 11), air dried specimens of each species were removed from the substrate, placed on a carbon-covered SEM-mount, sputtered by gold/palladium and examined under a Carl Zeiss LEO 1530 Gemini field emission scanning-electron microscope.

Figure 1. Typical habitats of *Chaenothecopsis* species from Podocarpaceae in northern New Zealand **A** collecting specimens of *Chaenothecopsis novae-zelandiae* (PDD 110742) from a trunk of *Prumnopitys taxifolia* along Te Whaiti Road **B** (detail of **A**): *Prumnopitys taxifolia* with old, partly charred lesions **C** *Prumnopitys taxifolia* hosting *Chaenothecopsis matai* (PDD 110746) along Ruatahuna Road **D** colonized exudate of *Prumnopitys taxifolia* **E** (detail of **D**): exudate colonized by *Chaenothecopsis matai* (PDD 110746). Scale bars: 4 cm (**D**); 2 cm (**E**).

Spore isolation and cultivation

Cultures were obtained by transferring single ascocarps from the substrate to cavity glass slides containing a drop of sterile 0.9% sodium chloride. All adhering substrate particles were removed and a single mature ascocarp was transferred to a fresh cavity glass slide containing a drop of sterile 0.9% sodium chloride and gently crushed with a sterile scalpel to liberate the spores. Spores were further diluted in 200–300µl sterile 0.9% sodium chloride and transferred to solid potato dextrose media (PDA, Carl Roth, Germany: 4 g/l potato infusion, 20 g/l glucose, 15 g/l agar, pH = 5.6 ± 0.2) using pipettes and filter tips. Inoculates were investigated under a Carl Zeiss StereoDiscovery V8 dissection microscope, initially every 2 days, until germination started. Cultures were subsequently stored in the dark

and checked every week in order to detect possible contamination at an early stage. After 5–6 months, cultures were identified using molecular analysis of internal transcribed spacer region (ITS).

DNA extraction, PCR amplification and sequencing

DNA was extracted from all collected representative specimens of *Chaenothecopsis*. Between 5–10 ascomata of each specimen were crushed with a fine glass mortar and pestle (Carl Roth, Karlsruhe, Germany) prior to DNA-extraction. DNA was subsequently extracted using the DNA Micro Kit from Quiagen (Hilden, Germany) following the manufacturer's protocol, but modifying the incubation time to at least 24 hours. Samples were held in micro-glass mortars closed with parafilm during the whole incubation time.

The large subunit of nuclear ribosomal RNA (LSU) was amplified using primers pairs LR0R and LR3 (Vilgalys and Hester 1990; Rehner and Samuels 1994), as well as LR5 and LR7 (Vilgalys and Hester 1990). The internal transcribed spacer region (ITS) of the ribosomal DNA was amplified using the primers ITS5 (White et al. 1990) or ITS1F (Gardes and Bruns 1993) and ITS4 (White et al. 1990). Polymerase chain reaction (PCR) was conducted using Taq DNA polymerase (Promega, Madison, WI) by following the manufacturer's recommendations and PCR conditions with the following steps: (1) hot start with 95 °C for 2 min; (2) 35 cycles of 45 s (ITS) to 60 s (LSU) at 95 °C, 60 s at 52–55 °C and 45 s (ITS) to 60 s (LSU) at 72 °C and (3) 10 min of final elongation at 72 °C. Subsequently, the ITS and LSU rDNA products were purified using PCRapace (Invitek, Berlin, Germany) and sequenced in both directions with a MegaBACE 1000 automated sequencing machine and DYEnamic ET Primer DNA sequencing reagent (Amersham Biosciences, Little Chalfont, UK). Sequences were assembled and edited using Bioedit 5.0.9 (Hall 1999).

Taxon sampling and phylogenetic analysis

While many different *Chaenothecopsis* species have been reported from New Zealand (Tibell 1987), sequences of only a few, including *Chaenothecopsis debilis* (Sm.) Tibell, *C. haematopus* Tibell and *C. schefflerae* (Samuels & D.E. Buchanan) Tibell, are available at present in Genbank. Most other sequences were obtained from specimens collected in Europe, primarily Sweden. Some Genbank sequences originating from cultures appeared inconsistent with the sequences from corresponding type material and were excluded from our analyses.

ITS and nucLSU from New Zealand specimens were sequenced in forward and backward direction and sequences were assembled using Bioedit 5.0.9 (Hall 1999). ITS and LSU data sets were aligned separately using MAFFT version 6 (Katoh and Toh 2008) and subsequently combined in Bioedit 5.0.9 (Hall 1999). For phylogenetic analyses only unambiguously alignable DNA regions were selected manually, using the mask function in Bioedit 5.0.9 (Hall 1999). The resulting data set comprises 401 basepairs (bp) of the ribosomal ITS region and 779 bp of the ribosomal LSU region.

The best fitting substitution model for each gene was chosen separately from seven substitution schemes included in the software package jModeltest 2.1.1 (Darriba et al. 2012), and models were selected according to the Bayesian information criterion (Schwarz 1978). The Bayesian information criterion supported the TIM2ef+I+G model as the best fit for the ITS region and the TrN+I+G model for the LSU gene. Both genes were combined in a single data matrix using Bioedit 5.0.9 (Hall 1999) and Bayesian analyses were carried out using Markov chain Monte Carlo in MrBayes 3.2.7 (Ronquist and Huelsenbeck 2003) on the CIPRES Science Gateway v. 3.3 (Miller et al. 2010) without using BEAGLE high-performance library (https://github.com/beagle-dev/beagle-lib).

Four chains were conducted simultaneously for 10 million generations each, sampling parameters every 1000th generation. Average standard deviations of split frequency < 0.01 were interpreted as indicative of independent Markov chain Monte Carlo convergence. A burn-in sample of 2500 trees was discarded for the run and the remaining trees were used to estimate branch lengths and posterior probabilities. Convergence and sufficient chain mixing (effective sample sizes > 200) were controlled using Tracer 1.7.2 (Rambaut and Drummond 2009). GenBank accession numbers of all fungal specimens used for phylogenetic reconstruction are provided in Table 1. The combined data matrix, settings for the Bayesian analyses, and resulting phylogenetic tree (Fig. 12) were deposited in TreeBASE, direct access: http://purl.org/phylo/treebase/phylows/study/TB2:S29864.

Table 1. GenBank accessions for the fungal ITS and LSU sequences used in this study for phylogenetic analysis (Fig. 12).

Species name	Voucher	GenBank accessions ITS/LSU	References
Brunneocarpos banksiae Giraldo & Crous	CPC 29841	NR_147648/NG_066277	Crous et al. (2016)
Caliciopsis indica J. Pratibha & Bhat	GUFCC 4947	GQ259981/GQ259980	Pratibha et al. (2011)
Chaenothecopsis sp. 1	Tuovila 09-052	X119110/JX119119	Tuovila et al. (2013)
Chaenothecopsis sp. 2	08-004 (TUR)	KC590480/KC590485	Tuovila (2014)
Chaenothecopsis consociata (Nádv.) A.F.W. Schmidt	Tibell 22472 (UPS)	AY795851/DQ008999	Tibell and Vinuesa (2005)
Chaenothecopsis debilis (Sm.) Tibell	Tibell 16643 (UPS)	AY795852/ AY795991	Tibell and Vinuesa (2005)
Chaenothecopsis diabolica Rikkinen & Tuovila	H:Tuovila 06-035	JX119109/JX119114	Tuovila (2013)
Chaenothecopsis dolichocephala Titov	Tibell 19281	AY795854/AY795993	Tibell and Vinuesa (2005)
Chaenothecopsis fennica (Laurila) Tibell	Tibell 16024 (UPS)	AY795857/AY795995	Tibell and Vinuesa (2005)
Chaenothecopsis golubkovae Tibell & Titov	Titov 6707 (UPS)	AY795859/AY795996	Tibell and Vinuesa (2005)
Chaenothecopsis haematopus Tibell	16625 (UPS)	AY795861/AY795997	Tibell and Vinuesa (2005)
Chaenothecopsis khayensis Rikkinen & Tuovila	JR 04G058	JX122785/HQ172895	Tuovila et al. (2011a)
Chaenothecopsis montana Rikkinen	H:Tuovila 07-086	JX119105/JX119114	Tuovila et al. (2013)
Chaenothecopsis neocaledonica Rikkinen, Tuovila & A.R. Schmidt	Rikkinen 010179	KF815196/KF815197	Rikkinen et al. (2014)
Chaenothecopsis nigripunctata Rikkinen	H:Tuovila 06-013	JX119103/JX119112	Tuovila et al. (2013)
Chaenothecopsis matai Rikkinen, Beimforde,	PDD 110746	OQ308931/OQ308874	This study
Tuovila & A.R. Schmidt	PDD 110749	OQ308932/OQ308875	This study
Chaenothecopsis nodosa Beimforde, Tuovila,	PDD 110743	OQ308933/OQ308876	This study
Rikkinen & A.R. Schmidt	PDD 110745	OQ308934/OQ308877	This study
Chaenothecopsis novae-zelandiae Rikkinen,	PDD 110742	OQ308935/OQ308878	This study
Beimforde, Tuovila & A.R. Schmidt	PDD 110744	OQ308936/OQ308879	This study

Species name	Voucher	GenBank accessions ITS/LSU	References
Chaenothecopsis pallida Rikkinen & Tuovila	H:JR 010652	JX122779/JX122781	Tuovila et al. (2013)
Chaenothecopsis pusilla (A. Massal.) A.F.W. Schmidt	Tibell 16580 (UPS)	-/ DQ009000.1	Tibell and Vinuesa (2005)
Chaenothecopsis pusiola (Ach.) Vain.	H:Tuovila 09-047	JX119106/JX119115	Tuovila et al. (2013)
Chaenothecopsis quintralis Messuti, Amico, Lorenzo & Vidal-Russ.	BCRU:05233	-/JQ267741	Messuti et al. (2012)
Chaenothecopsis resinophila Rikkinen & Tuovila	H:JR000424	JX122780/JX122782	Tuovila et al. (2013)
Chaenothecopsis schefflerae (Samuels & D.E. Buchanan) Tibell	Rikkinen 13183	KY499965/ KY499967	Beimforde et al. (2017)
Chaenothecopsis sitchensis Rikkinen	H:Tuovila 06-033	JX119102/JX119111	Tuovila et al. (2013)
Chaenothecopsis subparoica (Nyl.) Tibell	Tretiach (hb. Tretiach)	AY795869/-	Tibell and Vinuesa (2005)
Chaenothecopsis tsugae	H:JR07005B	JX119104/JX119113	Tuovila et al. (2013)
Chaenothecopsis viridireagens Rikkinen	Tibell 22803 (UPS)	AY795872/ DQ013257	Tibell and Vinuesa (2005)
Fusichalara minuta Hol.-Jech.	CBS 709.88	KX537754/ KX537758	Réblová et al. (2017)
Mycocalicium albonigrum (Nyl.) Tibell	Tibell 19038	AF223966/ AY796001	Tibell and Vinuesa (2005)
Mycocalicium subtile (Pers.) Szatala	JR6450	OQ308930/OQ308873	This study
Mycocalicium sp.	Tuovila 09-131 (TUR)	KC590482/KC590487	Tuovila et al. (2014)
Sphinctrina leucopoda Nyl.	Kalb 33829 (hb. Kalb)	AY795875/AY796006	Tibell and Vinuesa (2005)
Sphinctrina turbinata (Pers.) De Not.	Tibell 23093 (UPS)	AY795877/DQ009001	Tibell and Vinuesa (2005)
	Tibell 22478 (UPS)	AY795876/-	Geiser et al. (2006)
	AFTOL-ID 1721	-/ EF413632	Geiser et al. (2006)
Stenocybe pullatula (Ach.) Stein	Tibell 17117 (UPS)	AY795878/AY796008	Tibell and Vinuesa (2005)
Phaeocalicium populneum (Brond. & Duby) A.F.W. Schmidt	Tibell 19286 (UPS)	AY795874/AY796009	Tibell and Vinuesa (2005)
Phaeocalicium praecedens (Nyl.) A.F.W. Schmidt	Tuovila 09-240 (TUR)	KC590481/KC590486	Tuovila et al. (2014)
Pyrgillus javanicus (Mont. & Bosch) Nyl.	AFTOL-ID 342	DQ826741/DQ823103	James et al. (2006)
Pyrenula minutispora Aptroot & M. Cáceres	ABL AA11877	KT820119/-	Gueidan et al. (2016)
Pyrenula nitida (Weigel) Ach.	F 5929	JQ927458/ DQ329023	del Prado et al. (2006); Weerakoon et al. (2016)
Rhopalophora clavispora (W. Gams) Réblová	CBS 129.74	KX537751/ MH872573	Réblová et al. (2017)
	CBS 281.75	KX537752/ KX537756	Réblová et al. (2017)
Verrucaria inverecundula Pykälä & Myllys	FILIC650-13	MK138796/-	Pykälä et al. (2019)

Results

Taxonomy

Chaenothecopsis novae-zelandiae **Rikkinen, Beimforde, Tuovila & A.R. Schmidt, sp. nov.**

MycoBank No: MB846458

Figs 2–4

Type. New Zealand, South Island, State Highway 6 close to Makarora, Otago, ca. 44°13.787'S, 169°13.9708'E, on exudate of *Prumnopitys taxifolia*, 5 February 2017, holotype: PDD110744, New Zealand Fungarium (PDD), Landcare Research in Auckland, GenBank accession OQ308936/OQ308879.

Diagnosis. *Chaenothecopsis novae-zelandiae* differs from other *Chaenothecopsis* species by forming mostly solitary ascomata on podocarpous plant exudates, and by having inner ascomatal structures firmly connected by amorphous material and finely ornamented spores, which can be slightly constricted at the septum.

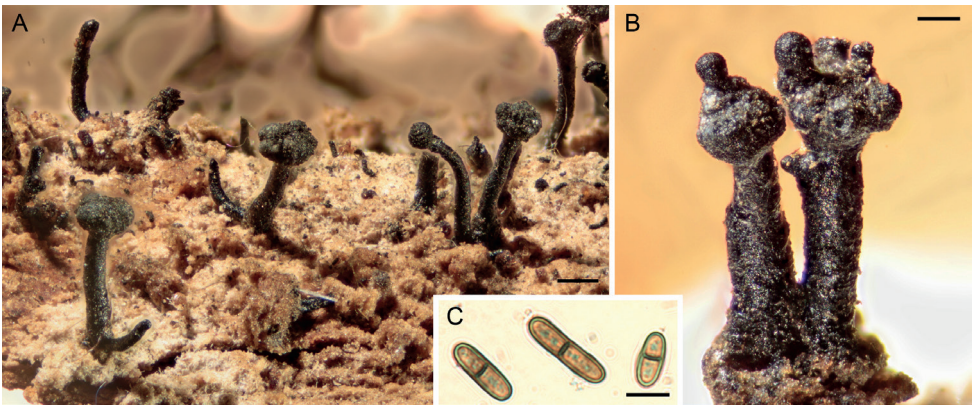

Figure 2. Light micrographs of *Chaenothecopsis novae-zelandiae* sp. nov. (PDD 110744). **A** apothecia on hardened exudate of *Prumnopitys taxifolia* **B** apothecia with proliferating capitula **C** ascospores. Scale bars: 200 µm (**A**); 100 µm (**B**); 5 µm (**C**).

Etymology. The specific epithet refers to New Zealand where the species was first discovered.

Description. ***Apothecia*** growing on the exudate of *Prumnopitys taxifolia*, 0.6–1.6 mm tall, growing individually or grouped in small clusters, often branched or proliferating from the capitulum. ***Stipe*** glossy black, straight, 80–180 µm wide, sometimes slightly flexuous or curved, frequently branched at the base or, more rarely, in the upper parts. ***Stipe hyphae*** mostly covered with a layer of hard pigment partly dissolving in KOH, 6–8 µm wide, with walls two layered, the outer wall brown, 2–4 µm wide and cell walls fused, the inner wall pale to hyaline, *c.* 0.5–1.5 µm wide, with the hyphae intertwined (textura intricata prismatica), swelling in KOH and the yellowish brown pigment leaking into the medium; hyphae in inner part of the stipe hyaline, slightly intertwined, 3–4.6 µm, swelling in KOH. ***Capitulum*** black, in young apothecia hemispherical to sometimes almost spherical, sometimes lobed or multi-headed, 200–400 µm wide. ***Excipulum*** hyphae brownish to slightly green, 5–7 µm wide, periclinally arranged or slightly intertwined (textura prismatica), swelling in KOH, with some brown pigment leaking into the medium; wall 2–2.5 µm. ***Epithecium*** light green to emerald green, appearing as a crustose layer, usually with crystals, composed of hyphae extending from the excipulum; hyphae attached to the hymenium by the amorphous material; containing various amounts of orange to ruby-red pigment in most ascomata, usually occurring as crystals on the outer walls of hyphae, and sometimes also inside their lumina. ***Hypothecium*** light green to hyaline, with the hyphae swelling in KOH. ***Hymenium*** light brown to greenish to almost hyaline, swelling in KOH, full of amorphous material strongly congealing the asci and paraphyses together. ***Paraphyses*** hyaline, filiform, 1.5–2 µm wide (n = 10), branched, as long or slightly longer than the asci, variously covered with amorphous material, septate at 10–15 µm intervals. ***Asci*** cylindrical, 55–60 × 6.1 µm (n = 5), with the apex variously thickened, often penetrated by a short canal; mature asci usually without a thickening, variously covered

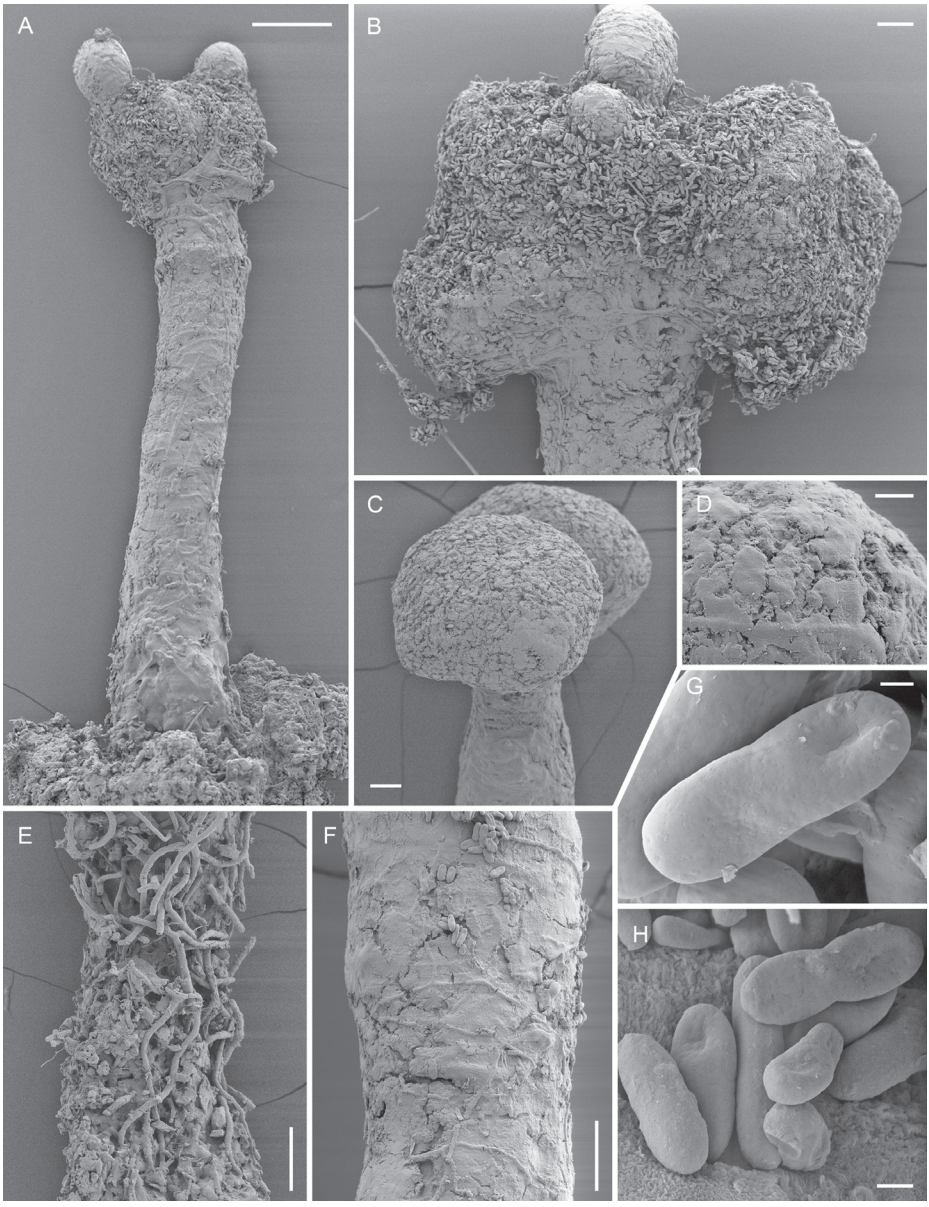

Figure 3. Scanning electron micrographs of *Chaenothecopsis novae-zelandiae* sp. nov. (PDD 110744/CBNZ073B) **A** proliferating apothecium **B** mature capitulum with ascospores and amorphous material **C** semi-mature capitulum **D** (detail of **C**): epithecium of semi-mature capitulum **E** orientation of hyphae at the base of deteriorating ascoma **F** stipe surface **G** ascospore **H** ascospores. Scale bars: 100 μm (**A**); 30 μm (**B, C, E, F**); 10 μm (**D**); 2 μm (**H**); 1 μm (**G**).

with light green to hyaline, amorphous material, formed with croziers. ***Ascospores*** uniseriate, sometimes partly biseriate, obliquely to periclinally oriented in asci, 1-septate, light brown, cylindrical to slightly ellipsoid, sometimes phaseoliform, smooth, or

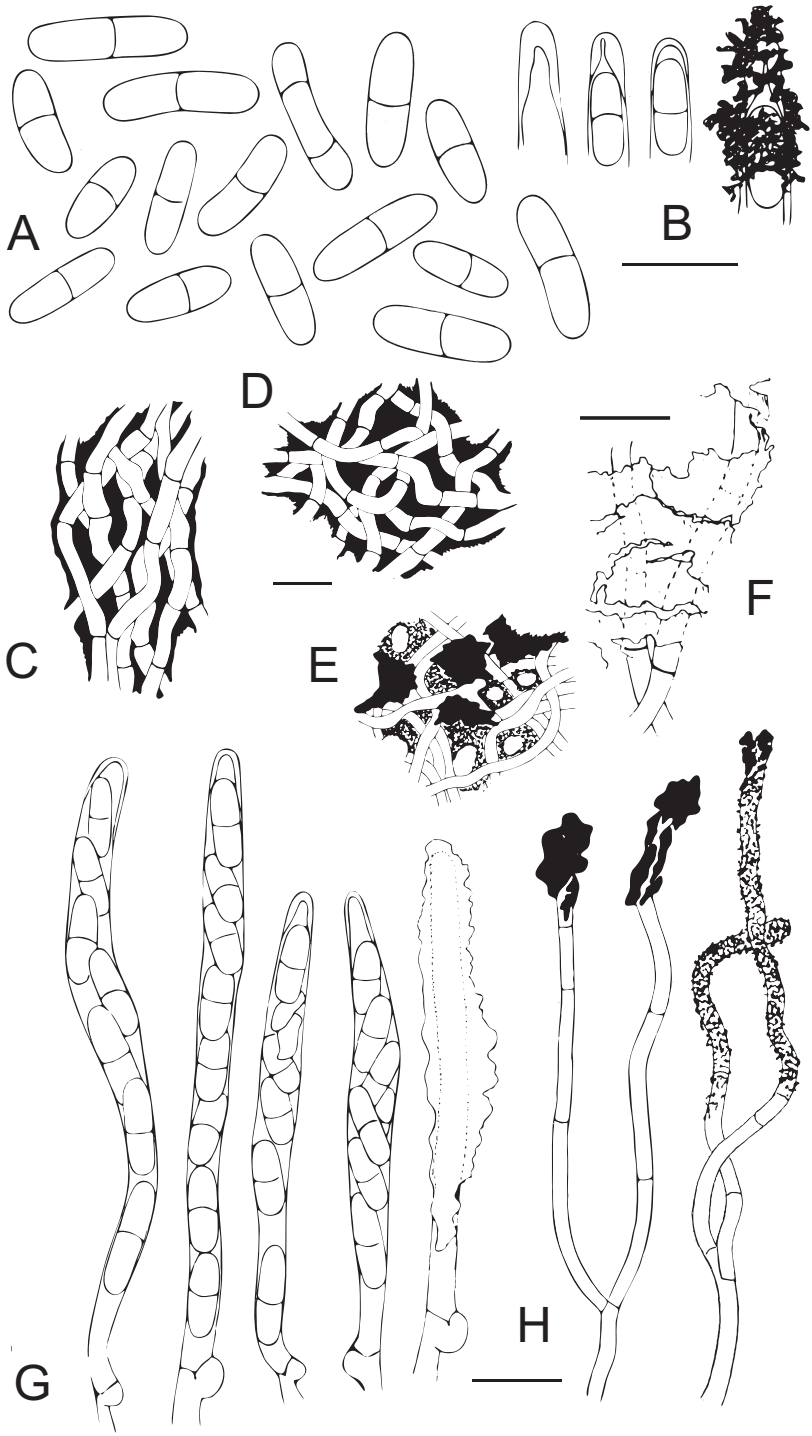

Figure 4. Anatomical details of *Chaenothecopsis novae-zelandiae* sp. nov. **A** ascospores **B** ascus tips **C** excipulum **D** stipe hyphae **E** epithecium with amorphous material and pores **F** hyphae of excipulum with amorphous material **G** asci with croziers **H** paraphyses. Scale bars: 10 µm.

with a very fine ornamentation, (7.7–) 8–13 (–15.4) × (2.8–) 3–3.9 (–4.5) µm (n = 70) [mean 10.3 × 3.4 µm, Q = (2.1–) 2.4–3.8 (–5.0), mean Q = 3.1]; septa as thick as the spore wall, sometimes constricted.

Ecology and distribution. *Chaenothecopsis novae-zelandiae* has been found only at two locations in temperate broad-leaved rainforests of New Zealand on semi-hardened exudate and exudate-soaked bark on the main trunk of *Prumnopitys taxifolia*, sometimes growing mixed with *Chaenothecopsis matai*.

Specimens examined. Specimens PDD110744 (Figs 2, 3A, B, F–H) and PDD 110742 (Figs 1A, B, 3C, D, E) on exudate of *Prumnopitys taxifolia*. The specimens are deposited in the New Zealand Fungarium (PDD), Landcare Research in Auckland, with a duplicate specimen (PDD 110742/JR13033) in Helsinki (H). The collection data and GenBank accession numbers are given in Suppl. material 1.

Chaenothecopsis matai **Rikkinen, Beimforde, Tuovila & A.R. Schmidt, sp. nov.**
MycoBank No: MB846459
Figs 5–7

Type. New Zealand, South Island, Croydon Bush, Dolamore Park, Southland, ca. 46°3.6657'S, 168°49.9135'E, on exudate of *Prumnopitys taxifolia*. 17 February 2017, Beimforde PDD110749, holotype; New Zealand Fungarium (PDD), Landcare Research in Auckland, GenBank accession OQ308932/OQ308875.

Diagnosis. *Chaenothecopsis matai* differs from other *Chaenothecopsis* species by forming extensive mat-like pseudostromata on podocarpous plant exudates with long, often multi-branched, partially translucent stipes, predominantly slender capitula and smooth septate spores that are often constricted at the septum.

Etymology. The specific epithet refers to the Maori name of *Prumnopitys taxifolia*, the exudate-producing tree on which the species was first discovered.

Description. ***Apothecia*** growing on the exudate of *Prumnopitys taxifolia*, arising from a dense mycelium mat which hardens in dry conditions and swells under humid conditions, forming a loose intertwined network with apices either remaining sterile or developing capitula, sometimes growing individually. ***Stipe*** glossy, crustose near stipe apices and pruinose parts, black to brownish, often with a hyaline base and/or apex, 90–240 µm wide, usually 2–7 mm long, or sometimes more than 1 cm long, flexuous or curved, multiple-branched, mostly uniformly thickened, tapering towards the apices, often with an orange to red pruina below the capitula. ***Stipe hyphae*** 2–8 µm wide, with walls two-layered, the outer wall brown and the cell walls fused, the inner walls hyaline, *c*. 0.5–1 µm wide, with the hyphae intertwined (textura prismatica-intricata), swelling in KOH; hyphae in the inner part of stipe hyaline to greenish, 2–6 µm wide, swelling in KOH. ***Capitulum*** black, 110–220 µm wide, 100–200 high, lentiform to cupulate, sometimes narrower than or as wide as the stipe. ***Excipulum*** hyphae brown to emerald green, 4–7 µm wide, intertwined (textura prismatica-intricata), with outer cell walls fused, swelling in KOH and some brown pigment leaking into the medium. ***Epithecium*** brownish to emerald green to hyaline, appearing

Figure 5. Light micrographs of *Chaenothecopsis matai* sp. nov. (PDD 110749) **A** branched and intertwined stipes, some developing capitula **B** ascomata with red pruina **C** young capitulum with ascospores **D** semi-mature capitulum **E** ascospores. Scale bars: 500 µm (**A**); 100 µm (**B, C**); 10 µm (**D**); 2 µm (**E**).

as crusty layer, usually with crystals, composed of the hyphae of the excipulum and paraphyses forming a variously thickened layer. Containing various amounts of orange to ruby-red pigments in most ascomata, usually occurring as crystals on the outer walls of hyphae, and sometimes also inside their lumina. ***Hypothecium*** light brown to greenish hyaline, with the hyphae swelling in KOH. ***Hymenium*** brownish to emerald to hyaline, with the hyphae swelling in KOH, orange to red pigments present, full of amorphous material strongly congealing asci and paraphyes together. ***Paraphyses*** hyaline, filiform, 1.5–2 µm wide (n = 10), branched, usually slightly longer than the asci, variously covered with amorphous material, septate at 9–19 µm intervals. ***Asci***

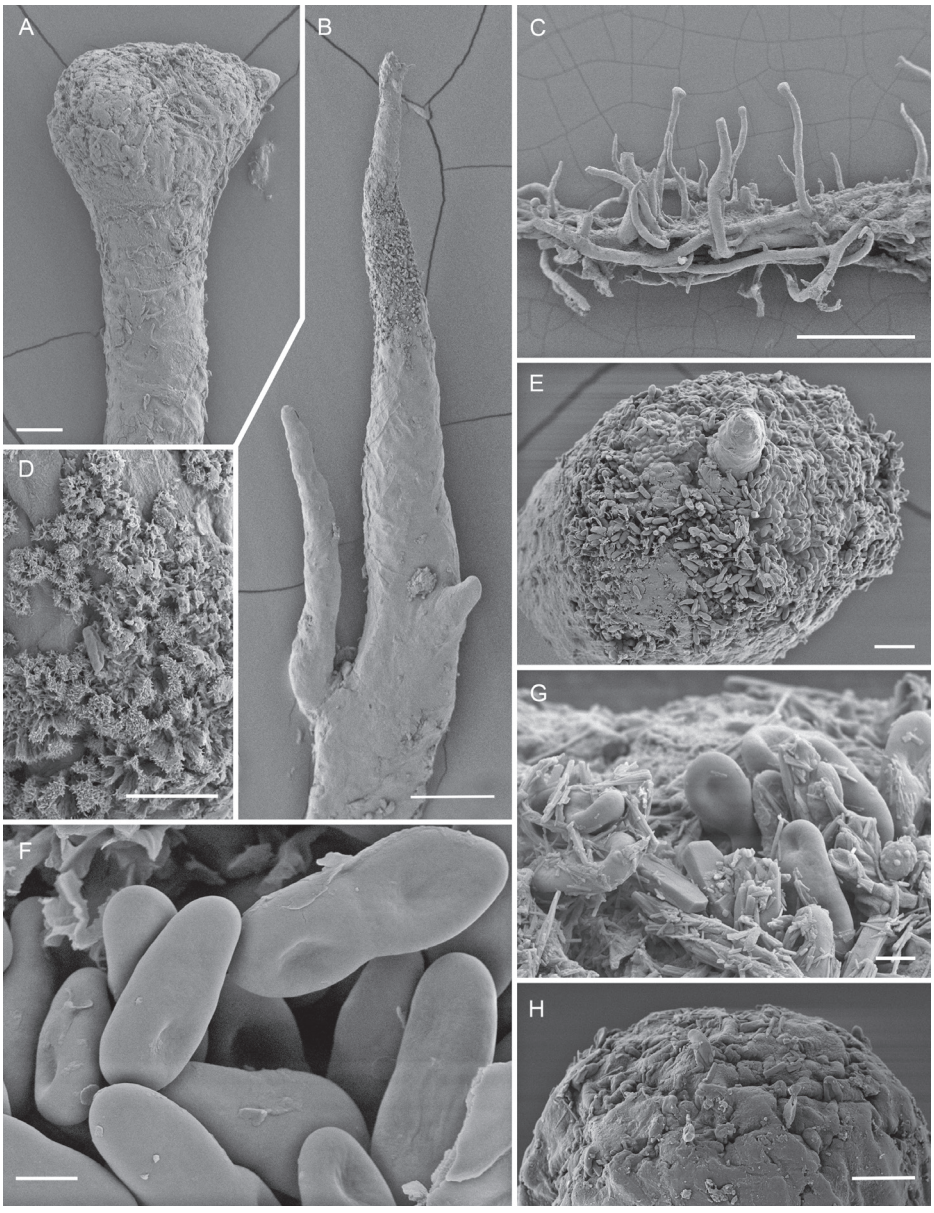

Figure 6. Scanning electron micrographs of *Chaenothecopsis matai* sp. nov. (PDD 110749) **A** semi-mature capitulum **B** upper part of apothecium **C** pseudostroma-like growth of apothecia **D** structure of pruina on stipe surface **E** proliferating growth of capitulum **F** ascospores **G** (detail of **E**): ascospores and crystals on capitulum surface **H** mature capitulum. Scale bars: 1 mm (**C**); 100 μm (**B**); 30 μm (**A**); 20 μm (**E**); 10 μm (**D, H**); 2 μm (**F, G**).

cylindrical, 47–77 μm high, 5–7 μm wide (n = 8), with the apex variously thickened, often penetrated by a poorly developed canal; mature asci usually without a thickening, formed with croziers, tightly embedded in the hymenium, with light brown-green

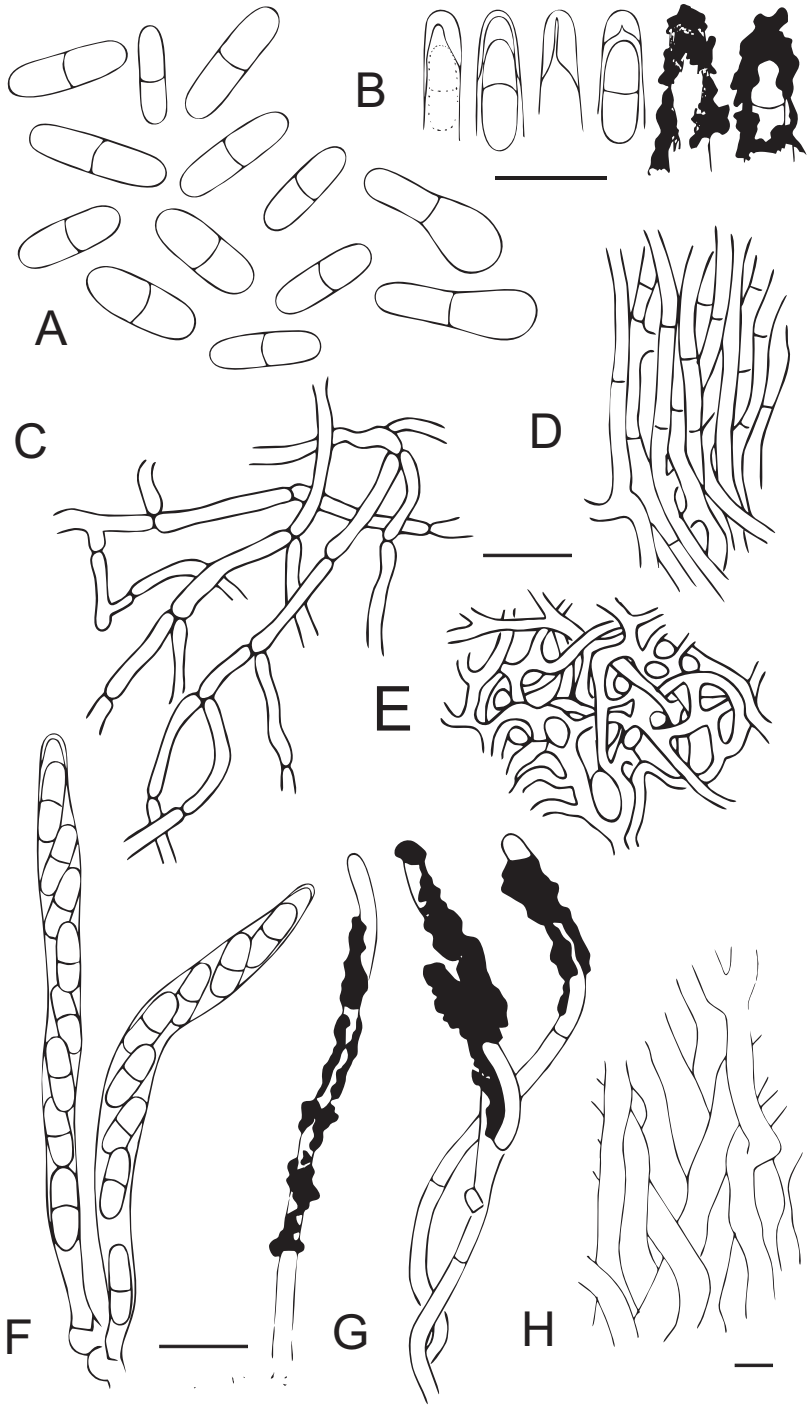

Figure 7. Anatomical details of *Chaenothecopsis matai* sp. nov. **A** ascospores **B** ascus tips **C** stipe hyphae **D** excipulum structure **E** epithecium structure **F** asci with corziers **G** paraphyses **H** inner stipe hyphae. Scale bars: 10 μm.

to hyaline amorphous material making individual asci difficult to observe. ***Ascospores***, smooth, uniseriate, periclinally (to slightly obliquely) oriented in asci, 1-septate, brown, cylindrical to slightly ellipsoid, (7.3–) 8–12.5 (–14) × (2.8–) 3–4.5 (–4.7) µm (n = 60), [mean 10.3 × 3.4 µm, Q = (2–) 3–4.3 (–4.5), mean Q = 3.2]; septa as thick as spore wall, sometimes constricted.

Ecology and distribution. *Chaenothecopsis matai* has been found at several locations in temperate broad-leaved rain forests of New Zealand on semi-hardened exudate and exudate-soaked wood and bark on the main trunk of *Prumnopitys taxifolia*, sometimes growing mixed with *Chaenothecopsis novae-zelandiae*. Some specimens of a morphologically-similar *Chaentohecopsis* species have also been collected from exudate of *Phyllocladus trichomanoides* (Podocarpaceae), but their detailed analysis awaits more material.

Specimens examined. PDD110746 (Fig. 1D–E), PDD110747, PDD110748, PDD110749 (Figs 5, 6) on exudate of *Prumnopitys taxifolia*. The specimens are deposited in the New Zealand Fungarium (PDD), Landcare Research, Auckland, with a duplicate of specimen JR13032 in Helsinki (H). The collection data and GenBank accession numbers are given in Suppl. material 1.

Chaenothecopsis nodosa **Beimforde, Tuovila, Rikkinen & A.R. Schmidt, sp. nov.**
MycoBank No: MB846460
Figs 8–10

Type. New Zealand, North Island, close to Kakaho Camp site, central North Island, ca. 38°34.0224'S, 175°43.0525'E, on exudate of *Prumnopitys taxifolia*, 5 April 2015, Beimforde PDD 110745, holotype; New Zealand Fungarium (PDD), Landcare Research in Auckland, GenBank accession OQ308934/OQ308877.

Diagnosis. *Chaenothecopsis nodosa* differs from other *Chaenothecopsis* species by producing capitula in a catenulate stack, consecutively on top of each other, typically covered with a white pruina.

Etymology. The specific epithet refers to the appearance of catenulate groups of sphaeric capitula stacked on top of each other

Description. ***Apothecia*** growing on the exudate of *Prumnopitys taxifolia*, 1.0–3.1 mm tall, growing individually and proliferating from the capitulum, often several from a single capitulum or from the stipe, eventually forming catenulate stacks of several capitula on top of each other. ***Stipe*** dark brown to black, straight to slightly curved, 100–190 µm wide, becoming crustose with age, often with a white pruina at upper stipe regions, and sometimes with an additional red pruina below. ***Stipe hyphae*** 3–8 µm wide, with walls two layered, the outer wall dark brown, 1.5–3.5 µm and with cell walls fused in most parts, the inner wall *c*. 0.5–1 µm, with the hyphae intertwined (textura prismatica-intricata), swelling in KOH; hyphae in inner parts yellowish to light brown, 2–5 µm wide, swelling in KOH. ***Capitulum*** black, lenticular to almost spherical or ellipsoid, 150–420 µm wide, 250–220µm high; typically a white pruina is macroscopically visible on the capitula. ***Excipulum*** hyphae light brown to

Figure 8. Light micrographs of *Chaenothecopsis nodosa* sp. nov. (PDD 110745) **A** branched ascoma with catenulate capitulum **B** development of this ascoma has involved at least 11 separate stages of capitulum proliferation **C** detail of compound capitulum **D** ascospores. Scale bars: 100 µm (**A, B, D**); 10 µm (**C**).

hyaline in younger ascomata, brown in older ascomata, 2–6 µm wide, intertwined (textura prismatica-intricata), swelling in KOH; often covered with a crusty layer of amorphous material and crystals. ***Epithecium*** light green to moss green, appearing as a crusty layer, variously (up to 20 µm) thickened, usually with crystals, composed of hyphae extending from the excipulum; hyphae attached to the hymenium by the amorphous material. ***Hymenium*** light brown to olive green, with the hyphae swelling in KOH, full of amorphous material strongly congealing the asci and paraphyses together. ***Paraphyses*** hyaline, filiform, 1.5–2.5 µm wide (n = 20), sometimes branched, as long as or slightly longer than asci, variously covered with amorphous material, septate at 10–25 µm intervals, with the apices intertwined and agglutinated with the hyphae of the epithecium. ***Asci*** cylindrical, 60–77 × 4.9–7.7 µm (n = 8), with the apex variously thickened, penetrated by a minute canal visible only in young asci; mature asci usually without a thickening, variously covered with light green to hyaline, amor-

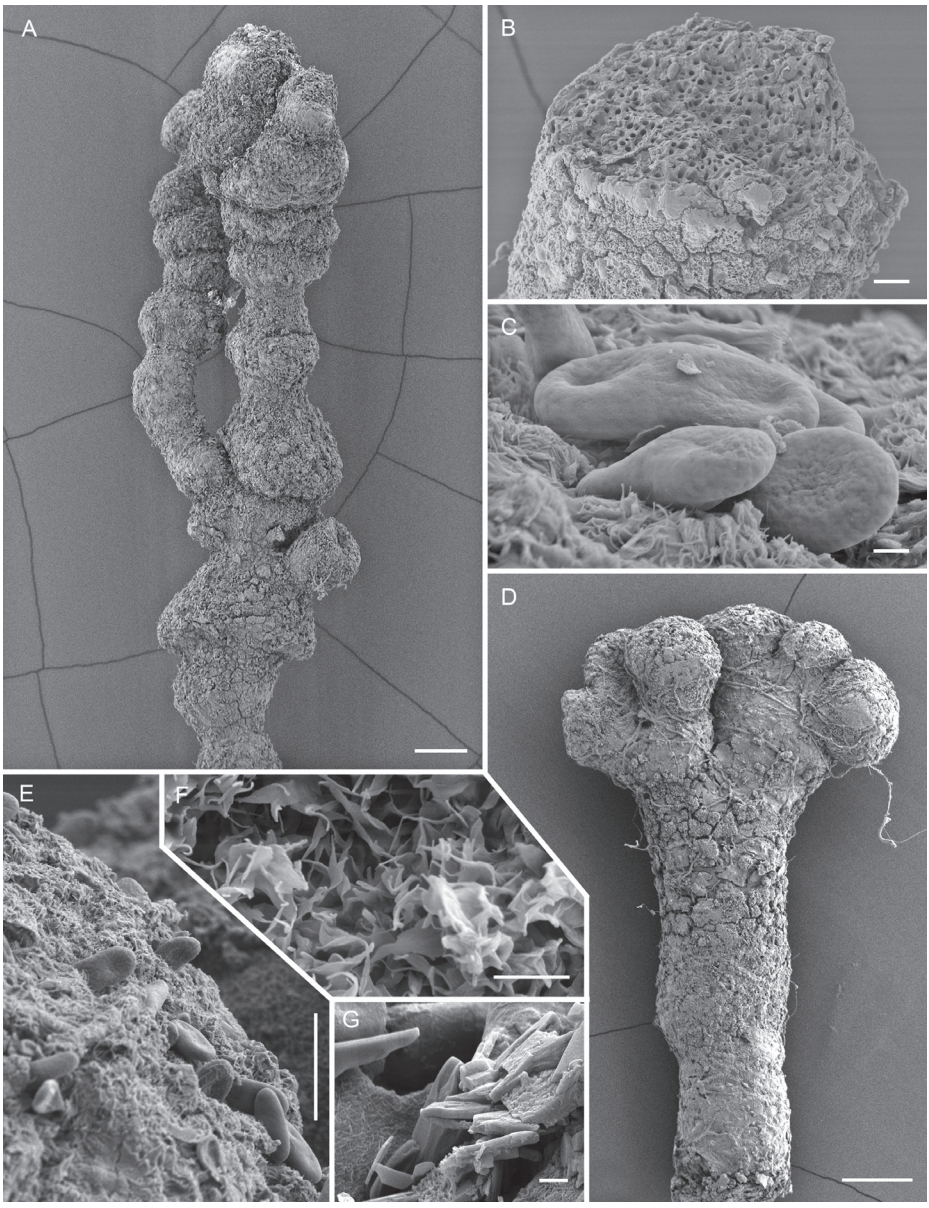

Figure 9. Scanning electron micrographs of *Chaenothecopsis nodosa* sp. nov. (PDD 110745) **A** branched ascoma with numerous tightly stacked capitula **B** cross section of stipe **C** ascospore ornamentation **D** compound capitula **E–G** details of capitulum surface **E** ascospores on capitulum surface **F** amorphous material on capitulum surface **G** crystals on capitulum surface. Scale bars: 100 μm (**A, D**); 10 μm (**B, E**); 1 μm (**C, F, G**).

phous material, formed with croziers; asci in older capitula disintegrated. ***Ascospores*** uniseriate, obliquely to periclinally oriented in the asci, 1-septate, brown, cylindrical to slightly ellipsoid, ornamented, (6.7–) 8.5–9.2 (–10.8) × (3.1–) 3.4–3.9 (–4.6) μm

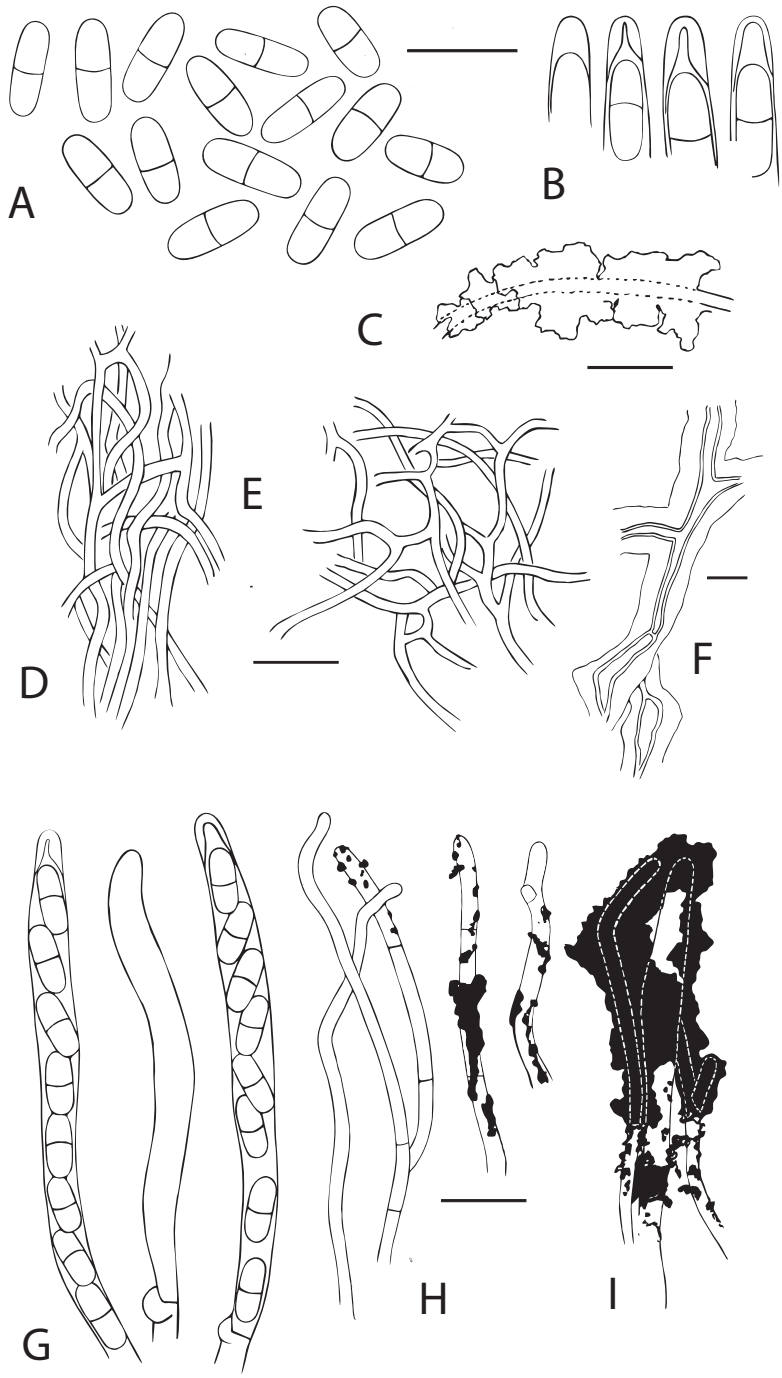

Figure 10. Anatomical details of *Chaenothecopsis nodosa* sp. nov. **A** ascospores **B** ascus tips **C** hypha of epithecium covered with amorphous material **D** excipulum structure **E** stipe hyphae **F** structure of the hyphae at the base of the stipe **G** asci with croziers **H** paraphyses **I** tips of paraphyses covered with amorphous material. Scale bars: 10 μm.

(n = 60) [mean 9.5 × 3.8 µm, Q = (2.8–) 3.5–4.6 (–5.4), mean Q = 3.8]; septa as thick as spore wall.

Ecology and distribution. *Chaenothecopsis nodosa* has to date been found only in temperate broad-leaved rainforests of New Zealand on semi-hardened exudate and exudate-soaked exposed wood and bark on the main trunk of *Prumnopitys taxifolia*.

Specimens examined. Specimens PDD 110743 and PDD 110745 (Figs 8, 9) on exudate of *Prumnopitys taxifolia*. The specimens are deposited in the New Zealand Fungarium (PDD), Landcare Research, Auckland. The collection data and GenBank accession numbers are given in Suppl. material 1.

Discussion

Taxonomy and systematics

The new species described here represent the first *Chaenothecopsis* species from exudates of New Zealand gymnosperms. Only *Chaenothecopsis schefflerae* had previously been found on New Zealand plant exudates, but this species is restricted to angiosperm exudates of endemic Araliaceae (Beimforde et al. 2017).

All three new species occur on the same substrate, i.e., exudate of *Prumnopitys taxifolia* and each has a distinctive macroscopic appearance. *Chaenothecopsis nodosa* tends to produce many capitula in a catenulate stack, consecutively on top of each other (Figs 8A, B, D, 9A) and typically produces a white prunia (Fig. 8A, D). In contrast, *C. matai* and *C. novae-zelandiae* produce a reddish pruina (Fig. 5B, C). Ascomata of *C. novae-zelandiae* have comparatively short stipes and tend to grow individually or in smaller groups (Fig. 2A), whereas *C. matai* usually produces extensive mat-like pseudostromata on its substrate (Figs 5A, 6C).

Chaenothecopsis matai may form very long, multiply-branched and interwoven stipes, often with hyaline parts at the base or apex (Fig. 5B). This species grows in areas of the host trees where exudate accumulates in a humid environment, e.g., in crevices of trunks or branches, or between forking trunks at the base of trees. In such places, *C. matai* sometimes forms dense mycelial mats which are soaked with the water-soluble *Prumnopitys* exudate and from which apothecia and sterile stalks arise, forming a pseudostroma-like network. A pseudostroma-like growth habit has also been observed in *Chaenothecopsis caespitosa* (W. Phillips) D. Hawksw., described by Hawksworth (1980). However, in contrast to *C. matai*, apothecia of *C. caespitosa* grow in tuft-like structures. Nor does *C. caespitosa* produce the long, abundantly branched stipes observed in *C. matai*. In addition, the former species has only been collected from rotting polypores on *Taxus* branches in Great Britain. A pseudostroma-like growth habit is also known from *Mycocalicium sequoia* Bonar (Bonar 1971), a mycocalicioid species growing on exudates of *Sequoia* Endl. and *Sequoiadendron* J.Buchholz. However, in contrast to *C. matai*, *M. sequioae* has a bright yellow pruina on the capitulum surface and tends to produce very compact stroma-like mycelia in which the stalked ascomata are almost completely embedded.

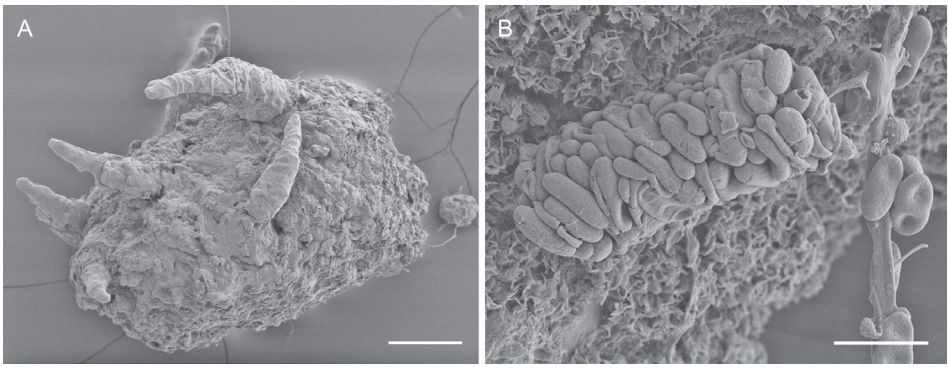

Figure 11. Insect fecal pellets associated with *Chaenothecopsis matai* (**A**) and *Chaenothecopsis nodosa* (**B**) **A** fecal pellet showing initial ascomata development **B** insect fecal pellets consisting predominantly of ascospores. Scale bars: 100 μm (**A**); 10 μm (**B**).

Chaenothecopsis nodosa is morphologically conspicuous and readily distinguishable from *C. matai*, *C. novae-zelandiae* and other resinicolous *Chaenothecopsis* species with proliferating ascomata, such as *C. diabolica* Rikkinen & Tuovila (Tuovila et al. 2011b), *C. dolichocephala* Titov (Tibell and Titov 1995), and *C. proliferatus* Rikkinen, A. R. Schmidt & Tuovila (Tuovila et al. 2013) on the basis of its catenulate, very tightly stacked capitula. Proliferating ascomata are produced by several resinicolous *Chaenothecopsis* species from different clades, and are also evident from fossil specimens from Paleogene Baltic and Bitterfeld amber (Tuovila et al. 2013; Rikkinen et al. 2018). One can assume that these types of ascomata can effectively rejuvenate if partially overrun by fresh exudate and thus represent a morphological adaptation to life on plant exudates (Tuovila et al. 2013).

In Mycocaliciales, the assignment of species to particular genera, and the delimitation of species is sometimes challenging when using morphological characters only (Schmidt 1970; Tibell 1984, 1987; Titov 2006; Tuovila 2013). For this reason, besides careful examination of microscopical diagnostic characters (for details see Tuovila and Huhtinen 2020), we used additional information from phylogenetically informative gene regions, the internal transcribed spacer region (ITS) and the large ribosomal subunit (LSU), for species identification and taxonomic assignment. Our phylogenetic tree (Fig. 12) accentuates unresolved issues of generic delimitation within Mycocaliciales (e.g. Tibell and Vinuesa 2005; Tuovila 2013) since species assigned to genera such as *Mycocalicium* Vain., *Phaeocalicium* A.F.W. Schmidt and *Chaenothecopsis* appear not to be monophyletic. The recently erected genus *Brunneocarpos* Giraldo & Crous (Crous et al. 2016) is nested within *Chaenothecopsis*, with *C. diabolica* constituting the sister taxon of *Brunneocarpos banksiae* Giraldo & Crous.

Our phylogenetic analysis (Fig. 12) places all three new *Chaenothecopsis* species in a monophyletic clade. The three species also share many morphological features. Additional specimens collected from *Phyllocladus trichomanoides* are most similar to *C. matai*, differing only by few base pairs in the ITS region. However, due to the very

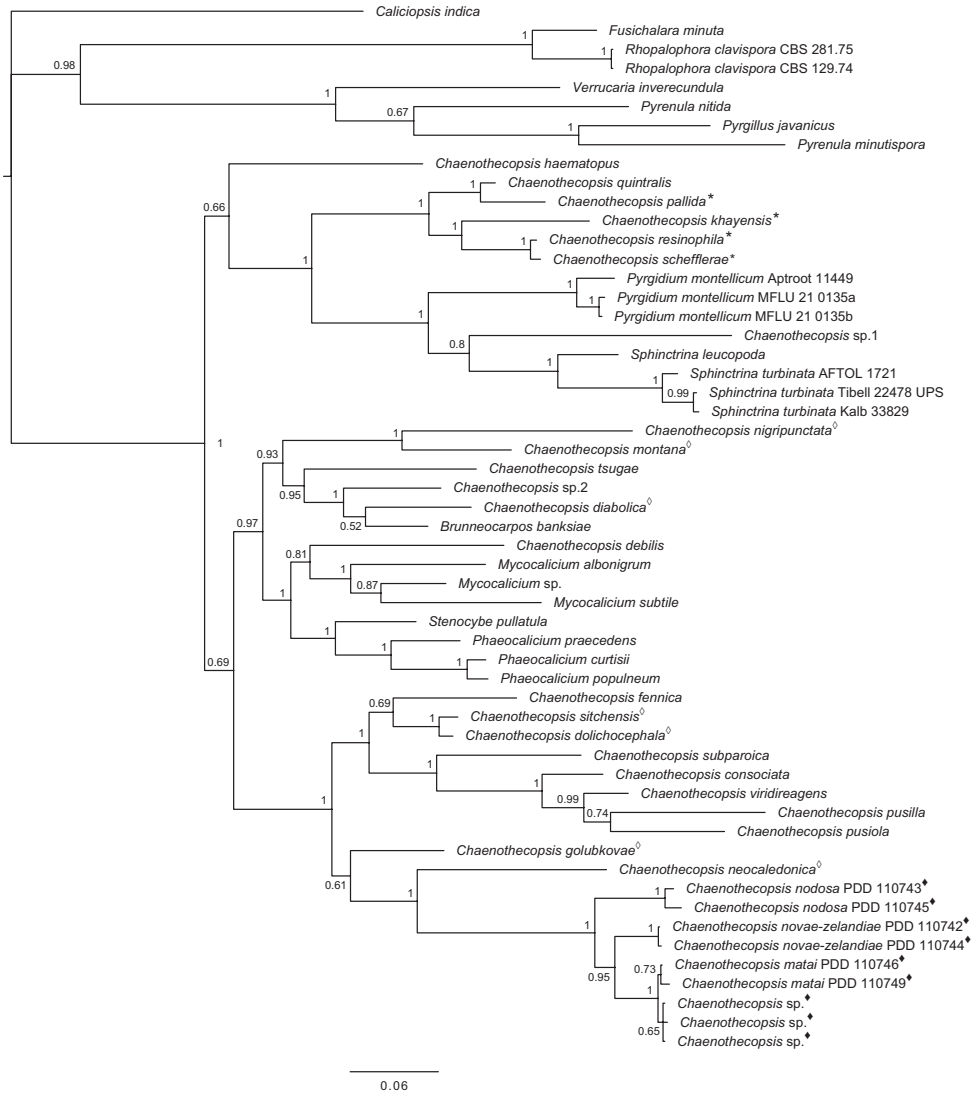

Figure 12. Phylogenetic relationships of mycocalicioid fungi (Mycocaliciales, Ascomycota). Bayesian tree based on partial sequences of the ribosomal internal transcribed spacer region (ITS) and the large ribosomal subunit (LSU). Numbers at branches indicate Bayesian posterior probabilities. The asterisks mark species from angiosperm exudate, white diamonds mark species from conifer resin, black diamonds mark species from podocarpous exudates.

limited sample material from *Phyllocladus* Rich. exudates, we were currently not able to study possible differences between *C. matai* specimens collected from *Prumnopitys* and *Phyllocladus* exudates in detail.

Chaenothecopsis neocaledonica Rikkinen, A.R.Schmidt & Tuovila is the sister taxon to the New Zealand clade in our phylogenetic tree (Fig. 12). *C. neocaledonica* grows

on resinous plant exudates of *Agathis ovata* (C.Moore ex Vieill.) Warb. (Araucariaceae Henkel & W.Hochst.), an endemic New Caledonian conifer (Rikkinen et al. 2014). This sister taxon relationship is conceivable due to their geographical proximity. Morphologically, all three New Zealand species differ from *C. neocaledonica* (and from other resinicolous species with one-septate spores) in the presence of peculiar amorphous material covering the asci and paraphyses, sometimes in a very thick layer (Figs 4B, F, H, 7B, G, 10C, H, I). This material also glues the whole hymenium tightly together and makes asci and paraphyses difficult to observe. In addition, the spores of the New Zealand species are on average narrower than those of *C. neocaledonica*, and at least some in each studied ascoma were phaseoliforme (resembling kidney-beans) or slightly constricted (*C. matai* and *C. novae-zelandiae*) at the septum, in contrast to the strictly cylindrical-fusoid spores of *C. neocaledonica*.

Endemism and spore dispersal

Most previously known *Chaenothecopsis* species from temperate forest systems of New Zealand are considered to be cosmopolitan and not strictly host specific. According to Tibell (1987), *C. debilis*, *C. nana* Tibell, *C. nivea* (F. Wilson) Tibell, *C. pusilla* (A. Massal.) A.F.W. Schmidt and *C. savonica* (Räsänen) Tibell occur on hard lignum and/or bark of various New Zealand gymnosperms or angiosperms. Other species, such as *C. haematopus*, *C. lignicola* (Nádv.) A.F.W. Schmidt, *C. nigra* Tibell and *C. nigropedata* Tibell, may also be associated with lichens or algae.

Previously only two *Chaenothecopsis* species, *C. brevipes* Tibell and *C. schefflerae*, were thought to be endemic to New Zealand (Tibell 1987). *C. brevipes* is a lichenicolous species, characterized by its short stalk and strict association with lichens of the genus *Arthonia* Ach. (Arthoniaceae). However, this species seems to be more widespread than previously assumed. In New Zealand *C. brevipes* occurs on *Arthonia platygraphella* Nyl. (Tibell 1987) but was later also noted on other *Arthonia* species e.g., in Russia (Titov and Tibell 1993), North America and Canada (Selva 2010). *C. schefflerae* is a species which appears to be endemic to New Zealand as it only occurs on exudates of endemic Araliaceae. This species was initially known only from exudates of *Schefflera digitata* (Araliaceae) but was later also found on exudates of *Pseudopanax* (Beimforde et al. 2017). In any case, *C. schefflerae* is not closely related to the species described here, as it belongs to a well-supported monophyletic group that includes all other known *Chaenothecopsis* species from angiosperm exudates.

Chaenothecopsis novae-zelandiae, *C. matai* and *C. nodosa* were predominantly found on exudates of *Prumnopitys taxifolia*. However, as mentioned above, we also found very limited material of a similar *Chaenothecopsis* species growing on exudates of *Phyllocladus trichomanoides*. Thus, it is possible that the new species may also occur on exudates of other *Phyllocladus* species and possibly even on *Prumnopitys ferruginea*, all of which are also endemic to New Zealand. Although a broader host range is thus possible, we expect that the three new *Chaenothecopsis* species described here all belong to New Zealand's endemic mycobiota, both due to their specialized substrates

and the fact that they group into a distinct monophyletic lineage in our phylogenetic analyses (Fig. 12).

The exudate outpourings of *Prumnopitys taxifolia* are sometimes densely covered by numerous *Chaenothecopsis* ascomata providing shelter to diverse arthropods. Some of our collected specimens, particularly those with numerous ascomata were abundantly littered with insect fecal pellets between or at the base of the ascomata. Scanning electron micrographs revealed spores on the outer surfaces of many fecal pellets, and some smaller fecal pellets consist almost entirely of *Chaenothecopsis* spores (Fig. 11B), suggesting that associated insects feed on the ascomata and defecate undigested ascospores. This notion is substantiated by our findings of fecal pellets with associated early stages of ascomata development (Fig. 11A). We detected a range of insects and insect remnants between the densely arranged ascomata in several samples, for example lepidopteran cocoons, mites, coleopterans such as a rove beetle (Staphylinidae Latreille) and possibly wood boring beetles as well as insect exuviae, pupae and larvae. These findings, together with the spores and initial ascomata development in the fecal pellets, indicate that the densely growing ascomata provide shelter and food source for diverse insects and that ascospores of the fungi are ingested, but probably not digested by insects. It is thus likely that insects are involved in the spore dispersal of the species described herein, as spores may be consumed by the insects and spread with their excrements or get attached to the insects' surface when they crawl over the apothecia. It might well be that the spore-dispersing insects are also associated with the host trees and thus guarantee that the spores reach the substrates that are essential for the fungal species to survive.

Ecology on plant exudates and evolution

Some fungi have developed defenses against the toxic components of plant exudates (e.g. Rautio et al. 2012; Adams et al. 2013) but it is uncertain whether this unusual, inherently toxic substrate is preferred to evade competition or whether exudates provide a nutrient source for the fungi. The dependence of some mycocalicioid fungi and other resinicolous ascomycetes on conifer resins and other plant exudates, and the fact that their hyphae grow randomly into this substrate (Beimforde et al. 2020) suggests a nutrient uptake from the exudates. Theoretically, resin and other plant exudates represent oxidizable organic matter, but it has not yet been proven empirically whether fungi are able to metabolize compounds of plant exudates.

Our culture experiments demonstrate that all three species described here grow *in vitro* on a carbohydrate-based medium (PDA). Still, we cannot exclude that phenolic and/or terpenoid substances of the *Prumnopitys* exudate may also be degraded by the species. The composition of plant exudate differs greatly between individual plant lineages. The exudates of angiosperms that serve as hosts for some *Chaenothecopsis* species (*Khaya* and *Rhus* (Anacardiaceae), *Ailanthus* (Simaroubaceae), *Kalopanax*, *Pseudopanax* and *Schefflera* (Araliaceae)) consist of complex hydrophilic, non-polymerized polysaccharides (Langenheim 2003), representing a conceivable nutrient source. In contrast, conifer host trees produce resinous exudates that consist of a mixture of hydrophobic,

phenolic and terpenoid components that are toxic for most microorganisms (Bednarek and Osbourn 2009; Sipponen and Laitinen 2011; Rautio et al. 2012) because they damage cell wall structures (Rautio et al. 2011). Nevertheless, terpenoid/phenolic conifer exudates may contain hybrid subgroups such as guaiac gums, guaiac resins, and kino resins (Lambert et al. 2021), which might be degradable by fungi. The composition of *Prumnopitys* exudate has not yet been studied in detail, but it appears to differ from other conifer exudates (Lambert et al. 2007). According to our observations, the exudate of *Prumnopitys taxifolia* differs from resins or exudates of most other conifer hosts in being water-soluble, in its dark tint and the strong phenolic fragrance of fresh outpourings. This means that, as recently shown for some Araucaria species (Seyfullah et al. 2022), distinct types of exudate (gum, resin, and gum resin) may co-occur in *Prumnopitys*.

Our phylogenetic analysis indicates that the three species from Podocarpaceae exudate descend from a common ancestor. Likewise, all known *Chaenothecopsis* species from various angiosperm exudates also originate from a common ancestor. In contrast, resinicolous species from terpenoid conifer resins have multiple origins and occur in several lineages within the Mycocaliciales, suggesting a longer and more complex evolutionary history. The age of the resinicolous ecology within Mycocaliciales remains uncertain since relationships between individual monophyletic clades have not yet been fully resolved. In any case, resinicolous *Chaenothecopsis* species from various ambers prove that this ecological mode on conifer resin has existed within the genus for at least 35 million years (Rikkinen and Poinar 2000; Tuovila et al. 2013; Rikkinen et al. 2018; Rikkinen and Schmidt 2018). Recent estimates of divergence times of the Ascomycota place the separation of Mycocaliales and Eurotiomycetes in the Carboniferous (Prieto and Wedin 2013; Beimforde et al. 2014) and the origin of the Mycocaliciales crown group in the late Jurassic, when diverse conifer lineages were present (Lubna et al. 2021). It is possible that Mycocaliciales could have colonized conifers at an early stage of conifer evolution in the Permian, and it might well be that the resinicolous ecology evolved at a very early stage within Mycocaliciales. The oldest New Zealand pollen and macrofossil records of *Prumnopitys* and *Phyllocladus* are from Paleocene and Eocene deposits (Lee et al. 2016) and thus fungi on their exudates could have existed since then. Based on the isolated phylogenetic position of this clade from Podocarpaceae exudates, it could well be that this lineage diverged from other *Chaenothecopsis* clades in the Paleocene or even earlier.

Acknowledgements

We thank Daphne Lee (Dunedin) for linguistic assistance, providing help with field work and information about palaeobotanical evidence in New Zealand, Adrienne Stanton (Landcare Research, Auckland) for providing voucher numbers and curating our specimens in the New Zealand Fungarium PDD – Plant Disease Division, Liz Girvan (Dunedin) and Dorothea Hause-Reitner (Göttingen) for assisting in scanning electron

microscopy. We also thank the anonymous reviewer for his detailed review of the manuscript. This study was supported by funds provided by the German Research Foundation (project 429296833) as well as by the Academy of Finland (project 343113).

References

Adams AS, Aylward FO, Adams SM, Erbilgin N, Aukema BH, Currie CR, Suen G, Raffa KF (2013) Mountain pine beetles colonizing historical and naive host trees are associated with a bacterial community highly enriched in genes contributing to terpene metabolism. Applied and Environmental Microbiology 79(11): 3468–3475. https://doi.org/10.1128/AEM.00068-13

Bednarek P, Osbourn A (2009) Plant-microbe interactions: Chemical diversity in plant defense. Science 324(5928): 746–748. https://doi.org/10.1126/science.1171661

Beimforde C, Feldberg K, Nylinder S, Rikkinen J, Tuovila H, Dörfelt H, Gube M, Jackson DJ, Reitner J, Seyfullah LJ, Schmidt AR (2014) Estimating the Phanerozoic history of the Ascomycota lineages: Combining fossil and molecular data. Molecular Phylogenetics and Evolution 78: 386–398. https://doi.org/10.1016/j.ympev.2014.04.024

Beimforde C, Tuovila H, Schmidt AR, Lee WG, Gube M, Rikkinen J (2017) *Chaenothecopsis schefflerae* (Ascomycota: Mycocaliciales): a widespread fungus on semi-hardened exudates of endemic New Zealand Araliaceae. New Zealand Journal of Botany 55(4): 387–406. https://doi.org/10.1080/0028825X.2017.1360368

Beimforde C, Schmidt AR, Rikkinen J, Mitchell JK (2020) Sareomycetes cl. nov.: A new proposal for placement of the resinicolous genus *Sarea* (Ascomycota, Pezizomycotina). Fungal Systematics and Evolution 6(1): 25–37. https://doi.org/10.3114/fuse.2020.06.02

Bonar L (1971) A new Mycocalicium on scarred Sequoia in California. Madroño 21: 62–69.

Crous PW, Wingfield MJ, Richardson DM, Leroux JJ, Strasberg D, Edwards J, Roets F, Hubka V, Taylor PWJ, Heykoop M, Martín MP, Moreno G, Sutton DA, Wiederhold NP, Barnes CW, Carlavilla JR, Gené J, Giraldo A, Guarnaccia V, Guarro J, Hernández-Restrepo M, Kolaik M, Manjón JL, Pascoe IG, Popov ES, Sandoval-Denis M, Woudenberg JHC, Acharya K, Alexandrova AV, Alvarado P, Barbosa RN, Baseia IG, Blanchette RA, Boekhout T, Burgess TI, Cano-Lira JF, Moková A, Dimitrov RA, Dyakov MY, Dueñas M, Dutta AK, Esteve-Raventós F, Fedosova AG, Fournier J, Gamboa P, Gouliamova DE, Grebenc T, Groenewald M, Hanse B, Hardy GESJ, Held BW, Jurjevi Kaewgrajang T, Latha KPD, Lombard L, Luangsa-ard JJ, Lysková P, Mallátová N, Manimohan P, Miller AN, Mirabolfathy M, Morozova OV, Obodai M, Oliveira NT, Ordóñez ME, Otto EC, Paloi S, Peterson SW, Phosri C, Roux J, Salazar WA, Sánchez A, Sarria GA, Shin HD, Silva BDB, Silva GA, Smith MT, Souza-Motta CM, Stchigel AM, Stoilova-Disheva MM, Sulzbacher MA, Telleria MT, Toapanta C, Traba JM, Valenzuela-Lopez N, Watling R, Groenewald JZ (2016) Fungal planet description sheets: 400–468. Persoonia 36(1): 450–451. https://doi.org/10.3767/003158516X692185

Darriba D, Taboada GL, Doallo R, Posada D (2012) jModelTest 2: More models, new heuristics and parallel computing. Nature Methods 9(8): e772. https://doi.org/10.1038/nmeth.2109

del Prado R, Schmitt I, Kautz S, Palice Z, Lücking R, Lumbsch HT (2006) Molecular data place Trypetheliaceae in Dothideomycetes. Mycological Research 110(5): 511–520. https://doi.org/10.1016/j.mycres.2005.08.013

Gardes M, Bruns TD (1993) ITS primers with enhanced specificity for basidiomycetes – application to the identification of mycorrhizae and rusts. Molecular Ecology 2(2): 113–118. https://doi.org/10.1111/j.1365-294X.1993.tb00005.x

Geiser DM, Gueidan C, Miadlikowska J, Lutzoni F, Kauff F, Hofstetter V, Fraker E, Schoch CL, Tibell L, Untereiner WA, Aptroot A (2006) Eurotiomycetes: Eurotiomycetidae and Chaetothyriomycetidae. Mycologia 98(6): 1053–1064. https://doi.org/10.1080/15572536.2006.11832633

Gueidan C, Aptroot A, da Silva Cáceres ME, Binh NQ (2016) Molecular phylogeny of the tropical lichen family Pyrenulaceae: Contribution from dried herbarium specimens and FTA card samples. Mycological Progress 15(1): 1–7. https://doi.org/10.1007/s11557-015-1154-8

Hall T (1999) BioEdit: A user-friendly biological sequence alignment editor and analysis program for Windows 95/98/NT. Nucleic Acids Symposium Series 41: 95–98.

Hawksworth DL (1980) Two little-known members of the Mycocaliciaceae on polypores (*Chaenothecopsis caespitosa*, *Phaeocalicium polyporaeum*, *Calicium*, *Mycocalicium*). Transactions of the British Mycological Society 74: 650–651. https://doi.org/10.1016/S0007-1536(80)80073-8

James TY, Kauff F, Schoch CL, Matheny PB, Hofstetter V, Cox CJ, Celio G, Gueidan C, Fraker E, Miadlikowska J, Lumbsch HT, Rauhut A, Reeb V, Arnold AE, Amtoft A, Stajich JE, Hosaka K, Sung GH, Johnson D, O'Rourke B, Crockett M, Binder M, Curtis JM, Slot JC, Wang Z, Wilson AW, Schüssler A, Longcore JE, O'Donnell K, Mozley-Standridge S, Porter D, Letcher PM, Powell MJ, Taylor JW, White MM, Griffith GW, Davies DR, Humber RA, Morton JB, Sugiyama J, Rossman AY, Rogers JD, Pfister DH, Hewitt D, Hansen K, Hambleton S, Shoemaker RA, Kohlmeyer J, Volkmann-Kohlmeyer B, Spotts RA, Serdani M, Crous PW, Hughes KW, Matsuura K, Langer E, Langer G, Untereiner WA, Lücking R, Büdel B, Geiser DM, Aptroot A, Diederich P, Schmitt I, Schultz M, Yahr R, Hibbett DS, Lutzoni F, McLaughlin DJ, Spatafora JW, Vilgalys R (2006) Reconstructing the early evolution of Fungi using a six-gene phylogeny. Nature 443(7113): 818–822. https://doi.org/10.1038/nature05110

Katoh K, Toh H (2008) Recent developments in the MAFFT multiple sequence alignment program. Briefings in Bioinformatics 9(4): 286–298. https://doi.org/10.1093/bib/bbn013

Lambert JB, Kozminski MA, Santiago-Blay JA (2007) Distinctions among conifer exudates by proton magnetic resonance spectroscopy. Journal of Natural Products 70(8): 1283–1294. https://doi.org/10.1021/np0701982

Lambert JB, Santiago-Blay JA, Wu Y, Contreras TA, Johnson CL, Bisulca CM (2021) Characterization of phenolic plant exudates by nuclear magnetic resonance spectroscopy. Journal of Natural Products 84(9): 2511–2524. https://doi.org/10.1021/acs.jnatprod.1c00522

Langenheim JH (2003) Plant Resins: Chemistry, Evolution, Ecology, and Ethnobotany. Timber Press, Portland, Cambridge.

Lee DE, Lee WG, Jordan GJ, Barreda VD (2016) The Cenozoic history of New Zealand temperate rainforests: Comparisons with southern Australia and South America. New Zealand Journal of Botany 54(2): 100–127. https://doi.org/10.1080/00288255X.2016.1144623

Lubna L, Asaf S, Khan AL, Jan R, Khan A, Khan A, Kim K-M, Lee I-J (2021) The dynamic history of gymnosperm plastomes: Insights from structural characterization, comparative analysis, phylogenomics, and time divergence. The Plant Genome 14(3): e20130. https://doi.org/10.1002/tpg2.20130

Messuti MI, Vidal-Russell R, Amico GC, Lorenzo LE (2012) *Chaenothecopsis quintralis*, a new species of calicioid fungus. Mycologia 104(5): 1222–1228. https://doi.org/10.3852/12-006

Miller MA, Pfeiffer W, Schwartz T (2010) Creating the CIPRES Science Gateway for inference of large phylogenetic trees. 2010 gateway computing environments workshop (GCE), New Orleans, 8 pp. https://doi.org/10.1109/GCE.2010.5676129

Pratibha J, Amandeep K, Shenoy BD, Bhat DJ (2010) *Caliciopsis indica* sp. nov. from India. Mycosphere. Journal of Fungal Biology 1: 65–72.

Prieto M, Wedin M (2013) Dating the diversification of the major lineages of ascomycota (Fungi). PLoS ONE 8(6): e65576. https://doi.org/10.1371/journal.pone.0065576

Pykälä J, Launis A, Myllys L (2019) Taxonomy of the *Verrucaria kalenskyi* – *V. xyloxena* species complex in Finland. Nova Hedwigia 109(3–4): 489–511. https://doi.org/10.1127/nova_hedwigia/2019/0553

Rambaut A, Drummond AJ (2009) Tracer. MCMC Trace analysis tool version v1.7.2. https://github.com/beast-dev/tracer/releases/tag/v1.7.2

Rautio M, Sipponen A, Lohi J, Lounatmaa K, Koukila-Kähkölä P, Laitinen K (2012) In vitro fungistatic effects of natural coniferous resin from Norway spruce (*Picea abies*). European Journal of Clinical Microbiology & Infectious Diseases 31(8): 1783–1789. https://doi.org/10.1007/s10096-011-1502-9

Réblová M, Untereiner WA, Stepanek V, Gams W (2017) Disentangling *Phialophora* section Catenulatae: Disposition of taxa with pigmented conidiophores and recognition of a new subclass, Sclerococcomycetidae (Eurotiomycetes). Mycological Progress 16(1): 27–46. https://doi.org/10.1007/s11557-016-1248-y

Rehner SA, Samuels GJ (1994) Taxonomy and phylogeny of *Gliocladium* analysed from nuclear large subunit ribosomal DNA sequences. Mycological Research 98(6): 625–634. https://doi.org/10.1016/S0953-7562(09)80409-7

Rikkinen J (1999) Two new species of resinicolous *Chaenothecopsis* (Mycocaliciaceae) from Western North America. The Bryologist 102(3): e366. https://doi.org/10.2307/3244223

Rikkinen J (2003) *Chaenothecopsis nigripunctata*, a remarkable new species of resinicolous Mycocaliciaceae from western North America. Mycologia 95(1): 98–103. https://doi.org/10.1080/15572536.2004.11833136

Rikkinen J, Poinar G (2000) A new species of resinicolous *Chaenothecopsis* (Mycocaliciaceae, Ascomycota) from 20 million year old Bitterfeld amber, with remarks on the biology of resinicolous fungi. Mycological Research 104(1): 7–15. https://doi.org/10.1017/S0953756299001884

Rikkinen J, Schmidt AR (2018) Morphological convergence in forest microfungi provides a proxy for Paleogene forest structure. In: Krings M, Harper CJ, Cúneo NR, Rothwell GW (Eds) Transformative Paleobotany. Academic Press, London, 527–549. https://doi.org/10.1016/B978-0-12-813012-4.00022-X

Rikkinen J, Tuovila H, Beimforde B, Seyfullah L, Perrichot V, Schmidt AR (2014) *Chaenothecopsis neocaledonica* sp. nov.: The first resinicolous mycocalicioid fungus from an araucarian conifer. Phytotaxa 173(1): 49–60. https://doi.org/10.11646/phytotaxa.173.1.4

Rikkinen J, Meinke K, Grabenhorst H, Gröhn C, Kobbert M, Wunderlich J, Schmidt AR (2018) Calicioid lichens and fungi in amber: Tracing extant lineages back to the Paleogene. Geobios 51(5): 469–479. https://doi.org/10.1016/j.geobios.2018.08.009

Ronquist F, Huelsenbeck JP (2003) MrBayes 3: Bayesian phylogenetic inference under mixed models. Bioinformatics 19(12): 1572–1574. https://doi.org/10.1093/bioinformatics/btg180

Samuels GJ, Buchanan DE (1983) Ascomycetes of New Zealand 5. *Mycocalicium schefflerae* sp. nov., its ascal ultrastructure and *Phialophora* anamorph GARY J. SAMUELS. New Zealand Journal of Botany 21(2): 163–169. https://doi.org/10.1080/0028825X.1983.10428540

Schmidt A (1970) Anatomisch-taxonoische Untersuchungen an europäischen Arten der Flechtenfamilie Caliciaceae. Mitteilungen aus dem Staatsinstitut für Allgemeine Botanik Hamburg 13: 111–166.

Schwarz G (1978) Estimating the dimension of a model. Annals of Statistics 6(2): 461–464. https://doi.org/10.1214/aos/1176344136

Selva SB (2010) New and interesting calicioid lichens and fungi from eastern North America. The Bryologist 113(2): 272–276. https://doi.org/10.1639/0007-2745-113.2.272

Seyfullah LJ, Roberts EA, Jardine PE, Rikkinen J, Schmidt AR (2022) Uncovering the natural variability of araucariacean exudates from ex situ and in situ tree populations in New Caledonia using FTIR spectroscopy. PeerJ Analytical Chemistry 4: e17. https://doi.org/10.7717/peerj-achem.17

Sipponen A, Laitinen K (2011) Antimicrobial properties of natural coniferous rosin in the European Pharmacopoeia challenge test. APMIS: Journal of Pathology, Microbiology and Immunology 119: 720–724. https://doi.org/10.1111/j.1600-0463.2011.02791.x

Tibell L (1984) A reappraisal of the taxonomy of Caliciales. Beiheft zur Nova Hedwigia 79: 597–713.

Tibell L (1987) Australasian Caliciales. Symbolae Botanicae Upsalienses 27: 1–276.

Tibell L, Titov A (1995) Species of *Chaenothecopsis* and *Mycocalicium* (Caliciales) on exudate. The Bryologist 98(4): e550. https://doi.org/10.2307/3243587

Tibell L, Vinuesa M (2005) *Chaenothecopsis* in a molecular phylogeny based on nuclear rDNA ITS and LSU sequences. Taxon 54(2): 427–442. https://doi.org/10.2307/25065370

Tibell L, Wedin M (2000) Mycocaliciales, a new order for nonlichenized calicioid fungi. Mycologia 92(3): 577–581. https://doi.org/10.1080/00275514.2000.12061195

Titov A (2006) Mikokalizievye griby (porjadok Mycocaliciales) Golarktiki [Mycocalicioid fungi (the order Mycocaliciales) of the Holarctic]. KMK Scientific Press, Moskva.

Titov A, Tibell L (1993) *Chaenothecopsis* in the Russian Far East. Nordic Journal of Botany 13(3): 313–329. https://doi.org/10.1111/j.1756-1051.1993.tb00055.x

Tuovila H (2013) Sticky business: Diversity and evolution of Mycocaliciales (Ascomycota) on plant exudates. Publications from the Department of Botany. University of Helsinki 44: 1–142.

Tuovila H, Huhtinen S (2020) New methods for mycocalicioid fungi. Lichenologist 52(6): 403–413. https://doi.org/10.1017/S0024282920000481

Tuovila H, Cobbinah JR, Rikkinen J (2011a) *Chaenothecopsis khayensis*, a new resinicolous calicioid fungus on African mahogany. Mycologia 103(3): 610–615. https://doi.org/10.3852/10-194

Tuovila H, Larsson P, Rikkinen J (2011b) Three resinicolous North American species of Mycocaliciales in Europe with a re-evaluation of *Chaenothecopsis oregana* Rikkinen. Karstenia 51(2): 37–49. https://doi.org/10.29203/ka.2011.447

Tuovila H, Schmidt AR, Beimforde C, Dörfelt H, Grabenhorst H, Rikkinen J (2013) Stuck in time – a new *Chaenothecopsis* species with proliferating ascomata from *Cunninghamia resin* and its fossil ancestors in European amber. Fungal Diversity 58(1): 199–213. https://doi.org/10.1007/s13225-012-0210-9

Tuovila H, Davey ML, Yan L, Huhtinen S, Rikkinen J (2014) New resinicolous *Chaenothecopsis* species from China. Mycologia 106(5): 989–1003. https://doi.org/10.3852/13-178

Vilgalys R, Hester M (1990) Rapid genetic identification and mapping of enzymatically amplified ribosomal DNA from several *Cryptococcus* species. Journal of Bacteriology 172(8): 4238–4246. https://doi.org/10.1128/jb.172.8.4238-4246.1990

Weerakoon G, Wolseley PA, Arachchige O, Eugenia da Silva Cáceres M, Jayalal U, Aptroot A (2016) Eight new lichen species and 88 new records from Sri Lanka. The Bryologist 119(2): 131–142. https://doi.org/10.1639/0007-2745-119.2.131

White TJ, Bruns T, Lee S, Taylor J (1990) Amplification and direct sequencing of fungal ribosomal RNA genes for phylogenetics. In: Innis MA, Gelfand DH, Sninsky JJ, White TJ (Eds) PCR Protocols: a Guide to Methods and Applications. Academic Press, New York, 315–322. https://doi.org/10.1016/B978-0-12-372180-8.50042-1

Supplementary material 1

Sampled specimens' information for the three new *Chaenothecopsis* species from Prodocarpaceae of New Zealand

Authors: Christina Beimforde, Alexander R. Schmidt, Hanna Tuovila, Uwe Kaulfuss, Juliane Germer, William G. Lee, Jouko Rikkinen

Data type: table (word document)

Explanation note: Species name, collection/voucher number, collection date/sites, fungal hosts and locations.

Link: https://doi.org/10.3897/mycokeys.95.97601.suppl1

MycoKeys 95: 131–162 (2023)
doi: 10.3897/mycokeys.95.98125
https://mycokeys.pensoft.net

RESEARCH ARTICLE

A peer-reviewed open-access journal
MycoKeys
Launched to accelerate biodiversity research

Segregation of the genus *Parahypoxylon* (Hypoxylaceae, Xylariales) from *Hypoxylon* by a polyphasic taxonomic approach

Marjorie Cedeño-Sanchez[1,2*], Esteban Charria-Girón[1,2*], Christopher Lambert[1,2,3], J. Jennifer Luangsa-ard[4], Cony Decock[5], Raimo Franke[6], Mark Brönstrup[6,7], Marc Stadler[1,2]

1 *Dept. Microbial Drugs, Helmholtz Centre for Infectiion Research, Inhoffenstrasse 7, 38124 Braunschweig, Germany* **2** *Institute of Microbiology, Technische Universität Braunschweig, Spielmannstraße 7, 38106 Braunschweig, Germany* **3** *Division of Molecular Cell Biology, Zoological Institute, Technische Universität Braunschweig, Spielmannstrasse 7, 38106 Braunschweig, Germany* **4** *National Center for Genetic Engineering and Biotechnology (BIOTEC), 113 Thailand Science Park, Phaholyothin Road, Klong Luang, Pathumthani 12120, Thailand* **5** *Mycothéque de l' Universite catholique de Louvain (BCCM/MUCL), Place Croix du Sud 3, B-1348 Louvain-la-Neuve, Belgium* **6** *Department of Chemical Biology, Helmholtz Centre for Infection Research, Partner site Hannover/Braunschweig, Inhoffenstrasse 7, 38124 Braunschweig, Germany* **7** *German Center for Infection Research (DZIF), Site Hannover-Braunschweig, 38124 Braunschweig, Germany*

Corresponding author: Marc Stadler (marc.stadler@helmholtz-hzi.de)

Academic editor: Andrew Miller | Received 28 November 2022 | Accepted 31 January 2023 | Published 20 February 2023

Citation: Cedeño-Sanchez M, Charria-Girón E, Lambert C, Luangsa-ard JJ, Decock C, Franke R, Brönstrup M, Stadler M (2023) Segregation of the genus *Parahypoxylon* (Hypoxylaceae, Xylariales) from *Hypoxylon* by a polyphasic taxonomic approach. MycoKeys 95: 131–162. https://doi.org/10.3897/mycokeys.95.98125

Abstract

During a mycological survey of the Democratic Republic of the Congo, a fungal specimen that morphologically resembled the American species *Hypoxylon papillatum* was encountered. A polyphasic approach including morphological and chemotaxonomic together with a multigene phylogenetic study (ITS, LSU, *tub2*, and *rpb2*) of *Hypoxylon* spp. and representatives of related genera revealed that this strain represents a new species of the Hypoxylaceae. However, the multi-locus phylogenetic inference indicated that the new fungus clustered with *H. papillatum* in a separate clade from the other species of *Hypoxylon*. Studies by ultrahigh performance liquid chromatography coupled to diode array detection and ion mobility tandem mass spectrometry (UHPLC-DAD-IM-MS/MS) were carried out on the stromatal extracts. In particular, the MS/MS spectra of the major stromatal metabolites of these species indicated the production of hitherto unreported azaphilone pigments with a similar core scaffold to the cohaerin-type metabolites, which are

* These authors contributed equally to this work.

exclusively found in the Hypoxylaceae. Based on these results, the new genus *Parahypoxylon* is introduced herein. Aside from *P. papillatum,* the genus also includes *P. ruwenzoriense* **sp. nov.**, which clustered together with the type species within a basal clade of the Hypoxylaceae together with its sister genus *Durotheca*.

Keywords
Ascomycota, metabolite annotation, one new genus, one new species, phylogeny, polythetic taxonomy, Xylariales

Introduction

The genus *Hypoxylon* Bull. 1791 remains one of the largest in the Xylariales, even after a turbulent taxonomic history, during which its generic concept has changed drastically. Its early taxonomic history has been reviewed in great detail by Ju and Rogers (1996). Therefore, we largely refer to this monograph for the taxonomic treatments that occurred in the 19th and early 20th century.

The first world monograph of *Hypoxylon* by Miller (1961) was mainly based on stromatal morphology and ascal micromorphology. He recognized four sections (*Hypoxylon*, *Annulata*, *Applanata* and *Papillata*, the latter of which was further subdivided into two subsections, *Papillata* and *Primocinerea*). Ju and Rogers (1996) then restricted *Hypoxylon* to sections *Hypoxylon* and *Annulata*, and included several species of section *Papillata* in their emended section *Hypoxylon*. The main criteria for this taxonomic change were the presence of stromatal pigments and a nodulisporium-like anamorph. Many of the species in sections *Applanata* and *Papillata* sensu Miller (1961) do not show the latter mentioned features and were accommodated in other genera (e.g., *Biscogniauxia*, *Nemania*, *Whalleya*), which were later transferred to different families (Wendt et al. 2018). For their current classification, we refer to Hyde et al. (2020).

With the advent of molecular phylogenetic studies, and chemotaxonomy as an additional tool, the taxonomic concepts of *Hypoxylon* and other stromatic genera of the Xylariales have been further refined. The holomorphic concepts developed by Ju and Rogers, as well as other mycologists who put more emphasis on the anamorphic characters than on stromatal and ascospore morphology, have largely been confirmed. Hsieh et al. (2005) used protein-coding genes of a large number of representative taxa to resolve the phylogeny of *Hypoxylon* s. lat., which resulted in the recognition of the genus *Annulohypoxylon*. The composition of the latter genus was then equivalent to that of sect. *Annulata* sensu Ju and Rogers (1996). Notably, a parallel approach to establish a phylogeny based on ITS nrDNA sequences resulted in a very low resolution of the hypoxyloid taxa (Triebel et al. 2005). Later studies revealed that a multi locus phylogeny involving both protein-coding genes and rDNA are suitable to achieve a sufficient phylogenetic resolution within *Hypoxylon* and its allies (Kuhnert et al. 2014b, 2015, 2017a; Sir et al. 2015) in scope of a polythetic concept. Concurrent chemotaxonomic studies have aided in establishing correlations between the genotypes and the phenotypes of these pyrenomycetes. Their stromatal pigments, as well as certain secondary metabolites of their mycelial cultures, turned out to be informative for

taxonomic segregation at the species or even genus level (cf. Helaly et al. 2018; Becker and Stadler 2021).

Based on the above accomplishments, Wendt et al. (2018) proposed a rearrangement of the families of the stromatic Xylariales, as well as the further segregation of genera from the mainstream of *Hypoxylon*. The Hypoxylaceae were resurrected to accommodate *Hypoxylon* and its closely related allies, and the Xylariaceae were restricted to the genera with geniculosporium-like anamorphs, which had already been recognized as phylogenetically distinct in earlier studies (e.g., Hsieh et al. 2010). *Annulohypoxylon* was further subdivided and largely restricted to those species that have ostiolar rings and do not produce cohaerin-type azaphilones. The genus *Jackrogersella* was erected to accommodate those species of *Annulohypoxylon* sensu Hsieh et al. (2005) that produce the aforementioned compounds and have papillate ostioles without rings. In addition, the genus *Pyrenopolyporus* was erected for species of *Hypoxylon* sensu Ju and Rogers (1996) that have massive stromata, long tubular perithecia, contain naphthopyrones in their stromata and (where this is known) produce a characteristic virgariella-like anamorph. A follow-up study by Lambert et al. (2019) provided evidence that the species of the *H. monticulosum* complex differ from *Hypoxylon* by the production of antifungal sporothriolides in culture. In addition, these fungi also lack the typical stromatal pigments of *Hypoxylon* (Fig. 1) and appear in a basal clade in the molecular phylogeny. The genus *Hypomontagnella* was therefore introduced to accommodate them.

The genus *Hypoxylon* in the current sense still appears heterogeneous and paraphyletic in the recently established phylogenies, also because its type species, *H. fragiforme* clustered in a relatively small clade comprising only a few species such as *H. howeanum*, *H. ticinense* and *H. rickii* (Wendt et al. 2018; Lambert et al. 2021). The latter species have in common that their stromatal pigments are of the mitorubrin type.

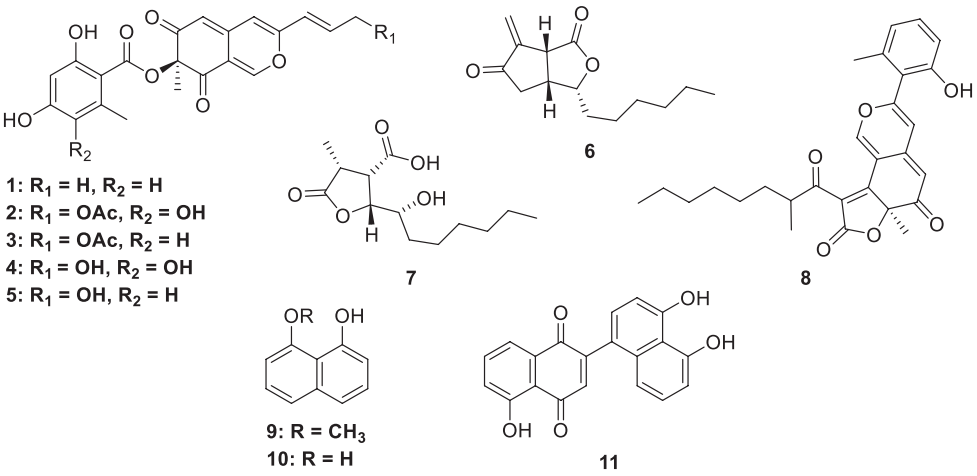

Figure 1. Characteristic stromatal pigments and other secondary metabolites of *Hypoxylon* species. (+)-mitorubrin (**1**); (+)-6˝-hydroxymitorubrinol acetate (**2**); (+)-mitorubrinol acetate (**3**); (+)-6˝-hydroxymitorubrinol (**4**); (+)-mitorubrinol (**5**); sporothriolide (**6**); dihydroisosporothric acid (**7**); cohaerin E (**8**); 8-methoxy naphthol (**9**); 1,8-naphthol (**10**); hypoxylone (**11**).

Another species that was retained in *Hypoxylon*, even though the DNA sequences of the only available strain formed an aberrant clade in the phylogeny by Wendt et al. (2018) is *H. papillatum* Ellis & Everh. This species is characterized by effused-pulvinate stromata featuring long tubular perithecia. Therefore, its stromata somewhat resemble those of *Pyrenopolyporus* and certain *Daldinia* species such as *D. placentiformis* that do not have internal concentric zones. Ju and Rogers (1996) have studied the type material and concluded that the syntypes they studied from BPI and NY (i.e., the specimens listed in the protologue by Ellis and Everhart (see Smith 1893) did not all correspond to the same taxon. They identified some of the specimens as *Hypoxylon placentiforme* (now: *Daldinia placentiformis*), which was confirmed by Stadler et al. (2014) in the *Daldinia* world monograph, and selected a lectotype from Ohio (Commons No. 2160) which showed a characteristic morphology and could easily be distinguished from the former taxon. They also listed several other specimens from North America and Trinidad that showed the same characteristics.

Rogers (1985) cultured this fungus and provided a detailed description of its nodulisporium-like anamorph and culture. The corresponding specimen was collected by him in West Virginia, USA, and could have served as epitype. The culture is deposited in ATCC and showed the typical characteristics of *H. papillatum* sensu Rogers (1985) and was included in the phylogeny by Wendt et al. (2018) as a representative of this taxon. However, it showed an aberrant phylogenetic position in a clade that appeared basal to the others in which the DNA sequences of *Hypoxylon* species were located. We have come across a very similar fungus that was collected in Central Africa and have studied it, along with several extant type and authentic specimens for comparison. The results of this study, which also relies on state-of-the art metabolomics, are reported herein.

Materials and methods

Sample sources

All scientific names of fungi are given without authorities or publication details, according to Index Fungorum (http://www.indexfungorum.org). Type and reference specimens were provided by Washington State University herbarium (**WSP**), U.S. National Fungus Collections (**BPI**) and the New York Botanical Garden (**NY**), USA. Fungal cultures were provided from the Belgian Coordinated Collections of Microorganisms (**MUCL**), Belgium and the Westerdijk Fungal Biodiversity Institute (**CBS**), The Netherlands.

Morphological characterization

The microscopic characteristics of the teleomorph were carried out as described by Pourmoghaddam et al. (2020). To observe the macro-morphology of the cultures, the strains were grown on Difco Oatmeal Agar (**OA**), 2% Malt Extract Agar (**MEA**) and Yeast Malt agar (**YM** agar; malt extract 10 g/L, yeast extract 4 g/L, D-glucose 4 g/L, agar 20 g/L, pH 6.3 before autoclaving) and the cultures checked at 15 days after inoculation. Pigment colors were determined following the color-codes by Rayner (1970).

DNA extraction, PCR and sequencing

The DNA was extracted from pure cultures grown on plates with YM agar. Small amounts of mycelia were harvested after five days of growth and transferred to a 1.5 ml homogenization tube filled with six to eight Precellys Ceramic beads (1.4 mm, Bertin Technologies, Montigny-le-Bretonneux, France).

DNA extraction was performed using the commercially available Fungal gDNA Miniprep Kit EZ-10 spin column (NBS Biologicals, Cambridgeshire, UK) following the manufacturer's instructions. The *tub2* (partial β-tubulin) gene region was amplified using the primers T1 and T22 (O'Donnell and Cigelnik 1997); ITS (nuc rDNA internal transcribed spacer) region using the primers ITS4 and ITS5 (White et al. 1990); LSU (Large subunit nuc 28S rDNA) using LR0R and LR7 (Vilgalys and Hester 1990) and *rpb2* (partial second largest subunit of the DNA-directed RNA polymerase II) using fRPB2-5F and fRPB2-7cR (Liu et al. 1999).

PCR reactions were performed by mixing template gDNA (2–3 µL), 12.5 µL JumpStart Taq Ready Mix (Sigma Aldrich, Deisenhofen, Germany), 0.5 µL of both forward and reverse primers (10 mM) and 8.5 to 9.5 µl of sterile filtered and sterilized water to a final volume of 25 µL. Amplification was achieved using a Mastercycler nexus Gradient (Eppendorf, Hamburg, Germany). Thermocycling for ITS commenced with an initial denaturation at 94 °C for 5 min followed by 34 cycles of denaturation (30 s at 94 °C), annealing (30 s at 52 °C), and elongation (1 min at 72 °C). The program concluded with a 10 min lasting elongation at 72 °C and reaction tubes were stored at 4 °C until further use. In the case of the other loci, the following steps were modified: LSU denaturation (1 min at 94 °C), annealing (1 min at 52 °C), and elongation (2 min at 72 °C); For *tub2* the cycle repetitions were raised to 38, annealing (30 s at 47 °C) and elongation (2 min 30 s at 72 °C); for *rpb2,* the cycle repetitions were raised to 38, annealing (1 min at 54 °C) and elongation (1 min 30 s at 72 °C).

Molecular phylogenetic analyses

Sequences were analyzed and processed in Geneious 7.1.9 (Kearse et al. 2012). The generated sequence data were complemented by available sequence data from GenBank and the data sets for each genetic marker were aligned using MAFFT online (http://mafft.cbrc.jp/alignment/server/, Katoh et al. 2019), and manually curated in MEGA 11 (Tamura et al. 2021). A maximum-likelihood phylogenetic tree was constructed using IQ-TREE v. 2.1.3 [-b 1000 -abayes -m MFP -nt AUTO] (Minh et al. 2020), The selection of the appropriate nucleotide exchange model was selected by ModelFinder (Chernomor et al. 2016; Kalyaanamoorthy et al. 2017) based on Bayesian inference criterion. Branch support was calculated with non-parametric bootstrap (Felsenstein 1985 and approximate Bayes test (Anisimova et al. 2011). The total 1000 bootstrap replicates were mapped onto the ML tree with the best (highest) ML score. Single locus trees were calculated following the identical methodology and checked for congruence with the multigene phylogenetic tree.

A second phylogenetic inference was carried out following a Bayesian approach using MrBayes 3.2.7a (Ronquist et al. 2012) with algorithm options set to the ones

reported by Matio Kemkuignou et al. (2022). The data matrix was subjected to PartitionFinder2 (Lanfear et al. 2016) as implemented in the program package phylosuite v. 1.2.2 (Zhang et al. 2020) with settings set to an un-linked determination of the best-fitting nucleotide substitution models following Bayesian information criterion (BIC) for the different partitions, restricted to the ones available in MrBayes. Posterior probabilities (PP) above 95% were regarded as significant. To determine the congruence of the topologies of ML and Bayes, an approximate unbiased (AU) topology test was carried out in IQ-TREE [iqtree -s example.phy -z example.treels -n 0 -zb 10000 -zw -au](Shimodaira 2022). All sequences used for the pyhlogeny are listed in Table 1.

UHPLC profiling and dereplication

The secondary metabolites were extracted using a small piece of the stromata (approx. 1 mm^3). Each piece was placed in 1.5 ml reaction tubes, covered with 1000 µl of methanol and placed for 30 min at 40 °C in an ultrasonic bath. The tubes were centrifuged at 14 000 rpm for 10 min. The methanol extract was separated from the remaining stromata, which was extracted again under the same procedure. Finally, both organic phases were combined and dried under nitrogen. Each sample was analyzed at a concentration of 450 µg/mL on an ultrahigh performance liquid chromatography system (Dionex Ultimate3000RS, Thermo Scientific, Dreieich, Germany), using a C18 column (Kinetex 1.7 µm, 2.1 × 150 mm, 100 Å; Phenomenex, Aschaffenburg, Germany) with a sample injection volume of 2 µL. The mobile phase consisted of A (H_2O + 0.1% formic acid) and B (ACN + 0.1% formic acid) with a constant flow rate of 0.3 mL/min. The gradient began with 1% B for 0.5 min, increasing to 5% B in 1 min, then to 100% B in 19 min and holding at 100% B for 5 min. The temperature of the column was kept at 40 °C and UV-Vis data were recorded with a DAD at 190–600 nm.

MS spectra were collected using a trapped ion mobility quadrupole time-of-flight mass spectrometer (timsTOF Pro, Bruker Daltonics, Bremen, Germany) with the following parameters: tims ramp time 100 ms, spectra rate 9.52 Hz, PASEF on, cycle time 320 ms, MS/MS scans 2, scan range (*m/z*, 100–1800 Da; $1/k_0$, 0.55–2.0 V·s/cm^2). For the stromatal extracts and the standards ESI mass spectra were acquired in positive ion mode. Raw data were pre-processed with MetaboScape 2022 (Bruker Daltonics, Bremen, Germany) in the retention time range of 0.5 to 25 min. The obtained features were dereplicated against our in-house database comprising MS/MS spectra of standards from characteristic secondary metabolites of hypoxylaceous species (e.g. azaphilones, asterriquinones, binaphthalenes, cytochalasins, macrolides and sesquiterpenoids) in MetaboScape. A molecular network was created with the Feature-Based Molecular Networking (FBMN) (Nothias et al. 2020) and the Spec2Vec (Huber et al. 2021) workflows on the GNPS platform (Wang et al. 2016) using the pre-processed feature table from MetaboScape. Fragmentation ions resulting from the MS/MS spectra of cohaerin E, cohaerin H, and minutellin A were assigned using CFM-ID 4.0 web server (Wang et al. 2021) and validated with the SmartFormula 3D tool from MetaboScape. The datasets generated/analyzed for this study are included in Suppl. material 1.

Table 1. Strains used in the phylogenetic analyses, including the strain IDs, GenBank accession numbers, and the references where the sequence data have been originally generated. Type specimens are labeled with T (holotype), IT (isotype), PT (paratype) and ET (epitype).

Species	Strain number	GenBank Accession Number				Origin	References
		ITS	LSU	*rpb2*	*tub2*		
Annulohypoxylon annulatum	CBS 140775	KY610418	KY610418	KY624263	KX376353	USA (ET)	Kuhnert et al. (2017a; *tub2*), Wendt et al. (2018: ITS, LSU, *rpb2*)
Annulohypoxylon michelianum	CBS 119993	KX376320	KY610423	KY624234	KX271239	Spain	Kuhnert et al. (2014a; ITS, *tub2*), Wendt et al. (2018; LSU, *rpb2*)
Annulohypoxylon truncatum	CBS 140778	KY610419	KY610419	KY624277	KX376352	USA (ET)	Kuhnert et al. (2017a; *tub2*), Wendt et al. (2018; ITS, LSU, *rpb2*)
Daldinia bambusicola	CBS 122872	KY610385	KY610431	KY624241	AY951688	Thailand (T)	Hsieh et al. (2005; *tub2*), Wendt et al. (2018; ITS, LSU, *rpb2*)
Daldinia childiae	CBS 122881	KU683757	MH874773	KU684290	KU684129	France (T)	U'Ren et al. (2016; ITS, *tub2*, *rpb2*), Vu et al. (2019; LSU)
Daldinia concentrica	CBS 113277	AY616683	KY610434	KY624243	KC977274	Germany	Triebel et al. (2005; ITS), Kuhnert et al. (2014a; *tub2*), Wendt et al. (2018; LSU, *rpb2*)
Daldinia dennisii	CBS 114741	JX658477	KY610435	KY624244	KC977262	Australia (T)	Stadler et al. (2014; ITS), Kuhnert et al. (2014a; *tub2*), Wendt et al. (2018; LSU, *rpb2*)
Daldinia eschscholtzii	MUCL 45435	JX658484	KY610437	KY624246	KC977266	Benin	Stadler et al. (2014a; ITS), Kuhnert et al. (2014a; *tub2*), Wendt et al. (2018; LSU, *rpb2*)
Daldinia petriniae	MUCL 49214	AM749937	KY610439	KY624248	KC977261	Austria (ET)	Bitzer et al. (2008; ITS), Kuhnert et al. (2014a; *tub2*), Wendt et al. (2018; LSU, *rpb2*)
Daldinia placentiformis	MUCL 47603	AM749921	KY610440	KY624249	KC977278	Mexico	Stadler et al. (2014a; ITS), Kuhnert et al. (2014a; *tub2*), Wendt et al. (2018; LSU, *rpb2*)
Daldinia vernicosa	CBS 119316	KY610395	KY610442	KY624252	KC977260	Germany (ET)	Kuhnert et al. (2014a; *tub2*), Wendt et al. (2018; ITS, LSU, *rpb2*)
Durotheca rogersii	YMJ 92031201	EF026127		JX507794	EF025612	Taiwan	Ju et al. (2007) as *Theissenia*
Durotheca comedens	YMJ 90071615	EF026128		JX507793	EF025613	Taiwan (T)	Ju et al. (2003) as *Theissenia*
Durotheca crateriformis	GMBC0205	MH645426	MH645425	MH645427	MH049441	China (T)	de Long et al. (2019)
Durotheca guizhouensis	GMBC0065	MH645423	MH645421	MH645422	MH049439	China (T)	de Long et al. (2019)
Durotheca rogersii	GMBC0204	MH645433	MH645434	MH645435	MH049449	China	de Long et al. (2019)
Graphostroma platystomum	CBS 270.87	JX658535	DQ836906	KY624296	HG934108	France (T)	Zhang et al. (2006; LSU), Stadler et al. (2014; ITS), Koukol et al. (2015; *tub2*), Wendt et al. (2018; *rpb2*)
Hypomontagnella barbarensis	STMA 14081	MK131720	MK131718	MK135891	MK135893	Argentina (T)	Lambert et al. (2019)
Hypomontagnella monticulosa	MUCL 54604	KY610404	KY610487	KY624305	KX271273	French Guiana	Wendt et al. (2018)
Hypomontagnella submonticulosa	CBS 115280	KC968923	KY610457	KY624226	KC977267	France	Kuhnert et al. (2014a; ITS, *tub2*), Wendt et al. (2018; LSU, *rpb2*)
Hypoxylon addis	MUCL 52797	KC968931	ON954141	OP251037	KC977287	Ethiopia (T)	Kuhnert et al. (2014a; ITS, *tub2*), This study
Hypoxylon aveirense	MUM 19.40	MN053021	ON954142	OP251028	MN066636	Portugal (T)	Vicente et al. (2021; ITS, *tub2*), This study
Hypoxylon baruense	UCH9545	MN056428	ON954143		MK908142	Panama (T)	Cedeño–Sanchez et al. (2020; ITS, *tub2*); This study
Hypoxylon canariense	MUCL 47224	ON792787	ON954140	OP251029	ON813073	Spain, Canary Islands (PT)	This study. (Species described by Stadler et al. 2008)
Hypoxylon carneum	MUCL 54177	KY610400	KY610480	KY624297	KX271270	France	Wendt et al. (2018)
Hypoxylon cercidicola	CBS 119009	KC968908	KY610444	KY624254	KC977263	France	Kuhnert et al. (2014a; ITS, *tub2*), Wendt et al. (2018; LSU, *rpb2*)
Hypoxylon chionostomum	STMA 14060	KU604563	ON954144	OP251030	ON813072	Argentina	Sir et al. (2016; ITS); This study

Species	Strain number	GenBank Accession Number				Origin	References
		ITS	LSU	*rpb2*	*tub2*		
Hypoxylon chrysalidosporum	FCATAS2710	OL467294	OL615106	OL584222	OL584229	China (T)	Ma et al. (2022)
Hypoxylon crocopeplum	CBS 119004	KC968907	KY610445	KY624255	KC977268	France	Kuhnert et al. (2014a; ITS, *tub2*), Wendt et al. (2018; LSU, *rpb2*)
Hypoxylon cyclobalanopsidis	FCATAS2714	OL467298	OL615108	OL584225	OL584232	China (T)	Ma et al. (2022)
Hypoxylon erythrostroma	MUCL 53759	KC968910	ON954154	OP251031	KC977296	Martinique	Kuhnert et al. (2014a; ITS2, TUB), This study
Hypoxylon eurasiaticum	MUCL 57720	MW367851		MW373852	MW373861	Iran (T)	Lambert et al. (2021)
Hypoxylon fendleri	MUCL 54792	KF234421	KY610481	KY624298	KF300547	French Guiana	Kuhnert et al. (2014a; ITS, *tub2*), Wendt et al. (2018; LSU, *rpb2*)
Hypoxylon ferrugineum	CBS 141259	KX090079			KX090080	Austria	Friebes and Wendelin (2016)
Hypoxylon fragiforme	MUCL 51264	KC477229	KM186295	MK887342	KX271282	Germany (ET)	Stadler et al. (2013; ITS), Daranagama et al. (2015; LSU, *rpb2*), Wendt et al. (2018; *tub2*)
Hypoxylon fuscoides	MUCL 52670	ON792789	ON954145	OP251038	ON813076	France (T)	This study. (Species described by Fournier et al. 2010a)
Hypoxylon fuscum	CBS 113049	KY610401	KY610482	KY624299	KX271271	Germany (ET)	Wendt et al. (2018)
Hypoxylon gibriacense	MUCL 52698	KC968930	ON954146	OP251026	ON813074	France (T)	Kuhnert et al. (2014a; ITS). This study
Hypoxylon griseobrunneum	CBS 331.73	KY610402	KY610483	KY624300	KC977303	India (T)	Kuhnert et al. (2014a; *tub2*), Wendt et al. (2018; ITS, LSU, *rpb2*)
Hypoxylon guilanense	MUCL 57726	MT214997	MT214992	MT212235	MT212239	Iran (T)	Pourmoghaddam et al. (2020)
Hypoxylon haematostroma	MUCL 53301	KC968911	KY610484	KY624301	KC977291	Martinique (ET)	Wendt et al. (2018; LSU, *rpb2*), Kuhnert et al. (2014a; ITS, *tub2*),
Hypoxylon hainanense	FCATAS2712	OL467296	OL616132	OL584224	OL584231	China (T)	Ma et al. (2022)
Hypoxylon hinnuleum	ATCC 36255, MUCL 3621	MK287537	MK287549	MK287562	MK287575	USA (T)	Sir et al. (2019)
Hypoxylon howeanum	MUCL 47599	AM749928	KY610448	KY624258	KC977277	Germany	Bitzer et al. (2008; ITS), Kuhnert et al. (2014a; *tub2*), Wendt et al. (2018; LSU, *rpb2*)
Hypoxylon hypomiltum	MUCL 51845	KY610403	KY610449	KY624302	KX271249	Guadeloupe	Wendt et al. (2018)
Hypoxylon invadens	MUCL 51475	MT809133	MT809132	MT813037	MT813038	France (T)	Becker et al. (2020)
Hypoxylon investiens	CBS 118183	KC968925	KY610450	KY624259	KC977270	Malaysia	Kuhnert et al. (2014a; ITS, *tub2*), Wendt et al. (2018; LSU, *rpb2*)
Hypoxylon isabellinum	MUCL 53308	KC968935	ON954155	OP251032	KC977295	Martinique (T)	Kuhnert et al. (2014a; ITS, *tub2*), This study
Hypoxylon laschii	MUCL 52796	JX658525	ON954147	OP251027	ON813075	France	Stadler et al. (2014; ITS), This study
Hypoxylon lateripigmentum	MUCL 53304	KC968933	KY610486	KY624304	KC977290	Martinique (T)	Kuhnert et al. (2014a; ITS, *tub2*), Wendt et al. (2018; LSU, *rpb2*)
Hypoxylon lechatii	MUCL 54609	KF923407	ON954148	OP251033	KF923405	French Guiana	Kuhnert et al. (2014b; ITS, *tub2*), This study
Hypoxylon lenormandii	CBS 119003	KC968943	KY610452	KY624261	KC977273	Ecuador	Kuhnert et al. (2014a; ITS, *tub2*), Wendt et al. (2018; LSU, *rpb2*)
Hypoxylon lienhwacheense	MFLUCC 14-1231	KU604558	MK287550	MK287563	KU159522	Thailand	Sir et al. (2016; ITS, *tub2*), Sir et al. (2019; LSU, *rpb2*)
Hypoxylon lividipigmentum	STMA14045	ON792788	ON954149		ON813077	Argentina	This study
Hypoxylon lividipigmentum	BCRC 34077	JN979433			AY951735	Mexico (IT)	Hsieh et al. (2005)
Hypoxylon macrocarpum	CBS119012	ON792785	ON954151	OP251034	ON813071	Germany	This study
Hypoxylon munkii	MUCL 53315	KC968912	ON954153	OP251035	KC977294	Martinique	Kuhnert et al. (2014a; ITS, *tub2*), This study
Hypoxylon musceum	MUCL 53765	KC968926	KY610488	KY624306	KC977280	Guadeloupe	Kuhnert et al. (2014a; ITS, *tub2*), Wendt et al. (2018; LSU, *rpb2*)
Hypoxylon ochraceum	MUCL 54625	KC968937		KY624271	KC977300	Martinique (ET)	Kuhnert et al. (2014a; ITS, *tub2*), Wendt et al. (2018; *rpb2*)

Species	Strain number	GenBank Accession Number				Origin	References
		ITS	LSU	*rpb2*	*tub2*		
Hypoxylon olivaceopigmentum	DSM 107924	MK287530	MK287542	MK287555	MK287568	USA (T)	Sir et al. (2019)
Hypoxylon perforatum	CBS115281	KY610391	KY610455	KY624224	KX271250	France	Wendt et al. (2018)
Hypoxylon petriniae	CBS 114746	KY610405	KY610491	KY624279	KX271274	France (T)	Wendt et al. (2018)
Hypoxylon pilgerianum	STMA 13455	KY610412	KY610412	KY624308	KY624315	Martinique	Wendt et al. (2018)
Hypoxylon porphyreum	CBS 119022	KC968921	KY610456	KY624225	KC977264	France	Kuhnert et al. (2014a; ITS, *tub2*), Wendt et al. (2018; LSU, *rpb2*)
Hypoxylon pseudofuscum	DSM112038	MW367857	MW367848	MW373858	MW373867	Germany (T)	Lambert et al. (2021)
Hypoxylon pulicicidum	CBS 122622	JX183075	KY610492	KY624280	JX183072	Martinique (T)	Bills et al. (2012; ITS, *tub2*), Wendt et al. (2018; LSU, *rpb2*)
Hypoxylon rickii	MUCL 53309	KC968932	KY610416	KY624281	KC977288	Martinique (ET)	Kuhnert et al. (2014a; ITS, *tub2*), Wendt et al. (2018; LSU, *rpb2*)
Hypoxylon rubiginosum	MUCL 52887	KC477232	KY610469	KY624266	KY624311	Germany (ET)	Stadler et al. (2013; ITS), Wendt et al. (2018; *tub2*, LSU, *rpb2*)
Hypoxylon samuelsii	MUCL 51843	KC968916	KY610466	KY624269	KC977286	Guadeloupe (ET)	Kuhnert et al. (2014a; ITS, *tub2*), Wendt et al. (2018; LSU, *rpb2*)
Hypoxylon sporistriatatunicum		MN056426	ON954150	OP251036	MK908140	Panama (T)	Cedeño-Sanchez et al. (2020; ITS, *tub2*); This study
Hypoxylon subticinense	MUCL 53752	KC968913	ON954152		KC977297	French Guiana	Kuhnert et al. (2014a; ITS, *tub2*), This study
Hypoxylon texense	DSM 107933	MK287536	MK287548	MK287561	MK287574	USA (T)	Sir et al. (2019)
Hypoxylon ticinense	CBS 115271	JQ009317	KY610471	KY624272	AY951757	France	Hsieh et al. (2005; ITS, *tub2*), Wendt et al. (2018; LSU, *rpb2*)
Hypoxylon trugodes	MUCL 54794	KF234422	KY610493	KY624282	KF300548	Sri Lanka (ET)	Kuhnert et al. (2014a; ITS, *tub2*), Wendt et al. (2018; LSU, *rpb2*)
Hypoxylon vogesiacum	CBS 115273	KC968920	KY610417	KY624283	KX271275	France	Kuhnert et al. (2014a; ITS), Kuhnert et al. (2017a; *tub2*), Wendt et al. (2018; LSU, *rpb2*)
Hypoxylon wuzhishanense	FCATAS2708	OL467292	OL615104	OL584220	OL584227	China (T)	Ma et al. (2022)
Jackrogersella cohaerens	CBS 119126	KY610396	KY610497	KY624270	KY624314	Germany	Wendt et al. (2018)
Jackrogersella multiformis	CBS 119016	KC477234	KY610473	KY624290	KX271262	Germany (ET)	Kuhnert et al. (2014a ; ITS), Kuhnert et al. (2017a; *tub2*), Wendt et al. (2018; LSU, *rpb2*)
Natonodosa speciosa	CLM-RV86	MF380435	MF380435	MH745150		Mexico (T)	Heredia et al. (2020)
Parahypoxylon papillatum comb. nov.	ATCC 58729	KC968919	KY610454	KY624223	KC977258	USA (T)	Kuhnert et al. (2014a; ITS, *tub2*), Wendt et al. (2018; LSU, *rpb2*)
Parahypoxylon ruwenzoriense sp. nov.	MUCL51392	ON792786	ON954156	OP251039	ON813078	D. R. Congo (T)	This study
Pyrenopolyporus hunteri	MUCL 52673	KY610421	KY610472	KY624309	KU159530	Ivory Coast (ET)	Kuhnert et al. (2017a; *tub2*), Wendt et al. (2018; ITS, LSU, *rpb2*)
Pyrenopolyporus laminosus	MUCL 53305	KC968934	KY610485	KY624303	KC977292	Martinique (T)	Kuhnert et al. (2014a; ITS, *tub2*), Wendt et al. (2018; LSU, *rpb2*)
Pyrenopolyporus nicaraguense	CBS 117739	AM749922	KY610489	KY624307	KC977272	Burkina_Faso	Bitzer et al. (2008; ITS), Kuhnert et al. (2014a; *tub2*), Wendt et al. (2018; LSU, *rpb2*)
Rhopalostroma angolense	CBS 126414	KY610420	KY610459	KY624228	KX271277	Ivory Coast	Wendt et al. (2018)
Rostrohypoxylon terebratum	CBS 119137	DQ631943	DQ840069	DQ631954	DQ840097	Thailand (T)	Tang et al. (2007), Fournier et al. (2010b)
Ruwenzoria pseudoannulata	MUCL 51394	KY610406	KY610494	KY624286	KX271278	D. R. Congo (T)	Wendt et al. (2018)
Thamnomyces dendroidea	CBS 123578	FN428831	KY610467	KY624232	KY624313	French Guiana (T)	Stadler et al. (2010; ITS), Wendt et al. (2018; *tub2*, LSU, *rpb2*)
Xylaria arbuscula	CBS 126415	KY610394	KY610463	KY624287	KX271257	Germany	Fournier et al. (2011; ITS), Wendt et al. (2018; *tub2*, LSU, *rpb2*)
Xylaria hypoxylon	CBS 122620	KY610407	KY610495	KY624231	KX271279	Sweden (ET)	Wendt et al. (2018)

Results

Phylogenetic analyses

The final data matrix for the molecular phylogenetic analysis (Fig. 2) comprised 345 sequences (44 generated in this study, and complemented by sequences available from GenBank, NCBI) derived from 89 strains and four loci, namely ITS, LSU, *rpb2* and *tub2.* The final MAFFT alignments consisted of 4018 nucleotides for the ITS alignment, 3642 for the LSU alignment, 2238 for the *tub2* alignment and 4023 positions for the *rpb2* alignment. The alignment of each locus is available in the Suppl. material 1: table S3–S6. Sequences of representatives for each molecularly well-established genus of the Hypoxylaceae were included: *Annulohypoxylon* (3 strains), *Daldinia* (8 strains), *Durotheca* (5 strains), *Hypomontagnella* (3 strains), *Hypoxylon* (58 strains), *Jackrogersella* (2 strains), *Natonodosa* (1 strain), *Pyrenopolyporus* (3 strains), as well as *Rhopalostroma*, *Rostrohypoxylon*, *Ruwenzoria*, and *Thamnomyces* (1 strain each). Three members of Xylariaceae and Graphostromataceae (*Xylaria hypoxylon*, *X. arbuscula* and *Graphostroma platystomum*) served as outgroup.

The inference of phylogenetic relationship using a Maximum-Likelihood and Bayesian approach yielded two different, discongruent topologies. An approximate unbiased (AU) topology test implemented in IQTree indicated that the tree resulting from Bayesian inference received a significantly ($p < 0.05$) lower maximum likelihood score, suggesting its rejection. Hence, we included support values of the approximate Bayes test implemented in IQTree to access posterior probability support values of the inferred phylogenetic tree. The combined rooted phylogenetic tree showed a clade consisting of the core members of the Hypoxylaceae, such as *Hypoxylon*, *Daldinia*, *Pyrenopolyporus*, *Hypomontagnella*, *Jackrogersella*, *Rostrohypoxylon*, *Thamnomyces* and *Ruwenzoria* with medium BS and high PP support (1/90), which was placed in a sister position to a clade consisting of members of *Parahypoxylon* gen. nov., and *Durotheca* (Hypoxylaceae) at the base of the tree with strong support (1/100). The genus *Hypoxylon* could be confirmed as paraphyletic, as has been described already by Wendt et al. (2018), Lambert et al. (2019), and Becker et al. (2020). The sequences assigned to *Parahypoxylon ruwenzoriense* formed a highly supported (1/100) cluster with the sequences derived from *Parahypoxylon papillatum*. The topology of *Durotheca* and the newly described genus *Parahypoxylon* as a basal lineage in the Hypoxylaceae are further reflected upon in the taxonomic part of this study.

Taxonomy

Lecto- and epitypification

Hypomontagnella monticulosa (Mont.) Sir, L. Wendt & C. Lamb.

Type. French Guiana, Cayenne, Leprieur, C. 1176, dead wood (PC, holotype; FH, isotype of *H. monticulosum*).

Epitype (designated here). France. French Guyana, Sinnamary, Paracou, Amazonian rain forest, bark of unknown tree, June 2012, leg J. Fournier (LIP, ex-epitype

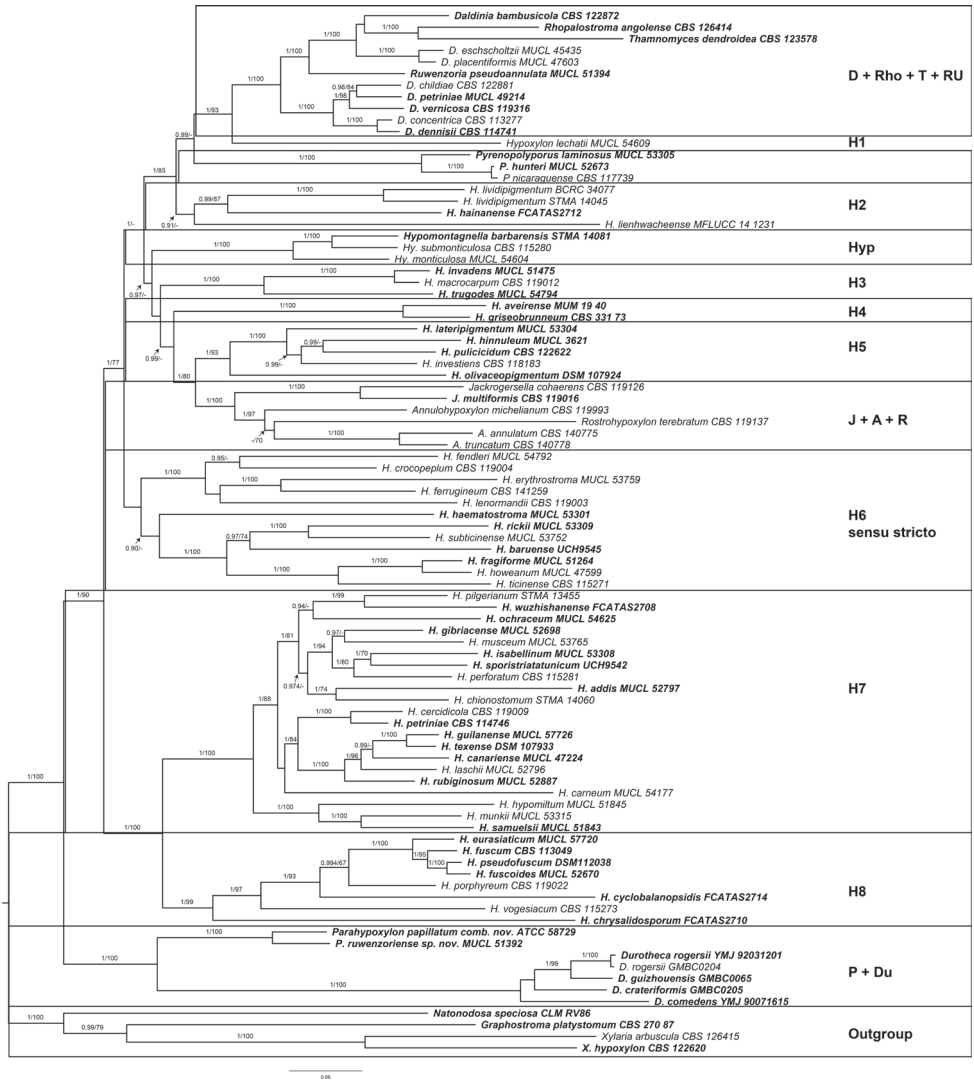

Figure 2. Inferred molecular phylogenetic maximum Likelihood (lLn = -122825.7921) tree of selected Hypoxylaceae, Graphostromataceae and Xylariaceae sequences. The analysis was calculated by using IQ-Tree with posterior probability support calculated from Bayesian inference methodology and support values generated from 1000 bootstrap replicates using a multigene alignment (ITS, LSU, *tub*2 and *rpb*2). The tree was rooted with *Xylaria hypoxylon* CBS 122620, *X. arbuscula* CBS 126415 (Xylariaceae) and *Graphostroma platystomum* CBS 27087 (Graphostromataceae). Type material is highlighted in **bold** letters. Bayesian posterior probability scores ≥ 0.95 / Bootstrap support values ≥ 70 are indicated along branches.

culture MUCL 54604). GenBank acc. nos for DNA sequences: KY610404 and KJ810556 (ITS), KY610487 (LSU), KY624305 (*rpb*2), KX271273 (*tub2*); MT889334 (sporothriolide gene cluster published by Tian et al. 2020).

MBT no: 10010042.

Notes. The strain designated here as epitype was used by Lambert et al. (2019) and the subsequent publications on genome analysis (Stadler et al. 2020; Tian et al. 2020; Kuhnert et al. 2021; Wibberg et al. 2021). The specimen and culture are perfectly suitable, because it was collected from the same geographic area as the holotype.

Parahypoxylon **M. Cedeño-Sanchez, E. Charria-Girón & M. Stadler, gen. nov.**
MycoBank No: 845463

Etymology. Refers to the morphological similarity to *Hypoxylon*, from which the genus is phylogenetically distinct.

Diagnosis. Differs from the genus *Durotheca* by the presence of greenish KOH-extractable pigments and by having an amyloid ascal apical apparatus. Differs from the genus *Hypoxylon* by containing yet unknown cohaerin-type azaphilones and by its basal position in the molecular phylogenetic inference using am ITS, LSU, *rpb2* and *tub2* matrix.

Parahypoxylon papillatum **(Ellis & Everh) M. Cedeño-Sanchez, E. Charria-Girón & M. Stadler, comb. nov.**
MycoBank No: 845462
Figs 3, 4

Hypoxylon papillatum Ellis & Everh. in Smith, Bull. Lab. Nat. Hist. Iowa State Univ. 2: 408 (1893). Syn.

Lectotype. USA. Ohio, Delaware, 21 Jul 1893, A. Commons 2160, rotten wood of *Carya* (NY [2 pks.], selected by Ju and Rogers (1996).

Epitype. USA. West Virginia, Mason Co., Bruce's Chapel, 18 Aug 1983, wood of *Acer*, J.D. Rogers (WSP 7557; ex-epitype culture ATCC 58729).

MBT no: 10011515.

Teleomorph. Stromata superficial, effused-pulvinate to plane, with inconspicuous to conspicuous perithecial mounds, up to 12.5 cm long × up to 4 cm broad × 1.8–4.0 mm thick; surface Honey (64) to Isabelline (65), Isabelline (65) to Gray Olivaceous (107), or Isabelline (65) to Olivaceous (48); blackish granules immediately beneath surface and between perithecia, with KOH-extractable pigments Isabelline (65); the tissue below the perithecial layer conspicuous, black, 1.0–2.5 mm thick. Perithecia long-tubular, 0.3–0.4 mm diam × 0.8–1.5 mm high. Ostioles umbilicate. Asci with amyloid, discoid apical apparatus, 1–2 µm high × 3.5 µm wide, stipe up 137–180 µm long × 8–10 µm broad, the spore-bearing parts 93–110 µm long, the stipes 30–80 µm long. Ascospores brown to dark brown, unicellular, ellipsoid, nearly equilateral, with broadly to narrowly rounded ends, 12.0–18.5 × 6.5–9.0 µm, with straight germ slit spore-length; perispore indehiscent in 10% KOH; epispore smooth.

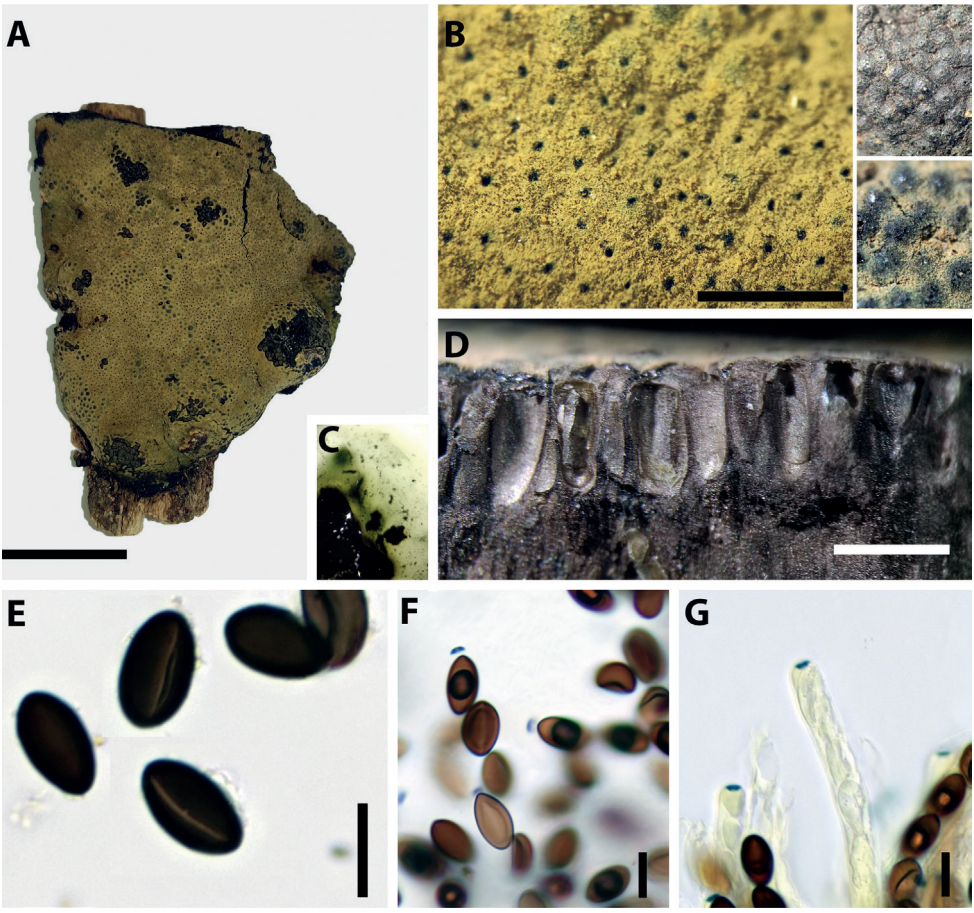

Figure 3. *Parahypoxylon papillatum* comb. nov. **A** stroma **B** ostioles **C** KOH extractable stromatal pigments **D** perithecia (cross section) **E** ascospores with straight germ slits **F** amyloid apical apparatus in a mature ascus treated with Melzer's reagent **G** amyloid apical apparatus in an immature ascus treated with Melzer's reagent. Scale bars: 1 cm (**A**); 10 µm (**E–F**); 10 µm (**G**).

Cultures and anamorph. Colonies on MEA, OA, and YM covering a 9 cm Petri plate in 2 weeks, with white, flat, mycelium, margins filamentous. Reverse at first white, becoming yellowish at the center. The anamorph has been described by Rogers (1985), but we were unable to confirm the presence of conidial structures when we studied the strain more than 30 years later.

Secondary metabolites. Stromata contain BNT and cohaerin type azaphilones according to the MS/MS analysis.

Notes. We were not only able to confirm the morphometric results of Ju and Rogers (1996) but even established that this species is characterized by a rather specific metabolite profile. This species has to our knowledge still not been reported from outside America and seems to be most frequently encountered in the Eastern USA.

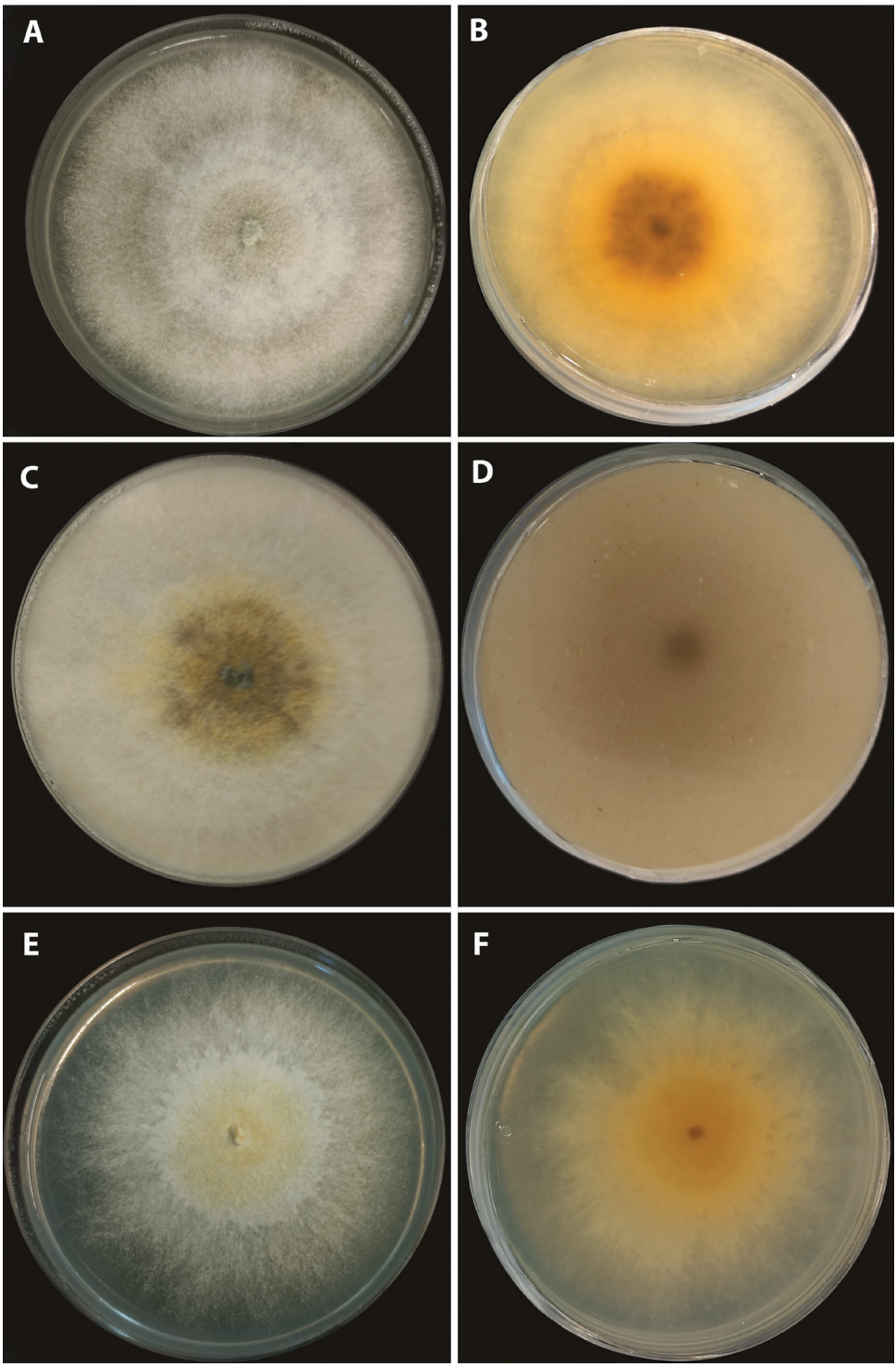

Figure 4. *Parahypoxylon papillatum* comb. nov. (ATCC 58729) Colonies after 2 weeks (**A, B**) on 2% MEA (**C, D**) on OA (**E, F**) on YM.

Further specimens examined. USA. Kansas, on decorticated wood, Feb 1884, F.W. Cragin 257 (NY00830462, syntype of *H. papillatum*); Pennsylvania, Allegheny Co., on dead wood, 14 Aug 1941, Henry, L.K. 4885 (BPI 591033); Pennsylvania, Meadville, old log, 17 Oct 1922, E.C. Smith 353 (BPI 591030); CANADA., on wood, J. Dearness (BPI 591035A, syntype of *H. papillatum*).

***Parahypoxylon ruwenzoriense* M. Cedeño-Sanchez, E. Charria-Girón & M. Stadler, sp. nov.**
MycoBank No: 845457
Figs 5–6

Holotype. Democratic Republic Of The Congo. North Kivu: Mt. Ruwenzori, about 00°33.961'N, 29°81.795'E, between 2,138 and 2,400 m alt., 3–5 Feb 2008, tropical mountain forest, C. Decock (MUCL 51392, ex-holotype culture MUCL 51392).

Etymology. Named after the Ruwenzori Mountains, where the species was collected.

Teleomorph. Stromata superficial, incomplete, effused-pulvinate, 60 mm long × 40 mm broad × 3–5 mm thick; surface Fawn (87), with inconspicuous perithecial mounds, with a black, shiny hard crust 100–150 µm thick above perithecia, without visible granules, with KOH-extractable pigments Hazel (88); the pruina hyphae turn violet in KOH; the tissue below the perithecia 2–4 mm thick, vertically fibrose, dark grey. Perithecia tubular, 0.90–1.50 mm high × 0.2–0.3 mm diam (n=18). Ostioles umbilicate, surrounded by a white substance. Asci cylindrical, 8-spored, the spore-bearing parts 82–105 µm long × 5.5–6.0 µm broad, the stipes 38–130 µm long, with amyloid, discoid apical ring 0.7–2.0 µm high × 2.5–3.5 µm (n=21) broad. Ascospores smooth, unicellular, brown to dark brown, narrowly ellipsoid, nearly equilateral with narrowly rounded ends, 10.5–13.8 × 4.0–5.6 µm (n=40), with a faint, straight germ slit; perispore indehiscent in 10% KOH.

Cultures and anamorph. Colonies on MEA, OA, and YM covering a 9 cm Petri plate in 2 weeks, with mycelium white at first, flat to raised in some zones, to becoming greenish in the center. Reverse at first yellowish, to become orange with a black spot at the center. Conidiophores not produced.

Secondary metabolites. Stromata contain BNT and cohaerin type azaphilones according to the MS/MS analysis.

Notes. *P. ruwenzoriense* is phylogenetically close to *P. papillatum* but differs by its KOH-extractable pigments Hazel (88) and by smaller ascospores.

Metabolomic profiling of stromata

As explained in the Experimental section, stromata of five herbarium specimens assignable to *Parahypoxylon* were extracted and analysed by UHPLC-DAD-IM-MS/MS. The raw data sets were pre-processed and the obtained feature table dereplicated using high resolution *m/z*, MS/MS spectra, retention time, CCS value, and UV/Vis spectra and reference data obtained from our in-house library of common secondary metabolites of the Hypoxylaceae (data not shown).

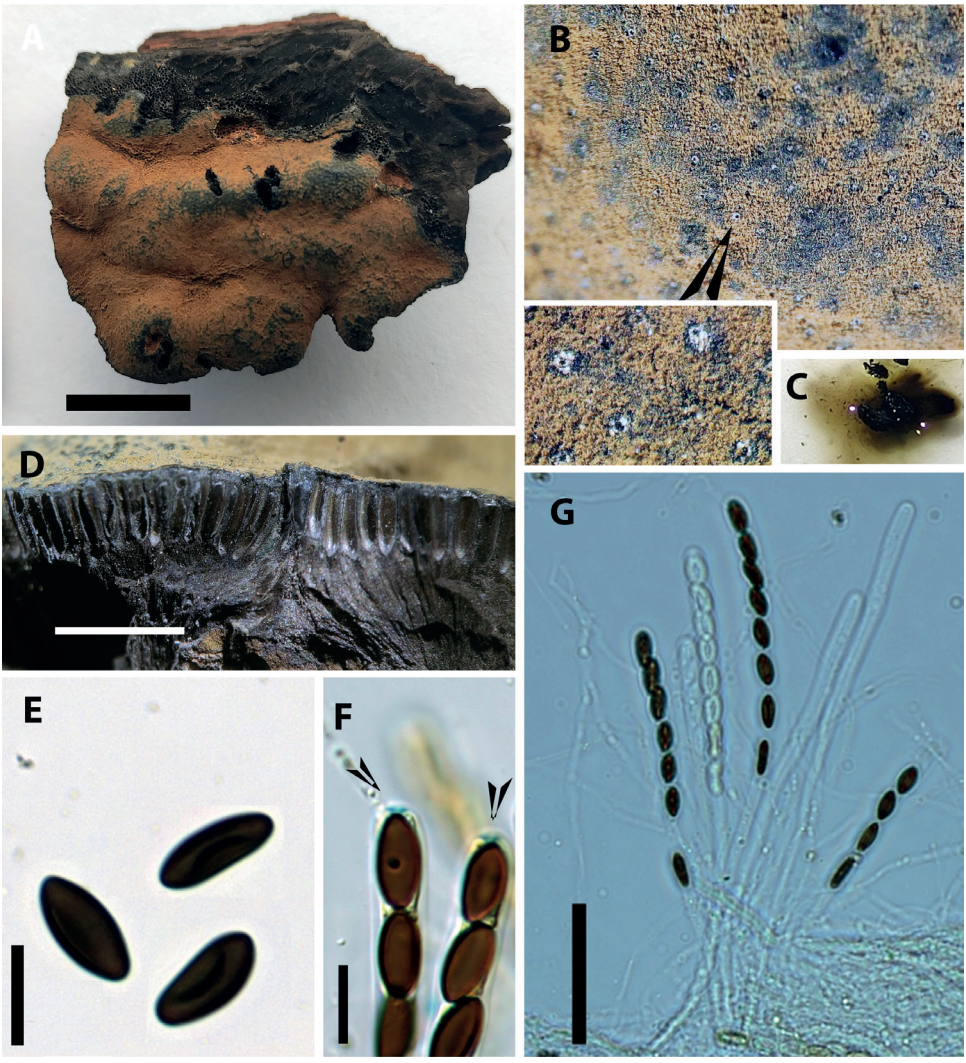

Figure 5. *Parahypoxylon ruwenzoriense* sp. nov. (MUCL 51392). **A** stroma **B** ostioles with white ring **C** KOH extractable stromatal pigments **D** perithecia (cross section) **E** ascospores **F** amyloid apical apparatus (blueing in Melzer's reagent) indicated by arrowheads **G** asci. Scale bars: 1 cm (**A**); 2 mm (**D**); 10 µm (**E, F**); 50 µm (**G**).

From the base peak chromatograms (BPC) of the stromatal extracts of the studied specimens, six major peaks could be distinguished (Fig. 7). An additional MS/MS similarity search without matching the precursor mass against our in-house library in MetaboScape yielded a MS/MS score > 700 for compounds **2** and **5** when compared with cohaerin E, cohaerin H, and minutellin A standards, which were not contained in the stromatal extracts (Suppl. material 1: fig. S2). This tentatively advocated

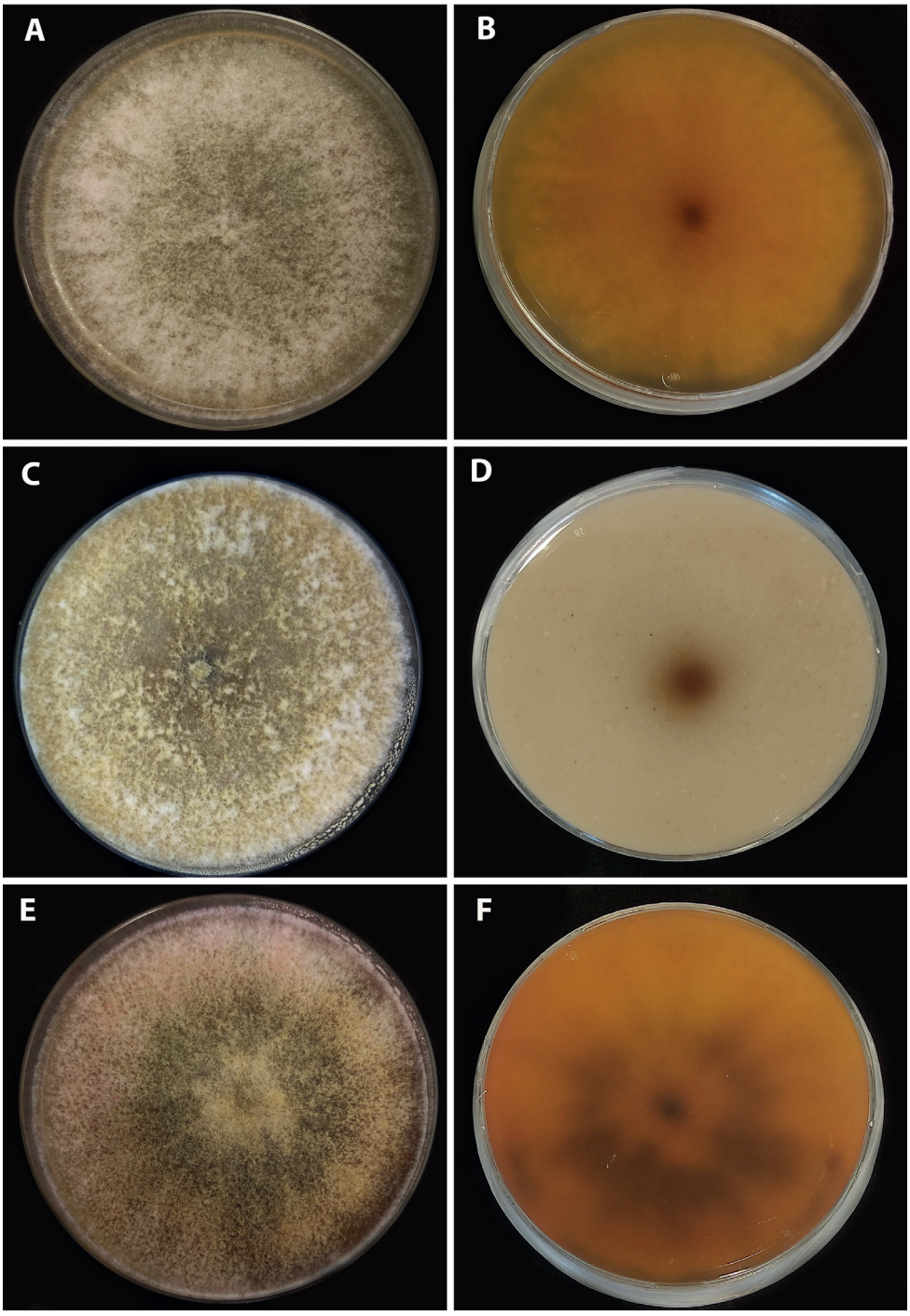

Figure 6. *Parahypoxylon ruwenzoriense* sp. nov. (MUCL 51392) Colonies after 2 weeks (**A, B**) on 2% MEA (**C, D**) on OA (**E, F**) on YM.

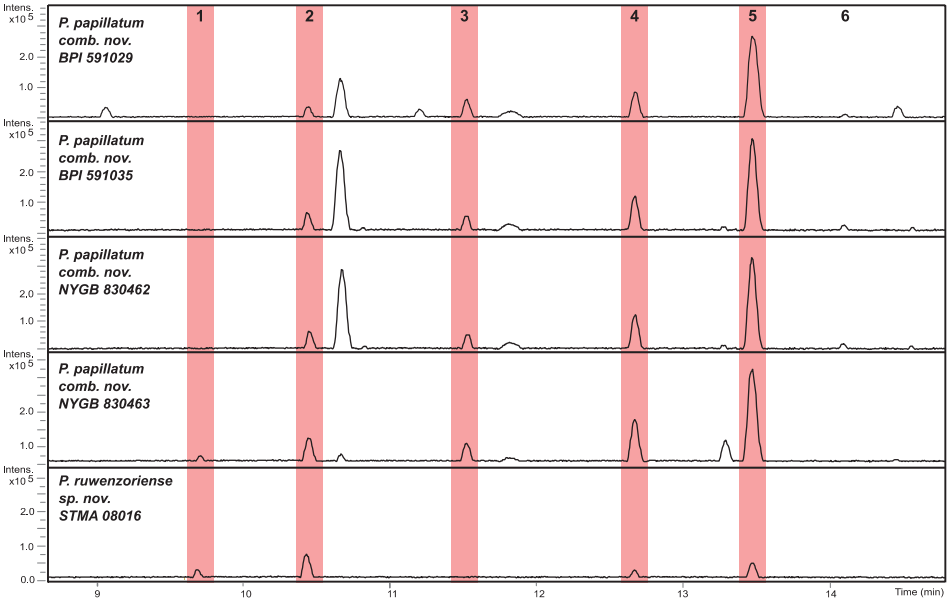

Figure 7. Base peak chromatograms (BPCs) from UHPLC-MS analysis of the stromatal extracts of *P. papillatum* (BPI 591029), *P. papillatum* (BPI 591035), *P. papillatum* (NYGB 830462), *P. papillatum* (NYGB 830463), and *Parahypoxylon ruwenzoriense* sp. nov. (STMA 08016). Compounds common between several species (numbered **1**–**6**) are highlighted in red.

a structural relation to the azaphilone family (Fig. 8a). Molecular formulae for compounds **1**–**6** were predicted as $C_{23}H_{24}O_7$, $C_{23}H_{22}O_7$, $C_{23}H_{20}O_8$, $C_{23}H_{22}O_6$, $C_{23}H_{20}O_6$, and $C_{23}H_{21}NO_5$ (Suppl. material 1: table S7), with a lower number of carbons than cohaerin E ($C_{28}H_{30}O_6$), cohaerin H ($C_{28}H_{32}O_6$), and minutellin A ($C_{28}H_{30}O_7$). To further validate the presence of cohaerin E-like azaphilones in the stromatal extracts of the *Parahypoxylon* spp. a molecular networking (MN) approach was pursued. The above mentioned tool can be employed to organize in an automatic basis MS/MS spectra into groups based on similarities in their fragmentation patterns and the hypothesis that structurally related molecules will yield similar MS/MS spectra (Duncan et al. 2015). For this analysis, we compared the MS/MS spectra of cohaerin E, cohaerin H, and minutellin A (Suppl. material 1: table S7, fig. S2) with all MS/MS spectra obtained from the *Parahypoxylon* gen. nov. stromatal extracts by means of the unsupervised machine learning approach Spec2Vec. As a result, the molecular cluster containing the cohaerin standards consisted of 29 consensus spectra (nodes), which included compounds **1**–**6** (Fig. 8b). In addition, cohaerin E and H have UV/Vis absorptions at λ_{max} 226–223 and 344–380 nm, which are resembling UV/Vis absorptions from compounds **1**, **3**, **4**, and **6**. Minutellin A displayed UV/Vis absorptions at λ_{max} 224, 271, and 343 nm, a pattern identified also for compounds **2** and **5** (Fig. 8c).

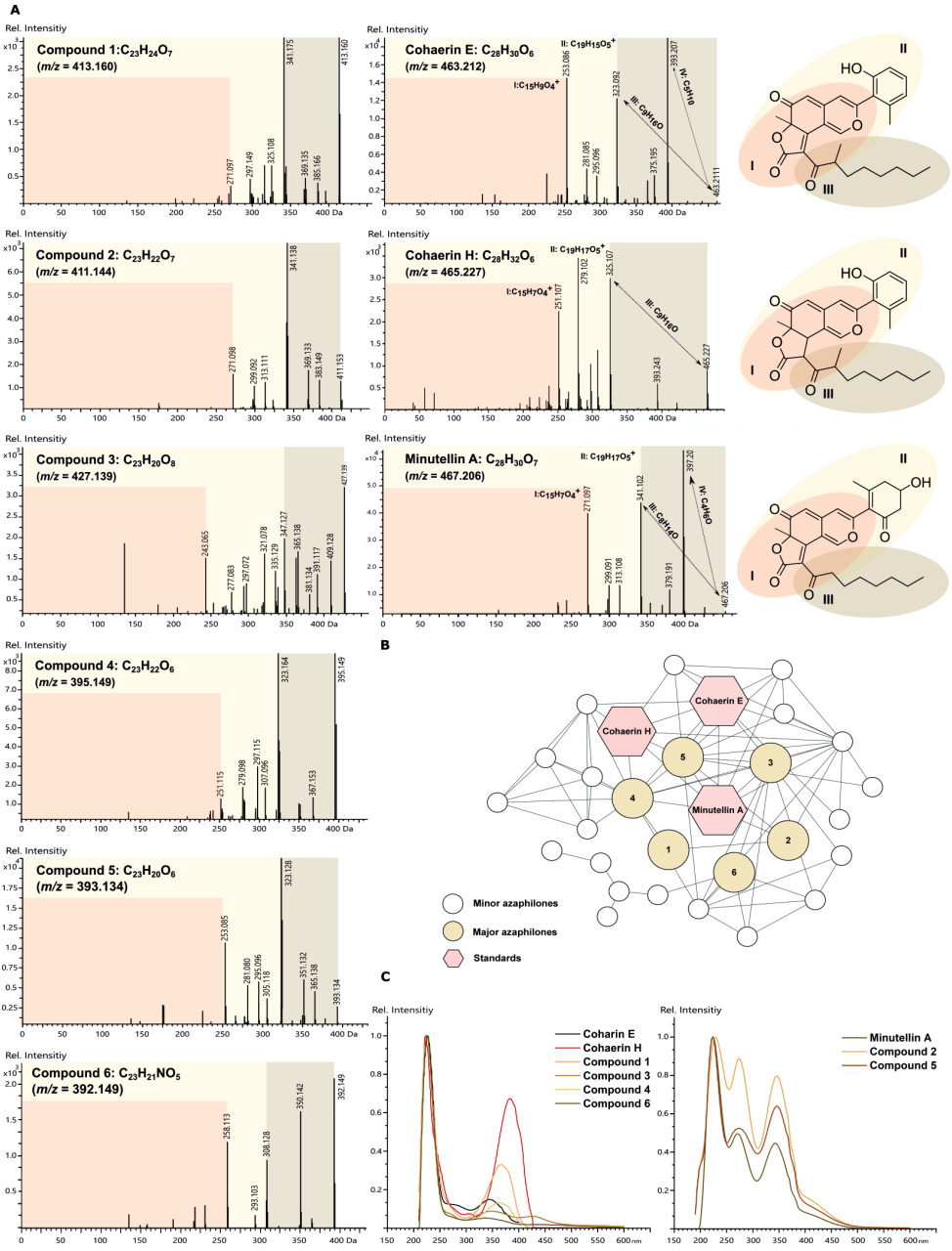

Figure 8. A Reference MS/MS spectra of cohaerin E, cohaerin H, and minutellin A standards, and the six major azaphilones identified in the UHPLC-MS chromatograms of stromatal extracts from the *Parahypoxylon* spp. **B** azaphilone cluster in a molecular network created from the *Parahypoxylon* spp. stromatal extracts and MS/MS spectra from selected standards **C** UV/Vis profile comparison from compound **1**–**6**, cohaerin E, cohaerin H, and minutellin A.

Cohaerin-type azaphilones present as well a distinct MS fragmentation pattern. In MS/MS experiments, cohaerin E generated fragment ions at 393.207 Da, 323.092 Da, 281.085 Da, and 253.086 Da, while minutellin A generated fragment ions at 397.201 Da, 341.102 Da, 299.091 Da, and 271.097 Da. The most abundant fragments were annotated using the CFM-ID 4.0 peak assignment module. In both cases, the most abundant fragments were traced down to the azaphilone backbone (Fig. 9). For instance, the mass difference of 18 Da between 323.092 Da and 341.102 Da could be interpreted as H_2O, reflecting the different substitution of the 3-methylphenol moiety. Fragment ions at 281.085 Da and 253.086 Da for cohaerin E represent the tricyclic portion of the molecule, while fragment ions at 299.091 Da and 271.097 Da represent the same part of the molecule in minutellin A. Analogously, MS fragmentation patterns for cohaerin H (Fig. 8) resembles the generated fragments for cohaerin E. As some typical cohaerin-type azaphilones fragmentation patterns were conserved, we assume that the changes found for the stromatal metabolites of **1**–**6** occur in the side chain of the molecules. In summary, the UHPLC-DAD-IM-MS/MS and UV/Vis data, combined with a comparison of molecular networking analyses, indicated the presence of novel azaphilones related to the cohaerin family in the stromatal extracts from the *Parahypoxylon* spp., in contrast to the absence of other common secondary metabolites of the Hypoxylaceae.

Discussion

The genus *Hypoxylon* in the current taxonomic concept has frequently been shown to be paraphyletic (Wendt et al. 2018; Lambert et al. 2019), which has once more been confirmed in this study, foreshadowing again future rearrangements for a thorough revision of its systematics. This is especially apparent because the type species *H. fragiforme* forms a relatively small clade clustering with a small subset of closely related taxa. Therefore, further segregation will eventually be unavoidable once more data to safely delineate the different lineages becomes available. Here, we gathered chemotaxonomic, morphological and sequence data to enable a polyphasic characterization of a basal clade formerly phylogenetically resolved inside *Hypoxylon*, containing specimen closely related to *H. papillatum*, for which we propose the erection of the new genus *Parahypoxylon*, sharing many salient features with *Hypoxylon* in the "traditional" definition.

The investigation of the stromatal metabolite extracts by HPLC has proven to be a valuable resource to achieve a more natural classification of hypoxylaceous taxa (Kuhnert et al. 2015; Wendt et al. 2018; Lambert et al. 2019). Recent advances in the analytics for in-depth characterization of natural products, mainly driven by metabolomics-based strategies, have enabled a better understanding of complex natural systems (Van der Hooft et al. 2020). The current MS-based techniques can help as a predictor for the discovery of new carbon skeletons to help and prioritize their isolation

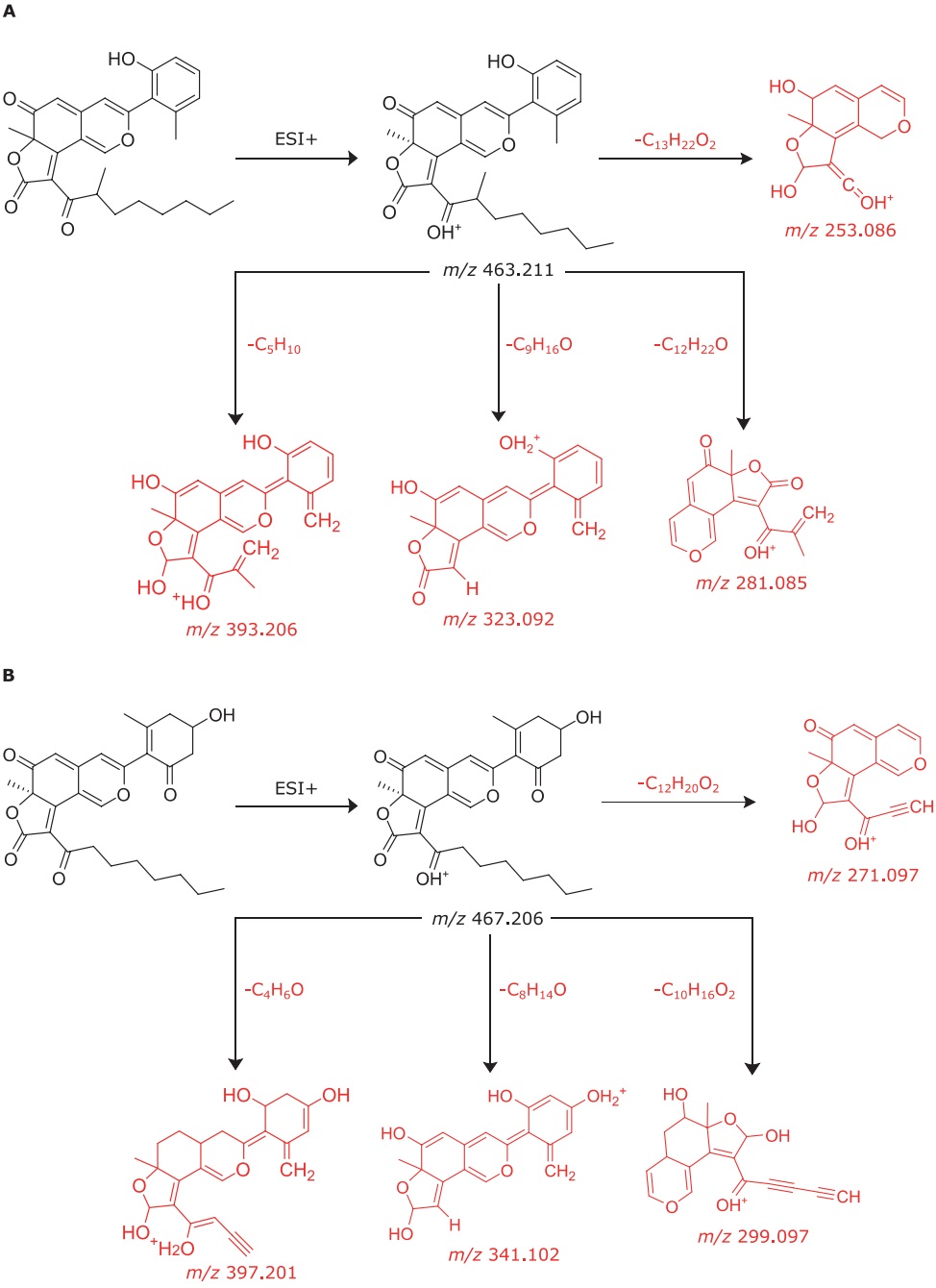

Figure 9. A most abundant fragment ions observed in MS/MS spectra for cohaerin E and associated structures as predicted by CFM-ID 4.0 **B** most abundant fragment ions observed in MS/MS spectrum for minutellin A and associated structures as predicted by CFM-ID 4.0.

and description instead of the isolation of new derivatives of already known metabolite scaffolds. Nevertheless, relying mainly on MS/MS fragmentation spectra could lead to an underestimation of chemical diversity. The complex chemical space produced by a single BGC may result in completely different fragmentation patterns only by the addition of small structural changes (McCaughey et al. 2022). Still, a general methodology for characterizing and classifying structural analogs with a common biosynthetic origin is absent particularly in the field of fungal natural products (Almeida et al. 2020).

However, in many occasions and applications, the isolation and structure elucidation of yet unidentified compounds is not possible, such as in the example of isolating pigments from natural sources, as is the case in the genus *Hypoxylon*. Even very old specimens have been reported to harbor intact secondary metabolites, as has been described for fossilized stromata assigned to *Hypoxylon fragiforme* in a study of archeological samples by Surup et al. (2018). Here, fortunately the original species could be recollected in German woods, but for rarer specimens, or specimens only producing scarce amounts of stromata, this is not a practicable option. Instability of the contained metabolites during e.g. purification further complicates the issue (Stadler et al. 2008; Kuhnert et al. 2014b; Sir et al. 2019). In this study, we demonstrated the value of integrating metabolomics-based tools to characterize the secondary metabolite profile of the type and authentic specimens of *P. papillatum* and the new species from the D.R. Congo.

An MS/MS analysis of the major metabolites suggested the presence of six unknown compounds assignable to the azaphilones related to the cohaerin family, which have been predicted to harbor a smaller carbon skeleton than the known cohaerins, and which still conserve some of the distinctive fragmentation patterns of these secondary metabolites (Suppl. material 1: fig. S3). This phenomenon has been exemplified within the Hypoxylaceae, which present a highly diverse group of PKS-derived pigments, among which the different subfamilies present different attached side chains at the C-8 oxygen (Kuhnert et al. 2021). The above findings suggest that the type of azaphilone produced by the studied species belong to a different type of azaphilones with a shorter side chain, but with a shared backbone in comparison to the cohaerins and minutellins. Additionally, the number of nodes found in the MN analysis suggests that the chemical diversity of the azaphilones produced by the strains belonging to *Parahypoxylon* gen. nov. is much higher than thought. In general, following a similar approach, the MolNetEnhancer workflow allowed the characterization of triterpenoid metabolites with several distinct phenolic acid modifications (e.g., vanillate, protocatechuate) in a different taxonomic background in the plant family Rhamnaceae (Ernst et al. 2019). The same methodology enabled the annotation of molecular families with known chemical motifs previously unreported for *Salinispora*, *Streptomyces*, and *Xenorhabdus* bacterial extracts (Ernst et al. 2019). Even though the ideal scenario would remain to isolate and elucidate the structures of the secondary metabolites, these tools are a powerful resource to classify chemical structural annotation and enhance our understanding of chemodiversity by adding biological and chemical insights of complex metabolic mixtures. It is worth noting that the stromatal material could eventually become available in the future from forthcoming collection campaigns, and

therefore the aforementioned hypothesis might be confirmed through isolation and chemical characterization of the major metabolites.

In this context, the stromatal metabolite profile of the specimens of *P. papillatum* and the new species *P. ruwenzoriense* are rather unique, even though it exhibits related chemotaxonomic features more likely to be found in the Hypoxylaceae. The cohaerin type azaphilones (which include also the multiformins and minutellins) have first been reported by Quang et al. (2005a, b, 2006), Surup et al. (2013) and Kuhnert et al. (2017b) and were recently found to possess interesting antiviral effects (Jansen-Olliges et al. 2023). Their producers are now all classified in *Jackrogersella* (Wendt et al. 2018) and were formerly placed in *Hypoxylon* sect. *Annulata* or (Ju and Rogers 1996) *Annulohypoxylon* (Hsieh et al. 2005), respectively. Kuhnert et al. (2017a) already reported that the species of *Annulohypoxylon* are divided into two chemotypes, one of which is characterized by stromata with papillate ostioles and cohaerin type azaphilones. The other chemotype is devoid of these compounds and produces binaphthalenes as prevailing stromatal metabolites. It includes *A. truncatum*, the type species of *Annulohypoxylon*, and many other species that feature ostiolar discs. Since this coincided with the molecular phylogeny by Wendt et al. (2018), the new genus *Jackrogersella* was erected for the cohaerin-containing species with papillate, diskless ostioles. There is only one species in *Annulohypoxylon* (i.e., *A. michelianum*) that has such ostiolar rings and also produces cohaerins. It was left at interim in *Annulohypoxylon*, even though its DNA sequence occupied a separate clade in the phylogeny by Wendt et al. (2018). The reason is that the strain studied did not constitute type material, and we felt that the erection of a separate genus should only be carried out by including fresh material from the geographic area and host (*Laurus* in South Europe) from which the holotype specimen was reported. Aside from the above-mentioned fungi, metabolites with cohaerin-like characteristics (i.e. characteristic mass and diode array spectra) have even been detected in species of *Hypoxylon*, such as *H. pulicicidum* (Bills et al. 2012). A recent study based on the analysis of full genomes based on 3rd generation sequencing techniques, such as PacBio and Oxford nanopore (Wibberg et al. 2021), has even revealed the corresponding biosynthetic gene clusters encoding for these azaphilone pigments to be present in the studied *Jackrogersella* species and *H. pulicicidum* (Kuhnert et al. 2021). For instance, the identified BGC in *H. pulicicidum* carries the core set of conserved genes for this family of azaphilones, but the additional presence of additional tailoring enzymes indicates that the produced metabolites might have different structural features compared to the known cohaerins (Kuhnert et al. 2021).

In the future, it will become easier to tell if the genetic information for the successful biosynthesis of such secondary metabolites is present in the genomes of the respective organisms even if the products cannot be detected. Chemotaxonomic evidence can also be used to segregate the new genus from the species that are located in neighboring basal clades in the current phylogeny (i.e., *Hypoxylon aeruginosum* and *Durotheca* spp.). Interestingly, these species neither contain azaphilones nor binaphthalenes, with *H. aeruginosum* and the related genus *Chlorostroma* reported to have lepraric acid derivatives as major stromatal metabolites (Læssøe et al. 2010), which are

otherwise unique and only occur in some lichenized ascomycetes. *Durotheca*, on the other hand, appears to be poor in stromatal metabolites, and Læssøe et al. (2013) only found traces of lepraric acids in one of the species they studied. The current study has further confirmed the results by de Long et al. (2019), who found that *Durotheca* is a hypoxylaceous genus, even though its species have a distinctive ascospore morphology and other secondary metabolites.

The integration of state-of-the-art metabolomic-based tools in chemotaxonomic surveys will further accelerate and assist the systematic study of paraphyletic taxa within the concept of polyphasic taxonomy as herein demonstrated for the introduction of *Parahypoxylon*.

Acknowledgements

This work was funded by the DFG (Deutsche Forschungsgemeinschaft) priority program "Taxon-Omics: New Approaches for Discovering and Naming Biodiversity" (SPP 1991). It also benefited from the European Union's H2020 Research and Innovation Staff Exchange program (RISE) [Grant No. 101008129: MYCOBIOMICS], granted to J.J. Luangsa-ard and M. Stadler. MCS gratefully acknowledges a PhD stipend from The National Secretariat of Science, Technology and Innovation of the Republic of Panama (SENACYT) and the Institute for the Development of Human Resources (IFARHU). E. Charria-Girón was funded by the HZI POF IV Cooperativity and Creativity Project Call. Additionally, we gratefully acknowledge support from the curators of the international herbaria, above all Lisa A Castlebury (BPI), Laura Briscoe (NY) and Monique Slipher (WSP), who provided important specimens for this study. Additionally, we are grateful for the expert and technical advice from Ulrike Beutling and Frank Surup.

References

Almeida H, Palys S, Tsang A, Diallo AB (2020) TOUCAN: A framework for fungal biosynthetic gene cluster discovery. NAR Genomics and Bioinformatics 2(4): 1–11. https://doi.org/10.1093/nargab/lqaa098

Anisimova M, Gil M, Dufayard JF, Dessimoz C, Gascuel O (2011) Survey of branch support methods demonstrates accuracy, power, and robustness of fast likelihood-based approximation schemes. Systematic Biology 60(5): 685–699. https://doi.org/10.1093/sysbio/syr041

Becker K, Stadler M (2021) Recent progress in biodiversity research on the Xylariales and their secondary metabolism. The Journal of Antibiotics 74(1): 1–23. https://doi.org/10.1038/s41429-020-00376-0

Becker K, Lambert C, Wieschhaus J, Stadler M (2020) Phylogenetic assignment of the fungicolous *Hypoxylon invadens* (Ascomycota, Xylariales) and investigation of its secondary metabolites. Microorganisms 8(9): 1397. https://doi.org/10.3390/microorganisms8091397

Bills GF, González-Menéndez V, Martín J, Platas G, Fournier J, Peršoh D, Stadler M (2012) *Hypoxylon pulicicidum* sp. nov. (Ascomycota, Xylariales), a pantropical insecticide-producing endophyte. PLoS ONE 7(10): e46687. https://doi.org/10.1371/journal.pone.0046687

Bitzer J, Læssøe T, Fournier J, Kummer V, Decock C, Tichy H-V, Piepenbring M, Peršoh D, Stadler M (2008) Affinities of *Phylacia* and the daldinoid Xylariaceae, inferred from chemotypes of cultures and ribosomal DNA sequences. Mycological Research 112(2): 251–270. https://doi.org/10.1016/j.mycres.2007.07.004

Cedeño-Sanchez M, Wendt L, Stadler M, Mejía LC (2020) Three new species of *Hypoxylon* and new records of Xylariales from Panama. Mycosphere 11(1): 1457–1476. https://doi.org/10.5943/mycosphere/11/1/9

Chernomor O, Von Haeseler A, Minh BQ (2016) Terrace aware data structure for phylogenomic inference from supermatrices. Systematic Biology 65(6): 997–1008. https://doi.org/10.1093/sysbio/syw037

Daranagama DA, Camporesi E, Tian Q, Liu X, Chamyuang S, Stadler M, Hyde KD (2015) *Anthostomella* is polyphyletic comprising several genera in Xylariaceae. Fungal Diversity 73(1): 203–238. https://doi.org/10.1007/s13225-015-0329-6

Daranagama DA, Hyde KD, Sir EB, Thambugala KM, Tian Q, Samarakoon MC, McKenzie EHC, Jayasiri SC, Tibpromma S, Bhat JD, Liu X, Stadler M (2018) Towards a natural classification and backbone tree for Graphostromataceae, Hypoxylaceae, Lopadostomataceae and Xylariaceae. Fungal Diversity 88(1): 1–165. https://doi.org/10.1007/s13225-017-0388-y

de Long Q, Liu LL, Zhang X, Wen TC, Kang JC, Hyde KD, Shen XC, Li QR (2019) Contributions to species of Xylariales in China-1. *Durotheca* species. Mycological Progress 18(3): 495–510. https://doi.org/10.1007/s11557-018-1458-6

Duncan KR, Crüsemann M, Lechner A, Sarkar A, Li J, Ziemert N, Wang M, Bandeira N, Moore BS, Dorrestein PC, Jensen PR (2015) Molecular networking and pattern-based genome mining improves discovery of biosynthetic gene clusters and their products from *Salinispora* species. Chemistry & Biology 22(4): 460–471. https://doi.org/10.1016/j.chembiol.2015.03.010

Ernst M, Kang K, Caraballo-Rodríguez AM, Nothias L-F, Wandy J, Chen C, Wang M, Rogers S, Medema MH, Dorrestein PC, van der Hooft JJJ (2019) Molnetenhancer: Enhanced molecular networks by integrating metabolome mining and annotation tools. Metabolites 9(7): 144. https://doi.org/10.3390/metabo9070144

Felsenstein J (1985) Confidence limits on phylogenies: An approach using the bootstrap. Evolution 39(4): 783–791. https://doi.org/10.2307/2408678

Fournier J, Köpcke B, Stadler M (2010a) New species of *Hypoxylon* from western Europe and Ethiopia. Mycotaxon 113(1): 209–235. https://doi.org/10.5248/113.209

Fournier J, Stadler M, Hyde KD, Duong LM (2010b) The new genus *Rostrohypoxylon* and two new *Annulohypoxylon* species from Northern Thailand. Fungal Diversity 40(1): 23–36. https://doi.org/10.1007/s13225-010-0026-4

Fournier J, Flessa F, Peršoh D, Stadler M (2011) Three new *Xylaria* species from Southwestern Europe. Mycological Progress 10(1): 33–52. https://doi.org/10.1007/s11557-010-0671-8

Friebes G, Wendelin I (2016) Studies on *Hypoxylon ferrugineum* (Xylariaceae), a rarely reported species collected in the urban area of Graz (Austria). Ascomycete.org 8: 83–90.

Helaly SE, Thongbai B, Stadler M (2018) Diversity of biologically active secondary metabolites from endophytic and saprotrophic fungi of the ascomycete order Xylariales. Natural Product Reports 35(9): 992–1014. https://doi.org/10.1039/C8NP00010G

Heredia G, Li DW, Wendt L, Réblová M, Arias RM, Gamboa-Angulo M, Štěpánek V, Stadler M, Castañeda-Ruíz RF (2020) *Natonodosa speciosa* gen. et sp. nov. and rediscovery of *Poroisariopsis inornata*: Neotropical anamorphic fungi in Xylariales. Mycological Progress 19(1): 15–30. https://doi.org/10.1007/s11557-019-01537-8

Hsieh H-M, Ju Y-M, Rogers JD (2005) Molecular phylogeny of *Hypoxylon* and closely related genera. Mycologia 97(4): 844–865. https://doi.org/10.1080/15572536.2006.11832776

Hsieh H-M, Lin C-R, Fang M-J, Rogers JD, Fournier J, Lechat C, Ju Y-M (2010) Phylogenetic status of *Xylaria* subgenus *Pseudoxylaria* among taxa of the subfamily Xylarioideae (Xylariaceae) and phylogeny of the taxa involved in the subfamily. Molecular Phylogenetics and Evolution 54(3): 957–969. https://doi.org/10.1016/j.ympev.2009.12.015

Huber F, Ridder L, Verhoeven S, Spaaks JH, Diblen F, Rogers S, Van Der Hooft JJJ (2021) Spec2Vec: Improved mass spectral similarity scoring through learning of structural relationships. PLoS Computational Biology 17(2): e1008724. https://doi.org/10.1371/journal.pcbi.1008724

Hyde K, Norphanphoun C, Maharachchikumbura SSN, Bhat DJ, Jones EBG, Bundhun D, Chen YJ, Bao DF, Boonmee S, Calabon MS, Chaiwan N, Chethana KWT, Dai DQ, Dayarathne MC, Devadatha B, Dissanayake AJ, Dissanayake LS, Doilom M, Dong W, Fan XL30 , Goonasekara ID, Hongsanan S, Huang SK, Jayawardena RS, Jeewon R, Karunarathna A, Konta S, Kumar V, Lin CG, Liu JK, Liu NG, Luangsa-ard J, Lumyong S, Luo ZL, Marasinghe DS, McKenzie EHC, Niego AGT, Niranjan M, Perera RH, Phukhamsakda C, Rathnayaka AR, Samarakoon MC, Samarakoon SMBC, Sarma VV, Senanayake IC, Shang QJ, Stadler M, Tibpromma S, Wanasinghe DN, Wei DP, Wijayawardene NN, Xiao YP, Yang J, Zeng XY, Zhang SN, Xiang MM (2020) Refined families of Sordariomycetes. Mycosphere 11(1): 305–1059. https://doi.org/10.5943/mycosphere/11/1/7

Jansen-Olliges L, Chatterjee S, Jia L, Stahl F, Bär C, Stadler M, Surup F, Zeilinger C (2022) Cohaerin-type azaphilones prevent SARS-CoV-2 binding to ACE2 receptor. Cells 12(1): 83. https://doi.org/10.3390/cells12010083

Ju Y, Rogers JD (1996) A revision of the genus *Hypoxylon*. Mycologia Memoir No. 20. American Phytopathological Society, APS Press.

Ju Y-M, Rogers JD, Hsieh H-M (2003) The genus *Theissenia*: *T. pyrenocrata*, *T. cinerea* sp. nov., and *T. eurima* sp. nov. Mycologia 95(1): 109–116. https://doi.org/10.1080/15572536.2004.11833138

Ju Y-M, Hsieh H-M, Ho M-C, Szu D-H, Fang M-J (2007) *Theissenia rogersii* sp. nov. and phylogenetic position of *Theissenia*. Mycologia 99(4): 612–621. https://doi.org/10.1080/15572536.2007.11832555

Kalyaanamoorthy S, Minh BQ, Wong TKF, von Haeseler A, Jermiin LS (2017) ModelFinder: Fast model selection for accurate phylogenetic estimates. Nature Methods 14(6): 587–589. https://doi.org/10.1038/nmeth.4285

Katoh K, Rozewicki J, Yamada KD (2019) MAFFT online service: Multiple sequence alignment, interactive sequence choice and visualization. Briefings in Bioinformatics 20(4): 1160–1166. https://doi.org/10.1093/bib/bbx108

Kearse M, Moir R, Wilson A, Stones-Havas S, Cheung M, Sturrock S, Buxton S, Cooper A, Markowitz S, Duran C, Thierer T, Ashton B, Meintjes P, Drummond A (2012) Geneious Basic: An integrated and extendable desktop software platform for the organization and analysis of sequence data. Bioinformatics 28(12): 1647–1649. https://doi.org/10.1093/bioinformatics/bts199

Koukol O, Kelnarová I, Černý K (2015) Recent observations of sooty bark disease of sycamore maple in Prague (Czech Republic) and the phylogenetic placement of *Cryptostroma corticale*. Forest Pathology 45(1): 21–27. https://doi.org/10.1111/efp.12129

Kuhnert E, Heitkämper S, Fournier J, Surup F, Stadler M (2014a) Hypoxyvermelhotins A–C, new pigments from *Hypoxylon lechatii* sp. nov. Fungal Biology 118(2): 242–252. https://doi.org/10.1016/j.funbio.2013.12.003

Kuhnert E, Fournier J, Peršoh D, Luangsa-ard JJD, Stadler M (2014b) New *Hypoxylon* species from Martinique and new evidence on the molecular phylogeny of *Hypoxylon* based on ITS rDNA and β-tubulin data. Fungal Diversity 64(1): 181–203. https://doi.org/10.1007/s13225-013-0264-3

Kuhnert E, Surup F, Sir EB, Lambert C, Hyde KD, Hladki AI, Romero AI, Stadler M (2015) Lenormandins A—G, new azaphilones from *Hypoxylon lenormandii* and *Hypoxylon jaklitschii* sp. nov., recognised by chemotaxonomic data. Fungal Diversity 71(1): 165–184. https://doi.org/10.1007/s13225-014-0318-1

Kuhnert E, Sir EB, Lambert C, Hyde KD, Hladki AI, Romero AI, Rohde M, Stadler M (2017a) Phylogenetic and chemotaxonomic resolution of the genus *Annulohypoxylon* (Xylariaceae) including four new species. Fungal Diversity 85(1): 1–43. https://doi.org/10.1007/s13225-016-0377-6

Kuhnert E, Surup F, Halecker S, Stadler M (2017b) Minutellins A – D, azaphilones from the stromata of *Annulohypoxylon minutellum* (Xylariaceae). Phytochemistry 137: 67–71. https://doi.org/10.1016/j.phytochem.2017.02.014

Kuhnert E, Navarro-Muñoz JC, Becker K, Stadler M, Collemare J, Cox RJ (2021) Secondary metabolite biosynthetic diversity in the fungal family Hypoxylaceae and *Xylaria hypoxylon*. Studies in Mycology 99(1): 100118. https://doi.org/10.1016/j.simyco.2021.100118

Læssøe T, Srikitikulchai P, Fournier J, Köpcke B, Stadler M (2010) Lepraric acid derivatives as chemotaxonomic markers in *Hypoxylon aeruginosum*, *Chlorostroma subcubisporum* and *C. cyaninum*, sp. nov. Fungal Biology 114(5–6): 481–489. https://doi.org/10.1016/j.funbio.2010.03.010

Læssøe T, Srikitikulchai P, Luangsa-ard JJD, Stadler M (2013) *Theissenia* reconsidered, including molecular phylogeny of the type species *T. pyrenocrata* and a new genus *Durotheca* (Xylariaceae, Ascomycota). IMA Fungus 4(1): 57–69. https://doi.org/10.5598/imafungus.2013.04.01.07

Lambert C, Wendt L, Hladki AI, Stadler M, Sir EB (2019) *Hypomontagnella* (Hypoxylaceae): A new genus segregated from *Hypoxylon* by a polyphasic taxonomic approach. Mycological Progress 18(1–2): 187–201. https://doi.org/10.1007/s11557-018-1452-z

Lambert C, Pourmoghaddam MJ, Cedeño-Sanchez M, Surup F, Khodaparast SA, Krisai-Greilhuber I, Voglmayr H, Stradal TEB, Stadler M (2021) Resolution of the *Hypoxylon fuscum* complex (Hypoxylaceae, Xylariales) and discovery and biological characterization of two of its prominent secondary metabolites. Journal of Fungi 7(2): 131. https://doi.org/10.3390/jof7020131

Lanfear R, Frandsen PB, Wright AM, Senfeld T, Calcott B (2016) PartitionFinder 2: New methods for selecting partitioned models of evolution for molecular and morphological phylogenetic analyses. Molecular Biology and Evolution 34: 772–773. https://doi.org/10.1093/molbev/msw260

Liu YJ, Whelen S, Hall BD (1999) Phylogenetic relationships among ascomycetes: Evidence from an RNA polymerase II subunit. Molecular Biology and Evolution 16(12): 1799–1808. https://doi.org/10.1093/oxfordjournals.molbev.a026092

Ma H, Song Z, Pan X, Li Y, Yang Z, Qu Z (2022) Multi-gene phylogeny and taxonomy of *Hypoxylon* (Hypoxylaceae, Ascomycota) from China. Diversity (Basel) 14(1): 37. https://doi.org/10.3390/d14010037

Matio Kemkuignou B, Schweizer L, Lambert C, Anoumedem EGM, Kouam SF, Stadler M, Marin-Felix Y (2022) New polyketides from the liquid culture of *Diaporthe breyniae* sp. nov. (Diaporthales, Diaporthaceae). MycoKeys 90: 85–118. https://doi.org/10.3897/mycokeys.90.82871

McCaughey CS, van Santen JA, van der Hooft JJJ, Medema MH, Linington RG (2022) An isotopic labeling approach linking natural products with biosynthetic gene clusters. Nature Chemical Biology 18(3): 295–304. https://doi.org/10.1038/s41589-021-00949-6

Miller JH (1961) A monograph of the world species of *Hypoxylon*. Univ. Georgia Press, Athens, 158 pp.

Minh BQ, Schmidt HA, Chernomor O, Schrempf D, Woodhams MD, von Haeseler A, Lanfear R (2020) IQ-TREE 2: New models and efficient methods for phylogenetic inference in the genomic era. Molecular Biology and Evolution 37(5): 1530–1534. https://doi.org/10.1093/molbev/msaa015

Nothias LF, Petras D, Schmid R, Dührkop K, Rainer J, Sarvepalli A, Protsyuk I, Ernst M, Tsugawa H, Fleischauer M, Aicheler F, Aksenov AA, Alka O, Allard PM, Barsch A, Cachet X, Caraballo-Rodriguez AM, Da Silva RR, Dang T, Garg N, Gauglitz JM, Gurevich A, Isaac G, Jarmusch AK, Kameník Z, Kang K, Kessler N, Koester I, Korf A, Le Gouellec A, Ludwig M, Martin H C, McCall L-I, McSayles J, Meyer SW, Mohimani H, Morsy M, Moyne O, Neumann S, Neuweger H, Nguyen NH, Nothias-Esposito M, Paolini J, Phelan VV, Pluskal T, Quinn RA, Rogers S, Shrestha B, Tripathi A, van der Hooft JJJ, Vargas F, Weldon KC, Witting M, Yang H, Zhang Z, Zubeil F, Kohlbacher O, Böcker S, Alexandrov T, Bandeira N, Wang M, Dorrestein PC (2020) Feature-based molecular networking in the GNPS analysis environment. Nature Methods 17(9): 905–908. https://doi.org/10.1038/s41592-020-0933-6

O'Donnell K, Cigelnik E (1997) Two divergent intragenomic rDNA ITS2 types within a monophyletic lineage of the fungus *Fusarium* are nonorthologous. Molecular Phylogenetics and Evolution 7(1): 103–116. https://doi.org/10.1006/mpev.1996.0376

Pourmoghaddam MJ, Lambert C, Surup F, Khodaparast SA, Krisai-Greilhuber I, Voglmayr H, Stadler M (2020) Discovery of a new species of the *Hypoxylon rubiginosum* complex from Iran and antagonistic activities of *Hypoxylon* spp. against the Ash Dieback pathogen, *Hymenoscyphus fraxineus*, in dual culture. MycoKeys 66: 105–133. https://doi.org/10.3897/mycokeys.66.50946

Quang DN, Hashimoto T, Nomura Y, Wollweber H, Hellwig V, Fournier J, Stadler M, Asakawa Y (2005a) Cohaerins A and B, azaphilones from the fungus *Hypoxylon cohaerens*,

and comparison of HPLC-based imetabolite profiles in *Hypoxylon* sect. *Annulata*. Phytochemistry 66: 797–809. 1 https://doi.org/10.1016/j.phytochem.2005.02.006

Quang DN, Hashimoto T, Stadler M, Radulović N, Asakawa Y (2005b) Antimicrobial azaphilones from the fungus *Hypoxylon multiforme*. Planta Medica 71(11): 1058–1062. https://doi.org/10.1055/s-2005-873129

Quang DN, Stadler M, Fournier J, Tomita A, Hashimoto T (2006) Cohaerins C–F, four azaphilones from the xylariaceous fungus *Annulohypoxylon cohaerens*. Tetrahedron 62(26): 6349–6354. https://doi.org/10.1016/j.tet.2006.04.040

Rayner RW (1970) A Mycological Colour Chart. Commonwealth Mycological Institute, Kew and British Mycological Society.

Rogers J (1985) *Hypoxylon duranii* sp. nov. and the anamorphs of *H. caries*, *H. papillatum*, and *Rosellinia subiculata*. Mycotaxon 23: 429–437.

Ronquist F, Teslenko M, van der Mark P, Ayres DL, Darling A, Höhna S, Larget B, Liu L, Suchard MA, Huelsenbeck JP (2012) MrBayes 3.2: Efficient Bayesian Phylogenetic Inference and model choice across a large model space. Systematic Biology 61(3): 539–542. https://doi.org/10.1093/sysbio/sys029

Shimodaira H (2022) An approximately unbiased test of phylogenetic tree selection. Systematic Biology 51(3): 492–508. https://doi.org/10.1080/10635150290069913

Sir EB, Kuhnert E, Surup F, Hyde KD, Stadler M (2015) Discovery of new mitorubrin derivatives from *Hypoxylon fulvo-sulphureum* sp. nov. (Ascomycota, Xylariales). Mycological Progress 14(5): 28. https://doi.org/10.1007/s11557-015-1043-1

Sir EB, Kuhnert E, Lambert C, Hladki AI, Romero AI, Stadler M (2016) New species and reports of *Hypoxylon* from Argentina recognized by a polyphasic approach. Mycological Progress 15(4): 42. https://doi.org/10.1007/s11557-016-1182-z

Sir EB, Becker K, Lambert C, Bills GF, Kuhnert E (2019) Observations on Texas hypoxylons, including two new *Hypoxylon* species and widespread environmental isolates of the *H. croceum* complex identified by a polyphasic approach. Mycologia 111(5): 832–856. https://doi.org/10.1080/00275514.2019.1637705

Smith CL (1893) Some Central American Pyrenomycetes. Bulletin from the laboratories of natural history of the State University of Iowa 2: 408.

Stadler M, Fournier J, Granmo A, Beltrán-Tejera E (2008) The "red Hypoxylons" of the temperate and subtropical Northern hemisphere. North American Fungi 3: 73–125. https://doi.org/10.2509/naf2008.003.0075

Stadler M, Fournier J, Læssøe T, Chlebicki A, Lechat C, Flessa F, Rambold G, Peršoh D (2010) Chemotaxonomic and phylogenetic studies of *Thamnomyces* (Xylariaceae). Mycoscience 51(3): 189–207. https://doi.org/10.1007/S10267-009-0028-9

Stadler M, Kuhnert E, Peršoh D, Fournier J (2013) The Xylariaceae as model example for a unified nomenclature following the "One Fungus-One Name" (1F1N) concept. Mycology 4: 5–21. https://doi.org/10.1080/21501203.2013.782478

Stadler M, Læssøe T, Fournier J, Decock C, Schmieschek B, Tichy H-V, Peršoh D (2014) A polyphasic taxonomy of *Daldinia* (Xylariaceae)1. Studies in Mycology 77: 1–143. https://doi.org/10.3114/sim0016

Stadler M, Lambert C, Wibberg D, Kalinowski J, Cox RJ, Kolařík M, Kuhnert E (2020) Intragenomic polymorphisms in the ITS region of high-quality genomes of the Hypoxylaceae

(Xylariales, Ascomycota). Mycological Progress 19(3): 235–245. https://doi.org/10.1007/s11557-019-01552-9

Surup F, Mohr KI, Jansen R, Stadler M (2013) Cohaerins G-K, azaphilone pigments from *Annulohypoxylon cohaerens* and absolute stereochemistry of cohaerins C–K. Phytochemistry 95: 252–258. https://doi.org/10.1016/j.phytochem.2013.07.027

Surup F, Narmani A, Wendt L, Pfütze S, Kretz R, Becker K, Menbrivès C, Giosa A, Elliott M, Petit C, Rohde M, Stadler M (2018) Identification of fungal fossils and novel azaphilone pigments in ancient carbonised specimens of *Hypoxylon fragiforme* from forest soils of Châtillon-sur-Seine (Burgundy). Fungal Diversity 92(1): 345–356. https://doi.org/10.1007/s13225-018-0412-x

Tang A, Jeewon R, Hyde KD (2009) A re-evaluation of the evolutionary relationships within the Xylariaceae based on ribosomal and protein-coding gene sequences. Fungal Diversity 34: 127–155.

Tamura K, Stecher G, Kumar S (2021) MEGA11: Molecular evolutionary genetics analysis Version 11. Molecular Biology and Evolution 38(7): 3022–3027. https://doi.org/10.1093/molbev/msab120

Tian DS, Kuhnert E, Ouazzani J, Wibberg D, Kalinowski J, Cox RJ (2020) The sporothriolides. A new biosynthetic family of fungal secondary metabolites. Chemical Science 11(46): 12477–12484. https://doi.org/10.1039/D0SC04886K

Triebel D, Peršoh D, Wollweber H, Stadler M (2005) Phylogenetic relationships among *Daldinia*, *Entonaema* and *Hypoxylon* as inferred from ITS nrDNA analyses of Xylariales. Nova Hedwigia 80(1–2): 25–43. https://doi.org/10.1127/0029-5035/2005/0080-0025

U'Ren JM, Miadlikowska J, Zimmerman NB, Lutzoni F, Stajich JE, Arnold AE, U'Ren JM (2016) Contributions of North American endophytes to the phylogeny, ecology, and taxonomy of Xylariaceae (Sordariomycetes, Ascomycota). Molecular Phylogenetics and Evolution 98: 210–232. https://doi.org/10.1016/j.ympev.2016.02.010

Van der Hooft JJJ, Mohimani H, Bauermeister A, Dorrestein PC, Duncan KR, Medema MH (2020) Linking genomics and metabolomics to chart specialized metabolic diversity. Chemical Society Reviews 49(11): 3297–3314. https://doi.org/10.1039/D0CS00162G

Vicente TFL, Gonçalves MFM, Brandão C, Fidalgo C, Alves A (2021) Diversity of fungi associated with macroalgae from an estuarine environment and description of *Cladosporium rubrum* sp. nov. and *Hypoxylon aveirense* sp. nov. International Journal of Systematic and Evolutionary Microbiology 71(2): 004630. https://doi.org/10.1099/ijsem.0.004630

Vilgalys R, Hester M (1990) Rapid genetic identification and mapping of enzymatically amplified ribosomal DNA from several *Cryptococcus* species. Journal of Bacteriology 172(8): 4238–4246. https://doi.org/10.1128/jb.172.8.4238-4246.1990

Vu D, Groenewald M, de Vries M, Gehrmann T, Stielow B, Eberhardt U, Al-Hatmi A, Groenewald JZ, Cardinali G, Houbraken J, Boekhout T, Crous PW, Robert V, Verkley GJM (2019) Large-scale generation and analysis of filamentous fungal DNA barcodes boosts coverage for kingdom fungi and reveals thresholds for fungal species and higher taxon delimitation. Studies in Mycology 92(1): 135–154. https://doi.org/10.1016/j.simyco.2018.05.001

Wang M, Carver JJ, Phelan VV, Sanchez LM, Garg N, Peng Y, Nguyen DD, Watrous J, Kapono CA, Luzzatto-Knaan T, Porto C, Bouslimani A, Melnik AV, Meehan MJ, Liu WT, Crüsemann M, Boudreau PD, Esquenazi E, Sandoval-Calderón M, Kersten RD, Pace LA, Quinn RA, Duncan KR, Hsu CC, Floros DJ, Gavilan RG, Kleigrewe K, Northen T, Dutton RJ, Parrot D, Carlson EE, Aigle B, Michelsen CF, Jelsbak L, Sohlenkamp C, Pevzner P, Edlund A, McLean J, Piel J, Murphy BT, Gerwick L, Liaw CC, Yang YL, Humpf HU, Maansson M, Keyzers RA, Sims AC, Johnson AR, Sidebottom AM, Sedio BE, Klitgaard A, Larson CB, Boya CAP, Torres-Mendoza D, Gonzalez DJ, Silva DB, Marques LM, Demarque DP, Pociute E, O'Neill EC, Briand E, Helfrich EJN, Granatosky EA, Glukhov E, Ryffel F, Houson H, Mohimani H, Kharbush JJ, Zeng Y, Vorholt JA, Kurita KL, Charusanti P, McPhail KL, Nielsen KF, Vuong L, Elfeki M, Traxler MF, Engene N, Koyama N, Vining OB, Baric R, Silva RR, Mascuch SJ, Tomasi S, Jenkins S, Macherla V, Hoffman T, Agarwal V, Williams PG, Dai J, Neupane R, Gurr J, Rodríguez AMC, Lamsa A, Zhang C, Dorrestein K, Duggan BM, Almaliti J, Allard PM, Phapale P, Nothias LF, Alexandrov T, Litaudon M, Wolfender JL, Kyle JE, Metz TO, Peryea T, Nguyen DT, VanLeer D, Shinn P, Jadhav A, Müller R, Waters KM, Shi W, Liu X, Zhang L, Knight R, Jensen PR, Palsson B, Pogliano K, Linington RG, Gutiérrez M, Lopes NP, Gerwick WH, Moore BS, Dorrestein PC, Bandeira N (2016) Sharing and community curation of mass spectrometry data with Global Natural Products Social Molecular Networking. Nature Biotechnology 34(8): 828–837. https://doi.org/10.1038/nbt.3597

Wang F, Liigand J, Tian S, Arndt D, Greiner R, Wishart DS (2021) CFM-ID 4.0: More Accurate ESI-MS/MS Spectral Prediction and Compound Identification. Analytical Chemistry 93(34): 11692–11700. https://doi.org/10.1021/acs.analchem.1c01465

Wendt L, Sir EB, Kuhnert E, Heitkämper S, Lambert C, Hladki AI, Romero AI, Luangsa-ard JJ, Srikitikulchai P, Peršoh D, Stadler M (2018) Resurrection and emendation of the Hypoxylaceae, recognised from a multigene phylogeny of the Xylariales. Mycological Progress 17(1–2): 115–154. https://doi.org/10.1007/s11557-017-1311-3

White TJ, Bruns TD, Lee S, Taylor JW (1990) Amplification and direct sequencing of fungal ribosomal RNA for phylogenetics. In: Innis MA, et al. (Eds) PCR protocols: a guide to methods and applications. Academic Press, San Diego, 315–322. https://doi.org/10.1016/B978-0-12-372180-8.50042-1

Wibberg D, Stadler M, Lambert C, Bunk B, Spröer C, Rückert C, Kalinowski J, Cox RJ, Kuhnert E (2021) High quality genome sequences of thirteen Hypoxylaceae (Ascomycota) strengthen the phylogenetic family backbone and enable the discovery of new taxa. Fungal Diversity 106(1): 7–28. https://doi.org/10.1007/s13225-020-00447-5

Zhang N, Castlebury LA, Miller AN, Huhndorf SM, Schoch CL, Seifert KA, Rossman AY, Rogers JD, Kohlmeyer J, Volkmann-Kohlmeyer B, Sung G-H (2006) An overview of the systematics of the Sordariomycetes based on a four-gene phylogeny. Mycologia 98(6): 1076–1087. https://doi.org/10.1080/15572536.2006.11832635

Zhang D, Gao F, Jakovlić I, Zou H, Zhang J, Li WX, Wang GT (2020) PhyloSuite: An integrated and scalable desktop platform for streamlined molecular sequence data management and evolutionary phylogenetics studies. Molecular Ecology Resources 20(1): 348–355. https://doi.org/10.1111/1755-0998.13096

Supplementary material 1

Supplementary information

Authors: Marjorie Cedeño-Sanchez, Esteban Charria-Girón, Christopher Lambert, J. Jennifer Luangsa-ard, Cony Decock, Raimo Franke, Mark Brönstrup, Marc Stadler

Data type: Alignments and MS raw data (PDF file)

Link: https://doi.org/10.3897/mycokeys.95.98125.suppl1

MycoKeys 95: 163–188 (2023)
doi: 10.3897/mycokeys.95.87121
https://mycokeys.pensoft.net

RESEARCH ARTICLE

A peer-reviewed open-access journal
MycoKeys
Launched to accelerate biodiversity research

Endophytic *Colletotrichum* (Sordariomycetes, Glomerellaceae) species associated with *Citrus grandis* cv. "Tomentosa" in China

Jia-Wei Liu[1], Ishara S. Manawasinghe[1], Xuan-Ni Liao[1], Jin Mao[1], Zhang-Yong Dong[1], Ruvishika S. Jayawardena[2,3], Dhanushka N. Wanasinghe[4], Yong-Xin Shu[1,2,3], Mei Luo[1]

1 *Innovative Institute for Plant Health/ Key laboratory of Fruit and Vegetable Green Prevention and Control in South-China, Ministry of Agricul-ture and Rural Affairs, Zhongkai University of Agriculture and Engineering, Guangzhou 510225, China* **2** *Center of Excellence in Fungal Research, Mae Fah Luang University, Chiang Rai, Thailand* **3** *School of Science, Mae Fah Luang University, Chiang Rai, Thailand* **4** *Center for Mountain Futures, Kunming Institute of Botany, Chinese Academy of Sciences, Kunming, Honghe 654400, China*

Corresponding authors: Ishara S. Manawasinghe (ishara9017@gmail.com); Mei Luo (08luomei@163.com)

Academic editor: M. Ruszkiewicz-Michalska | Received 7 June 2022 | Accepted 9 February 2023 | Published 23 February 2023

Citation: Liu J-W, Manawasinghe IS, Liao X-N, Mao J, Dong Z-Y, Jayawardena RS, Wanasinghe DN, Shu Y-X, Luo M (2023) Endophytic *Colletotrichum* (Sordariomycetes, Glomerellaceae) species associated with *Citrus grandis* cv. "Tomentosa" in China. MycoKeys 95: 163–188. https://doi.org/10.3897/mycokeys.95.87121

Abstract

Colletotrichum species are well-known plant pathogens, saprobes, endophytes, human pathogens and entomopathogens. However, little is known about *Colletotrichum* as endophytes of plants and cultivars including *Citrus grandis* cv. "Tomentosa". In the present study, 12 endophytic *Colletotrichum* isolates were obtained from this host in Huazhou, Guangdong Province (China) in 2019. Based on morphology and combined multigene phylogeny [nuclear ribosomal internal transcribed spacer (ITS), glyceraldehyde-3-phosphate dehydrogenase (*gapdh*), chitin synthase 1 (*chs-1*), histone H3 (*his3*) actin (*act*), beta-tubulin (β-*tubulin*) and glutamine synthetase (*gs*)], six *Colletotrichum* species were identified, including two new species, namely *Colletotrichum guangdongense* and *C. tomentosae*. *Colletotrichum asianum*, *C. plurivorum*, *C. siamense* and *C. tainanense* are identified as being the first reports on *C. grandis* cv. "Tomentosa" worldwide. This study is the first comprehensive study on endophytic *Colletotrichum* species on *C. grandis* cv. "Tomentosa" in China.

Keywords

Chinese traditional medicinal plants, new ascomycete, phylogeny, six new host records, taxonomy, two new species

Introduction

Citrus grandis cv. "Tomentosa" is an important traditional medicinal plant which contains essential oils, flavonoids and polysaccharides. In traditional Chinese medicine, *Citrus grandis* cv. "Tomentosa" has been used for treatments due to its anti-inflammatory effect (Zhao et al. 2017). It has also been used in the treatment of coughs, asthma, food stagnation, vomiting and other symptoms (Peng et al. 2019). Current research on *C. grandis* cv. "Tomentosa" is still focused on medicinal components, with a relatively long timescale needed to accumulate the effective ingredient. It is likely that the endophytic community living inside the host affects the metabolites of the plant. Dai et al. (2017) found that nine species of *Taxus* endophytic fungi could produce paclitaxel. Hasan et al. (2022) found endophytic fungi, *Penicillium crustosum* from *Annona muricata* L. has anti-cancer activity against HeLa cells. Therefore, it is necessary to study the effects of the endophytic community associated with these traditional medicinal plants. The findings of this research can help in finding potential new natural medicines and form the basis for subsequent screening of strains.

Colletotrichum Corda (1831), belongs to Glomerellaceae (Sordariomycetes), which comprises plant pathogens, endophytes and saprobes on a wide range of hosts (Christy et al. 2020; Jayawardena et al. 2021). They are one of the most often isolated endophytic fungal groups encompassing a wide range of hosts. These endophytic *Colletotrichum* species have some advantages to the host, such as providing disease resistance, drought tolerance and promoting growth of the host (Hacquard et al. 2016; Dini-Andreote 2020). Endophytic species can also change their lifestyle and become pathogenic (Photita et al. 2004). Liu et al. (2022) accepted 280 *Colletotrichum* species, from which 23 species have been identified from *Citrus* spp. Therefore, studying diversity and clarifying taxonomic affinities of isolates can answer a range of important ecological and evolutionary questions. Although there have been several studies on *Colletotrichum* species associated with *Citrus* (Damm et al. 2012; Huang et al. 2013; Guarnaccia et al. 2017), there is still imprecise identification of endophytes of *Colletotrichum* species on *C. grandis* cv. "Tomentosa".

Species delineation of *Colletotrichum* is challenging because there are few distinctive morphological characters available (Bhunjun et al. 2021). *Colletotrichum* is characterised as an intricate genus with 16 species complexes and 15 singleton species (Liu et al. 2022). Although host specificity was the most used character for identification in early studies, current taxonomic classifications and species delineations are based on morphology alongside multi-locus phylogeny (Bhunjun et al. 2021; Jayawardena et al. 2021; Liu et al. 2022). Phylogenetic analyses of *Colletotrichum* have been based on ITS, *gapdh*, *chs-1*, *act* and β-*tubulin* and multi-loci phylogeny. However, some complexes that cannot be distinguished by five loci required additional loci for identification (Bhunjun et al. 2021; Jayawardena et al. 2021; Liu et al. 2022). Therefore, the selection of gene combinations depends on the species complex (Jayawardena et al. 2021).

The objectives of this study were to isolate and identify the dominant endophytic *Colletotrichum* species associated with healthy *C. grandis* cv. "Tomentosa" in Huazhou, Guangdong, China. Morphology, molecular phylogeny and recombination analysis

were used for the species characterisation. This resulted in two new species and six new host records. Detailed descriptions and coloured illustrations have been given for the novel taxa identified.

Materials and methods

Sample collection and isolation

Healthy leaves and twigs of *Citrus grandis* cv. "Tomentosa" were randomly collected from a *Citrus* orchard in Huazhou, Guangdong Province, China (21°66'N, 110°63'E). A total of 20 trees were randomly selected for the collection. Ten samples were collected from the upper, middle and lower parts of each plant. Asymptomatic samples were packed into zip-lock bags in a foam box with ice and were then brought to the plant pathology laboratory of Zhongkai University of Agriculture and Engineering where they were preserved at 4 °C before processing. Isolation was undertaken within 48 h after collection, following the procedure by Dong et al. (2021).

Endophytic fungi were isolated following the methods described by da Silva et al. (2020). The samples were initially washed with running tap water followed by sterile water. The leaves were cut into 3 mm × 3 mm segments, while the twigs were cut into 3 mm long pieces. Each piece was then surface sterilised by being dipped sequentially into 75% ethanol for 30 s, 2.5% NaClO (sodium hypochlorite) for 30–60 s (leaves for 30 s, twigs for 60 s), before being rinsed three times with sterilised water. They were then dried on sterilised filter paper. The cuttings were then placed on potato dextrose agar (PDA: 200 g potato, 20 g dextrose, 20 g agar per 1 litre of water). Plates were incubated at 25 °C with 12 h of dark and 12 h of fluorescent light. Pure cultures were cultured on PDA for 7 to 14 days at 25 °C. All the pure cultures obtained in this study were deposited in the Culture Collection of Zhongkai University of Agriculture and Engineering (**ZHKUCC**). The living cultures (ex-type) of new species identified in this study were deposited in the Culture Collection of the Chinese Academy of Sciences (CGMCC, *C. guangdongense* for the holotype with CGMCC 3.24127 and *C. tomentosae* with CGMCC 3.24128). Herbarium materials as dry cultures of novel species were deposited in the Herbarium of Zhongkai University of Agriculture and Engineering (**ZHKU**). The strain numbers belonging to all isolates (from ZHKUCC 21-0095 to 21-0106 and 22-041 to 22-0042) for this study are presented in Appendix 1.

Morphological studies

For macro- and micro-morphological characterisation, 5 mm diameter agar plugs were cut from all the actively growing pure cultures on PDA and were then transferred on to new PDA. The colony diameter was measured daily for 5–9 d to determine the growth rate (mm/day) on the PDA at 25 °C under 12 h of dark and 12 h of fluorescent light. Appressoria formation was observed following Johnston and Jones (1997) and Cai et al. (2009). The cultures were incubated for 2–4 weeks and morphological characters (appressoria,

ascomata, asci, ascospores, conidiophores and conidia) were observed. Macro-morphological characters were photographed using a SteREO Discovery.V20 (Zeiss, Germany) stereomicroscope. Fruiting bodies were cut into thin sections by a CM1860 freezing sliding microtome (LEICA, Germany). Digital images were captured with an Eclipse 80i photographic microscope (Nikon, Japan). Measurements were taken using NIS Elements BR 3.2 (Nikon, Japan). The mean values were calculated with their standard deviations (SDs).

DNA extraction, PCR amplification and sequencing

Total genomic DNA was extracted from mycelium grown on PDA and incubated for approx. seven days at 25 °C using the CTAB method (Sun et al. 2009). The ITS region was amplified and sequenced. The resulting sequences were subjected to BLASTn searches in GenBank (https://blast.ncbi.nlm.nih.gov) to identify them to the genus level. Once the BLAST results had confirmed isolates as being *Colletotrichum* species, an additional six gene regions, namely *gapdh*, *chs-1*, *his3*, *act*, β-*tubulin* and *gs*, were amplified and sequenced. The PCR conditions for each primer pair are given below (Table 1). The amplicons were observed on 1% agarose electrophoresis gel and positive amplicons were sequenced by Tianyi Huiyuan Biotechnology Co., Ltd., Guangzhou, China. The initial sequence quality was checked using BioEdit v. 7.25 (Hall 2006). A total of 66 sequences generated in this study were submitted to GenBank (Appendix 1).

Phylogenetic analysis

For the phylogenetic analysis, reference sequences for *Colletotrichum* species and related taxa were obtained from NCBI GenBank (Appendix 1). Each locus was aligned together with the sequences obtained in the present study using MAFFT (https://www.ebi.ac.uk/Tools/msa/mafft/) (Katoh et al. 2019). Alignments were checked and manually adjusted where necessary with BioEdit v. 7.25 (Hall 2006). Alignment results were automatically trimmed using the Trimal tool in PhyloSuite (v.1.2.1) (Zhang et al. 2020). Phylogenetic analyses were conducted according to Maximum Likelihood (ML) in RAxML (Silvestro

Table 1. Gene regions, respective primer pairs and PCR protocols used in the study.

Gene	Primer pair	Optimised PCR protocols	References
ITS	ITS1 ITS4	94 °C: 5 min (94 °C: 30 s, 53 °C: 30 s, 72 °C: 1 min) × 32 cycles, 72 °C: 10 min	White et al. (1990)
gapdh	GDF GDR	94 °C: 5 min (94 °C: 30 s, 60 °C: 30 s, 72 °C: 1 min) × 32 cycles, 72 °C: 10 min	Guerber et al. (2003)
chs-1	CHS-79F CHS-345R	94 °C: 5 min (94 °C: 30 s, 49 °C: 30 s, 72 °C: 1 min) × 32 cycles, 72 °C: 10 min	Carbone and Kohn (1999)
his3	CYLH3F CYLH3R	94 °C: 5 min (94 °C: 30 s, 53 °C: 30 s, 72 °C: 1 min) × 32 cycles, 72 °C: 10 min	Crous et al. (2004)
act	ACT-512F ACT-783R	94 °C: 5 min (94 °C: 30 s, 54 °C: 30 s, 72 °C: 1 min) × 32 cycles, 72 °C: 10 min	Carbone and Kohn (1999)
β-tubulin	Bt2a Bt2b	94 °C: 5 min (94 °C: 30 s, 58 °C: 30 s, 72 °C: 1 min) × 32 cycles, 72 °C: 10 min	Glass and Donaldson (1995)
gs	GSF1 GSR1	94 °C: 5 min (94 °C: 30 s, 60 °C: 60 s, 72 °C: 1 min) × 35 cycles, 72 °C: 30 min	Guerber et al. (2003)

and Michalak 2010), maximum parsimony (MP) in PAUP (v.4.0) (Swofford 2002) and Bayesian analyses (BP) in MrBayes (v. 3.1.2) (Ronquist and Huelsenbeck 2003). The final analyses of the *Colletotrichum gloeosporioides* complex were made using the concatenated dataset of *act*, *chs-1*, *gapdh*, ITS, β-*tubulin* and *gs*, following Liu et al. (2022). The other two complexes: *Colletotrichum orchidearum* complex and *Colletotrichum magnum* complex were analysed using *act*, *chs-1*, *gapdh*, *his3*, ITS and β-*tubulin*, following Liu et al. (2022).

In the MP analysis, ambiguous regions were excluded and gaps were treated as missing data. Tree stability was evaluated with 1,000 bootstrap replications. Zero-length branches were collapsed and all the parsimonious trees were saved. Tree parameters: tree length (TL), consistency index (CI), retention index (RI), relative consistency index (RC) and homoplasy index (HI) were calculated. Kishino-Hasegawa tests (KHT) were conducted to evaluate the differences between the trees inferred as being under different optimality criteria (Kishino and Hasegawa 1989). MrModelTest v. 2.3 (Nylander 2004) was used to determine the evolutionary models for each locus to be used in Bayesian and Maximum Likelihood analyses. The Maximum Likelihood analyses were conducted using RAxML-HPC2 on XSEDE (8.2.8) (Stamatakis 2014) in the CIPRES Science Gateway platform (Miller et al. 2010). The GTR + I + G evolutionary model was employed with 1,000 non-parametric bootstrapping iterations. Bayesian analysis was performed in MrBayes v. 3.1.2 (Ronquist and Huelsenbeck 2003). Posterior probabilities (PPs) were determined using Markov Chain Monte Carlo sampling (MCMC). Six simultaneous Markov chains were run for 10^8 generations, with sampling the trees at each 1000th generation. From the 10,000 trees obtained, the first 2,500 representing the burn-in phase were discarded. The remaining 7,500 trees were then used to calculate the posterior probabilities (BPs) in a majority rule consensus tree. Taxonomic novelties were submitted to the FacesofFungi database (Jayasiri et al. 2015) and Index Fungorum (http://www.indexfungorum.org). The final sequence alignments generated in this study were submitted to TreeBASE (http://www.treebase.org) under the submission ID 29668.

Pairwise homoplasy index (PHI) analysis

Recombination analyses were conducted to provide evidence for genetic distances for two new species identified, based on the phylogenetic analyses. The pairwise homoplasy index (Φw) (Bruen et al. 2006) was calculated in SplitsTree (version 4.1.4.4) using Kimura's two-parameter (K2P) models for low genetic distance datasets. The standard deviation of split frequencies in the PHI test results (Φw) < 0.05 indicates significant recombination within the dataset.

Results

In total, 12 endophytic *Colletotrichum* strains were obtained: seven from leaves and five from twigs. Based on the initial species identification undertaken through BLASTn searches, taxa isolated in this study belonged to three species complexes, namely the *C. gloeosporioides*, *C. magnum* and *C. orchidearum* complexes.

Colletotrichum gloeosporioides complex

In the present study, eight *Colletotrichum* isolates were initially recognised as belonging to the *C. gloeosporioides* complex. Phylogenetic analyses of a combined *act* (1–281), *chs-1* (282–573), *gapdh* (574–850), ITS (851–1384), β-*tubulin* (1385–1846) and *gs* (1847–2616) sequence alignment were conducted using 89 *Colletotrichum* strains. *Colletotrichum boninense* (ICMP 17904) and *C. hippeastri* (ICMP 17920) were used as outgroup taxa. The best-scoring MP tree is shown in Fig. 1. The dataset comprised 2,616 characters with 1,757 constant characters, 370 parsimony-informative and 489 parsimony-uninformative characters. The maximum number of trees generated was 1,000 and the most parsimonious trees had a length of 1,492 steps (CI = 0.707, RI = 0.848, RC = 0.600, HI = 0.293). The final ML tree topology was in line with the MP and BP trees. The best-scoring ML tree has a final likelihood value of –12,639.274168. The matrix consisted of 1,060 distinct alignment patterns, with 15.26% undetermined characters or gaps. For the Bayesian Inference, the TPM2uf+G model was selected for *act*, TIM1ef+G for *chs-1*, HKY+I for *gapdh*, TrNef+I+G for ITS, TIM3ef+G for β-*tubulin* and TVM+G for *gs*. In the phylogenetic analysis, three isolates (ZHKUCC 21-0103, ZHKUCC 21-0104 and ZHKUCC 22-0041) from this study developed a sister clade from other known species. The new species of *C. tomentosae* showed a close relationship to *C. syzygicola* (MFLUCC 10-0624) with 92% ML, 90% MP and 1.00 BP support. Three strains (ZHKUCC 21-0096, ZHKUCC 21-0097 and ZHKUCC 21-0098) from this study cluster together with *C. siamense* (ICMP 18578) with 0.99 BP support in the multi-locus phylogenetic tree. The strain ZHKUCC 21-0095 was clustered with *C. asianum* (ICMP 18580) with 100% ML, 100% MP and 1.00 BP in the phylogenetic tree. A single strain (ZHKUCC 21-0101) belongs to *C. tainanense* (CBS 143666) with 93% ML, 83% MP and 1.00 BP support. The PHI value indicates that there is no significant evidence for recombination amongst the species used in this analysis (p = 1.0) (Fig. 2). Based on this, we identified these isolates as novel *Colletotrichum* species. Species descriptions and illustrations of the new species, identified from the *C. gloeosporioides* complex, are presented below.

Taxonomy

Colletotrichum asianum **Prihast., L. Cai & K.D. Hyde, Fungal Diversity 39: 96 (2009)**
Index Fungorum Number: IF515408
Facesoffungi Number: FoF10689

Material examined. China, Guangdong Province, Huazhou, isolated from healthy twigs of *Citrus grandis* cv. "Tomentosa", May 2019, Y.X. Shu, (dried culture ZHKU 21-0084); living culture ZHKUCC 21-095.

Notes. The single isolate (ZHKUCC 21-0095) obtained in this study clustered with the *Colletotrichum asianum* ex-type strain (ICMP: 1850) with 100% ML, 100% MP and 1.0 BP values (Fig. 1). Morphologically, the isolate obtained in this study is similar to those in the original description of *C. asianum* (Prihastuti et al. 2009). This is the first report of *C. asianum* on *C. grandis* cv. "Tomentosa".

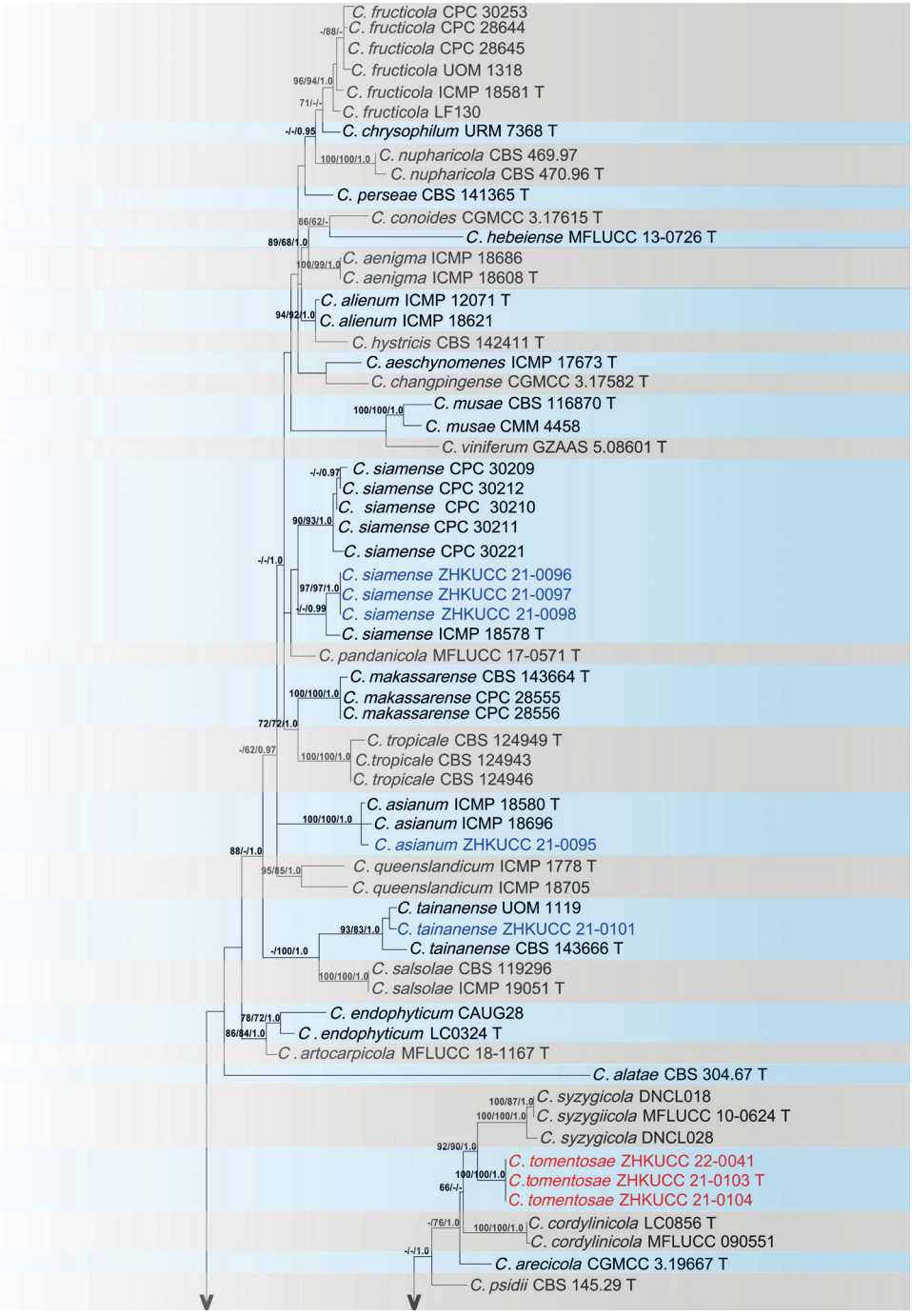

Figure 1. The most parsimonious tree of the *gloeosporioides* complex developed using combined *act*, *chs-1*, *gapdh*, ITS, β-*tubulin* and *gs* sequences. *Colletotrichum boninense* and *C. hippeastri* were used as outgroup taxa. Bootstrap values equal to or greater than 60% in MP and ML and BP equal to or greater than 0.95 are shown as MP/ML/BP above the respective node. The isolates belonging to the current study are given in blue for known species and new species are shown in red. Ex-type strains are noted with T.

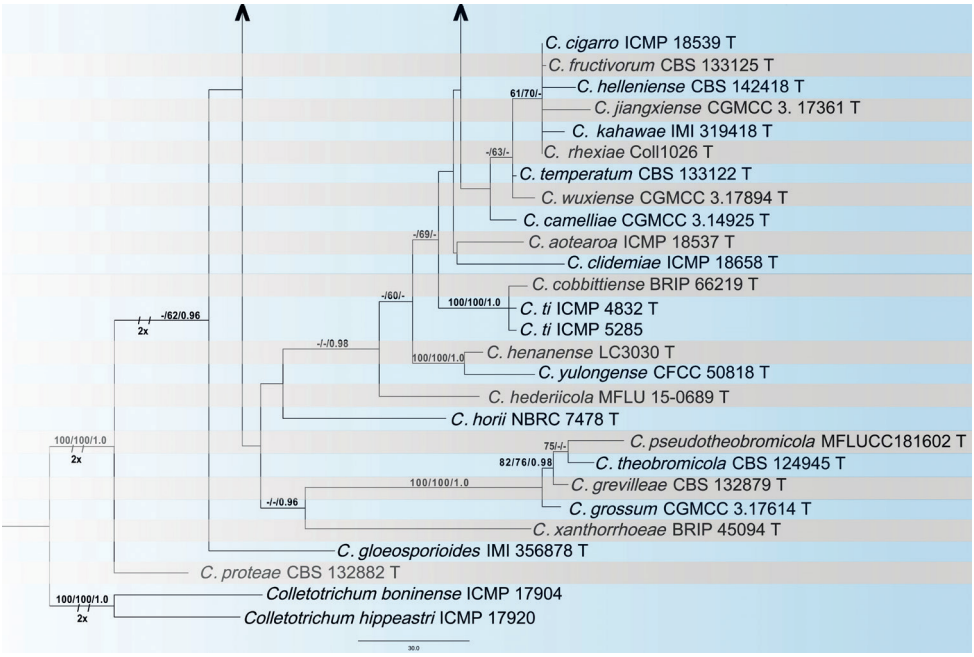

Figure 1. Continued.

Colletotrichum siamense **Prihast., L. Cai & K.D. Hyde, Fungal Diversity 39: 98 (2009)**
Index Fungorum Number: IF515410
Facesoffungi Number: FoF03599

Material examined. China, Guangdong Province, Huazhou, isolated from healthy leaf of *Citrus grandis* cv. "Tomentosa", May 2019, Y.X. Shu, (dried culture ZHKU 21-0085); living cultures ZHKUCC 21-0096, ZHKUCC 21-0097, ZHKUCC 21-0098).

Notes. Three isolates obtained in this study (ZHKUCC 21-0096–100) clustered with the ex-type strain of *Colletotrichum siamense* (ICMP: 18578) with 67% MP and 0.99 BP values (Fig. 1). Morphologically, the isolate obtained in this study is similar to those in the original description of *C. siamense* (Prihastuti et al. 2009). This is the first report of *C. siamense* on *C. grandis* cv. "Tomentosa".

Colletotrichum tainanense **de Silva, Crous & P.W.J. Taylor, IMA Fungus 10(1): 23 (2019)**
Index Fungorum Number: IF827692
Facesoffungi Number: FoF10690

Material examined. China, Guangdong Province, Huazhou, isolated from healthy leaf of *Citrus grandis* cv. "Tomentosa", May 2019, Y.X. Shu, (dried culture ZHKU 21-0086); living culture ZHKUCC 21-0101.

Notes. A single isolate obtained in this study (ZHKUCC 21-0101) clustered with the *Colletotrichum tainanense* (CBS 143666) ex-type strain with 93% ML, 83% MP bootstrap and 1.0 BP values (Fig. 1). Morphologically, the isolate obtained in this study is similar to those in the original description of *C. tainanense* (de Silva et al. 2019). To our knowledge, this is the first report of *C. tainanense* on *C. grandis* cv. "Tomentosa".

Colletotrichum tomentosae **J.W. Liu, Manawas. & M. Luo, sp. nov.**
Index Fungorum Number: IF559482
Facesoffungi Number: FoF10692
Fig. 2

Etymology. The epithet refers to the cultivar of the host plant – *Citrus grandis* cv. "Tomentosa".

Holotype. ZHKUCC 21-0103.

Description. Endophytic in *C. grandis* cv. "Tomentosa" leaf. ***Sexual morph*****:** not observed. ***Asexual morph*****:** Conidiophores 20–40 × 3–5 µm ($\bar{x}$ = 29.8 ± 5.5 × 3.7 ± 0.6 µm, n = 30), hyaline, cylindrical, 1–3-celled, unbranched or branched at the base. Conidia 10–20 × 3–6 µm ($\bar{x}$ = 12.5 ± 1.6 × 4.4 ± 0.6 µm, n = 50), 1–2-guttulate, aseptate, straight, hyaline, smooth-walled, middle part cylindrical both ends obtuse, middle part occasionally shrinkage or bulging. Appressoria 5–15 × 5–10 µm ($\bar{x}$ = 10 ± 1.8 × 7 ± 1.5 µm, n = 50) solitary or in loose groups, light brown to medium brown, Ellipsoidal to subcircular or irregular-shaped.

Cultural characteristics. Colonies on PDA reach 70 mm diam. in seven days, with 10–11 mm/day ($\bar{x}$ = 10 mm, n = 6) growth rate. Colonies flat with entire margin, floccose cottony, surface grey in the centre with glaucous margin. Reverse buff in the centre with off-white margin.

Material examined. China, Guangdong Province, Huazhou, isolated from a healthy leaf of *Citrus grandis* cv. "Tomentosa", May 2019, Y.X. Shu, (dried cultures ZHKU 21-0088 ***holotype***); ex-type culture ZHKUCC 21-0103 (= CGMCC 3.24128), ex-isotype ZHKUCC 21-0104, ZHKUCC 22-0041).

Notes. In the phylogenetic analysis of combined six genes, *Colletotrichum tomentosae* formed an independent clade (Fig. 1). This species is phylogenetically distinct from *C. syzygicola*. Morphologically, appressoria developed by *C. syzygicola* (DNCL021; Udayanga et al. (2013)) are longer than *C. tomentosae* (5–15 × 18–24 µm vs. 18–24 µm). *Colletotrichum tomentosae* has longer conidiophores (20–40 × 3–5 vs. 12–16 × 4–5 µm). This species can be distinguished from *C. syzygicola* by 32 nucleotide differences (1/511 in the ITS region, 2/229 in the *gapdh* region, 7/242 in the *act* region and 22/906 in the *gs* region). The PHI test revealed no significant evidence for a recombination (p = 1.0) event amongst *C. syzygicola* and its closely-related taxa (Fig. 3). Therefore, we have described this fungus as a novel species.

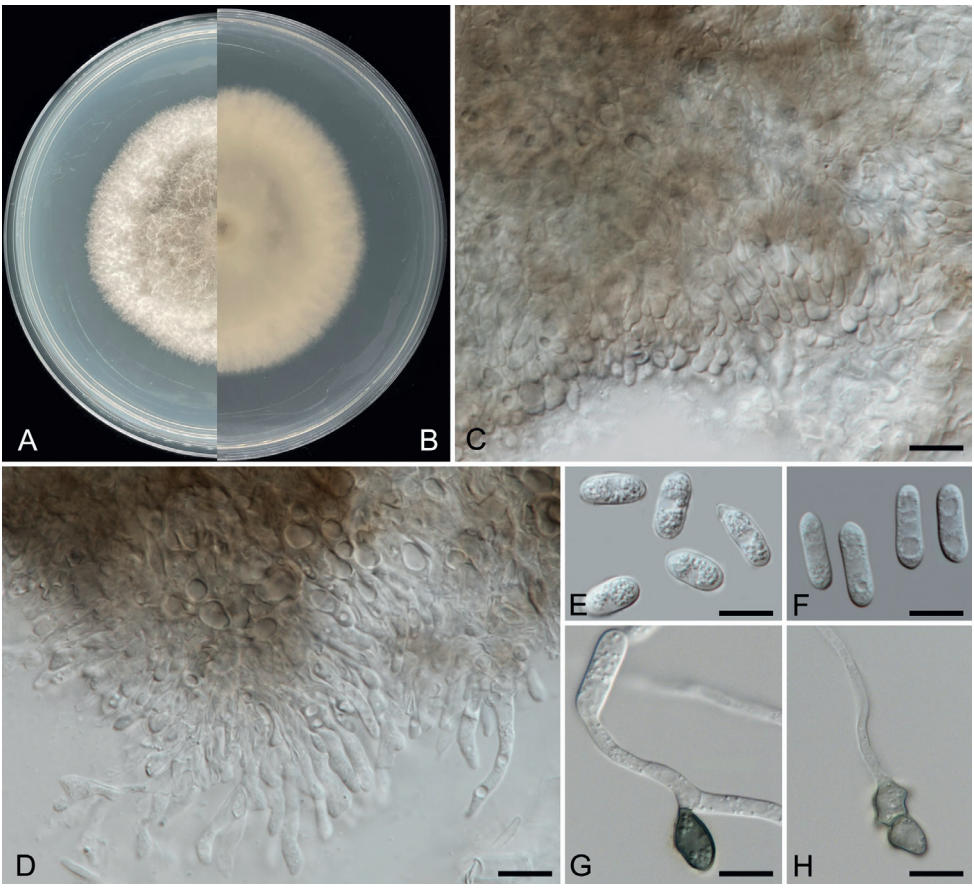

Figure 2. *Colletotrichum tomentosae* (ZHKUCC 21-0103, holotype) **A, B** upper and reverse side of cultures on PDA seven days after inoculation **C, D** conidiophores with developing conidia **E, F** conidia **G, H** appressoria. Scale bars: 10 μm (**C–H**).

Colletotrichum orchidearum complex

In the present study, a single isolate was recognised as belonging to the *Colletotrichum orchidearum* complex. The phylogenetic analysis of a combined ITS, *gapdh*, *chs-1*, *his3*, *act* and β-*tubulin* sequence alignment was constructed using 30 *Colletotrichum* strains. *Colletotrichum magnum* (CBS 519.97) and *C. brevisporum* (BCC 38876) were used as the outgroup. The best scoring MP tree is presented in Fig. 4. The dataset comprised 2,422 characters with 2,055 constant characters and 242 parsimony-informative and 125 parsimony-uninformative characters. The maximum number of trees generated was 1,000 and the most parsimonious trees had a length of 475 steps (CI = 0.874, RI = 0.904, RC = 0.790, HI = 0.126). The final ML tree topology was similar to the MP and BP trees. The best-scoring ML tree with a final likelihood value of –6,065.417493 is shown in Fig. 4. The matrix comprised 479 distinct alignment patterns, with 10.74% of undetermined characters or gaps. The estimated base frequencies were as follows: A = 0.214401, C = 0.319513, G = 0.254583, T = 0.211503;

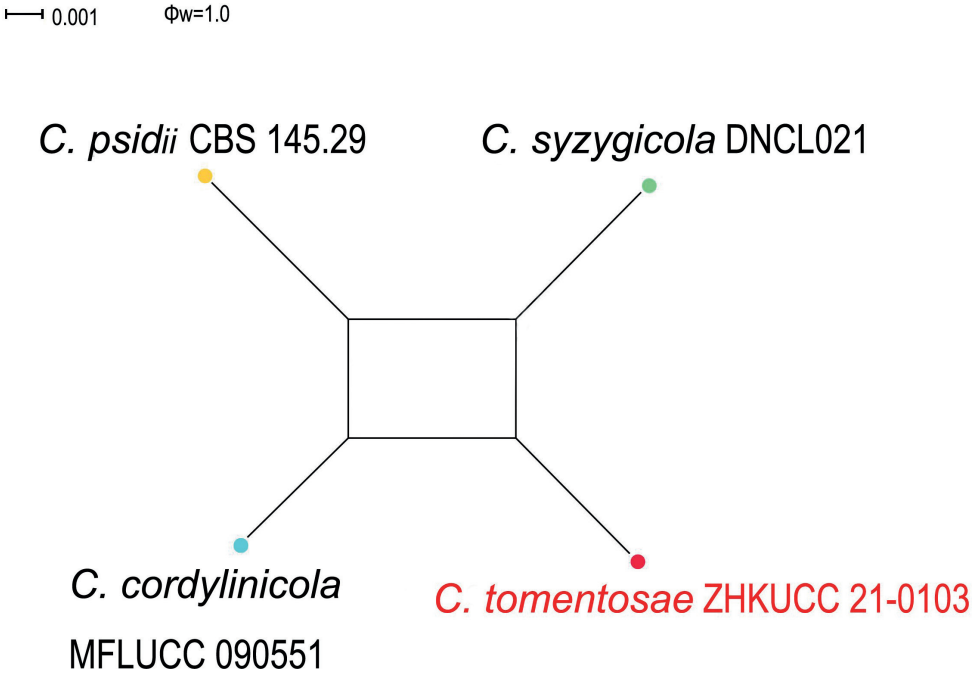

Figure 3. PHI analysis of combined ITS, *gapdh*, *chs-1*, *act* and β-*tubulin* sequence data. PHI test result (Φw) < 0.05 indicates significant recombination within the dataset.

substitution rates AC = 0.9523776, AG = 3.421321, AT = 0.568275, CG = 0.738898, CT = 6.093168, GT = 1.000000; gamma distribution shape parameter a = 0.814817. For the Bayesian Inference, the TPM1uf+I model was selected for *act*, GTR+I+G for *chs-1*, HKY+I for *gapdh*, TIM2+G for *his3*, TIM1+I for ITS and HKY+G for β-*tubulin*. In the phylogenetic analysis, isolates from this study clustered together with *C. plurivorum*. The species description and illustration are given below.

***Colletotrichum plurivorum* Damm, Alizadeh & Toy. Sato, Studies in Mycology 92: 31 (2019)**

Index Fungorum Number: IF824228
Facesoffungi Number: FoF10691

Material examined. China, Guangdong Province, Huazhou, isolated from healthy leaf of *Citrus grandis* cv. "Tomentosa", May 2019, YX Shu, (dried culture ZHKU 21-0087), living culture ZHKUCC 21-0102.

Notes. A single isolate (ZHKUCC 21-0102) obtained in this study clustered with the ex-type strain of *C. plurivorum* (CBS 125474) with 99% ML, 97% MP and 1.0 BP support values (Fig. 4). Morphologically, the isolate obtained in this study is similar to those in the original description of *C. plurivorum* (Damm et al. 2019). *Colletotrichum plurivorum* was first introduced by Damm et al. (2019) as a pathogen

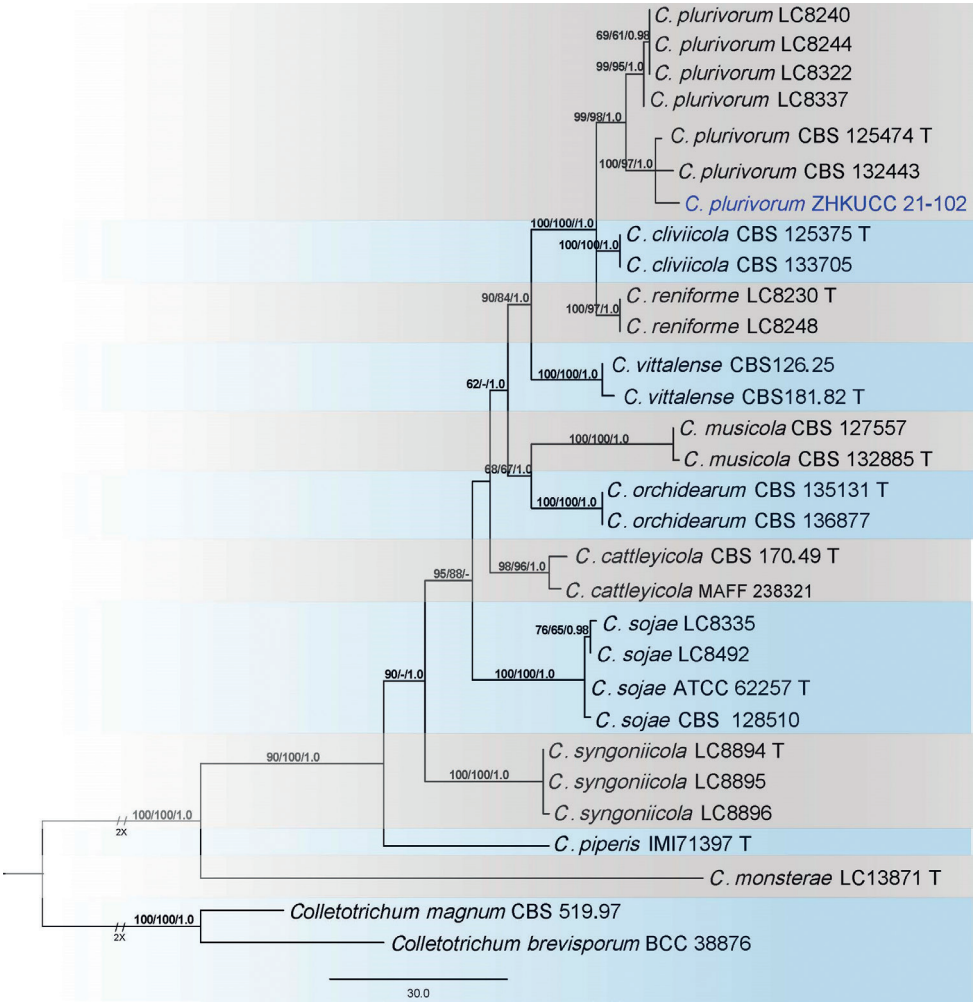

Figure 4. The most parsimonious tree for *Colletotrichum orchidearum* complex using a combined *act*, *chs-1*, *gapdh*, *his3*, ITS, and β-*tubulin* sequences. The tree is rooted to *Colletotrichum brevisporum* and *C. magnum*. Bootstrap support values equal to or greater than 60% in MP and ML and BP equal to or greater than 0.95 are shown as MP/ML/BP above the respective nodes. The isolates belonging to the current study is given in blue. Ex-type strains are noted with T.

on *Capsicum annuum* fruits and subsequently, has been reported as pathogens causing anthracnose or leaf spot diseases (Farr and Rossman 2022). This is the first report of *C. plurivorum* as an endophyte on *Citrus grandis* cv. "Tomentosa".

Colletotrichum magnum complex

Three of our isolates were initially recognised as belonging to the *Colletotrichum magnum* species complex. The phylogenetic analysis of combined *act*, *chs-1*, *gapdh*, *his3*, ITS and β-*tubulin* sequence alignment was conducted using 17 *Colletotrichum* strains.

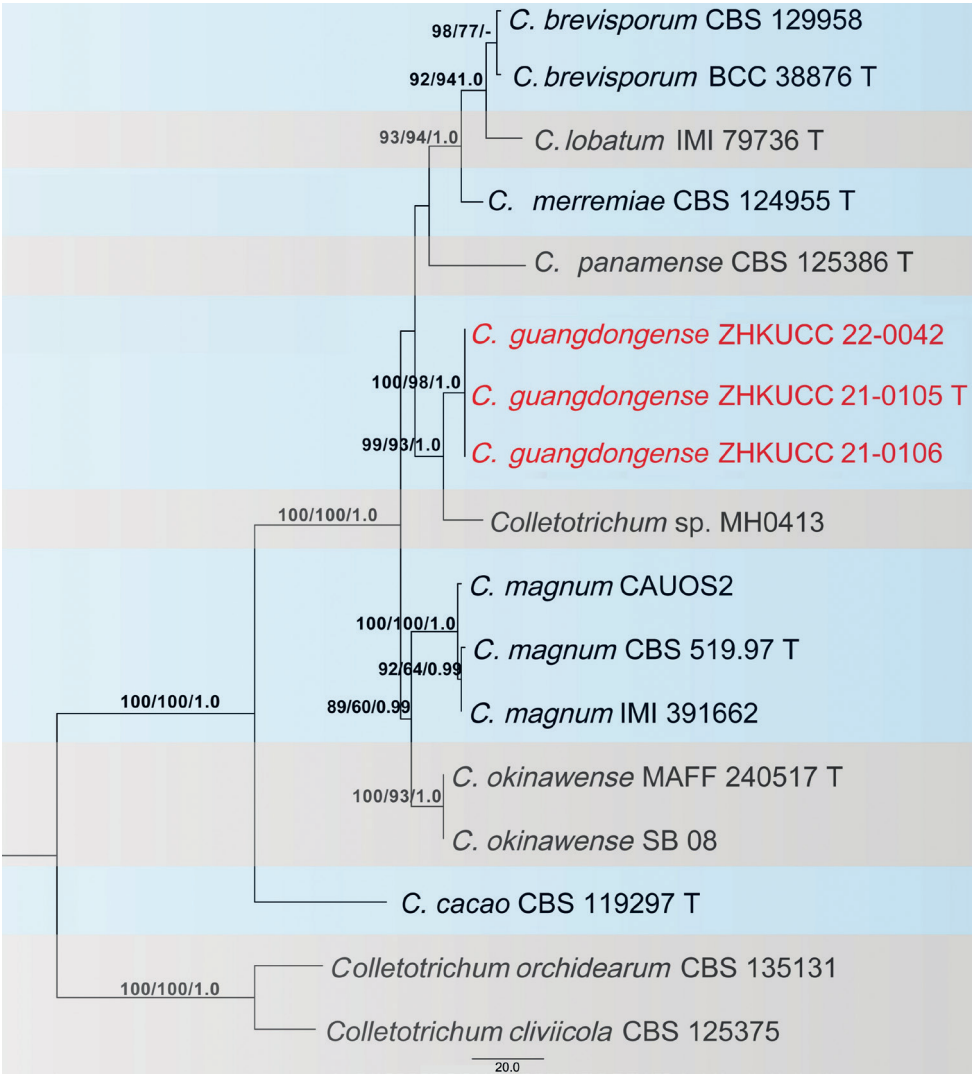

Figure 5. The most parsimonious tree of the *Colletotrichum magnum* complex using combined *act*, *chs-1*, *gapdh*, *his3*, ITS and β-*tubulin* sequences. *Colletotrichum cliviicola* and *C. orchidearum* were used as outgroup taxa. Bootstrap support values equal to or greater than 60% in MP and ML and BP equal to or greater than 0.95 are shown as MP/ML/BP above the respective nodes. The isolates of the novel taxon described in the current study are highlighted in red. Ex-type strains are noted with T.

Colletotrichum orchidearum (CBS 135131) and *C. cliviicola* (CBS 125375) were used as outgroup taxa. The best-scoring MP tree is given in Fig. 5. The dataset consisted of 2,296 characters with 2,013 constant characters and 196 parsimony-informative and 87 parsimony-uninformative characters. The maximum number of trees generated was 1,000 and the most parsimonious trees had a length of 350 steps (CI = 0.883, RI = 0.882, RC = 0.779, HI = 0.117). The final ML tree topology was similar to the MP and BP trees. The best-scoring ML tree had a –5198.901460 final likelihood

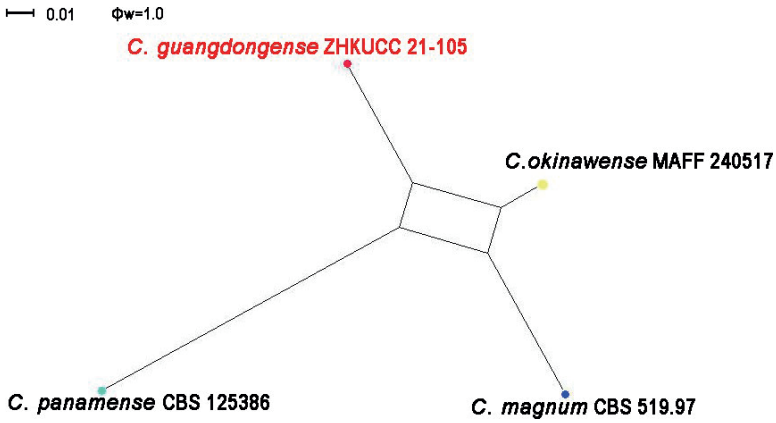

Figure 6. PHI analysis of combined *act*, *chs-1*, *gapdh*, *his3*, ITS and β-*tubulin* sequence data. A PHI test result (Φw) < 0.05 indicates significant recombination within the dataset.

value. The ML matrix comprised 258 distinct alignment patterns, with 6.18% undetermined characters or gaps. For the Bayesian Inference, the HKY model was selected for *act*, TIM2ef+G for *chs-1*, HKY+G for *gapdh*, TrN+G for *his3*, TIM1+I for ITS and TIM1+G for β-*tubulin*. In the phylogenetic analysis, isolates from this study developed to show the presence of an independent clade with high bootstrap and BP support. To confirm that these isolates belonged to novel species, the PHI index was calculated. The PHI test revealed no significant evidence for recombination (p = 1.0) amongst the taxon from this study and its closely-related taxa (Fig. 6).

Colletotrichum guangdongense **J.W. Liu, Manawas. & M. Luo, sp. nov.**
Index Fungorum Number: IF559483
Facesoffungi Number: FoF10693
Fig. 7

Etymology. The epithet refers to the Guangdong Province where the fungus was collected.

Holotype. ZHKUCC 21-0105

Description. Isolated from a *Citrus grandis* cv. "Tomentosa" twig. ***Sexual morph*****:** not observed. ***Asexual morph*****.** Conidiomata formed directly on hyphae, conidial masses abundant, coral. Setae pale to dark brown, smooth-walled, straight or flexuous, 2–4-septate, 60–136 µm long, basal cell cylindrical, 3.5–4.8 µm diam., tip more or less acute. Conidiophores 20–70 × 3–7 µm ($\bar{x}$ = 39.1 ± 10.7 × 4.7 ± 0.7 µm, n = 50), cylindrical, hyaline, smooth-walled, 1–4-celled, unbranched or branched at the base. Conidia 14–22 × 3–7 µm ($\bar{x}$ = 18.2 ± 1.6 × 4.9 ± 0.5 µm, n = 50), straight, hyaline and smooth-walled. Appressoria 7–12 × 5–10 µm ($\bar{x}$ = 10.2 ± 1.8 × 7.3 ± 0.9 µm, n = 50), single, medium brown, round, oval to irregular in outline.

Cultural characteristics. Colonies on PDA reach 65 mm diameter after seven days, with 8–11 mm/day ($\bar{x}$ = 10 mm, n = 6) growth rate. Colonies circular, slightly

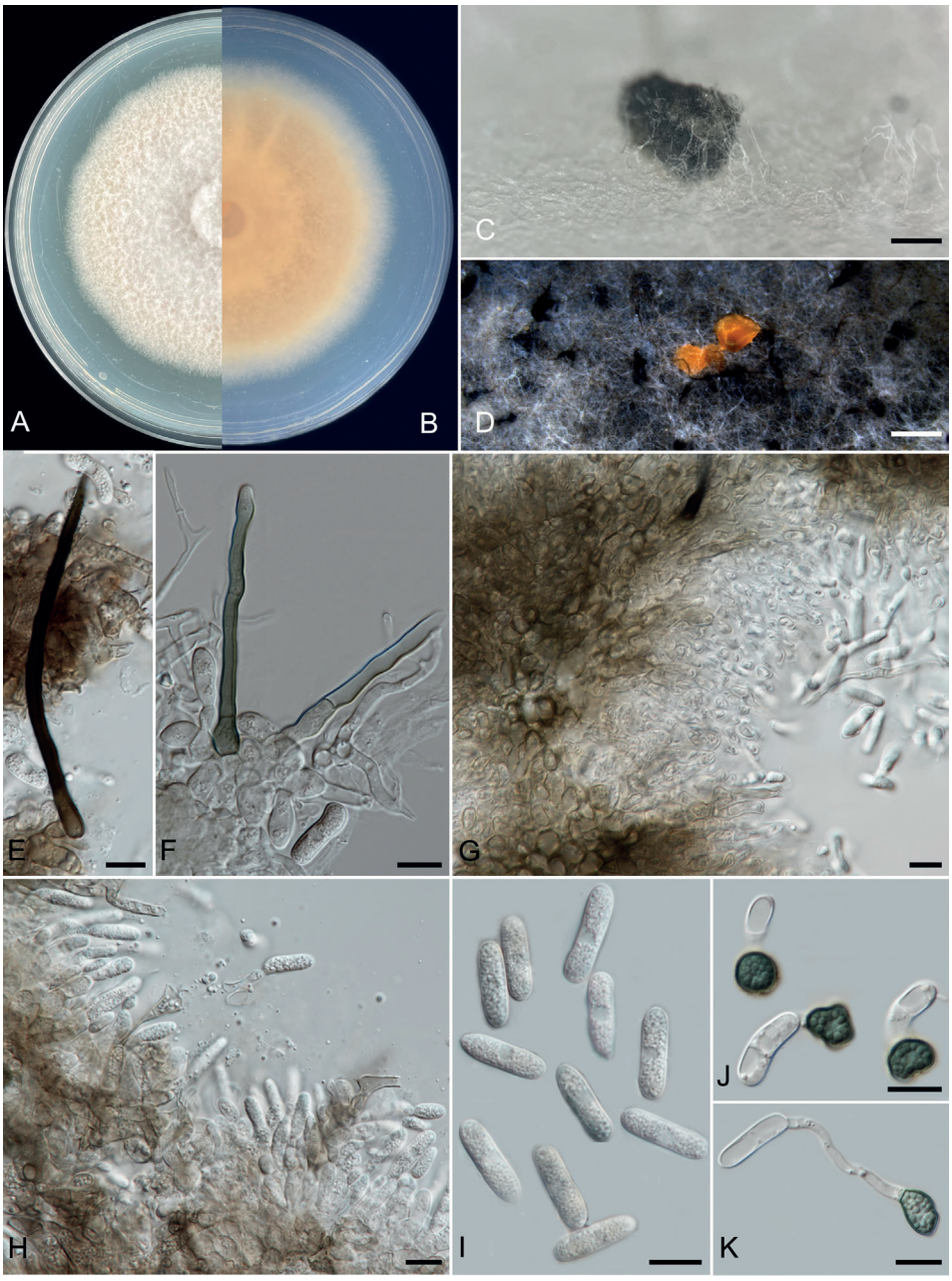

Figure 7. *Colletotrichum guangdongense* (ZHKUCC 21-0105, holotype) **A, B** upper and reverse sides of cultures on PDA seven days after inoculation **C, D** conidioma **E, F** setae **G, H** conidiophores **I** conidia **J, K** appressoria. Scale bars: 1 mm (**C, D**); 10 μm (**E–K**).

raised, flat, with pale coral red to light pink margin. Reverse dark vermillion to light ivory. Colonies on SNA flat, with entire margin, glaucous, reverse buff. Sporulates after 14 d on SNA.

Material examined. China, Guangdong Province, Huazhou, isolated from healthy twigs of *Citrus grandis* cv. "Tomentosa", May 2019, Y.X. Shu (dried cultures ZHKU 21-0089 ***holotype***); living cultures ZHKUCC 21-0105 (= CGMCC 3.24127) ex-type, ZHKUCC 21-0106 and ZHKUCC 22-0042 isotype).

Notes. In the phylogenetic analysis of combined *act*, *chs-1*, *gapdh*, *his3*, ITS and β-*tubulin* sequences, three isolates (ZHKUCC 21-0105, ZHKUCC 21-0106 and ZHKUCC 22-0042) obtained in this study developed a sister clade to *Colletotrichum* sp. MH0413 with 89% ML bootstrap, 60% MP bootstrap and 1.00 BP (Fig. 5). *Colletotrichum guangdongense* is also closely related to *C. magnum* (CBS 519.97) and *C. panamense* (CBS 125386). It can be distinguished from *C. magnum* (CBS 519.97) by having smaller conidia (10–20 × 4–6 μm vs. 17–24 × 3.5–5 μm) and longer conidiophores (20–70 μm vs. 20 μm) (Damm et al. 2019). *Colletotrichum panamense* (CBS 125386) has conidiophores shorter than *C. guangdongense* (30 μm vs. 20–70 μm). *Colletotrichum guangdongense* can be distinguished from *C. magnum* (CBS 519.97) also by 39 different nucleotides (4/538 in the ITS region, 9/204 in the *gapdh* region, 3/251 in the *chs-1* region, 9/235 *act*, 5/431 *tub2* and 9/403 *his3*) and from *C. panamense* (CBS 125386) by 39 different nucleotides (4/538 in the ITS region, 9/204 in the *gapdh* region, 3/251 in the *chs-1* region, 9/235 *act*, 2/431 *tub2* and 12/403 *his3*). The PHI test revealed no significant recombination event amongst *C. guangdongense* and its closely-related taxa (Fig. 6). Therefore, we have described this fungus as a novel species.

Discussion

In the present study, endophytic *Colletotrichum* species were isolated from *Citrus grandis* cv. "Tomentosa" in Guangdong Province, China. Guangdong Province has a mild subtropical monsoon climate with abundant rainfall and high average annual temperatures. Vigorous fruit trees provide suitable conditions for the colonisation of *Colletotrichum* species (Jayawardena et al. 2021). When the host is healthy, the endophyte has a symbiotic relationship with the host (Jayawardena et al. 2021). However, sometimes the interaction between the plant and the endophyte can switch from mutualistic to antagonistic or pathogenic (da Silva et al. 2020). Thus, the identification and characterisation of endophytic fungi are necessary. Based on the phylogenetic analysis using a combined seven loci (ITS, *gapdh*, *chs-1*, *act*, *his3*, *tub2* and *gs*), 12 isolates from this study were identified as being six distinct species within the three *Colletotrichum* species complexes (Figs 1, 4, 5). These results included two new species, namely *C. guangdongense*, *C. tomentosae* and three new host records for *C. asianum*, *C. plurivorum* and *C. tainanense*. *Colletotrichum siamense* has also been identified and described as being associated with *Citrus*. The present study has re-affirmed that more than one *Colletotrichum* species can colonise a single host, which is consistent with the conclusion of Damm et al. (2012).

Species belonging to the *C. gloeosporioides* complex were often found as endophytes (Damm et al. 2012; Weir et al. 2012; Jayawardena et al. 2016). Here, we identified seven strains representing four species as endophytes from the *C. gloeosporioides* complex. *Colletotrichum siamense* was previously reported as an epiphyte and an endophyte asso-

ciated with coffee berries in northern Thailand (Prihastuti et al. 2009) and tea plants in China (Liu et al. 2015). *Colletotrichum siamense* has also been reported as a pathogen of many plants (Liu et al. 2022). In the present study, this species was isolated from leaves. Liu et al. (2015) identified six species from symptomatic and asymptomatic leaf tissue, all of which belonged to the *C. gloeosporioides* species complex, namely *C. camelliae*, *C. fructicola*, *C. gloeosporioides*, *C. jiangxiense* and *C. siamense*, providing convincing evidence that these species could switch their lifestyle from endophytic to pathogenic. Therefore, further studies are necessary to understand the pathogenicity of these endophytic strains and the factors affecting these taxa becoming pathogenic on *Citrus*.

Colletotrichum species belonging to the *C. magnum* and *C. orchidearum* complexes were found on tropical or subtropical plants (Damm et al. 2019). It has been proposed that some of these species might be host- and region-specific (Damm et al. 2019). *Colletotrichum plurivorum* is widely distributed in several hosts and most of them are pathogens. This study is the first report of the species from *Citrus*. Here, we introduce a new taxon belonging to the *C. magnum* species complex. Whether it is host-specific or not needs further confirmation.

Endophytic fungal colonisation might vary in different tissues of the same plant (Taylor et al. 1999; Huang et al. 2015). Different fungal genera could have different tissue specificities and preferences. In the present study, endophytes were isolated from leaves and twigs. Additionally, there were higher numbers of *Colletotrichum* species from leaves in *Citrus* (Hakimeh et al. 2019) and some other plants like *Dendrobium* (Chen et al. 2011; Ma et al. 2018). Huang et al. (2015) and Dong et al. (2021) have observed that endophytic *Diaporthe* species are less abundant on leaves, whereas endophytic *Colletotrichum* species are abundantly isolated from the *Dendrobium* spp. leaves (Chen et al. 2011; Ma et al. 2018). These variations may be the result of differences in the tissue organisational structure, different nutrition contents of each tissue type or the lifestyle of each genus, locality or season (Zhou et al. 2014; Huang et al. 2015). To date, the reasons for these variations are not yet known.

Overall, in the present study, two novel endophytic *Colletotrichum* species have been described and illustrated. Our study is the first comprehensive study on endophytic *Colletotrichum* species associated with *Citrus grandis* cv. "Tomentosa". Moreover, our molecular data and novel species introduced in this study contribute to understanding the diversity and biology of the genus *Colletotrichum*. These results provide an important resource and basis for plant pathologists and fungal taxonomists. However, future studies are necessary to understand the lifestyle changes of the endophytic taxa towards the pathogenicity, as well as the effects of fungus-related medicinal properties of *Citrus grandis* cv. "Tomentosa".

Acknowledgements

We would like to thank Dr Shaun Pennycook, Nomenclature Editor of Mycotaxon, for his guidance on the species names. M. Luo would like to thank for the grant from the Guangdong Rural Science and Technology Commissioner project (KTP20210313)

and the Research Project of Innovative Institute for Plant Health (KA21031H101). Z.Y. Dong would like to thank the Key Realm R & D Program of Guangdong Province (2018B020205003). R.S. Jayawardena would like to thank Thailand Science Research and Innovation, grant number 652A01003 entitled 'Biodiversity, taxonomy, phylogeny and evolution of *Colletotrichum* on Avocado, *Citrus*, Durian and Mango in northern Thailand'. Ishara S Manawasinghe would like to thank the Research Project of the Innovative Institute for Plant Health (KA21031H101) and the project of the Zhongkai University of Agriculture and Engineering, Guangzhou, China (KA210319288).

References

Bhunjun CS, Phukhamsakda C, Jayawardena RS, Jeewon R, Promputtha I, Hyde KD (2021) Investigating species boundaries in *Colletotrichum*. Fungal Diversity 107(1): 107–127. https://doi.org/10.1007/s13225-021-00471-z

Bruen TC, Philippe H, Bryant D (2006) A simple and robust statistical test for detecting the presence of recombination. Genetics 172(4): 2665–2681. https://doi.org/10.1534/genetics.105.048975

Cai L, Hyde KD, Taylor P, Weir BS, Waller J, Abang MM, Zhang JZ, Yang YL, Phoulivong S, Liu ZY (2009) A polyphasic approach for studying *Colletotrichum*. Fungal Diversity 39: 183–204. https://fungaldiversity.org/fdp/sfdp/FD39-8.pdf

Carbone I, Kohn LM (1999) A method for designing primer sets for speciation studies in filamentous ascomycetes. Mycologia 91(3): 553–556. https://doi.org/10.1080/00275514.1999.12061051

Chen J, Hu KX, Hou XQ, Guo SX (2011) Endophytic fungi assemblages from 10 *Dendrobium* medicinal plants (*Orchidaceae*). World Journal of Microbiology & Biotechnology 27(5): 1009–1016. https://doi.org/10.1007/s11274-010-0544-y

Christy JS, Balraj A, Agarwal A (2020) A Rare Case of *Colletotrichum truncatum* keratitis in a young boy with complete healing after medical treatment. Indian Journal of Medical Microbiology 38(3–4): 475–477. https://doi.org/10.4103/ijmm.IJMM_20_146

Corda ACI (1831) Die Pilze Deutschlands. In: Sturm J (Ed.) Deutschlands Flora in Abbildungen nach der Natur mit Beschreibungen. Sturm, Nürnberg 3: 33–64.

Crous PW, Gams W, Stalpers JA, Robert V, Stegehuis G (2004) MycoBank: An online initiative to launch mycology into the 21st century. Studies in Mycology 50: 19–22. https://doi.org/10.1023/B:MYCO.0000012225.79969.29

da Silva LL, Moreno HLA, Correia HLN, Santana MF, de Queiroz MV (2020) *Colletotrichum*: Species complexes, lifestyle, and peculiarities of some sources of genetic variability. Applied Microbiology and Biotechnology 104(5): 1891–1904. https://doi.org/10.1007/s00253-020-10363-y

Dai HY, He D, Liu MZ (2017) Progress and trends on researches of taxol-producing endophytic fungi. Western Forestry Science 46: 169–187. [in Chinese]

Damm U, Cannon PF, Woudenberg JHC, Crous PW (2012) The *Colletotrichum acutatum* species complex. Studies in Mycology 73: 37–113. https://doi.org/10.3114/sim0010

Damm U, Sato T, Alizadeh A, Groenewald JZ, Crous PW (2019) The *Colletotrichum dracaenophilum*, *C. magnum* and *C. orchidearum* species complexes. Studies in Mycology 92(1): 1–46. https://doi.org/10.1016/j.simyco.2018.04.001

de Silva DD, Groenewald JZ, Crous PW, Ades PK, Nasruddin A, Mongkolporn O, Taylor PWJ (2019) Identification, prevalence and pathogenicity of *Colletotrichum* species causing anthracnose of *Capsicum annuum* in Asia. IMA Fungus 10(1): 1–8. https://doi.org/10.1186/s43008-019-0001-y

Dini-Andreote F (2020) Endophytes: the second layer of plant defense. Trends in Plant Science 25(4): 319–322. https://doi.org/10.1016/j.tplants.2020.01.007

Dong ZY, Manawasinghe IS, Huang YH, Shu YX, Phillips AJL, Dissanayake DJ, Hyde KD, Xiang MM, Luo M (2021) Endophytic *Diaporthe* associated with *Citrus grandis* cv. Tomentosa in China. Frontiers in Microbiology 11: e609387. https://doi.org/10.3389/fmicb.2020.609387

Farr DF, Rossman AY (2022) Fungal Databases. U.S. National Fungus Collections, ARS, USDA. https://nt.ars-grin.gov/fungaldatabases/

Glass NL, Donaldson GC (1995) Development of primer sets designed for use with the PCR to amplify conserved genes from filamentous ascomycetes. Applied and Environmental Microbiology 61(4): 1323–1330. https://doi.org/10.1128/aem.61.4.1323-1330.1995

Guarnaccia V, Groenewald JZ, Polizzi G, Crous PW (2017) High species diversity in *Colletotrichum* associated with *Citrus* diseases in Europe. Persoonia 39(1): 32–50. https://doi.org/10.3767/persoonia.2017.39.02

Guerber JC, Liu B, Correll JC, Johnston PR (2003) Characterization of diversity in *Colletotrichum acutatum* sensu lato by sequence analysis of two gene introns, mtDNA and intron RFLPs, and mating compatibility. Mycologia 95(5): 872–895. https://doi.org/10.1080/15572536.2004.11833047

Hacquard T, Kracher B, Hiruma K, Munch PC, Garrido-Oter G, Thon MR, Weimann A, Damm U, Dallery JF, Hainaut M, Henrissat B, Lespinet O, Sacristan S, Themaat EVL, Kemen E, McHardy AC, Schulze-Lefert P, O'Connell RJ (2016) Survival trade-offs in plant roots during colonization by closely related beneficial and pathogenic fungi. Nature Communications 7(1): e11362. https://doi.org/10.1038/ncomms11362

Hakimeh ZJ, Mohammad ATG, Heshmat R, Kaivan K (2019) Seasonal, tissue and age influences on frequency and biodiversity of endophytic fungi of *Citrus sinensis* in Iran. Forest Pathology 49(6): e12559. https://doi.org/10.1111/efp.12559

Hall T (2006) Bioedit. Raleigh, NC: Department of Microbiology, North Carolina State University. http://www.mbio.ncsu.edu/BioEdit/page2.html

Hasan AEZ, Julistiono H, Bermawie N, Riyanti EI, Arifni FR (2022) Soursop leaves (*Annona muricata* L.) endophytic fungi anticancer activity against HeLa cells. Saudi Journal of Biological Sciences 29(8): e103354. https://doi.org/10.1016/j.sjbs.2022.103354

Huang F, Chen GQ, Hou X, Fu YS, Cai L, Hyde KD, Li HY (2013) *Colletotrichum* species associated with cultivated *Citrus* in China. Fungal Diversity 61(1): 61–74. https://doi.org/10.1007/s13225-013-0232-y

Huang F, Udayanga D, Wang XH, Hou X, Mei XF, Fu YS, Hyde KD, Li HY (2015) Endophytic *Diaporthe* associated with *Citrus*: A phylogenetic reassessment with seven new species from China. Fungal Biology 119(5): 331–347. https://doi.org/10.1016/j.funbio.2015.02.006

Jayasiri SC, Hyde KD, Ariyawansa HA, Bhat J, Buyck B, Cai L, Dai YC, Abd-Elsalam KA, Ertz D, Hidayat I, Jeeon R, Gareth Jones EB, Bahkali AH, Karunarathna SC, Liu JK, Luangsa-ard JJ, Lumbsch HT, Maharachchikumbura S, McKenzie EHC, Moncalvo JM, Ghobad-Nejhad M, Nilsson H, Pang KL, Pereira OL, Phillips A, Raspe O, Rollins AW, Romero AI, Etayo J, Sulcuk

F, Stephenson S, Suetrong S, Taylor JE, Tsui C, Boonmee S, Dai D, Daranagama D, Dissanayake A, Ekanayaka A, Fryar S, Hongsanan S, Jayawardena R, Li W-J, Perera R, Phookamsak R, de Silva N, Thambugala K, Tian Q, Wijayawardene N, Zhao RL, Zhao Q, Kang JC, Promputtha I (2015) The faces of fungi database: fungal names linked with morphology, phylogeny and human impacts. Fungal Diversity 74(1): 3–18. https://doi.org/10.1007/s13225-015-0351-8

Jayawardena RS, Hyde KD, Damm U, Cai L, Liu M, Li XH, Zhang W, Zhao W, Yan J (2016) Notes on currently accepted species of *Colletotrichum*. Mycosphere: Journal of Fungal Biology 7(8): 1192–1260. https://doi.org/10.5943/mycosphere/si/2c/9

Jayawardena RS, Bhunjun CS, Gentekaki E, Hyde KD, Promputtha I (2021) *Colletotrichum*: Lifestyles, biology, morpho-species, species complexes and accepted species. Mycosphere: Journal of Fungal Biology 12(1): 519–669. https://doi.org/10.5943/mycosphere/12/1/7

Johnston PR, Jones D (1997) Relationships among *Colletotrichum* isolates from fruit-rots assessed using rDNA sequences. Mycologia 89(3): 420–430. https://doi.org/10.1080/00275514.1997.12026801

Katoh R, Rozewicki J, Yamada KD (2019) MAFFT online service: Multiple sequence alignment, interactive sequence choice and visualization. Briefings in Bioinformatics 20(4): 1160–1166. https://doi.org/10.1093/bib/bbx108

Kishino H, Hasegawa M (1989) Evaluation of the maximum likelihood estimate of the evolutionary tree topologies from DNA sequence data, and the branching order in *Homeinoidea*. Journal of Molecular Evolution 29(2): 170–179. https://doi.org/10.1007/BF02100115

Liu F, Weir BS, Damm U, Crous PW, Wang Y, Liu B, Wang M, Zhang M, Cai L (2015) Unravelling *Colletotrichum* species associated with *Camellia*, employing *apmat* and *gs* loci to resolve species in the *C. gloeosporioides* complex. Persoonia 35(1): 63–86. https://doi.org/10.3767/003158515X687597

Liu F, Ma ZY, Hou LW, Diao YZ, Wu WP, Damm U, Song S, Cai L (2022) Updating species diversity of *Colletotrichum*, with a phylogenomic overview. Studies in Mycology 101(1): 1–56. https://doi.org/10.3114/sim.2022.101.01

Ma X, Nontachaiyapoom S, Jayawardena RS, Hyde KD, Gentekaki E, Zhou S, Qian YX, Wen TC, Kang JC (2018) Endophytic *Colletotrichum* species from *Dendrobium* spp. in China and Northern Thailand. MycoKeys 43: 23–57. https://doi.org/10.3897/mycokeys.43.25081

Miller MA, Pfeiffer W, Schwartz T (2010) Creating the CIPRES Science Gateway for inference of large phylogenetic trees, in Proceedings of the Gateway Computing Environments Workshop (GCE) 14 Nov 2010. Institute of Electrical and Electronics Engineers, New Orleans. https://doi.org/10.1109/GCE.2010.5676129

Nylander JAA (2004) MrModeltest 2.0. Program distributed by the author. Uppsala, Sweden: Evolutionary Biology Centre Uppsala University. http://www.abc.se/~nylander/mrmodeltest2/mrmodeltest2.html

Peng Y, Hu MJ, Lu Q, Tian Y, He WY, Chen L, Pan SY (2019) Flavonoids derived from *Exocarpium* Citri Grandis inhibit LPS-induced inflammatory response via suppressing MAPK and NF-kB signalling pathways. Food and Agricultural Immunology 30: 564–580. https://doi.org/10.1080/09540105.2018.1550056

Photita W, Lumyong S, Lumyong P, McKenzie EHC, Hyde KD (2004) Are some endophytes of *Musa acuminata* latent pathogens? Fungal Diversity 16: 131–140. https://www.fungaldiversity.org/fdp/sfdp/16-4.pdf

Prihastuti H, Cai L, Chen H, McKenzie EHC, Hyde KD (2009) Characterization of *Colletotrichum* species associated with coffee berries in northern Thailand. Fungal Diversity 39: 89–109. https://doi.org/10.1016/j.riam.2009.11.001

Ronquist F, Huelsenbeck JP (2003) MrBayes 3: Bayesian phylogenetic inference under mixed models. Bioinformatics 19(12): 1572–1574. https://doi.org/10.1093/bioinformatics/btg180

Silvestro D, Michalak I (2010) RaxmlGUI: a Graphical Front-End for RAxML. https://doi.org/10.1007/s13127-011-0056-0 [Accessed June 2, 2022]

Stamatakis A (2014) RAxML version 8: A tool for phylogenetic analysis and post-analysis of large phylogenies. Bioinformatics 30(9): 1312–1313. https://doi.org/10.1093/bioinformatics/btu033

Sun LF, Zhang YH, Pei KQ (2009) A rapid extraction of genomic DNA from fungi. Mycosystema 28: 299–302. [In Chinese]

Swofford DL (2002) PAUP: Phylogenetic Analysis Using Parsimony (and Other Methods) Version 4.0b10. Sinauer Associates, Sunderland. https://doi.org/10.1111/j.0014-3820.2002.tb00191.x

Taylor JE, Hyde KD, Jones EBG (1999) Endophytic fungi associated with the temperate palm, *Trachycarpus fortunei*, within and outside its natural geographic range. The New Phytologist 142(2): 335–346. https://doi.org/10.1046/j.1469-8137.1999.00391.x

Udayanga D, Manamgoda DS, Liu X, Chukeatirote E, Hyde KD (2013) What are the common anthracnose pathogens of tropical fruits? Fungal Diversity 61(1): 165–179. https://doi.org/10.1007/s13225-013-0257-2

Weir BS, Johnston PR, Damm U (2012) The *Colletotrichum gloeosporioides* species complex. Studies in Mycology 73: 115–180. https://doi.org/10.3114/sim0011

White TJ, Bruns T, Lee S, Taylor JW (1990) Amplification and direct sequencing of fungal ribosomal RNA genes for phylogenetics. PCR protocols: a guide to methods and applications 18. Academic Press, San Diego, 315–322. https://doi.org/10.1016/B978-0-12-372180-8.50042-1

Zhang D, Gao F, Jakovlić I, Zou H, Zhang J, Li WX, Wang GT (2020) PhyloSuite: An integrated and scalable desktop platform for streamlined molecular sequence data management and evolutionary phylogenetics studies. Molecular Ecology Resources 20(1): 348–355. https://doi.org/10.1111/1755-0998.13096

Zhao Y, Kao CP, Liao KC, Zhou X, Ho YL, Chang YS (2017) Chemical compositions, chromatographic fingerprints and antioxidant activities of Citri Exocarpium Rubrum (Juhong). Chinese Medicine 12: 1–6. https://doi.org/10.1186/s13020-017-0127-z

Zhou CR, Huang J, Li ZE, Li SB (2014) Diversity and tissue distribution of fungal endophytes in: An important south-China medicinal plant. China journal of Chinese materia medica 39: 3023–3029. https://doi.org/10.4268/cjcmm20141605

Appendix 1

Table A1. Fungal isolates and sequences of molecular marker used in *Colletotrichum* phylogenetic analysis.

Species	Culture	Type	Genbank accession number						
			ITS	*gapdh*	*chs-1*	*his3*	*act*	*tub2*	*gs*
C. gloeosporioides complex									
C. aenigma	ICMP 18608	Holotype	JX010244	JX010044	JX009774	-	JX009443	JX010389	JX010078
	ICMP 18686		JX010243	JX009913	JX009789	-	JX009519	JX010390	JX010079
C. aeschynomenes	ICMP 17673	Holotype	JX010176	JX009930	JX009799	-	JX009483	JX010392	JX009799
C. alatae	ICMP 17919	Holotype	JX010190	JX009990	JX009837	-	JX009471	JX010383	JX010065
C. alienum	ICMP 12071	Holotype	JX010251	JX010028	JX009882	-	JX009572	JX010411	JX010101
	ICMP 18621		JX010246	JX009959	JX009755	-	JX009552	JX010386	JX010075
C. aotearoa	ICMP 18537	Holotype	JX010205	JX010005	JX009853	-	JX009854	JX010420	JX010113
C. arecicola	CGMCC 3.19667	Holotype	NR171191	-	-	-	-	-	-
C. artocarpicola	MFLUCC 181167	Holotype	MN415991	-	-	-	-	-	-
C. asianum	ICMP 18580	Holotype	JX010196	JX010053	JX009867	-	JX009584	JX010406	JX010096
	ICMP 18696		JX010192	JX009915	JX009753	-	JX009576	JX010384	JX010073
	ZHKUCC 21-0095		OL708418	OL855857	OL855867	-	OL855877	OL855883	-
C. boninense	ICMP 17904		JX010292	JX009905	JX009827	-	JX009583	-	-
C. camelliae	CGMCC3 14925	Holotype	KJ955081	KJ954782	MZ799255	-	KJ954363	KJ955230	KJ954932
C. changpingense	MFLUCC 150022	Holotype	KP683152	KP852469	KP852449	-	KP683093	KP852490	-
C. chrysophilum	CMM 4268	Holotype	KX094252	KX094183	KX094083	-	KX093982	KX094285	KX094204
C. cigarro	ICMP 18539	Holotype	JX010230	JX009966	-	-	JX009523	-	-
C. clidemiae	ICMP 18658	Holotype	JX010265	JX009989	JX009877	-	JX009537	JX010438	JX010129
C. cobbittiense	BRIP 66219	Holotype	NR_163538	MH094133	MH094135	-	MH094134	MH094137	-
C. conoides	CAUG17	Holotype	KP890168	KP890162	KP890156	-	KP890144	KP890174	-
C. cordylinicola	ICMP 18579	Holotype	JX010226	JX009975	JX009864	-	JX009586	JX010440	JX010122
	LC0856		HM470246	HM470240	-	-	HM470234	HM470249	HM470243
C. endophytica	CAUG28		KP145441	KP145413	KP145385	-	KP145329	KP145469	-
	MFLUCC 13-0418	Holotype	KC633854	KC832854	-	-	KF306258	-	-
C. fructicola	LF130		KJ955083	KJ954784	-	-	KJ954365	KJ955232	-
	CPC:28644		MH728811	MH707465	MH805851	-	MH781481	MH846564	-
	CPC:28645		MH728810	MH707466	MH805852	-	MH781482	MH846565	-
	CPC:30253		MH728817	MH707463	MH805846	-	MH781476	MH846559	-
	UOM 1138		MH728808	MH707468	MH805854	-	MH781484	MH846567	-

Species	Culture	Type	Genbank accession number						
			ITS	*gapdh*	*chs-1*	*his3*	*act*	*tub2*	*gs*
C. fructicola	ICMP 18581	Holotype	JX010165	JX010033	JX009866	-	JX009501	JX010405	JX010095
C. fructivorum	CBS 133125	Holotype	JX145145	MZ664047	MZ799259	-	MZ664126	JX145196	-
C. gloeosporioides	IMI 356878		JX010152	JX010056	JX009818	-	JX009531	JX010445	JX010085
C. grevilleae	CBS 132879	Holotype	KC297078	KC297010	KC296987	-	KC296941	KC297102	KC297033
C. grossum	CAUG7	Holotype	KP890165	KP890159	KP890153	-	KP890141	KP890171	-
C. hebeiense	MFLUCC 13-0726	Holotype	KF156863	KF377495	KF289008	-	KF377532	KF288975	-
C. hederiicola	MFLU 150689	Holotype	MN631384	-	MN635794	-	MN635795	-	-
C. helleniense	CPC:26844		KY856446	KY856270	KY856186	-	KY856019	KY856528	-
C. henanense	CGMCC 3.17354	Holotype	KJ955109	KJ954810	MZ799256	-	KM023257	KJ955257	KJ954960
C. hippeastri	ICMP 17920		JX010293	JX009932	JX009838	-	JX009485	-	-
C. horii	NBRC 7478	Holotype	GQ329690	GQ329681	JX009752	-	JX009438	JX010450	JN937000
C. hystricis	CBS 142411	Holotype	KY856450	KY856274	KY856190	-	KY856023	KY856532	-
C. jiangxiense	CGMCC 3.17363	Holotype	KJ955201	KJ954902	-	-	KJ954471	KJ955348	KJ955051
C. kahawae	ICMP 17816		JX010231	JX010012	JX009813	-	JX009452	JX010444	JX010130
C. makassarense	CPC:28612	Holotype	MH728812	MH728820	MH805850	-	MH781480	MH846563	MH748264
	CPC:28555		MH728816	MH728822	MH805847	-	MH781477	MH846560	MH748261
	CPC:28556		MH728815	MH728821	MH805848	-	MH781478	MH846561	MH748262
C. musae	CBS:116870	Holotype	JX010146	JX010050	JX009896	-	JX009433	HQ596280	JX010103
	CMM 4458		KX094249	KX094191	KX094080	-	KX093967	KX094292	KX094234
C. nupharicola	CBS 470.96	Holotype	JX010187	JX009972	JX009835	-	JX009437	JX010398	-
	CBS 469.96		JX010189	JX009936	JX009834	-	JX009486	JX010397	-
C. pandanicola	MFLUCC 170571	Holotype	MG646967	MG646934	MG646931	-	MG646938	MG646926	-
C. perseae	GA100	Holotype	KX620308	KX620242	-	-	KX620145	KX620341	KX620275
C. proteae	CBS 132882	Holotype	KC297079	KC297009	KC296986	-	KC296940	KC297101	KC297032
C. pseudotheobromicola	MFLUCC 181602	Holotype	MH817395	MH853675	MH853678	-	MH853681	MH853684	-
C. psidii	CBS 145.29	Holotype	JX010219	JX009967	JX009901	-	JX009515	JX010443	JX010133
C. queenslandicum	ICMP 1778	Holotype	JX010276	JX009934	JX009899	-	JX009447	JX010414	JX010104
	ICMP 18705		JX010185	JX010036	JX009890	-	JX009490	JX010412	JX010102
C. rhexiae	CBS 133134	Holotype	NR_144797	MZ664046	MZ799258	-	MZ664127	-	-
C. salsolae	ICMP 19051	Holotype	JX010242	JX009916	JX009863	-	JX009562	JX010403	JX010093
	CBS 119296		JX010241	JX009917	JX009791	-	JX009559	-	-
C. siamense	ICMP 18578	Holotype	JX010171	JX009924	JX009865	-	FJ907423	JX010404	JX010094
	CPC:30210		MH707472	MH707453	MH805835	-	MH781465	MH846548	MH748232

Species	Culture	Type	Genbank accession number						
			ITS	*gapdh*	*chs-1*	*his3*	*act*	*tub2*	*gs*
C. siamense	CPC:30211		MH707473	MH707454	MH805836	-	MH781466	MH846549	MH748233
	CPC:30212		MH707474	MH707455	MH805837	-	MH781467	MH846550	MH748234
	CPC:30221		MH707475	MH707456	MH805838	-	MH781468	MH846551	MH748235
	CPC:30209		MH707471	MH707452	MH805834	-	MH781464	MH846547	MH748231
	ZHKUCC 21-0096		OL708414	OL855849	OL855859	-	OL855869	OL855879	-
	ZHKUCC 21-0097		OL708424	OL855852	OL855862	-	OL855872	OL855881	-
	ZHKUCC 21-0098		OL708423	OL855851	OL855861	-	OL855871	OL855880	-
C. syzygicola	DNCL021	Holotype	KF242094	KF242156	-	-	KF157801	KF254880	KF242125
	DNCL028		KF242095	KF242157	-	-	KF157802	KF254881	KF242126
	DNCL018		KF242093	KF242155	-	-	KF157800	KF254879	KF242124
C. tainanense	CBS 143666	Holotype	MH728818	MH728823	MH805845	-	MH781475	MH846558	MH748259
	UOM 1119		MH728805	MH728819	MH805857	-	MH781487	MH846570	-
	ZHKUCC 21-0101		OL708421	OL855858	OL855868	-	OL855878	OL855884	-
C. temperatum	CBS 133122	Holotype	MH877532	MZ664045	MZ799254	-	MZ664125	-	-
C. theobromicola	CBS 124945	Holotype	JX010294	JX010006	JX009869	-	JX009444	JX010447	JX010139
C. ti	ICMP 4832	Holotype	JX010269	JX009952	JX009898	-	JX009520	JX010442	JX010123
	ICMP 5285		JX010267	JX009910	JX009897	-	JX009553	JX010441	JX010124
C. tomentosae	ZHKUCC 21-0103 CGMCC 3.24128 Dry culture: ZHKU 21-0088	Holotype	OL708422	OL855850	OL855860	-	OL855870	OL855887	ON315373
	ZHKUCC 21-0104		OL708419	OL855856	OL855866	-	OL855873	OL855888	ON315374
	ZHKUCC 22-0041		ON303476	ON315382	ON315376	-	ON315380	ON315378	ON315375
C. tropicale	CBS 124946		KC566806	KC566660	KC566373	-	KC566952	KC566228	-
	CBS 124943		JX010277	JX010014	JX009868	-	JX009570	-	-
	CBS 124949	Holotype	JX010264	JX010007	JX009870	-	JX009489	JX010407	JX010097
C. viniferum	GZAAS 5.08601	Holotype	JN412804	JN412798	-	-	JN412795	JN412813	-
C. wuxiense	CGMCC 3.17894	Holotype	KU251591	KU252045	KU251939	-	KU251672	KU252200	KU252101
C. xanthorrhoeae	BRIP 45094	Holotype	JX010261	JX009927	JX009823	-	JX009478	JX010448	JX010138
C. yulongense	CFCC 50818	Holotype	MH751507	MK108986	MH793605	-	MH777394	MK108987	MK108988
			C. magnum complex						
C. brevisporum	BCC 38876	Holotype	JN050238	JN050227	MZ799287	MZ673841	JN050216	JN050244	-
	CBS 129958		MG600763	MG600823	MG600870	MG600909	MG600967	MG601030	-
C. cacao	CBS 119297	Holotype	MG600772	MG600832	MG600878	MG600916	MG600976	MG601039	-
C. cliviicola	CBS 125375		MG600733	MG600795	MG600850	MG600892	MG600939	MG601000	-

Species	Culture	Type	Genbank accession number						
			ITS	*gapdh*	*chs-1*	*his3*	*act*	*tub2*	*gs*
C. guangdongense	ZHKUCC 21-0105 CGMCC 3.24127 Dry culture: ZHKU 21-0089	Holotype	OL708415	OL855854	OL855864	ON315370	OL855875	OL855885	-
	ZHKUCC 21-0106		OL708420	OL855855	OL855865	ON315371	OL855876	OL855886	-
	ZHKUCC 22-0042		ON303474	ON315383	ON315377	ON315372	ON315381	ON315379	-
C. lobatum	IMI79736	Holotype	MG600828	MG600874	MG600912	MG600972	MG600972	MG601035	-
C. magnum	CBS519.97	Holotype	MG600769	MG600829	MG600875	MG600913	MG600973	MG601036	-
	IMI391662		MG600771	MG600831	MG600877	MG600915	MG600975	MG601038	-
	CAUOS2		MZ595839	MZ848400	OK236385	MZ673858	OK236387	MZ673960	-
C. merremiae	CBS124955	Holotype	MG600765	MG600825	MG600872	MG600910	MG600969	MG601032	-
C. okinawense	MAFF240517	Holotype	MG600767	MG600827	-	-	MG600971	MG601034	-
	SB 08		MK830706	MK820658	-	MK820660	MK820659	-	-
C. orchidearum	CBS135131		MG600738	MG600800	MG600855	MG600897	MG600944	MG601005	-
C. panamense	CBS125386	Holotype	MG600766	MG600826	MG600873	MG600911	MG600970	MG601033	-
Colletotrichum sp.	MH0413		MZ595871	MZ664109	MZ799289	MZ673891	MZ664169	MZ673990	-
			C. orchidearum complex						
C. brevisporum	BCC 38876		JN050238	JN050227	MZ799287	MZ673841	JN050216	JN050244	-
C. cattleyicola	CBS 170.49	Holotype	MG600758	MG600819	MG600866	MG600905	MG600963	MG601025	-
	MAFF 238321		MG600759	-	-	-	-	MG601026	-
C. cliviicola	CBS 133705		MG600732	MG600794	MG600849	MG600891	MG600938	MG600999	-
	CBS 125375	Holotype	MG600733	MG600795	MG600850	MG600892	MG600939	MG601000	-
C. magnum	CBS519.97		MG600769	MG600829	MG600875	MG600913	MG600973	MG601036	-
C. monsteriae	LC13871	Holotype	MZ595897	MZ664121	MZ799351	MZ673917	MZ664195	MZ674015	-
C. musicola	CBS132885	Holotype	MG600736	MG600798	MG600853	MG600895	MG600942	MG601003	-
	CBS127557		MG600737	MG600799	MG600854	MG600896	MG600943	MG601004	-
C. orchidearum	CBS135131	Holotype	MG600738	MG600800	MG600855	MG600897	MG600944	MG601005	-
	CBS136877		MG600739	MG600801	MG600856	MG600898	MG600945	MG601006	-
C. piperis	IMI71397	Holotype	MG600760	MG600820	MG600867	MG600906	MG600964	MG601027	-
C. plurivorum	CBS125474	Holotype	MG600718	MG600781	MG600841	MG600887	MG600925	MG600985	-
	CBS132443		MG600719	MG600782	MG600842	MG600888	MG600926	MG600986	-
	LC8240		MZ595848	MZ664113	MZ799291	MZ673868	MZ664146	MZ673969	-
	LC8244		MZ595849	MZ772868	MZ799292	MZ673869	MZ664147	MZ673970	-
	LC8322		MZ595853	MZ664114	MZ799293	MZ673873	MZ664151	MZ673974	-
	LC8337		MZ595855	MZ664115	MZ799294	MZ673875	MZ664153	MZ673976	-
	ZHKUCC 21-0102		OL708416	OL855874	OL855863	-	OL855853	OL855882	-

Species	Culture	Type	Genbank accession number						
			ITS	*gapdh*	*chs-1*	*his3*	*act*	*tub2*	*gs*
C. reniforme	LC8230	Holotype	MZ595847	MZ664110	MZ799290	MZ673867	MZ664145	MZ673968	-
	LC8248		MZ595850	MZ664111	MZ799295	MZ673870	MZ664148	MZ673971	-
C. sojae	ATCC62257	Holotype	MG600749	MG600810	MG600860	MG600899	MG600954	MG601016	-
	CBS128510		MG600751	MG600812	MG600862	MG600901	MG600956	MG601018	-
	LC8335		MZ595854	MZ664112	MZ799300	MZ673874	MZ664152	MZ673975	-
	LC8492		MZ595858	MZ664116	MZ799301	MZ673878	MZ664156	MZ673979	-
C. syngoniicola	LC8894	Holotype	MZ595863	MZ664117	MZ799296	MZ673883	MZ664161	MZ673982	-
	LC8895		MZ595864	MZ664118	MZ799297	MZ673884	MZ664162	MZ673983	-
	LC8896		MZ595865	MZ664119	MZ799298	MZ673885	MZ664163	MZ673984	-
C. vittalense	CBS126.25		MG600735	MG600797	MG600852	MG600894	MG600941	MG601002	-
	CBS181.82	Holotype	MG600734	MG600796	MG600851	MG600893	MG600940	MG601001	-

MycoKeys 95: 189–207 (2023)
doi: 10.3897/mycokeys.95.100414
https://mycokeys.pensoft.net

RESEARCH ARTICLE

A peer-reviewed open-access journal
MycoKeys
Launched to accelerate biodiversity research

Multi-gene phylogeny and morphology of two new *Phyllosticta* (Phyllostictaceae, Botryosphaeriales) species from China

Cheng-Bin Wang[1], Jing Yang[2], Yong Li[1], Han Xue[1], Chun-Gen Piao[1], Ning Jiang[1]

1 *Key Laboratory of Biodiversity Conservation of National Forestry and Grassland Administration, Ecology and Nature Conservation Institute, Chinese Academy of Forestry, Beijing 100091, China* **2** *Natural Resources and Planning Bureau of Rizhao City, Rizhao 276827, China*

Corresponding author: Ning Jiang (n.jiang@caf.ac.cn)

Academic editor: C. Bhunjun | Received 11 January 2023 | Accepted 21 February 2023 | Published 1 March 2023

Citation: Wang C-B, Yang J, Li Y, Xue H, Piao C-G, Jiang N (2023) Multi-gene phylogeny and morphology of two new *Phyllosticta* (Phyllostictaceae, Botryosphaeriales) species from China. MycoKeys 95: 189–207. https://doi.org/10.3897/mycokeys.95.100414

Abstract

Phyllosticta (Phyllostictaceae, Botryosphaeriales) includes plant pathogens, endophytes and saprobes, occurring on various hosts worldwide. During the present study, isolates associated with leaf spots were obtained from the hosts *Quercus aliena* and *Viburnum odoratissimum*, and identified based on morphological features and phylogenetic inference from the analyses of five loci (ITS, LSU, *tef1*, *act* and *gapdh*). Results supported the introduction of two novel species, namely *Phyllosticta anhuiensis* and *P. guangdongensis*. Phylogenetically, *P. anhuiensis* and *P. guangdongensis* formed two well-separated lineages in the *P. concentrica* and *P. capitalensis* species complexes, distinguishing from all presently accepted species in this genus by DNA sequence data. Morphologically, *P. anhuiensis* and *P. guangdongensis* have the typical structure of the genus *Phyllosticta*, and differed from their closely related species by the length of the conidial appendage.

Keywords

Ascomycota, morphology, new species, phylogeny, plant disease, taxonomy

Introduction

The genus *Phyllosticta* was established by Persoon (1818) and classified in Phyllostictaceae (Botryosphaeriales) (Phillips et al. 2019; Wijayawardene et al. 2020). Initially, *Phyllosticta* was placed in the Phyllostictaceae (Fries 1849). In a multi-

locus phylogeny in the Dothideomycetes, Schoch et al. (2006) placed *Phyllosticta* into Botryosphaeriaceae (Botryosphaeriales), which was agreed upon by Crous et al. (2006) and Liu et al. (2012). Subsequently, Slippers et al. (2013) reinstated the Phyllostictaceae to accommodate *Phyllosticta* in terms of phylogenetic relationships. Recently, *Pseudofusicoccum* was added in this family based on the morphological characters of the conidia covered by a mucous sheath and molecular evidence (Phillips et al. 2019). The asexual morph of *Phyllosticta* is characterized by pycnidial conidiomata containing aseptate conidia surrounding with a mucoid layer and bearing a single apical appendage (van der Aa 1973; van der Aa and Vanev 2002; Wikee et al. 2011). The sexual morph of *Phyllosticta* is characterized by erumpent ascomata, 8-spored, clavate to broadly ellipsoid asci, ellipsoid to limoniform ascospores (van der Aa 1973; Wikee et al. 2011). Following the implementation of "one fungus one name" nomenclature rules, the name *Phyllosticta* (asexual state) was used over *Guignardia* (sexual state) and *Leptodothiorella* (spermatial state) (Glienke et al. 2011; Wikee et al. 2011).

The *Phyllosticta* species identification solely delimited by morphology and host association may be difficult to assess (Wikee et al. 2011; Su and Cai 2012). Many species are difficult to distinguish due to slight morphological variation, and the mucoid layer or appendage will be absent or invisible in some species (van der Aa and Vanev 2002; Jin 2011; Wikee et al. 2011). Besides, the host range of *Phyllosticta* is unclear; some species exhibit the broadest host range while others do not (Wikee et al. 2011; Rashmi et al. 2019; Norphanphoun et al. 2020). To overcome the lack of morphological features and host range, phylogenetic approaches based on molecular loci were used to resolve the classification and identification of *Phyllosticta* species (Baayen et al. 2002; Wulandari et al. 2009; Wong et al. 2012; Wikee et al. 2013a). Based on the phylogenetic analyses of a combined ITS, LSU, *tef1*, *act* and *gapdh* sequence data, the current taxonomic classification of *Phyllosticta* comprises six species complexes i.e., *P. capitalensis*, *P. concentrica*, *P. cruenta*, *P. owaniana*, *P. rhodorae* and *P. vaccinii* species complexes (Norphanphoun et al. 2020). Currently, the polyphasic approach involving phylogenetic, morphological, and other analyses is used to clarify species boundaries (Norphanphoun et al. 2020; Zhang et al. 2022).

Members of *Phyllosticta* species are known as pathogenic, endophytic, or rarely saprobic fungi associated with a variety of plants and have a worldwide distribution (van der Aa and Vanev 2002; Glienke et al. 2011; Wikee et al. 2011; Jiang et al. 2021; Wang et al. 2023). As pathogens, *Phyllosticta* species cause spots on the leaves or fruits of many economical plants (e.g., *Musa* spp., *Citrus* spp. and *Vitis* spp.), leading to substantial economic losses (Wang et al. 2012; Wong et al. 2012; Wikee et al. 2013b; Tran et al. 2017). As endophytes, some species were found associated with leaf spots but did not cause any symptom in pathogenicity tests, e.g., *P. oblongifoliae* was isolated from leaf spots of *Garcinia oblongifolia*, *P. pterospermi* was isolated from leaf spots of *Pterospermum heterophyllum*, and *P. capitalensis* was isolated from leaf spots of *Citrus* spp. (Wikee et al. 2013b; Tran et al. 2019; Zhang et al. 2022). In this study, two novel

fungal species named *P. anhuiensis* and *P. guangdongensis*, were isolated from diseased leaves of *Quercus aliena* in Anhui Province and *Viburnum odoratissimum* in Guangdong Province, respectively. This paper describes these species based on molecular evidence and morphological characteristics.

Materials and methods

Isolation and morphological observations

Samples of *Quercus aliena* and *Viburnum odoratissimum* showing necrotic spots were obtained and collected from Anhui and Guangdong Provinces. Samples were surface-sterilized in 75% ethanol for 30 s, then sterilized in 1.5% sodium hypochlorite for 1 min, followed by three rinses with sterilized water and dried on sterilized filter paper, and cut into small sections (3 × 3 mm) from the margins of infected tissues. The sections were plated onto potato dextrose agar (PDA) plates and incubated at 25 °C. Hyphal tips from the edge of emerging colonies were transferred on fresh PDA plates and purified by single-spore culturing (Choi et al. 1999). The cultures and dried specimens of the new isolates have been deposited with the China Forestry Culture Collection Center (**CFCC**; http://cfcc.caf.ac.cn/) and the herbarium of the Chinese Academy of Forestry (**CAF**; http://museum.caf.ac.cn/).

Colony features of cultures on PDA medium, synthetic low-nutrient agar (SNA), and malt extract agar (MEA) were recorded after 14 d incubation at 25 °C. After conidiomata appeared, fungal structures (including conidia, conidiogenous cells, and appendage) were measured and captured at least 50 measurements using a Nikon Eclipse 80i compound microscope with differential interference contrast optics.

DNA extraction, PCR amplification, and sequencing

Genomic DNA was extracted from fungal cultures grown on PDA medium using a CTAB method (Doyle and Doyle 1990). Polymerase chain reaction (PCR) amplification of the ITS, LSU, *tef1*, *act*, and *gapdh* loci were amplified using the primers: ITS1/ITS4 (White et al. 1990), EF1-728F/EF2 (O'Donnell et al. 1998; Carbone and Kohn 1999), ACT-512F/ACT-783R (Carbone and Kohn 1999) and Gpd1-LM/Gpd2-LM (Myllys et al. 2002), respectively. Amplification reactions were performed in a 20 μl reaction volume system containing 10 μl of 2× Taq Mix (Tiangen, China), 1 μl of each primer (10 μM), 1 μl template DNA (20 ng/μl) and 7 μL RNase-free water. PCR parameters were as follows: an initial denaturation step of 5 min at 94 °C, followed by 35 cycles of 30 s at 94 °C, 50 s at 55 °C for ITS, 51 °C for LSU, 48 °C for *tef1* or 52 °C for *act* and *gapdh*, and 1 min at 72 °C, and a final elongation step of 10 min at 72 °C. The PCR products were purified and sequenced in Shanghai Invitrogen Biological Technology Company Limited (Beijing, China).

Phylogenetic analyses

Newly generated in this study were combined using SeqMan v. 7.1.0, and reference sequences (Table 1) were downloaded from GenBank, according to the recent publication (Hattori et al. 2020; Norphanphoun et al. 2020; Crous et al. 2021; Bhunjun et al. 2022; Nguyen et al. 2022; Tan and Shivas 2022; Zhang et al. 2022). Alignments were done by MAFFT v. 7.036 (https://maft.cbrc.jp/alignment/server/) using default settings and manually improved using MEGA v.7.0 (Kumar et al. 2016). The phylogenetic analyses of the combined five loci (ITS, LSU, *tef1*, *act* and *gapdh*) were performed by maximum likelihood (ML) and Bayesian inference (BI). The ML research was conducted with the CIPRES web portal (Miller et al. 2017) using RAxML v. 8.2.12 (Stamatakis 2014) under the GTR+GAMMA model with 1000 bootstrap iterations. The BI analyses was performed by MrBayes 3.1.2 (Ronquist and Huelsenbeck 2003). MrModelTest v. 2.3 (Nylander 2004) was used to determine the best-fit evolution model for each locus. Bayesian posterior probabilities (BYPP) were evaluated by Markov Chain Monte Carlo sampling (MCMC). Four Markov chains were performed for 2 million generations in two independent runs until the split deviation frequencies decreased below 0.01, and sampling every 100 generations. The first 25% of sampled trees were discarded as burn-in, and the remaining ones were used to calculate BYPP. Trees were visualized in FigTree 1.4 (http://tree.bio.ed.ac.uk/software/figtree), and the ML bootstraps (ML-BS) ≥ 50% and BYPP ≥ 0.9 were presented on nodes of the ML tree.

Results

Phylogenetic analyses

In this study, phylogenetic analyses contained sequences from 131 fungal samples representing 93 taxa, including two outgroup taxa, viz., *Botryosphaeria obtusa* (CMW 8232) and *B. stevensii* (CBS 112553). The multi-locus datasets comprised 2460 characters including gaps, 521 for ITS, 764 for LSU, 297 for *tef1*, 248 for *act* and 630 for *gapdh*, with 1499/2460 conserved sites, 187/2460 variable sites, and 774/2460 parsimony informative. The best scoring RAxML tree with a final likelihood value of -22751.44. Estimated base frequencies were: A = 0.206387, C = 0.294301, G = 0.279093, T = 0.220219; substitution rates AC = 1.049607, AG = 3.135926, AT = 1.344881, CG = 1.068545, CT = 6.294467, GT = 1.00000; gamma distribution shape parameter α = 0.690585. In the phylogenetic tree (Fig. 1), *Phyllosticta* was divided into six distinct lineages as six species complexes, and our isolates formed two separate lineages represented two new species viz., *P. anhuiensis* (CFCC 54840, CFCC 55887 and CFCC 58849) and *P. guangdongensis* (CFCC 58144, CFCC 58766 and CFCC 58772).

Table 1. Species and GenBank accession numbers of DNA sequences used for phylogenetic analyses in this study.

Species	Strain no.*	Host	Location	GenBank no.				
				ITS	LSU	*tef1*	*act*	*gapdh*
***Phyllosticta capitalensis* species complex**								
P. acaciigena	CPC 28295 T	*Acacia suaveolens*	Australia	KY173433	KY173523	NA	KY173570	NA
P. aloeicola	CPC 21020 T	*Aloe ferox*	South Africa	KF154280	KF206214	KF289193	KF289311	KF289124
	CPC 21021	*Aloe ferox*	South Africa	KF154281	KF206213	KF289194	KF289312	KF289125
P. ardisiicola	NBRC 102261 T	*Ardisia crenata*	Japan	AB454274	NA	NA	AB704216	NA
P. aristolochiicola	BRIP 53316 T	*Aristolochia acuminata*	Australia	JX486129	NA	NA	NA	NA
P. azevinhi	MUCC0088	*Ilex pedunculosa*	Japan	AB454302	NA	NA	AB704226	NA
P. beaumarisii	CBS 535.87	*Muehlenbekia adpressa*	Australia	NR_145235	NG_058040	KF766429	KF306232	KF289074
P. brazilianiae	LGMF 330 T	*Mangifera indica*	Brazil	JF343572	KF206217	JF343593	JF343656	JF343758
	LGMF 334	*Mangifera indica*	Brazil	JF343566	KF206215	JF343587	JF343650	JF343752
P. capitalensis	CBS 114751	*Vaccinium* sp.	New Zealand	EU167584	EU167584	FJ538407	FJ538465	KF289088
	CBS 128856 T	*Stanhopea* sp.	Brazil	JF261465	KF206304	JF261507	JF343647	JF343776
P. carochlae	CGMCC 3.17317 T	*Caryota ochlandra*	China	KJ847422	NA	KF289178	KF289273	KF289092
P. cavendishii	BRIP 57384	*Musa* cv. *Lady finger*	Australia	KC117644	KU697330	KF009695	KF014059	KU716085
	BRIP 57383	*Musa* cv. *Lady finger*	Australia	KC117643	KU697329	KF009694	KF014058	KU716084
P. cordylinophila	MFLUCC 10-0166 T	*Cordyline fruticosa*	Thailand	KF170287	KF206242	KF289172	KF289295	KF289076
	MFLUCC 12-0014	*Cordyline fruticosa*	Thailand	KF170288	KF206228	KF289171	KF289301	KF289075
P. doitungensis	MFLU 21-0175 T	*Dasymaschalon obtusipetalum*	Thailand	OK661033	OK661034	OL345581	NA	NA
P. eugeniae	CBS 445.82 T	*Eugenia aromatica*	Indonesia	AY042926	KF206288	KF289208	KF289246	KF289139
P. fallopiae	MUCC0113 T	*Fallopia japonica*	Japan	AB454307	NA	NA	AB704228	NA
P. guangdongensis	CFCC 58144 T	*Viburnum odoratissimum*	China	OQ202160	OQ202170	OQ267758	OQ267764	OQ267770
	CFCC 58766	*Viburnum odoratissimum*	China	OQ202161	OQ202171	OQ267759	OQ267765	OQ267771
	CFCC 58772	*Viburnum odoratissimum*	China	OQ202162	OQ202172	OQ267760	OQ267766	OQ267772
P. ilicis-aquifolii	CGMCC 3.14358 T	*Ilex aquifolium*	China	JN692538	NA	JN692526	JN692514	NA
	CGMCC 3.14359	*Ilex aquifolium*	China	JN692539	NA	JN692527	JN692515	NA
P. maculata	CPC 18347 T	*Musa* cv. *Golygoly pot-pot*	Australia	JQ743570	NA	KF009700	KF014016	NA
	BRIP 46622	*Musa* cv. *Golygoly pot-pot*	Australia	JQ743567	NA	KF009692	KF014013	NA
P. mangiferae	IMI 260576 T	*Mangifera indica*	India	JF261459	KF206222	JF261501	JF343641	JF343748
P. mangifera-indicae	MFLUCC 10-0029 T	*Mangifera indica*	Thailand	KF170305	KF206240	KF289190	KF289296	KF289121
P. musaechinensis	GZAAS 6.1247	*Musa* sp.	China	KF955294	NA	KM816639	KM816627	KM816633
	GZAAS 6.1384	*Musa* sp.	China	KF955295	NA	KM816640	KM816628	KM816634

Species	Strain no.*	Host	Location	GenBank no.				
				ITS	LSU	*tef1*	*act*	*gapdh*
P. musarum	BRIP 57803	*Musa* sp.	Malaysia	JX997138	NA	KF009737	KF014055	NA
	BRIP 58028	*Musa* sp.	Australia	KC988377	NA	KF009738	KF014054	NA
P. oblongifoliae	SAUCC210055	*Garcinia oblongifolia*	China	OM248442	OM232085	OM273890	OM273894	OM273898
	SAUCC210052 T	*Garcinia oblongifolia*	China	OM248445	OM232088	OM273893	OM273897	OM273901
P. paracapitalensis	CPC 26517 T	*Citrus floridana*	Italy	KY855622	KY855796	KY855951	KY855677	KY855735
	CPC 26518	*Citrus floridana*	Italy	KY855623	KY855797	KY855952	KY855678	KY855736
P. parthenocissi	CBS 111645 T	*Parthenocissus quinquefolia*	USA	EU683672	NA	JN692530	JN692518	NA
P. partricuspidatae	NBRC 9466 T	*Parthenocissus tricuspidata*	Japan	KJ847424	NA	KJ847446	KJ847432	KJ847440
	NBRC 9757	*Parthenocissus tricuspidata*	Japan	KJ847425	NA	KJ847447	KJ847433	KJ847441
P. philoprina	CBS 587.69	*Ilex aquifolium*	Spain	KF154278	KF206297	KF289206	KF289250	KF289137
P. phoenicis	CBS 147091	*Phoenix reclinata*	South Africa	MW883442	MW883833	MW890098	MW890031	MW890050
P. pterospermi	SAUCC210104 T	*Pterospermum heterophyllum*	China	OM249954	OM249956	OM273902	OM273904	OM273906
	SAUCC210106	*Pterospermum heterophyllum*	China	OM249955	OM249957	OM273903	OM273905	OM273907
P. rhizophorae	NCYUCC 19-0352 T	*Rhizophora stylosa*	China	MT360030	MT360039	NA	MT363248	MT363250
	NCYUCC 19-0358	*Rhizophora stylosa*	China	MT360031	MT360040	NA	MT363249	MT363251
P. schimae	CGMCC 3.14354 T	*Schima superba*	China	JN692534	NA	JN692522	JN692510	JN692506
P. schimicola	CGMCC 3.17319 T	*Schima superba*	China	KJ847426	NA	KJ847448	KJ847434	KJ854895
	CGMCC 3.17320	*Schima superba*	China	KJ847427	NA	KJ847449	KJ847435	KJ854896
P. styracicola	CGMCC3.14985 T	*Styrax grandiflorus*	China	JX025040	NA	JX025045	JX025035	JX025030
	CGMCC3.14989	*Styrax grandiflorus*	China	JX025041	NA	JX025046	JX025036	JX025031
P. vitis-rotundifoliae	CGMCC 3.17322 T	*Vitis rotundifolia*	USA	KJ847428	NA	KJ847450	KJ847436	KJ847442
	CGMCC 3.17321	*Vitis rotundifolia*	USA	KJ847429	NA	KJ847451	KJ847437	KJ847443
***Phyllosticta concentrica* species complex**								
P. anhuiensis	CFCC 54840T	*Quercus aliena*	China	OQ202157	OQ202167	OQ267761	OQ267767	OQ267773
	CFCC 55887	*Quercus aliena*	China	OQ202158	OQ202168	OQ267762	OQ267768	OQ267774
	CFCC 58849	*Quercus aliena*	China	OQ202159	OQ202169	OQ267763	OQ267769	OQ267775
P. aspidistricola	NBRC 102244 T	*Aspidistra elatior*	Japan	AB454314	NA	NA	AB704204	NA
P. aucubae-japonicae	MAFF 236703 T	*Aucuba japonica*	Japan	KR233300	NA	KR233310	KR233305	NA
P. bifrenariae	CBS 128855 T	*Bifrenaria harrisoniae*	Brazil	JF343565	KF206209	JF343586	JF343649	JF343744
	CPC 17467	*Bifrenaria harrisoniae*	Brazil	KF170299	KF206260	KF289207	KF289283	KF289138
P. catimbauensis	URM 7672 T	*Mandevilla catimbauensis*	Brazil	MF466160	MF466163	MF466155	MF466157	NA
	URM 7674	*Mandevilla catimbauensis*	Brazil	MF466161	MF466164	MF466153	MF466158	NA
P. citriasiana	CBS 120486 T	*Citrus maxima*	Thailand	FJ538360	KF206314	FJ538418	FJ538476	JF343686

Species	Strain no.*	Host	Location	GenBank no.				
				ITS	LSU	*tef1*	*act*	*gapdh*
P. citriasiana	CBS 120487	*Citrus maxima*	China	FJ538361	KF206313	FJ538419	FJ538477	JF343687
P. citribraziliensis	CBS 100098 T	*Citrus limon*	Brazil	FJ538352	KF206221	FJ538410	FJ538468	JF343691
P. citricarpa	CBS 127454 T	*Citrus limon*	Australia	JF343583	KF206306	JF343604	JF343667	JF343771
P. citrichinensis	ZJUCC 200956 T	*Citrus reticulata*	China	JN791620	NA	JN791459	JN791533	NA
	ZJUCC 2010150	*Citrus maxima*	China	JN791662	NA	JN791514	JN791582	NA
P. citrimaxima	MFLUCC 10-0137 T	*Citrus maxima*	Thailand	KF170304	KF206229	KF289222	KF289300	KF289157
P. concentrica	CBS 937.70	*Hedera helix*	Italy	FJ538350	KF206291	FJ538408	KF289257	JF411745
	CPC 18842 T	*Hedera* sp.	Italy	KF170310	KF206256	KF289228	KF289288	KF289163
P. cussonia	CPC 14873 T	*Cussonia* sp.	South Africa	JF343578	KF206279	JF343599	JF343662	JF343764
	CPC 14875	*Cussonia* sp.	South Africa	JF343579	KF206278	JF343600	JF343663	JF343765
P. elongata	CBS 126.22 T	*Oxycoccus macrocarpos*	USA	FJ538353	NA	FJ538411	FJ538469	KF289164
P. ericarum	CBS 132534 T	*Erica gracilis*	South Africa	KF206170	KF206253	KF289227	KF289291	KF289162
P. gardeniicola	MUCC0117	*Gardenia jasminoides*	Japan	AB454310	NA	NA	AB704230	NA
	MUCC0089	*Gardenia jasminoides*	Japan	AB454303	NA	NA	NA	NA
P. gwangjuensis	CNUFC NJ1-12 T	*Torreya nucifera*	Korea	OK285195	NA	OM038511	OM001471	NA
	CNUFC NJ1-12-1	*Torreya nucifera*	Korea	OK285196	NA	OM038512	OM001472	NA
P. hostae	CGMCC 3.14355 T	*Hosta plantaginea*	China	JN692535	NA	JN692523	JN692511	JN692503
	CGMCC 3.14356	*Hosta plantaginea*	China	JN692536	NA	JN692524	JN692512	JN692504
P. hymenocallidicola	CBS 131309 T	*Hymenocallis littoralis*	Australia	JQ044423	JQ044443	KF289211	KF289242	KF289142
	CPC 19331	*Hymenocallislittoralis*	Australia	KF170303	KF206254	KF289212	KF289290	KF289143
P. hypoglossi	CBS 101.72	*Ruscus aculeatus*	Italy	FJ538365	KF206326	FJ538423	FJ538481	JF343694
	CBS 434.92 T	*Ruscus aculeatus*	Italy	FJ538367	KF206299	FJ538425	FJ538483	JF343695
P. iridigena	CBS 143410 T	*Iris* sp.	South Africa	MG934459	NA	MG934502	MG934466	NA
P. kerriae	MAFF 240047 T	*Kerria japonica*	Japan	AB454266	NA	NA	NA	NA
P. kobus	MUCC0049	*Magnolia kobus*	Japan	AB454286	NA	NA	AB704221	NA
P. ophiopogonis	KACC 47754	*Ophiopogon japonicus*	South Korea	KP197057	NA	NA	NA	NA
	LrLF11	*Lycoris radiata*	China	MG543713	NA	NA	NA	NA
P. paracitricarpa	CPC 27169 T	*Citrus limon*	Greece	KY855635	KY855809	KY855964	KY855690	KY855748
	ZJUCC 200933	*Citrus sinensis*	China	JN791626	KY855813	JN791468	JN791544	KY855752
P. pilospora	MUCC 2912a T	*Chamaecyparis pisifera* var. *plumose*	Japan	LC542597	LC543423	LC543445	LC543465	NA
P. speewahensis	BRIP 58044 T	Orchids	Australia	KF017269	NA	KF017268	NA	NA
P. spinarum	CBS 292.90	*Chamaecyparis pisifera*	France	JF343585	KF206301	JF343606	JF343669	JF343773
P. westeae	BRIP 72390c T	*Clerodendrum inerme*	Australia	OP599631	NA	OP627090	NA	NA

Species	Strain no.*	Host	Location	GenBank no.				
				ITS	LSU	*tef1*	*act*	*gapdh*
***Phyllosticta cruenta* species complex**								
P. abieticola	CBS 112067	*Abies concolor*	Canada	KF170306	EU754193	NA	KF289238	NA
P. cornicola	CBS 111639	*Cornus florida*	USA	KF170307	NA	NA	KF289234	NA
P. cruenta	CBS 858.71	*Polygonatum odoratum*	Czech Republic	MG934458	NA	MG934501	MG934465	MG934474
P. cruenta	MUCC0206	*Polygonatum odoratum* var. *pluriflorum*	Japan	AB454331	NA	NA	AB704237	NA
P. cryptomeriae	KACC 48643	*Juniperus chinensis* var. *sargentii*	Not given	MK396559	NA	NA	NA	NA
	MUCC0028	*Cryptomeria japonica*	Japan	AB454271	NA	NA	AB704213	NA
P. foliorum	CBS 447.68 T	*Taxus baccata*	Netherlands	KF170309	KF206287	KF289201	KF289247	KF289132
P. gaultheriae	CBS 447.70 T	*Gaultheria humifusa*	USA	JN692543	KF206298	JN692531	KF289248	JN692508
P. hakeicola	CBS 143492 T	*Hakea* sp.	Australia	MH107907	MH107953	MH108025	MH107984	MH107999
P. hamamelidis	MUCC149	*Hamamelis japonica*	Japan	KF170289	NA	NA	KF289309	NA
P. hubeiensis	CGMCC 3.14986 T	*Viburnum odoratissimim*	China	JX025037	NA	JX025042	JX025032	JX025027
	CGMCC 3.14987	*Viburnum odoratissimim*	China	JX025038	NA	JX025043	JX025033	JX025028
P. illicii	24-1-1 T	*Illicium verum*	China	MF198235	MF198240	MF198237	MF198243	NA
	16-16-1	*Illicium verum*	China	MF198234	MF198239	MF198236	MF198242	NA
P. leucothoicola	MUCC553 T	*Leucothoe catesbaei*	Japan	AB454370	AB454370	NA	KF289310	NA
P. ligustricola	MUCC0024 T	*Ligustrum obtusifolium*	Japan	AB454269	NA	NA	AB704212	NA
P. minima	CBS 585.84 T	*Acer rubrum*	USA	KF206176	KF206286	KF289204	KF289249	KF289135
P. neopyrolae	CPC 21879 T	*Pyrola asarifolia*	Japan	AB454318	AB454318	NA	AB704233	NA
P. pachysandricola	MUCC124 T	*Pachysandra terminalis*	Japan	AB454317	AB454317	NA	AB704232	NA
P. paxistimae	CBS 112527 T	*Paxistima mysinites*	USA	KF206172	KF206320	KF289209	KF289239	KF289140
P. podocarpicola	CBS 728.79 T	*Podocarpus maki*	USA	KF206173	KF206295	KF289203	KF289252	KF289134
P. pyrolae	IFO 32652	*Erica carnea*	Not given	AB041242	NA	NA	NA	NA
P. rubella	CBS 111635 T	*Acer rubrum*	USA	KF206171	EU754194	KF289198	KF289233	KF289129
P. sphaeropsoidea	CBS 756.70	*Aesculus hippocastanum*	Germany	AY042934	KF206294	KF289202	KF289253	KF289133
P. telopeae	CBS 777.97 T	*Telopea speciosissima*	Tasmania	KF206205	KF206285	KF289210	KF289255	KF289141
P. yuccae	CBS 112065	*Yucca elephantipes*	USA	KF206175	NA	NA	KF289237	NA
	CBS 117136	*Yucca elephantipes*	New Zealand	JN692541	KF766385	JN692529	JN692517	JN692507

Species	Strain no.*	Host	Location	GenBank no.				
				ITS	LSU	*tef1*	*act*	*gapdh*
***Phyllosticta owaniana* species complex**								
P. austroafricana	CBS 144593 ^{T}	leaf spots of unidentified deciduous tree	South Africa	MK442613	MK442549	MK442704	MK442640	NA
P. carissicola	CPC 25665 ^{T}	*Carissa macrocarpa*	South Africa	KT950849	KT950863	KT950879	KT950872	KT950876
P. hagahagaensis	CBS 144592 ^{T}	*Carissa bispinosa*	South Africa	MK442614	MK442550	MK442705	MK442641	MK442657
P. owaniana	CBS 776.97 ^{T}	*Brabejum stellatifolium*	South Africa	FJ538368	KF206293	FJ538426	KF289254	JF343767
	CPC 14901	*Brabejum stellatifolium*	South Africa	JF261462	KF206303	JF261504	KF289243	JF343766
P. podocarpi	CBS 111646	*Podocarpus falcatus*	South Africa	AF312013	KF206323	KC357671	KC357670	KF289169
	CBS 111647	*Podocarpus lanceolata*	South Africa	KF154276	KF206322	KF289232	KF289235	KF289168
P. pseudotsugae	CBS 111649	*Pseudotsuga menziesii*	USA	KF154277	KF206321	KF289231	KF289236	KF289167
***Phyllosticta rhodorae* species complex**								
P. mimusopisicola	CBS 138899 ^{T}	*Mimusops zeyheri*	South Africa	KP004447	MH878626	NA	NA	NA
P. rhodorae	CBS 901.69	*Rhododendron* sp.	Netherlands	KF206174	KF206292	KF289230	KF289256	KF289166
***Phyllosticta vaccinii* species complex**								
P. vaccinii	ATCC 46255 ^{T}	*Vaccinium macrocarpon*	China	KC193585	NA	KC193582	KC193580	KC193583
	LC 2795	*Vitis macrocarpon*	USA	KR233323	NA	NA	NA	NA
P. vacciniicola	CPC 18590 ^{T}	*Vaccinium macrocarpum*	USA	KF170312	KF206257	KF289229	KF289287	KF289165
Outgroup								
B. obtusa	CMW 8232 ^{T}	Conifers	South Africa	AY972105	NA	DQ280419	AY972111	NA
B. stevensii	CBS 112553 ^{T}	culture from isotype of *Diplodia mutila*	Not given	AY259093	AY928049	AY573219	NA	NA

Notes: *^{T} = ex-type strains, NA = not available.

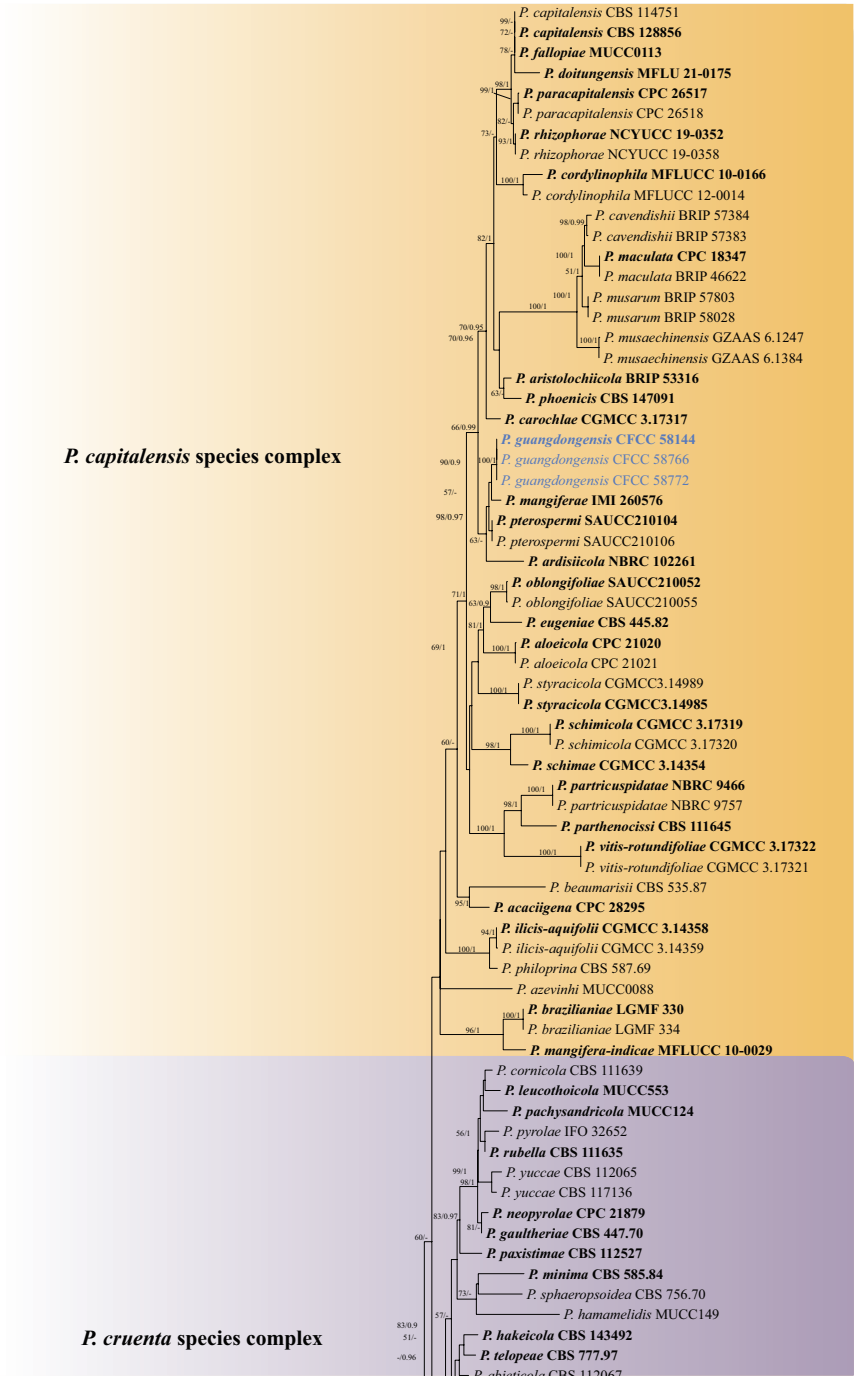

Figure 1. Phylogram of *Phyllosticta* genus resulting from a maximum likelihood analysis based on a combined matrix of ITS, LSU, *tef1*, *act* and *gapdh* loci. The tree is artificially rooted to *B. obtusa* (CMW 8232) and *B. stevensii* (CBS 112553). ML bootstrap values (left, ML-BS ≥ 50%) and Bayesian posterior probabilities (right, BYPP ≥ 0.9) are given at the nodes. Ex-type strains are indicated in bold. Strains from the present study are marked in blue.

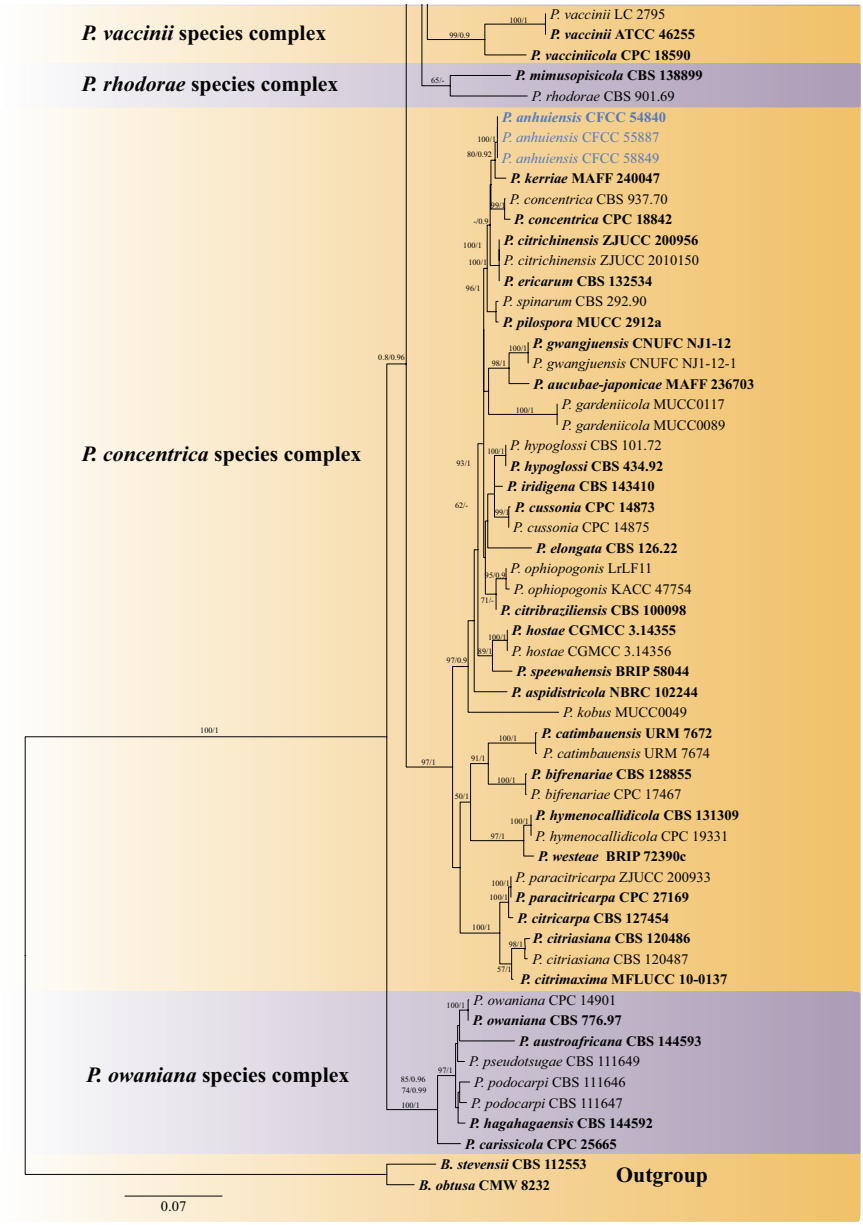

Figure 1. Continued.

Taxonomy

Phyllosticta anhuiensis **Ning Jiang & C.B. Wang, sp. nov.**
MycoBank No: 847160
Fig. 2

Etymology. Referring to the Anhui Province, where the species was first collected.

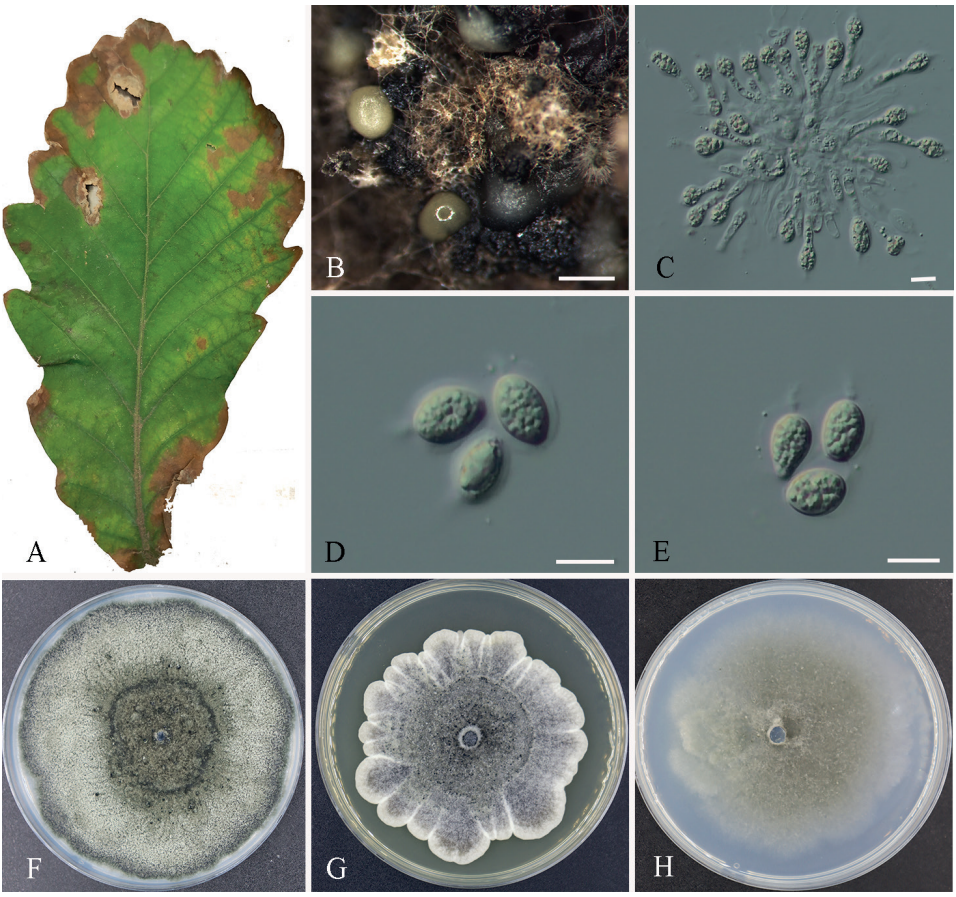

Figure 2. Morphology of *Phyllosticta anhuiensis* (CFCC 54840) **A** diseased leaf of *Quercus aliena* **B** conidiomata **C** conidiogenous cells **D, E** conidia **F–H** colonies on PDA, MEA and SNA after two weeks at 25 °C. Scale bars: 500 μm (**B**); 10 μm (**C–E**).

Description. ***Sexual morph*:** Unknown. ***Asexual morph*:** Conidiomata pycnidial, aggregated, black, erumpent, globose to pyriform, exuding gray to pale yellow conidial masses, 100–400 μm diam. Conidiophores subcylindrical to ampulliform, reduced to conidiogenous cells. Conidiogenous cells phialidic, hyaline, thin-walled, smooth, subcylindrical to ampulliform, 10–16 × 2.5–4.5 μm. Conidia 8.5–12 × 5.5–9 μm, (mean ± SD = 10 ± 1 × 7.2 ± 0.7 μm), solitary, hyaline, aseptate, thin and smooth-walled, coarsely guttulate, globose or ellipsoid to obvoid, enclosed in a thin persistent sheath, 1–1.5 μm thick, and bearing an apical mucoid appendage 4–6 × 1–2 μm, flexible, unbranched, tapering towards an acutely rounded tip.

Culture characters. Colonies on PDA flat, with irregular edge, slow growing, grayish-green to green, reaching a 90 mm diameter after two weeks. Colonies on MEA flat, undulate at the edge, slow growing, gray-white to gray, reaching a 70–80 mm diameter after two weeks. Colonies on SNA flat, slow growing, celandine green, reaching a 60–70 mm diameter after two weeks.

Specimens examined. China, Anhui Province, Hefei City, leaf spots of *Quercus aliena*, Yong Li & Dan-ran Bian, 10 August 2019 (holotype CAF800072; ex-type culture: CFCC 54840). Ibid. (cultures: CFCC 55887 and CFCC 58849).

Notes. In the phylogeny analyses, *P. anhuiensis* groups sister to *P. kerriae* (MAFF 240047). *P. kerriae* was associated with *Kerria japonica* in Japan (Motohashi et al. 2008). Comparison of DNA sequences of *P. anhuiensis* with *P. kerriae* (MAFF 240047), there is 99.4% (447/480 identities; 0/480 gaps) sequence similarity in ITS, 99.8% (554/555 identities, 0/480 gaps) in LSU, 98.6% (215/218 identities, 0/218 gaps) in *tef1*, and 97.7% (212/217 identities, 0/217 gaps) in *act*. Morphologically, *P. anhuiensis* can be distinguished from *P. kerriae* in having shorter appendage (4–6 μm in *P. anhuiensis* vs. 5–12.5 μm in *P. kerriae*) (Motohashi et al. 2008). Therefore, this species was regarded as a new species based on morphology and multi-locus phylogeny.

Phyllosticta guangdongensis **Ning Jiang & C.B. Wang, sp. nov.**
MycoBank No: 847161
Fig. 3

Etymology. Referring to the Guangdong Province, where the species was first collected.

Description. ***Sexual morph*****:** Unknown. ***Asexual morph*****:** Conidiomata pycnidial, aggregated, black, globose to pyriform, exuding opaque conidial masses, erumpent, 100–450 μm diam. Conidiophores subcylindrical to ampulliform, reduced to conidiogenous cells. Conidiogenous cells phialidic, subcylindrical to ampulliform, hyaline, smooth, 10–15 × 2.5–4 μm. Conidia 10–14 × 6–8 μm, (mean ± SD = 11.5 ± 1.3 × 7.5 ± 0.6 μm), solitary, hyaline, aseptate, thin and smooth-walled, ellipsoid to obovoid, coarsely guttulate, enclosed in a thin persistent mud sheath, 1–1.5 μm thick, with an apical mucoid appendage, 4.5–10 × 1–2 μm, flexible, unbranched, tapering towards an acutely rounded tip.

Culture characters. Colonies on PDA flat, slow growing, grayish-green in the center, and dark green at margin reaching 85 mm diameter after two weeks. Colonies on MEA slow growing, yellow in the center, white at undulate the margin, reaching a 20–25 mm diameter after two weeks. Colonies on SNA flat, slow growing, grayish-green, reaching a 25–30 mm diameter after two weeks.

Specimens examined. China, Guangdong Province, Guangzhou City, leaf spot of *Viburnum odoratissimum*, Yong Li, 20 September 2022 (holotype CAF800073; ex-type culture: CFCC 58144). Ibid. (cultures: CFCC 58766 and CFCC 58772).

Notes. Phylogeny indicates that *P. anhuiensis* groups sister to *P. mangiferae* (IMA 260576). *P. mangiferae* was associated with *Mangifera indica* leaves in Tanzania (Ebbels and Allen 1979; Glienke et al. 2011). Comparison of DNA sequences of *P. anhuiensis* with *P. mangiferae* (IMA 260576), there are 99.1% (471/475 identifies, 0/475 gaps) sequence similarity in ITS, 99.6% (760/763 identifies, 0/763 gaps) in LSU, 97.7% (211/216 identifies, 2/218 gaps) in *tef1*, 98.2% (221/225 identifies, 0/225 gaps) in *act*, and 98.4% (614/624 identifies, 6/624 gaps) in *gapdh*. Morphologically, *P. guangdongensis* can be distinguished from *P. mangiferae* in longer conidia (10–14 μm in

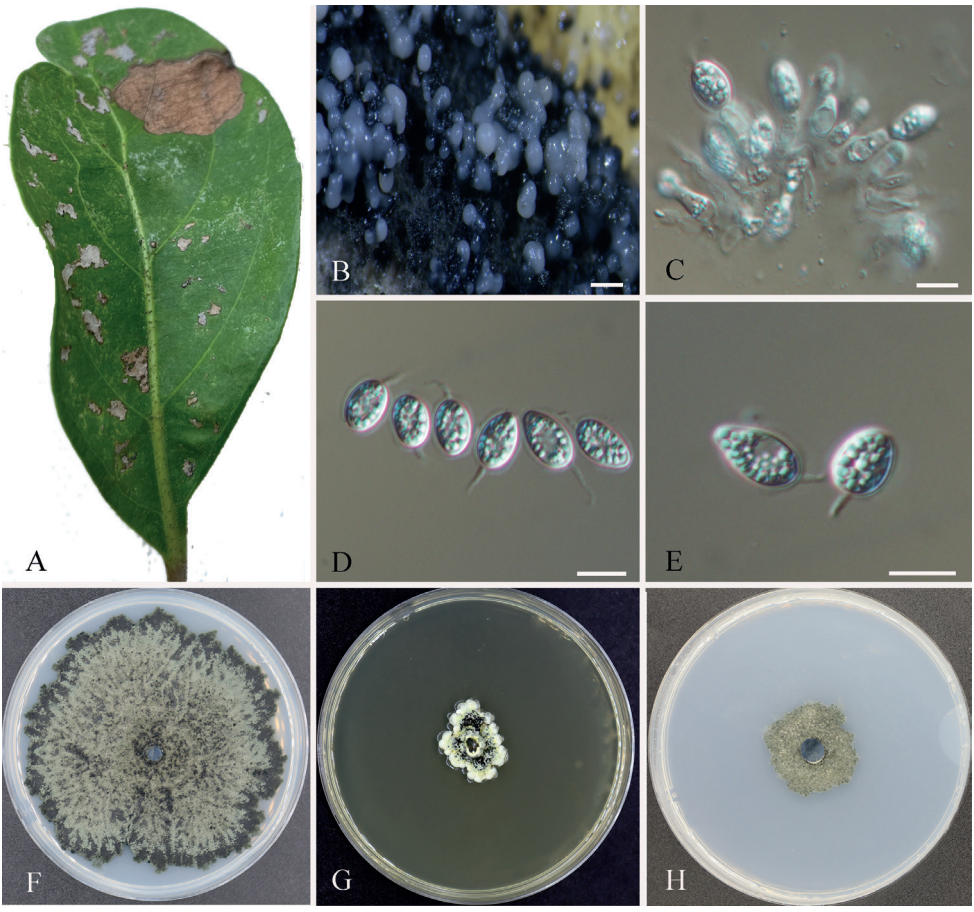

Figure 3. Morphology of *Phyllosticta guangdongensis* (CFCC 58144) **A** diseased leaf of *Viburnum odoratissimum* **B** conidiomata **C** conidiogenous cells **D, E** conidia **F–H** colonies on PDA, MEA and SNA after two weeks at 25 °C. Scale bars: 500 μm (**B**); 10 μm (**C–E**).

P. guangdongensis vs. 8–12 μm in *P. mangiferae*) and shorter appendage (4.5–10 μm in *P. guangdongensis* vs. 7–13 μm in *P. mangiferae*) (Glienke et al. 2011). Therefore, this species was regarded as a new species based on morphology and multi-locus phylogenetic analyses.

Discussion

Phyllosticta is a species-rich genus with more than 3211 records listed in the Index Fungorum (http://www.indexfungorum.org). For the *Phyllosticta* species identification, molecular data have proven useful in resolving species relationships (Okane et al. 2003; Su and Cai 2012; Guarnaccia et al. 2017; Norphanphoun et al. 2020; Zhang

et al. 2022). ITS is a genetic marker for genus level, and combining it with additional loci (LSU, *tef1*, *act* and *gapdh*) is enough for species-level resolution (Jayawardena et al. 2019; Norphanphoun et al. 2020). In this study, based on the phylogenetic analyses of presently accepted species using five loci (ITS, LSU, *tef1*, *act* and *gapdh*), there are six species complexes and 93 species accepted in *Phyllosticta* (Table 1), viz., *P. capitalensis* species complex (including 33 species), *P. concentrica* species complex (including 28 species), *P. cruenta* species complex (including 22 species), *P. owaniana* species complex (including six species), *P. rhodorae* species complex (including two species), and *P. vaccinii* species complex species complex (including two species). *P. anhuiensis* and *P. guangdongensis* formed two well separated clades in the *P. concentrica* and *P. capitalensis* species complexes, distinguishing from all accepted species in this genus by DNA sequences data.

Morphologically, our isolates have the typical structure of *Phyllosticta* (van der Aa and Vanev 2002). The asexual morph of species in the *P. concentrica* species complex is characterized by globose or ellipsoid to obvoid conidia enclosed in a thin persistent sheath with an apical mucoid appendage (Norphanphoun et al. 2020). The asexual morph of species in the *P. capitalensis* species complex are characterized by ellipsoid or ellipsoid to obovoid, ovoid, obpyriform conidia with a mucoid sheath with an apical mucoid appendage (Norphanphoun et al. 2020). Our isolates include the essential characteristics of their species complexes, and differ from their closest relatives by the size ranges of conidia and appendage (Motohashi et al. 2008; Glienke et al. 2011).

Phyllosticta anhuiensis was isolated from *Q. aliena* in Anhui Province, and *P. guangdongensis* was isolated from *V. odoratissimum* in Guangdong Province. Among *Phyllosticta* species recorded from *Quercus* and *Viburnum* with sequence date and morphological features, *P. capitalensis* was isolated from *Q. dentata* and *Q. variabilis* in Japan; *P. concentrica* was isolated from *Q. robur* in Poland and *Q. ilex* in Ukraine; and *P. hubeiensis* was isolated from *V. odoratissimum* in China (Okane et al. 2003; Mulenko et al. 2008; Zhang et al. 2013; Farr and Rossman 2022). *P. capitalensis* and *P. concentrica* are common species reported from various plants, and *P. hubeiensis* was only recorded from *V. odoratissimum* (Wikee et al. 2013a, b; Zhang et al. 2013; Farr and Rossman 2022). Our isolates formed individual lineages as shown in Fig. 1, segregated from those three species. Morphologically, *P. anhuiensis* differs from *P. capitalensis* and *P. concentrica* by having longer conidiogenous cells (10–16 × 2.5–4.5 μm in *P. anhuiensis* vs. 7–10 × 3–5 in *P. capitalensis* vs. 7–10 × 3–6 μm in *P. concentrica*), shorter conidia (8.5–12 × 5.5–9 μm in *P. anhuiensis* vs. 10–14 × 5–7 μm in *P. capitalensis* vs. 10–14 × 6–9 μm in *P. concentrica*) and shorter appendage (4–6 × 1–2 μm in *P. anhuiensis* vs. 5–15 × 1–1.5 μm in *P. concentrica*) (Glienke et al. 2011; Wikee et al. 2013a); *P. guangdongensis* can be distinguished from *P. hubeiensis* in having shorter appendage (4.5–10 μm in *P. guangdongensis* vs. 7–12 μm in *P. hubeiensis*) (Zhang et al. 2013).

In this study, we introduced two novel species from forestry trees. Previously, many *Phyllosticta* species were found in economic hosts, and with the investigation and study of *Phyllosticta*, many *Phyllosticta* will be found on forestry trees and this will improve our understanding of the species diversity.

Acknowledgements

This research was funded by the National Microbial Resource Center of the Ministry of Science and Technology of the People's Republic of China (NMRC-2022-7).

References

Baayen RP, Bonants P, Verkley G, Carroll GC, van der Aa HA, de Weerdt M, van Brouwershaven IR, Schutte GC, Maccheroni Jr W, Glienke de Blanco C, Azevedo JL (2002) Nonpathogenic isolates of the *Citrus* black spot fungus, *Guignardia citricarpa*, identified as a cosmopolitan endophyte of woody plants, *G. mangiferae* (*Phyllosticta capitalensis*). Phytopathology 92(5): 464–477. https://doi.org/10.1094/PHYTO.2002.92.5.464

Bhunjun CS, Niskanen T, Suwannarach N, Wannathes N, Chen YJ, McKenzie EHC, Maharachchikumbura SSN, Buyck B, Zhao CL, Fan YG, Zhang JY, Dissanayake AJ, Marasinghe DS, Jayawardena RS, Kumla J, Padamsee M, Chen YY, Liimatainen K, Ammirati JF, Phukhamsakda C, Liu JK, Phonrob W, Randrianjohany É, Hongsanan S, Cheewangkoon R, Bundhun D, Khuna S, Yu WJ, Deng LS, Lu YZ, Hyde KD, Lumyong S (2022) The numbers of fungi: Are the most specious genera truly diverse? Fungal Diversity 114(1): 387–462. https://doi.org/10.1007/s13225-022-00501-4

Carbone I, Kohn LM (1999) A method for designing primer sets for speciation studies in filamentous ascomycetes. Mycologia 91(3): 553–556. https://doi.org/10.1080/00275514.1999.12061051

Choi YW, Hyde KD, Ho W (1999) Single spore isolation of fungi. Fungal Diversity 3: 29–38.

Crous PW, Slippers B, Wingfield MJ, Rheeder J, Marasas WFO, Philips AJL, Alves A, Burgess T, Barber P, Groenewald JZ (2006) Phylogenetic lineages in the Botryosphaeriaceae. Studies in Mycology 55: 235–253. https://doi.org/10.3114/sim.55.1.235

Crous PW, Hernández-Restrepo M, Schumacher RK, Cowan DA, Maggs-Kölling G, Marais E, Wingfield MJ, Yilmaz N, Adan OCG, Akulov A, Duarte EÁ, Berraf-Tebbal A, Bulgakov TS, Carnegie AJ, de Beer ZW, Decock C, Dijksterhuis J, Duong TA, Eichmeier A, Hien LT, Houbraken JAMP, Khanh TN, Liem NV, Lombard L, Lutzoni FM, Miadlikowska JM, Nel WJ, Pascoe IG, Roets F, Roux J, Samson RA, Shen M, Spetik M, Thangavel R, Thanh HM, Thao LD, van Nieuwenhuijzen EJ, Zhang JQ, Zhang Y, Zhao LL, Groenewald JZ (2021) New and interesting fungi. 4. Fungal Systematics and Evolution 7(1): 255–343. https://doi.org/10.3114/fuse.2021.07.13

Doyle JJ, Doyle JL (1990) Isolation of plant DNA from fresh tissue. Focus 12: 13–15. https://doi.org/10.2307/2419362

Ebbels DL, Allen DJ (1979) A supplementary and annotated list of plant diseases, pathogens and associated fungi in Tanzania. Phytopathological papers 22: 1–89.

Farr DF, Rossman AY (2022) Fungal Databases, U.S. National Fungus Collections. https://nt.ars-grin.gov/fungaldatabases/ [Accessed 10 January 2023]

Fries EM (1849) Summa Vegetabilium Scandinaveae. Sectio posterior. Typographia Academica, Leipzig, 259–572.

Glienke C, Pereira OL, Stringari D, Fabris J, Kava-Cordeiro V, Galli-Terasawa L, Cunnington J, Shivas RG, Groenewald JZ, Crous PW (2011) Endophytic and pathogenic *Phyllosticta* species, with reference to those associated with *Citrus* black spot. Persoonia 26(1): 47–56. https://doi.org/10.3767/003158511X569169

Guarnaccia V, Groenewald JZ, Li H, Glienke C, Carstens E, Hattingh V, Fourie PH, Crous PW (2017) First report of *Phyllosticta citricarpa* and description of two new species, *P. paracapitalensis* and *P. paracitricarpa*, from *Citrus* in Europe. Studies in Mycology 87(1): 161–185. https://doi.org/10.1016/j.simyco.2017.05.003

Hattori Y, Motohashi K, Tanaka K, Nakashima C (2020) Taxonomical re-examination of the genus *Phyllosticta*–Parasitic fungi on Cupressaceae trees in Japan. Forest Pathology 50(5): e12630,1.

Jayawardena RS, Hyde KD, Jeewon R, Ghobad-Nejhad M, Wanasinghe DN, Liu NG, Phillips AJL, Oliveira-Filho JRC, da Silva GA, Gibertoni TB, Abeywikrama P, Carris LM, Chethana KWT, Dissanayake AJ, Hongsanan S, Jayasiri SC, McTaggart AR, Perera RH, Phutthacharoen K, Savchenko KG, Shivas RG, Thongklang N, Dong W, Wei D, Wijayawardena NN, Kang JC (2019) One stop shop II: taxonomic update with molecular phylogeny for important phytopathogenic genera: 26–50. Fungal Diversity 94(1): 41–129. https://doi.org/10.1007/s13225-019-00418-5

Jiang N, Fan X, Tian C (2021) Identification and characterization of leaf-inhabiting fungi from *Castanea* plantations in China. Journal of Fungi 7(1): 1–64. https://doi.org/10.3390/jof7010064

Jin J (2011) Conidial morphology changes in four *Phyllosticta* species. Mycotaxon 115(1): 401–406. https://doi.org/10.5248/115.401

Kumar S, Stecher G, Tamura K (2016) MEGA7: Molecular evolutionary genetics analysis version 7.0 for bigger datasets. Molecular Biology and Evolution 33(7): 1870–1874. https://doi.org/10.1093/molbev/msw054

Liu JK, Phookamsak R, Doilom M, Wikee S, Li YM, Ariyawansha H, Boonmee S, Chomnunti P, Dai DQ, Bhat JD, Romero AI, Zhuang WY, Monkai J, Jones EBG, Chukeatirote E, Zhao YC, Wang Y, Hyde KD (2012) Toward a natural classification of Botryosphaeriales. Fungal Diversity 57(1): 149–210. https://doi.org/10.1007/s13225-012-0207-4

Miller MA, Pfeiffer W, Schwartz T (2017) Creating the CIPRES Science Gateway for Inference of Large Phylogenetic Trees. 2010 gateway computing environments workshop (GCE), 8 pp. https://doi.org/10.1109/GCE.2010.5676129

Motohashi K, Araki I, Nakashima C (2008) Four new species of *Phyllosticta*, one new species of *Pseudocercospora*, and one new combination in *Passalora* from Japan. Mycoscience 49(2): 138–146. https://doi.org/10.1007/S10267-007-0395-Z

Mulenko W, Majewski T, Ruszkiewicz-Michalska M (2008) A preliminary checklist of micromycetes in Poland. W. Szafer Institute of Botany. Polish Academy of Sciences 9: e752.

Myllys L, Stenroos S, Thell A (2002) New genes for phylogenetic studies of lichenized fungi, glyceraldehyde-3-phosphate dehydrogenase and beta-tubulin genes. Lichenologist 34(3): 237–246. https://doi.org/10.1006/lich.2002.0390

Nguyen TTT, Lim HJ, Chu SJ, Lee HB (2022) Two new species and three new records of Ascomycetes in Korea. Mycobiology 50(1): 30–45. https://doi.org/10.1080/12298093.2022.2038843

Norphanphoun C, Hongsanan S, Gentekaki E, Chen YJ, Kuo CH, Hyde KD (2020) Differentiation of species complexes in *Phyllosticta* enables better species resolution. Mycosphere 11(1): 2542–2628. https://doi.org/10.5943/mycosphere/11/1/16

Nylander JAA (2004) MrModeltest Version 2. Program Distributed by the Author Evolutionary Biology Centre, Uppsala University, Uppsala.

O'Donnell K, Kistler HC, Cigelnik E, Ploetz RC (1998) Multiple evolutionary origins of the fungus causing panama disease of banana: Concordant evidence from nuclear and mitochondrial gene genealogies. Proceedings of the National Academy of Sciences of the United States of America 95(5): 2044–2049. https://doi.org/10.1073/pnas.95.5.2044

Okane I, Lumyong S, Ito T, Nakagiri A (2003) Extensive host range of an endophytic fungus, *Guignardia endophyllicola* (anamorph, *Phyllosticta capitalensis*). Mycoscience 44(5): 353–363. https://doi.org/10.1007/S10267-003-0128-X

Persoon CH (1818) Traité sur les champignons comestibles, contenant l'indication des espèces nuisibles; a l'histoire des champignons. Belin-Leprieur, Paris. https://doi.org/10.5962/bhl.title.110115

Phillips AJL, Hyde KD, Alves A, Liu JK (2019) Families in Botryosphaeriales: A phylogenetic, morphological and evolutionary perspective. Fungal Diversity 94(1): 1–22. https://doi.org/10.1007/s13225-018-0416-6

Rashmi M, Kushveer JS, Sarma VV (2019) A worldwide list of endophytic fungi with notes on ecology and diversity. Mycosphere 10(1): 798–1079. https://doi.org/10.5943/mycosphere/10/1/19

Ronquist F, Huelsenbeck JP (2003) MrBayes 3: Bayesian phylogenetic inference under mixed models. Bioinformatics 19(12): 1572–1574. https://doi.org/10.1093/bioinformatics/btg180

Schoch CL, Shoemaker RA, Seifert KA, Hambleton S, Spatafora JW, Crous PW (2006) A multigene phylogeny of the Dothideomycetes using four nuclear loci. Mycologia 98(6): 1041–1052. https://doi.org/10.1080/15572536.2006.11832632

Slippers B, Boissin E, Phillips AJL, Groenewald JZ, Lombard L, Wingfield MJ, Postma A, Burgess T, Crous PW (2013) Phylogenetic lineages in the Botryosphaeriales: A systematic and evolutionary framework. Studies in Mycology 76: 31–49. https://doi.org/10.3114/sim0020

Stamatakis A (2014) RAxML version 8: A tool for phylogenetic analysis and post-analysis of large phylogenies. Bioinformatics 30(9): 312–1313. https://doi.org/10.1093/bioinformatics/btu033

Su YY, Cai L (2012) Polyphasic characterisation of three new *Phyllosticta* spp. Persoonia 28(1): 76–84. https://doi.org/10.3767/003158512X645334

Tan YP, Shivas RG (2022) Nomenclatural novelties. Index of Australian Fungi 1: 1–18. https://zenodo.org/record/7250859

Tran NT, Miles AK, Dietzgen RG, Dewdney MM, Zhang K, Rollins JA, Drenth A (2017) Sexual reproduction in the *Citrus* black spot pathogen, *Phyllosticta citricarpa*. Phytopathology 107(6): 732–739. https://doi.org/10.1094/PHYTO-11-16-0419-R

Tran NT, Miles AK, Dietzgen RG, Drenth A (2019) *Phyllosticta capitalensis* and *P. paracapitalensis* are endophytic fungi that show potential to inhibit pathogenic *P. citricarpa* on

Citrus. Australasian Plant Pathology 48(3): 281–296. https://doi.org/10.1007/s13313-019-00628-0

van der Aa HA (1973) Studies in *Phyllosticta*. Studies in Mycology 5: 1–110.

van der Aa HA, Vanev S (2002) A Revision of the Species Described in *Phyllosticta*. Centraalbureau voor Schimmelcultures (CBS), Utrecht, The Netherlands.

Wang CB, Wang TT, Ma CY, Xue H, Li Y, Piao CG, Jiang N (2023) *Phyllosticta rizhaoensis* sp. nov. causing leaf blight of *Ophiopogon japonicus* in China. Fungal Systematics and Evolution 11: 43–50. https://doi.org/10.3114/fuse.2023.11.03

Wang X, Chen G, Huang F, Zhang J, Hyde KD, Li H (2012) *Phyllosticta* species associated with *Citrus* diseases in China. Fungal Diversity 52(1): 209–224. https://doi.org/10.1007/s13225-011-0140-y

White T, Burns T, Lee S, Taylor J (1990) Amplification and direct sequencing of ribosomal RNA genes for phylogenetics. In: Innis MA (Ed.) PCR Protocols: A Guide to Methods and Applications. Academic Press, New York, 315–322. https://doi.org/10.1016/B978-0-12-372180-8.50042-1

Wijayawardene NN, Hyde KD, Al-Ani LKT, Tedersoo L, Haelewaters D, Rajeshkumar KC, Zhao RL, Aptroot A, Leontyev DV, Saxena RK, Tokarev YS, Dai DQ, Letcher PM, Stephenson SL, Ertz D, Lumbsch HT, Kukwa M, Issi IV, Madrid H, Phillips AJL, Selbmann L, Pfliegler WP, Horváth E, Bensch K, Kirk PM, Kolaříková K, Raja HA, Radek R, Papp V, Dima V, Ma J, Malosso E, Takamatsu S, Rambold G, Gannibal PB, Triebel D, Gautam AK, Avasthi S, Suetrong S, Timdal E, Fryar SC, et al. (2020) Outline of fungi and fungus-like taxa. Mycosphere 11(1): 1060–1456. https://doi.org/10.5943/mycosphere/11/1/8

Wikee S, Udayanga D, Crous PW, Chukeatirote E, McKenzie EHC, Bahkali AH, Dai DQ, Hyde KD (2011) *Phyllosticta* – an overview of current status of species recognition. Fungal Diversity 51(1): 43–61. https://doi.org/10.1007/s13225-011-0146-5

Wikee S, Lombard L, Nakashima C, Motohashi K, Chukeatirote E, Cheewangkoon R, McKenzie EHC, Hyde KD, Crous PW (2013a) A phylogenetic re-evaluation of *Phyllosticta* (Botryosphaeriales). Studies in Mycology 76: 1–29. https://doi.org/10.3114/sim0019

Wikee S, Lombard L, Crous PW, Nakashima C, Motohashi K, Chukeatirote E, Alias SA, McKenzie EHC, Hyde KD (2013b) *Phyllosticta capitalensis*, a widespread endophyte of plants. Fungal Diversity 60(1): 91–105. https://doi.org/10.1007/s13225-013-0235-8

Wong MH, Crous PW, Henderson J, Groenewald JZ, Drenth A (2012) *Phyllosticta* species associated with freckle disease of banana. Fungal Diversity 56(1): 173–187. https://doi.org/10.1007/s13225-012-0182-9

Wulandari NF, Hyde KD, Duong LM, De Gruyter J, Meffert JP, Groenewald JZ, Crous PW (2009) *Phyllosticta citriasiana* sp. nov., the cause of citrus tan spot of *Citrus maxima* in Asia. Fungal Diversity 34: 23–39.

Zhang K, Su YY, Cai L (2013) Morphological and phylogenetic characterisation of two new species of *Phyllosticta* from China. Mycological Progress 12(3): 547–556. https://doi.org/10.1007/s11557-012-0861-7

Zhang Z, Liu X, Zhang X, Meng Z (2022) Morphological and phylogenetic analyses reveal two new species and a new record of *Phyllosticta* (Botryosphaeriales, Phyllostictaceae) from Hainan, China. MycoKeys 91: 1–23. https://doi.org/10.3897/mycokeys.91.84803

MycoKeys 95: 209–228 (2023)
doi: 10.3897/mycokeys.95.98969
https://mycokeys.pensoft.net

RESEARCH ARTICLE

A peer-reviewed open-access journal
MycoKeys
Launched to accelerate biodiversity research

Two new species of *Diaporthe* (Diaporthaceae, Diaporthales) in China

Ya-Quan Zhu[1], Chun-Yan Ma[2], Han Xue[1], Chun-Gen Piao[1], Yong Li[1], Ning Jiang[1]

1 *Key Laboratory of Biodiversity Conservation of National Forestry and Grassland Administration, Ecology and Nature Conservation Institute, Chinese Academy of Forestry, Beijing 100091, China* **2** *Natural Resources and Planning Bureau of Rizhao City, Rizhao 276827, China*

Corresponding author: Ning Jiang (n.jiang@caf.ac.cn)

Academic editor: S. Maharachchikumbura | Received 18 December 2022 | Accepted 17 February 2023 | Published 1 March 2023

Citation: Zhu Y-Q, Ma C-Y, Xue H, Piao C-G, Li Y, Jiang N (2023) Two new species of *Diaporthe* (Diaporthaceae, Diaporthales) in China. MycoKeys 95: 209–228. https://doi.org/10.3897/mycokeys.95.98969

Abstract

Species of *Diaporthe* have been reported as plant endophytes, pathogens and saprobes on a wide range of plant hosts. Strains of *Diaporthe* were isolated from leaf spots of *Smilax glabra* and dead culms of *Xanthium strumarium* in China, and identified based on morphology and molecular phylogenetic analyses of combined internal transcribed spacer region (ITS), calmodulin (*cal*), histone H3 (*his3*), translation elongation factor 1-alpha (*tef1*) and β-tubulin (*tub2*) loci. As a result, two new species named *Diaporthe rizhaoensis* and *D. smilacicola* are identified, described and illustrated in the present study.

Keywords

Leaf spots, morphology, multi-gene phylogeny, taxonomy

Introduction

Diaporthe (Diaporthaceae, Diaporthales) is a species-rich genus with its asexual morph previously known as *Phomopsis* (Rossman et al. 2007; Udayanga et al. 2011, 2012a, 2014a, 2015; Dissanayake et al. 2017; Guarnaccia et al. 2018). The genus *Diaporthe* was established by Nitschke in 1870 and predates its sexual morph established in 1905, thus *Diaporthe* is recommended to be used for this genus following "one fungus one name" nomenclature (Nitschke 1870; Rossman et al. 2015).

The sexual morph of *Diaporthe* is characterized by immersed ascomata and an erumpent pseudostroma with single or multiple tapering perithecial necks. Asci are unitunicate, sessile and clavate to cylindrical. Ascospores are elliptical to fusiform, septate or aseptate, hyaline, biseriate to uniseriate in the ascus and sometimes have appendages (Udayanga et al. 2011; Senanayake et al. 2017, 2018). The asexual morph is characterized by black or dark brown conidiomata, with cylindrical phialides producing three types of aseptate and hyaline conidia (Type I: α-conidia, hyaline, fusiform, straight, guttulate or eguttulate, aseptate, smooth-walled; type II: β-conidia, hyaline, filiform, straight or hamate, aseptate, smooth-walled, eguttulate; type III: γ-conidia, rarely produced, hyaline, multiguttulate, fusiform to subcylindrical with an acute or rounded apex, while the base is sometimes truncate) (Udayanga et al. 2011; Gomes et al. 2013).

Species of *Diaporthe* are widely distributed, and infect a broad plant host range, e.g., agricultural crops, forest trees, vegetables, and fruits (Farr et al. 2002a, b; Crous 2005; Rossman et al. 2007; Udayanga et al. 2011, 2012a, b, 2014a, b, 2015; Gomes et al. 2013; Du et al. 2016; Dissanayake et al. 2017; Guarnaccia and Crous 2017; Fan et al. 2018). As plant pathogens, *Diaporthe* spp. cause severe diseases, e.g., blights, cankers, decay, dieback, leaf spots and wilt of many economically important plants in genera *Castanea*, *Citrus*, *Helianthus*, *Macadamia*, *Rosa*, *Vaccinium* and *Vitis*, resulting in major losses (Thompson et al. 2011; Huang et al. 2015; Guarnaccia et al. 2018, 2020; Hilário et al. 2020; Wrona et al. 2020; Caio et al. 2021; Jiang et al. 2021a).

The genus *Diaporthe* includes over 1000 epithets, mostly based on morphological characteristics and host associations (van der Aa et al. 1990; Santos et al. 2010; Guarnaccia et al. 2018). However, recent studies have shown that many species of *Diaporthe* are not host-specific, i.e., one species may infect more than one host species (Vrandecic et al. 2011; Bai et al. 2015; Zhang et al. 2018). And many *Diaporthe* species that are morphologically similar have proven to be genetically distinct (van Rensburg et al. 2006; Udayanga et al. 2011; Jiang et al. 2021b). Thus, polyphasic taxonomy is essential to identify and comprehensively characterize *Diaporthe*.

In the present study, we have analyzed five-locus dataset of combined nuclear ribosomal internal transcribed spacer (ITS), calmodulin (*cal*), histone (*his3*), translation elongation factor 1-alpha (*tef1*) and beta-tubulin (*tub2*). To aid the identification of two new species, we followed Norphanphoun et al. (2022) for the taxonomic treatments of *Diaporthe*. Norphanphoun et al. (2022) clustered *Diaporthe* into 13 workable species complexes namely *D. arecae*, *D. biconispora*, *D. carpini*, *D. decedens*, *D. eres*, *D. oncostoma*, *D. pustulata*, *D. rudis*, *D. scobina*, *D. sojae*, *D. toxica*, *D. varians* and *D. vawdreyi* species complexes. In addition, nine species were retained as singletons, viz., *D. acerina*, *D. acutispora*, *D. crataegi*, *D. multiguttulata*, *D. ocoteae*, *D. perjuncta*, *D. pseudoalnea*, *D. spartinicola* and *D. undulata* based on multilocus phylogeny.

In previous studies, *Smilax glabra* and *Xanthium strumarium* have been reported as hosts of *Diaporthe* (Vrandecic et al. 2007, 2010; Gao et al. 2013; Thompson et al. 2018). *D. eres* (= *D. mahothocarpi*) and *D. lithocarpi* were identified as the cause agents of leaf spot disease based on morphology and phylogenetics on *S. glabra* in China (Gao et al. 2013). *D. helianthi* and *D. longicolla*, pathogens of *X. strumarium*, have

been collected from blighted stems and branches in Croatia (Vrandecic et al. 2007, 2010). *D. pseudolongicolla* (= *D. novem*) has been reported as a branch dieback agent in *X. strumarium* in Australia (Thompson et al. 2018).

In this study, we introduce two new species namely *Diaporthe rizhaoensis* and *D. smilacicola*, collected from diseased plant tissues in China. We further provide descriptions, illustrations, and DNA sequence-based phylogeny to verify identification and placement.

Materials and methods

Isolation and morphological characterization

During 2021 and 2022, investigations were conducted to inspect for the presence of *Diaporthe* species associated with plant diseases in China. Leaves of *Smilax glabra* and culms of *Xanthium strumarium* showing typical symptoms of *Diaporthe* were collected. Infected tissues were cut into 0.5 × 0.5 cm pieces using a double-edge blade, and surface sterilized as follows. These sections underwent initial immersion for 2 min in 0.5% sodium hypochlorite, followed by 1 min in sterile distilled water, 2 min in 75% ethanol, and, finally, 1 min in sterile distilled water. The disinfected fragments were then plated onto the surface of potato dextrose agar (**PDA**; 200 g potatoes, 20 g dextrose, 20 g agar per L) and malt extract agar (**MEA**; 30 g malt extract, 5 g mycological peptone, 15 g agar per L), and incubated at 25 °C to obtain the pure culture.

Species identification was based on morphological features of the new species produced on infected plant tissues and PDA plates. Conidiomata were sectioned by hand, using a double-edged blade and structures were observed under a dissecting microscope. Over 20 fruiting bodies were sectioned, and 50 conidia were selected randomly for measurement using Axio Imager 2 microscope (Zeiss, Oberkochen, Germany). Isolate characteristics incubated on PDA at 25 °C were observed and recorded at 7 days, including colony colour, texture and the arrangement of the conidiomata. The cultures were deposited in the China Forestry Culture Collection Center (**CFCC**; http://www.cfcc-caf.org.cn/), and the specimens in the herbarium of the Chinese Academy of Forestry (**CAF**; http://museum.caf.ac.cn/).

DNA extraction, amplification and sequencing

Genomic DNA was extracted from the fresh mycelium harvested from PDA plates after 7 days using a cetyltrimethylammonium bromide (**CTAB**) method (Doyle and Doyle 1990). For initial species confirmation, the internal transcribed spacer (**ITS**) region was sequenced for all isolates. The BLAST tool (https://blast.ncbi.nlm.nih.gov/Blast.cgi) was used to compare the resulting sequences with those in GenBank. After confirmation of *Diaporthe* species, four additional partial loci, including calmodulin (*cal*), histone H3 (*his3*), partial translation elongation factor 1-alpha (*tef1*) and part of the beta-tubulin

gene region (*tub2*) genes were amplified. The primer pairs and amplification conditions for each of the above-mentioned gene regions are provided in Table 1. A PCR reaction was conducted in a 20 μL reaction volume, and the components were as follows: 1 μL DNA template (20 ng/μl), 1 μL forward 10 μM primer, 1 μL reverse 10 μM primer, 10 μL T5 Super PCR Mix (containing Taq polymerase, dNTP and Mg^{2+}, Beijing TisingKe Biotech Co., Ltd., Beijing, China), and 7 μL sterile water. Amplifications were performed using a T100 Thermal Cycler (Bio-Rad, Hercules, CA, USA). Strands were sequenced in both directions using PCR primers. All amplified PCR products were estimated visually 1.4% agarose gels stained with ethidium bromide and then PCR positive products were sent to Sangon Biotech (Shanghai) Co., Ltd., (Beijing, China) for sequencing.

Phylogenetic analyses

Sequences were edited and condensed with SeqMan v.7.1.0. The sequences generated in this study were supplemented with additional sequences obtained from GenBank (Table 2) based on blast searches and recent publications of the genus *Diaporthe*. The sequences were aligned with the MAFFT v.7 after which the alignments were manually corrected using MEGA v. 7.0. (Katoh and Toh 2010; Kumar et al. 2016). Phylogenetic analyses including Maximum Likelihood (**ML**) and Bayesian Inference (**BI**) methods were conducted for the single gene sequence data sets of the ITS, *cal*, *his3*, *tef1* and *tub2*, and the combined data set of all five gene regions. ML analyses were conducted using RAxML-HPC BlackBox 8.2.10 on the CIPRES Science Gateway portal (https://www.phylo.org) (Miller et al. 2012), employing a GTRGAMMA substitution model with 1000 bootstrap replicates (Stamatakis 2014). BI analyses were conducted using a Markov Chain Monte Carlo (**MCMC**) algorithm in MrBayes v.3.0 (Ronquist and Huelsenbeck 2003). Two Markov chain Monte Carlo (**MCMC**) chains were run from a random starting tree for 1,000,000 generations, resulting in a total of 10,000 trees. The first 25% of trees sampled were discarded as burn-in and the remaining trees were used to calculate the posterior probabilities. Branches with significant Bayesian Posterior Probabilities (**BPP** > 0.9) were estimated in the remaining 7,500 trees. Phylogenetic trees were viewed with FigTree v. 1.4 and processed by Adobe Illustrator CS5. The nucleotide sequence data of the new taxa were deposited in GenBank, and the GenBank accession numbers of all accessions included in the phylogenetic analyses are listed in Table 2.

Table 1. Loci used in this study with PCR primers and process.

Loci	PCR primers	PCR: thermal cycles: (Annealing temp. in bold)	Reference
ITS	ITS1/ITS4	(95 °C: 30 s, **48 °C**: 30 s, 72 °C: 1 min) × 35 cycles	White et al. 1990
cal	CAL228F/CAL737R	(95 °C: 15 s, **54 °C**: 20 s, 72 °C: 1 min) × 35 cycles	Carbone and Kohn 1999
his3	CYLH3F/H3-1b	(95 °C: 30 s, **57 °C**: 30 s, 72 °C: 1 min) × 35 cycles	Crous et al. 2004
			Glass and Donaldson 1995
tef1	EF1-728F/EF1-986R	(95 °C: 15 s, **54 °C**: 20 s, 72 °C: 1 min) × 35 cycles	Carbone and Kohn 1999
tub2	T1(Bt2a)/Bt2b	(95 °C: 30 s, **55 °C**: 30 s, 72 °C: 1 min) × 35 cycles	Glass and Donaldson 1995
			O'Donnell and Cigelnik 1997

Table 2. Strains and GenBank accession numbers used in this study.

Species	Location	Host	Strain	GenBank Accession Number				
				ITS	*tef1*	*tub2*	*cal*	*his3*
Diaporthe absenteum	China	*Camellia sinensis*	LC3429*	KP267897	KP267971	KP293477	NA	KP293547
D. absenteum	China	*Camellia sinensis*	LC3564	KP267912	KP267986	KP293492	NA	KP293559
D. acaciarum	Tanzania	*Acacia tortilis*	CBS 138862*	KP004460	NA	KP004509	NA	KP004504
D. acericola	Italy	*Acer negundo*	MFLUCC 17-0956*	KY964224	KY964180	KY964074	KY964137	NA
D. aceris	Japan	*Acer* sp.	LC8112	KY491547	KY491557	KY491567	KY491575	NA
D. actinidiae	New Zealand	*Actinidia deliciosa*	ICMP 13683*	KC145886	KC145941	NA	NA	NA
D. acuta	China	*Pyrus pyrifolia*	CGMCC 3.19600*	MK626957	MK654802	MK691225	MK691124	MK726161
D. alangii	China	*Alangium kurzii*	CFCC 52556*	MH121491	MH121533	MH121573	MH121415	MH121451
D. alangii	China	*Alangium kurzii*	CFCC 52557	MH121492	MH121534	MH121574	MH121416	MH121452
D. alnea	Netherlands	*Alnus* sp.	CBS 146.46	KC343008	KC343734	KC343976	KC343250	KC343492
D. amaranthophila	Japan	*Amaranthus tricolor*	MAFF 246900	LC459575	LC459577	LC459579	LC459583	LC459581
D. ambigua	South Africa	*Pyrus communis*	CBS 114015*	KC343010	KC343736	KC343978	KC343252	KC343494
D. angelicae	Austria	*Heracleum sphondylium*	CBS 111592*	KC343027	KC343753	KC343995	KC343269	KC343511
D. anhuiensis	China	*Cunninghamia lanceolata*	CNUCC 201901*	MN219718	MN224668	MN227008	MN224549	MN224556
D. arctii	Austria	*Arctium lappa*	CBS 139280*	KJ590736	KJ590776	KJ610891	KJ612133	KJ659218
D. arecae	India	*Areca catechu*	CBS 161.64*	KC343032	KC343758	KC344000	KC343274	KC343516
D. arengae	Hong Kong	*Arenga engleri*	CBS 114979*	KC343034	KC343760	KC344002	KC343276	KC343518
D. arezzoensis	Italy	*Cytisus* sp.	MFLUCC 15-0127	MT185503	NA	NA	NA	NA
D. aseana	Thailand	*Unidentified dead leaf*	MFLUCC 12-0299a*	KT459414	KT459448	KT459432	KT459464	NA
D. australiana	Australia	*Macadamia*	CBS 146457	MN708222	MN696522	MN696530	NA	NA
D. batatas	USA	*Ipomoea batatas*	CBS 122.21*	KC343040	KC343766	KC344008	KC343282	KC343524
D. beilharziae	Australia	*Indigofera australis*	BRIP 54792*	JX862529	JX862535	KF170921	NA	NA
D. biconispora	China	*Citrus grandis*	ZJUD62	KJ490597	KJ490476	KJ490418	MT227578	KJ490539
D. biguttulata	China	*Citrus limon*	ZJUD47*	KJ490582	KJ490461	KJ490403	NA	KJ490524
D. brasiliensis	Brazil	*Aspidosperma* sp.	CBS 133183*	KC343042	KC343768	KC344010	KC343284	KC343526
D. caatingaensis	Brazil	*Tacinga inamoena*	CBS 141542*	KY085927	KY115603	KY115600	NA	KY115605
D. camelliae-oleiferae	China	*Camellia oleifera*	HNZZ027*	MZ509555	MZ504707	MZ504718	MZ504685	MZ504696
D. caryae	China	*Carya illinoensis*	CFCC 52563*	MH121498	MH121540	MH121580	MH121422	MH121458
D. caryae	China	*Carya illinoensis*	CFCC 52564	MH121499	MH121541	MH121581	MH121423	MH121459
D. cercidis	China	*Cercis chinensis*	CFCC 52565*	MH121500	MH121542	MH121582	MH121424	MH121460
D. cercidis	China	*Cercis chinensis*	CFCC 52566	MH121501	MH121543	MH121583	MH121425	MH121461
D. chiangraiensis	Thailand	*Bauhinia* sp.	MFLUCC 17-1669*	MF190119	MF377598	NA	NA	NA
D. chrysalidocarpi	China	*Chrysalidocarpus lutescens*	SAUCC194.35	MT822563	MT855760	MT855876	MT855646	MT855532
D. cichorii	Italy	*Cichorium intybus*	MFLUCC 17-1023*	KY964220	KY964176	KY964104	KY964133	NA
D. cinnomi	China	*Cinnamomum* sp.	CFCC 52569*	MH121504	MH121546	MH121586	NA	MH121464
D. cinnomi	China	*Cinnamomum* sp.	CFCC 52570	MH121505	MH121547	MH121587	NA	MH121465
D. citriasiana	China	*Citrus unshiu*	CGMCC 3.15224*	JQ954645	JQ954663	KC357459	KC357491	KJ490515
D. columnaris	USA	*Vaccinium vitisidaea*	AR3612*	AF439625	NA	NA	NA	NA
D. compacta	China	*Camellia sinensis*	CGMCC 3.17536*	KP267854	KP267928	KP293434	NA	KP293508
D. convolvuli	Turkey	*Convolvulus arvensis*	CBS 124654*	KC343054	KC343780	KC344022	KC343296	KC343538
D. cucurbitae	Canada	*Cucumis* sp.	DAOM 42078*	KM453210	KM453211	KP118848	NA	KM453212
D. cuppatea	South Africa	*Aspalathus linearis*	CBS 117499*	KC343057	KC343783	KC344025	KC343299	KC343541
D. cyatheae	Taiwan	*Cyathea lepifera*	YMJ 1364*	JX570889	KC465406	KC465403	KC465410	NA

Species	Location	Host	Strain	GenBank Accession Number				
				ITS	*tef1*	*tub2*	*cal*	*his3*
D. discoidispora	China	*Citrus unshiu*	ZJUD89*	KJ490624	KJ490503	KJ490445	NA	KJ490566
D. drenthii	Australia	*Macadamia*	CBS 146453	MN708229	MN696526	MN696537	NA	NA
D. durionigena	Vietnam	*Durio zibethinus*	VTCC 930005	MN453530	MT276157	MT276159	NA	NA
D. endocitricola	China	*Citrus maxima*	ZHKUCC 20-0012*	MT355682	MT409336	MT409290	MT409312	NA
D. endophytica	Brazil	*Schinus terebinthifolius*	CBS 133811*	KC343065	KC343791	KC344033	KC343307	KC343549
D. eucalyptorum	China	*Eucalyptus*	CBS 132525*	MH305525	NA	NA	NA	NA
D. eugeniae	Indonesia	*Eugenia aromatica*	CBS 444.82*	KC343098	KC343824	KC344066	KC343340	KC343582
D. fraxini-angustifoliae	Australia	*Fraxinus angustifolia*	BRIP 54781*	JX862528	JX862534	KF170920	NA	NA
D. fructicola	Japan	*Passiflora edulis* × *P. edulis f.*	MAFF 246408*	LC342734	LC342735	LC342736	LC342738	LC342737
D. fulvicolor	China	*Pyrus pyrifolia*	CGMCC 3.19601*	MK626859	MK654806	MK691236	MK691132	MK726163
D. ganjae	USA	*Cannabis sativa*	CBS 180.91*	KC343112	KC343838	KC344080	KC343354	KC343596
D. goulteri	Australia	*Helianthus annuus*	BRIP 55657a*	KJ197290	KJ197252	KJ197270	NA	NA
D. guangdongensis	China	*Citrus maxima*	ZHKUCC 20-0014*	MT355684	MT409338	MT409292	MT409314	NA
D. guangxiensis	China	*Vitis vinifera*	JZB320094*	MK335772	MK523566	MK500168	MK736727	NA
D. gulyae	Australia	*Helianthus annuus*	BRIP 54025*	JF431299	JN645803	KJ197271	NA	NA
D. guttulata	China	Unknown	CGMCC 3.20100	MT385950	MT424685	MT424705	MW022470	MW022491
D. helianthi	Serbia	*Helianthus annuus*	CBS 592.81*	KC343115	KC343841	KC344083	KC343357	KC343599
D. heterostemmatis	China	*Heterostemma grandiflorum*	SAUCC194.85*	MT822613	MT855925	MT855810	MT855692	MT855581
D. hongkongensis	China	*Dichroa febrifuga*	CBS 115448*	KC343119	KC343845	KC344087	KC343361	KC343603
D. hordei	Norway	*Hordeum vulgare*	CBS 481.92*	KC343120	KC343846	KC344088	KC343362	KC343604
D. huangshanensis	China	*Camellia oleifera*	CNUCC 201903*	MN219729	MN224670	MN227010	NA	MN224558
D. hubeiensis	China	*Vitis vinifera*	JZB320123	MK335809	MK523570	MK500148	MK500235	NA
D. hunanensis	China	*Camellia oleifera*	HNZZ023*	MZ509550	MZ504702	MZ504713	MZ504680	MZ504691
D. infecunda	Brazil	*Schinus* sp.	CBS 133812*	KC343126	KC343852	KC344094	KC343368	KC343610
D. infertilis	Suriname	*Camellia sinensis*	CBS 230.52*	KC343052	KC343778	KC344020	KC343294	KC343536
D. kochmanii	Australia	*Helianthus annuus*	BRIP 54033*	JF431295	JN645809	NA	NA	NA
D. kongii	Australia	*Portulaca grandifla*	BRIP 54031*	JF431301	JN645797	KJ197272	NA	NA
D. krabiensis	Thailand	marine based habitats	MFLUCC 17-2481*	MN047101	MN433215	MN431495	NA	NA
D. leucospermi	Australia	*Leucospermum* sp.	CBS 111980*	JN712460	KY435632	KY435673	KY435663	KY435653
D. limonicola	Malta	*Citrus limon*	CPC 28200*	NR_154980	MF418501	MF418582	MF418256	MF418342
D. litchiicola	Australia	*Litchi chinensis*	BRIP 54900*	JX862533	JX862539	KF170925	NA	NA
D. lithocarpi	China	*Lithocarpus glabra*	CGMCC 3.15175*	KC153104	KC153095	KF576311	KF576235	NA
D. longicolla	USA	*Glycine max*	FAU599	KJ590728	KJ590767	KJ610883	KJ612124	KJ659188
D. longispora	Canada	*Ribes* sp.	CBS 194.36*	KC343135	KC343861	KC344103	KC343377	KC343619
D. lusitanicae	Portugal	*Foeniculum vulgare*	CBS 123212	KC343136	KC343862	KC344104	KC343378	KC343620
D. lusitanicae	Portugal	*Foeniculum vulgare*	CBS 123213*	MH863280	KC343863	KC344105	KC343379	KC343621
D. malorum	Portugal	*Malus domestica*	CAA 734*	KY435638	KY435627	KY435668	KY435658	KY435648
D. manihotia	Rwanda	*Manihot utilissima*	CBS 505.76	KC343138	KC343864	KC344106	KC343380	KC343622
D. masirevicii	Australia	*Helianthus annuus*	BRIP 57892a*	KJ197276	KJ197239	KJ197257	NA	NA
D. mayteni	Brazil	*Maytenus ilicifolia*	CBS 133185	KC343139	KC343865	KC344107	KC343381	KC343623
D. megalospora	Not stated	*Sambucus canadensis*	CBS 143.27*	KC343140	KC343866	KC344108	KC343382	KC343624
D. melitensis	Malta	*Citrus limon*	CPC 27873*	MF418424	MF418503	MF418584	MF418258	MF418344
D. melonis	USA	*Cucumis melo*	CBS 507.78*	KC343142	KC343868	KC344110	KC343384	KC343626
D. melonis	Indonesia	*Glycine soja*	CBS 435.87	KC343141	KC343867	KC344109	KC343383	KC343625
D. middletonii	Australia	*Rapistrum rugostrum*	BRIP 54884e*	KJ197286	KJ197248	KJ197266	NA	NA
D. millettiae	China	*Millettia reticulata*	GUCC9167*	MK398674	MK480609	MK502089	MK502086	NA
D. minusculata	China	saprobic on decaying wood	CGMCC 3.20098*	MT385957	MT424692	MT424712	MW022475	MW022499

Species	Location	Host	Strain	GenBank Accession Number				
				ITS	*tef1*	*tub2*	*cal*	*his3*
D. miriciae	Australia	*Helianthus annuus*	BRIP 54736j*	KJ197282	KJ197244	KJ197262	NA	NA
D. musigena	Australia	*Musa* sp.	CBS 129519*	KC343143	KC343869	KC344111	KC343385	KC343267
D. myracrodruonis	Brazil	*Astronium urundeuva*	URM 7972*	MK205289	MK213408	MK205291	MK205290	17
D. nelumbonis	Taiwan	*Nelumbo nucifera*	R. Kirschner 4114*	KT821501	NA	LC086652	NA	NA
D. neoarctii	USA	*Ambrosia trifi*	CBS 109490*	KC343145	KC343871	KC344113	KC343387	KC343629
D. neoraonikayaporum	Thailand	*Tectona grandis*	MFLUCC 14-1136*	KU712449	KU749369	KU743988	KU749356	NA
D. oculi	Japan	*Homo sapiens*	HHUF 30565*	LC373514	LC373516	LC373518	NA	NA
D. osmanthi	China	*Osmanthus fragrans*	GUCC9165*	MK398675	MK480610	MK502091	MK502087	NA
D. ovalispora	China	*Citrus limon*	CGMCC 3.17256*	KJ490628	KJ490507	KJ490449	NA	KJ490570
D. oxe	Brazil	*Maytenus ilicifolia*	CBS 133186*	KC343164	KC343890	KC344132	KC343406	KC343648
D. pandanicola	Thailand	*Pandanus* sp.	MFLUCC 17-0607*	MG646974	NA	MG646930	NA	NA
D. paranensis	Brazil	*Maytenus ilicifolia*	CBS 133184*	KC343171	KC343897	KC344139	KC343413	KC343655
D. pascoei	Australia	*Persea americana*	BRIP 54847*	JX862532	JX862538	KF170924	NA	NA
D. passiflorae	South America	*Passiflora edulis*	CBS 132527*	JX069860	KY435633	KY435674	KY435664	KY435654
D. passifloricola	Malaysia	*Passiflora foetida*	CBS 141329*	KX228292	NA	KX228387	NA	KX228367
D. perseae	Netherlands	*Persea gratissima*	CBS 151.73*	KC343173	KC343899	KC343141	KC343415	KC343657
D. pescicola	China	*Prunus persica*	MFLUCC 16-0105*	KU557555	KU557623	KU557579	KU557603	NA
D. phaseolorum	USA	*Phaseolus vulgaris*	AR4203*	KJ590738	KJ590739	KJ610893	KJ612135	KJ659220
D. phoenicicola	India	*Areca catechu*	CBS 161.64*	MH858400	GQ250349	JX275440	JX197432	NA
D. podocarpi-macrophylli	China	*Podocarpus macrophyllus*	CGMCC 3.18281*	KX986774	KX999167	KX999207	KX999278	KX999246
D. pseudolongicolla	Serbia	*Glycine max*	PL42*	JQ697843	JQ697856	NA	NA	NA
D. pseudolongicolla	Croatia	*Glycine max*	CBS 127269	KC343155	KC343881	KC344123	KC343397	KC343639
D. pseudomangiferae	Dominican Republic	*Mangifera indica*	CBS 101339*	KC343181	KC343907	KC344149	KC343423	KC343665
D. pseudooculi	Japan	*Homo sapiens*	HHUF 30617*	NR_161019	LC373517	LC373519	NA	NA
D. pseudophoenicicola	Spain	*Phoenix dactylifera*	CBS 462.69*	KC343184	KC343910	KC344152	KC343426	KC343668
D. pseudophoenicicola	Iraq	*Mangifera indica*	CBS 176.77	KC343183	KC343909	KC344151	KC343425	KC343667
D. pterocarpicola	Thailand	*Pterocarpus indicus*	MFLUCC 10-0580a*	JQ619887	JX275403	JX275441	JX197433	NA
D. pyracanthae	Portugal	*Pyracantha coccinea*	CBS 142384*	KY435635	KY435625	KY435666	KY435656	KY435646
D. racemosae	South Africa	*Euclea racemosa*	CPC 26646*	MG600223	MG600225	MG600227	MG600219	MG600221
D. raonikayaporum	Brazil	*Spondias mombin*	CBS 133182*	KC343188	KC343914	KC344156	KC343430	KC343672
D. rhodomyrti	China	*Rhodomyrtus tomentosa*	CFCC 53101	MK432643	MK578119	MK578046	MK442965	MK442990
D. rhodomyrti	China	*Rhodomyrtus tomentosa*	CFCC 53102	MK432644	MK578120	MK578047	MK442966	MK442991
D. rizhaoensis	**China**	***Xanthium strumarium***	**CFCC 57562***	**OP955930**	**OP959767**	**OP959773**	**OP959782**	**OP959785**
D. rizhaoensis	**China**	***Xanthium strumarium***	**CFCC 57563**	**OP955931**	**OP959766**	**OP959772**	**OP959781**	**OP959784**
D. rizhaoensis	**China**	***Xanthium strumarium***	**CFCC 57564**	**OP955932**	**OP959765**	**OP959771**	**OP959780**	**OP959783**
D. rosae	Thailand	*Rosa* sp.	MFLUCC 17-2658*	MG828894	NA	MG843878	MG829273	NA
D. rosiphthora	Brazil	*Rosa* sp.	COAD 2914*	MT311197	MT313693	NA	MT313691	NA
D. rossmaniae	Portugal	*Vaccinium corymbosum*	CAA762*	MK792290	MK828063	MK837914	MK883822	MK871432
D. sackstonii	Australia	*Helianthus annuus*	BRIP 54669b*	KJ197287	KJ197249	KJ197267	NA	NA
D. salinicola	Thailand	*Xylocarpus* sp.	MFLU 18-0553*	MN047098	MN077073	NA	NA	NA

Species	Location	Host	Strain	GenBank Accession Number				
				ITS	*tef1*	*tub2*	*cal*	*his3*
D. sambucusii	China	*Sambucus williamsii*	CFCC 51986*	KY852495	KY852507	KY852511	KY852499	KY852503
D. sambucusii	China	*Sambucus williamsii*	CFCC 51987	KY852496	KY852508	KY852512	KY852500	KY852504
D. schimae	China	*Schima superba*	CFCC 53103*	MK432640	MK578116	MK578043	MK442962	MK442987
D. schimae	China	*Schima superba*	CFCC 53104	MK432641	MK578117	MK578044	MK442963	MK442988
D. schini	Brazil	*Schinus terebinthifolius*	CBS 133181*	KC343191	KC343917	KC344159	KC343433	KC343675
D. schoeni	Italy	*Schoenus nigricans*	MFLU 15-1279*	KY964226	KY964182	KY964109	KY964139	
D. sclerotioides	Netherlands	*Cucumis sativus*	CBS 296.67*	KC343193	KC343919	KC344161	KC343435	KC343677
D. searlei	Australia	*Macadamia*	CBS 146456*	MN708231	NA	MN696540	NA	NA
D. sennae	China	*Senna bicapsularis*	CFCC 51636*	KY203724	KY228885	KY228891	KY228875	NA
D. sennae	China	*Senna bicapsularis*	CFCC 51637	KY203725	KY228886	KY228892	KY228876	NA
D. serafiniae	Australia	*Helianthus annuus*	BRIP 55665a*	KJ197274	KJ197236	KJ197254	NA	NA
D. siamensis	Thailand	*Dasymaschalon* sp.	MFLUCC 10-0573a*	JQ619879	JX275393	JX275429	JX197423	NA
D. sinensis	China	*Amaranthus* sp.	ZJUP0033-4*	MK637451	MK660449	MK660447	NA	MK660451
D. smilacicola	**China**	***Smilax glabra***	**CFCC 54582***	**OP955933**	**OP959770**	**OP959776**	**OP959779**	**OP959788**
D. smilacicola	**China**	***Smilax glabra***	**CFCC 58764**	**OP955934**	**OP959769**	**OP959775**	**OP959778**	**OP959787**
D. smilacicola	**China**	***Smilax glabra***	**CFCC 58765**	**OP955935**	**OP959768**	**OP959774**	**OP959776**	**OP959786**
D. sojae	USA	*Glycine max*	FAU635*	KJ590719	KJ590762	KJ610875	KJ612116	KJ659208
D. spinosa	China	*Pyrus pyrifolia*	CGMCC 3.19602*	MK626849	MK654811	MK691234	MK691129	MK726156
D. stewartii	Not stated	*Cosmos bipinnatus*	CBS 193.36*	MH867279	GQ250324	JX275421	JX197415	NA
D. subellipicola	China	on dead wood	KUMCC 17-0153*	MG746632	MG746633	MG746634	NA	NA
D. subordinaria	New Zealand	*Plantago lanceolata*	CBS 464.90*	KC343214	KC343940	KC344182	KC343456	KC343698
D. taiwanensis	Taiwan	*Ixora chinensis*	NTUCC 18-105-1*	MT241257	MT251199	MT251202	MT251196	NA
D. taoicola	China	*Prunus persica*	MFLUCC 16-0117*	KU557567	KU557635	KU557591	NA	NA
D. tarchonanthi	South Africa	*Tarchonanthus littoralis*	CBS 146073*	MT223794	NA	MT223733	NA	MT223759
D. tecomae	Brazil	*Tabebuia* sp.	CBS 100547*	KC343215	KC343941	KC344183	KC343457	KC343699
D. tectonae	Thailand	*Tectona grandis*	MFLUCC 12-0777*	KU712430	KU749359	KU743977	KU749345	NA
D. tectonendophytica	Thailand	*Tectona grandis*	MFLUCC 13-0471*	KU712439	KU749367	KU743986	KU749354	NA
D. tectonigena	China	*Tectona grandis*	MFLUCC 12-0767*	KU712429	KU749371	KU743976	KU749358	NA
D. tectonigena	China	*Camellia sinensis*	LC6512	KX986782	KX999174	KX999214	KX999284	KX999254
D. terebinthifolii	Brazil	*Schinus terebinthifolius*	CBS 133180*	KC343216	KC343942	KC344184	KC343458	KC343700
D. thunbergiicola	Thailand	*Thunbergia laurifolia*	MFLUCC 12-0033*	KP715097	KP715098	NA	NA	NA
D. tulliensis	Australia	*Theobroma cacao*	BRIP 62248a*	KR936130	KR936133	KR936132	NA	NA
D. ueckeri	USA	*Cucumis melo*	FAU656*	KJ590726	KJ590747	KJ610881	KJ612122	KJ659215
D. unshiuensis	China	*Fortunella margarita*	CGMCC 3.17566*	KJ490584	KJ490463	KJ490405	NA	KJ490526
D. unshiuensis	China	*Carya illinoensis*	CFCC 52594	MH121529	MH121571	MH121606	MH121447	MH121487
D. unshiuensis	China	*Carya illinoensis*	CFCC 52595	MH121530	MH121572	MH121607	MH121448	MH121488
D. vawdreyi	Australia	*Psidium guajava*	BRIP 57887a	KR936126	KR936129	KR936128	NA	NA
D. vexans	USA	*Solanum melongena*	CBS 127.14	KC343229	KC343955	KC344197	KC343471	KC343713
D. viniferae	China	*Vitis vinifera*	JZB320071*	MK341550	MK500107	MK500112	MK500119	NA
D. vochysiae	Brazil	*Vochysia divergens*	LGMF1583*	MG976391	MK007526	MK007527	MK007528	MK033323
D. xishuangbanica	China	*Camellia sinensis*	CGMCC 3.18283*	KX986784	KX999176	KX999217	NA	NA
D. xishuangbanica	China	*Camellia sinensis*	LC6707	KX986783	KX999175	KX999216	NA	KX999255

Notes: NA, not applicable. * ex-type strains.

Results

Phylogeny

In the present study, we followed Norphanphoun et al. (2022) for the species complexes treatments of *Diaporthe*. Firstly, we conducted a genus tree including all species belonging to this genus according to Norphanphoun et al. (2022). After that, the phylogenetic analysis revealed that three isolates (CFCC 57562, CFCC 57563 and CFCC 57564) clustered in a distinct clade in the *D. sojae* species complex, and three isolates (CFCC 54582, CFCC 58764 and CFCC 58765) clustered in a distinct clade in the *D. arecae* species complex (Figs 1, 2). The combined sequence alignments of *D. arecae* species complex comprised 62 strains, with *D. vawdreyi* (BRIP 57887a) and *D. biconispora* (ZJUD62) as the outgroup taxa. The dataset comprised 2791 characters including alignment gaps (634 for ITS, 381 for *tef1*, 791 for *tub2*, 499 for *cal* and 486 for *his3*). The combined sequence alignments of *D. sojae* species complex comprised 111 strains, with *D. aceris* (LC8112) and *D. alnea* (CBS 146.46) as the outgroup taxa. The dataset comprised 2799 characters including alignment gaps (671 for ITS, 483 for *tef1*, 483 for *tub2*, 593 for *cal* and 569 for *his3*). The final maximum likelihood tree topology was similar to Bayesian analysis.

Taxonomy

Diaporthe rizhaoensis **Y.Q. Zhu & Ning Jiang, sp. nov.**
MycoBank No: 846816
Fig. 3

Etymology. Named after the collection site of the type specimen, Rizhao City.

Description. ***Conidiomata*** pycnidial, small, scattered, slightly erumpent through bark surface, nearly flat, discoid, with a solitary undivided locule, 150–400 μm diam. ***Conidiogenous cells*** 6.7–11.4 × 1.6–3.0 μm, hyaline, unbranched, densely aggregated, mostly ampulliform, guttulate, aseptate, straight or slightly curved, swelling at base, tapering towards apex. ***Beta conidia*** 12.9–23.4 × 1.1–2.1 μm (mean = 18.7 × 1.4 μm, n = 50), hyaline, filiform, straight or slightly curved, aseptate, base subtruncate, tapering towards the base. ***Alpha conidia and gamma conidia*** not observed. ***Sexual morph*** not observed.

Culture characters. Colonies on potato dextrose agar (PDA) flat, spreading, with flocculent aerial mycelium and entire edge, white, reaching a 90 mm diameter after 14 days at 25 °C; on malt extract agar (MEA) flat, spreading, with flocculent aerial mycelium and crenate edge, white, reaching a 90 mm diameter after 14 days at 25 °C, forming black conidiomata with black conidial masses; on synthetic low nutrient agar (SNA) flat, spreading, with flocculent aerial mycelium forming concentric rings and entire edge, white, reaching a 90 mm diameter after 14 days at 25 °C.

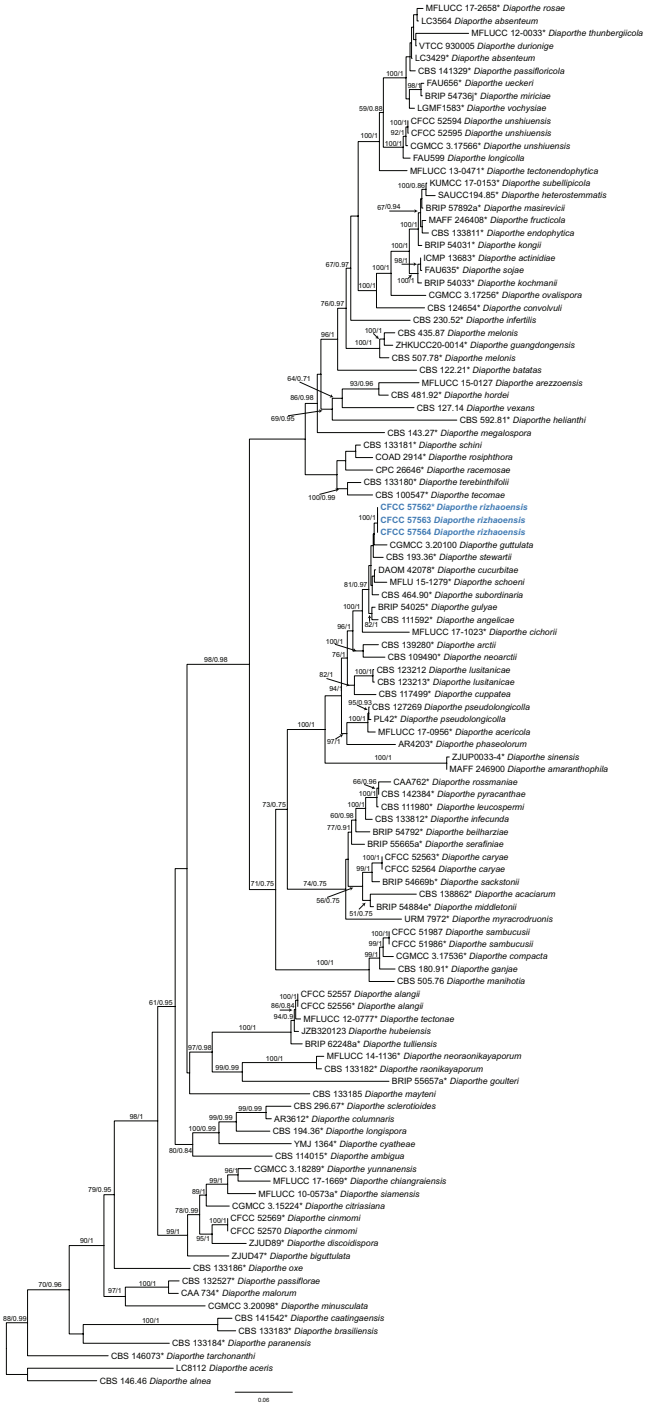

Figure 1. Phylogram of *Diaporthe sojae* species complex resulting from a maximum likelihood analysis based on a combined matrix of ITS, *cal*, *his3*, *tef1* and *tub2* loci. Numbers above the branches indicate ML bootstrap values (left, ML BS ≥ 50%) and Bayesian posterior probabilities (right, BPP ≥ 0.9). Isolates from the present study are marked in bold blue.

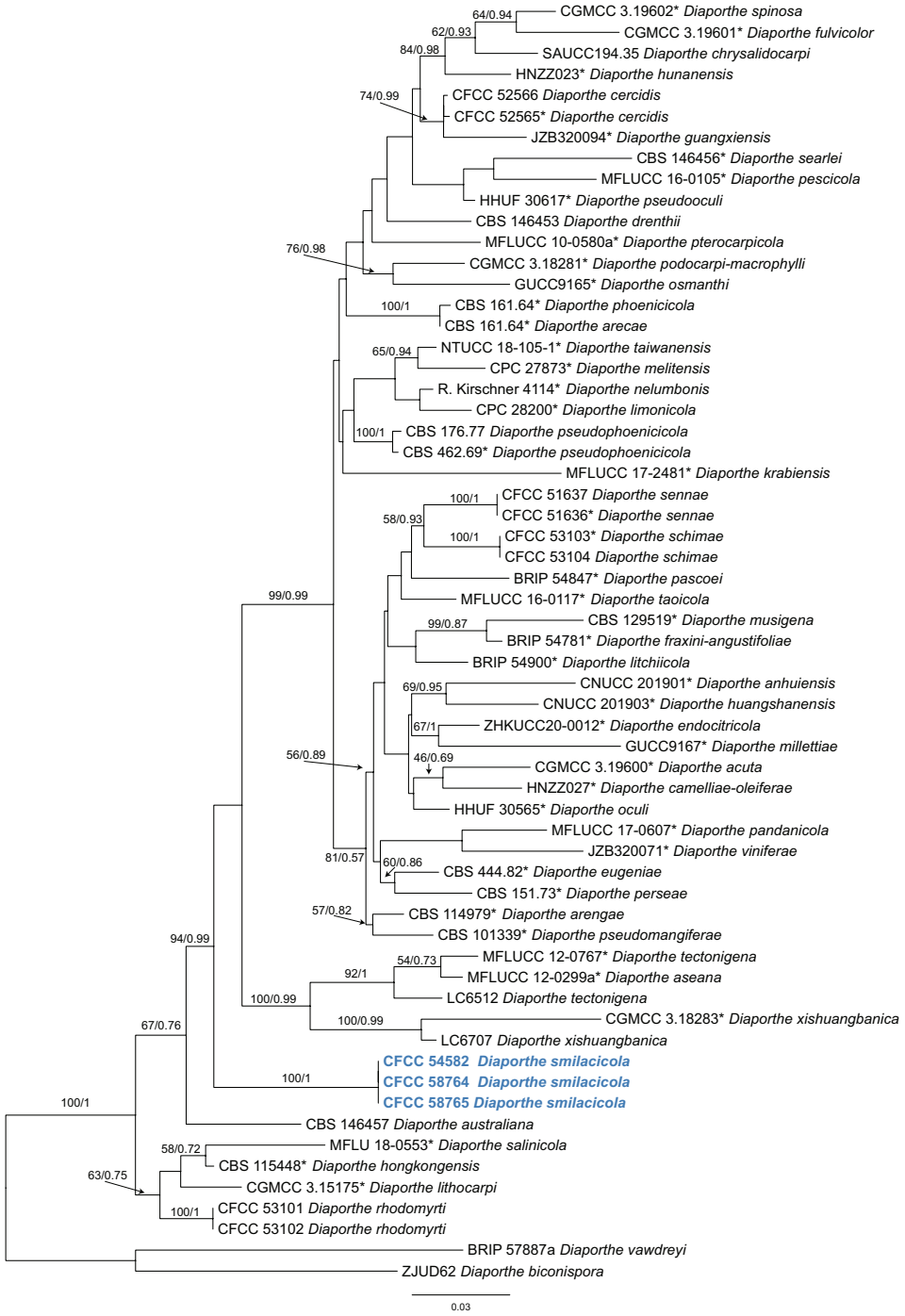

Figure 2. Phylogram of *Diaporthe arecae* species complex resulting from a maximum likelihood analysis based on a combined matrix of ITS, *cal*, *his3*, *tef1* and *tub2* loci. Numbers above the branches indicate ML bootstrap values (left, ML BS ≥ 50%) and Bayesian posterior probabilities (right, BPP ≥ 0.9). Isolates from the present study are marked in bold blue.

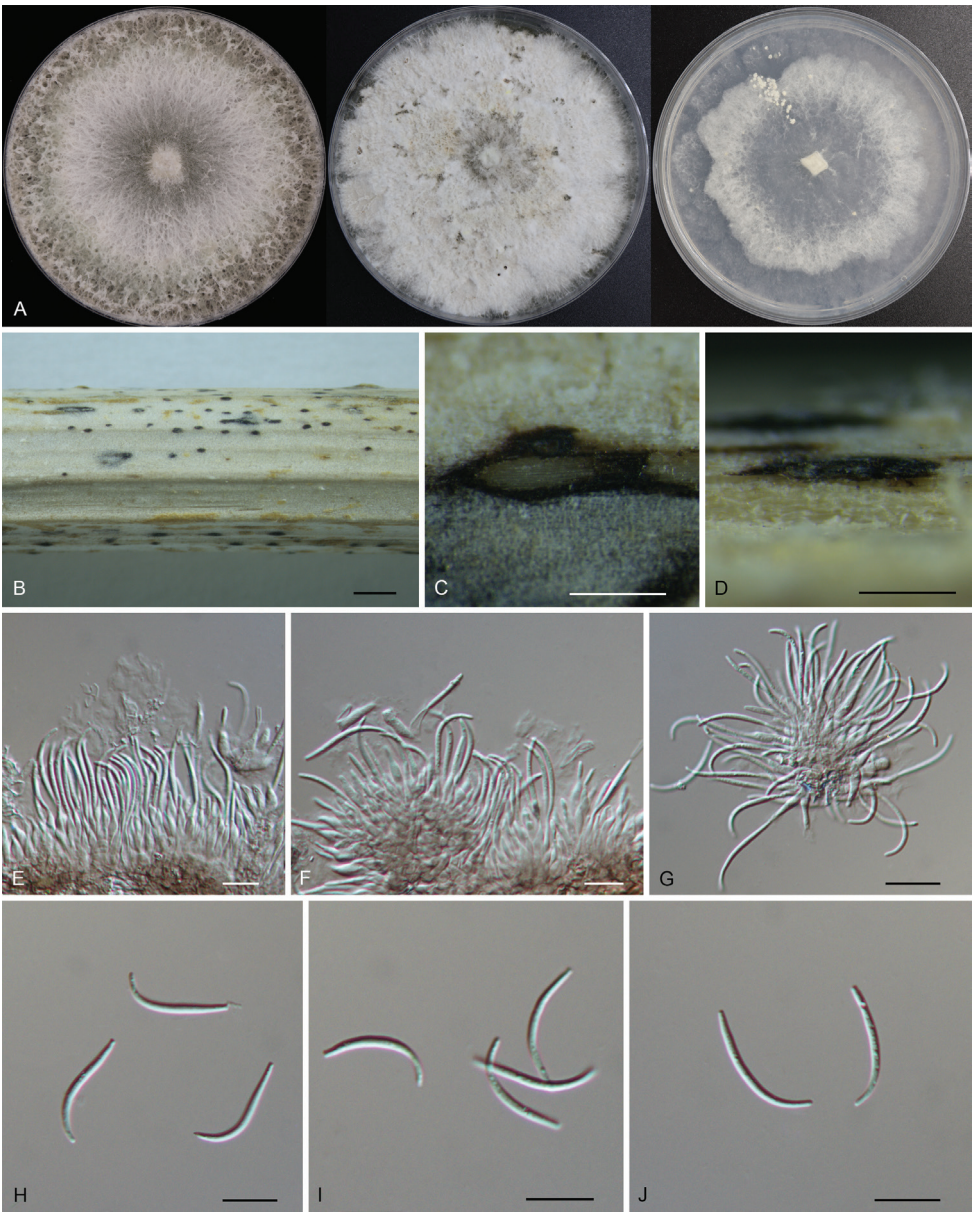

Figure 3. Morphology of *Diaporthe rizhaoensis* **A** colonies on PDA, MEA and SNA at 25 °C after 2 weeks **B** habit of conidiomata on the host **C** transverse section of the conidioma **D** longitudinal section through the conidioma **E–G** conidiogenous cells with attached beta conidia **H–J** beta conidia. Scale bars: 500 µm (**B**); 100 µm (**C, D**); 10 µm (**E–J**).

Materials examined. China, Shandong Province, Rizhao City, Wulian County, Zhongzhi Town, on dead culms of *Xanthium strumarium*, 5 May 2022, Ning Jiang & Chengbin Wang (holotype CAF 800069; ex-holotype culture CFCC 57562).

Shandong Province, Rizhao City, Wulian County, Xumeng Town, on dead culms of *Xanthium strumarium*, 5 May 2022, Ning Jiang & Chengbin Wang (cultures CFCC 57563 and CFCC 57564).

Notes. *Diaporthe rizhaoensis* formed a distinct clade with high support (ML/BI = 100/1), and was close to *D. guttulata* and *D. stewartia* (Fig. 1). *Diaporthe rizhaoensis* is different from *D. stewartia* by host association (*D. rizhaoensis* on *Xanthium strumarium* vs. *D. stewartia* on *Cosmos bipinnatus*) (Harrison 1935; Dissanayake et al. 2020). In addition, *D. guttulata* and *D. stewartia* are only known in sexual morph. Moreover, *Diaporthe rizhaoensis* can be distinguished from *D. guttulata* (15/364 in *cal*, 5/428 in *his3*, 5/313 in *tef1*, and 1/408 in *tub2*) and *D. stewartii* (3/532 in ITS, 7/451 in *cal*, and 7/369 in *tub2*) by sequence data. *Diaporthe helianthi*, *D. longicolla*, *D. pseudolongicolla* (= *D. novem*) and *D. rizhaoensis* have been reported form the host *Xanthium strumarium* (Vrandecic et al. 2007, 2010; Petrović et al. 2018; Thompson et al. 2018). Morphologically, *Diaporthe helianthi* is a bit longer than *D. rizhaoensis* in the beta conidia, but not fully distinguished (Vrandecic et al. 2007, 2010). Morphology of *D. longicolla* and *D. pseudolongicolla* on *Xanthium strumarium* were not available. However, these four species are phylogenetically distinguished in the phylogram of *D. sojae* species complex (Fig. 1).

Diaporthe smilacicola **Y.Q. Zhu & Ning Jiang, sp. nov.**
MycoBank No: 846818
Fig. 4

Etymology. Named after the host genus, *Smilax*.

Description. ***Leaf spots*** subcircular to irregular, pale brown to brown, with dark brown margin. ***Conidiomata*** pycnidial, scattered, subglobose to globose, black, erumpent, exuding faint yellow translucent conidial droplets from central ostioles, 150–350 µm diam. ***Conidiogenous cells*** 11–16.2 × 1.8–2.4 µm, hyaline, phialidic, cylindrical, terminal, slightly tapering towards the apex. ***Alpha conidia*** 5.7–9.7 × 2.0–3.5 µm (mean = 7.8 × 2.6 µm, n = 50), hyaline, aseptate, smooth, guttulate, ellipsoidal to oblong ellipsoidal, with both ends obtuse. ***Beta conidia and gamma conidia*** not observed. ***Sexual morph*** not observed.

Culture characters. Colonies on PDA flat, with flocculent aerial mycelium and crenate edge, white to gray, reaching a 90 mm diameter after 14 days at 25 °C, forming black conidiomata with black conidial masses; on MEA flat, spreading, with flocculent aerial mycelium forming concentric rings, off-white to luteous, reaching a 90 mm diameter after 14 days at 25 °C; on SNA flat, spreading, with flocculent aerial mycelium forming concentric rings and entire edge, white, reaching a 90 mm diameter after 14 days at 25 °C.

Materials examined. China, Hunan Province, Changsha City, Changsha County, Kaihui Town, on leaf spots of *Smilax glabra*, 2 November 2020, Ning Jiang (holotype CAF 800070; ex-holotype culture CFCC 54582). Hunan Province, Shaoshan City, on leaf spots of *Smilax glabra*, 2 November 2020, Ning Jiang (cultures CFCC 58764 and CFCC 58765).

Notes. Three *Diaporthe* isolates representing *D. smilacicola* formed a well-supported clade (ML/BI = 100/1), and appear to be distinct from the other *Diaporthe* species phylogenetically (Fig. 2). *Diaporthe eres* (= *D. mahothocarpi*), *D. lithocarpi* and *D. smilacicola* have been reported from the host *S. glabra* (Gao et al. 2013; Chaisiri et al. 2021). Morphologically, these three species are similar in conidial shape and size. However, *Diaporthe eres* belongs to *D. eres* species complex, which is different from *D. lithocarpi* and *D. smilacicola* in *D. arecae* species complex. *D. smilacicola* is obviously different from *D. lithocarpi* based on sequence data (22/467 in ITS, 31/393 in *cal*, 52/317 in *tef1*, 19/420 in *tub2*) (Fig. 2).

Discussion

Based on the morphology and the multi-locus phylogeny, six isolates from the present study can be recognized as two new species of *Diaporthe*, viz. *D. rizhaoensis* from dead culms of *Xanthium strumarium* and *D. smilacicola* from leaf spots of *Smilax glabra*.

Species identification in *Diaporthe* was primarily based on the assumption of host-specificity, which has largely impeded the progress of establishing a proper taxonomy of *Diaporthe* (Gomes et al. 2013). More than one species of *Diaporthe* can often be recovered from a single host and one species was found to be associated with different host plants (Gomes et al. 2013; Gao et al. 2017; Guarnaccia and Crous 2017; Guarnaccia et al. 2018; Guo et al. 2020). For example, *D. eres* can infect blackberry (Vrandecic et al. 2011), pear (Bai et al. 2015), and jujube (Zhang et al. 2018); *D. pometiae* was isolated from *Heliconia metallica* and *Persea americana* (Huang et al 2021); *D. melastomatis* was collected from three hosts namely *Camellia sinensis*, *Melastoma malabathricum* and *Millettia reticulata* (Sun et al. 2021); *D. australiana*, *D. drenthii*, *D. macadamiae* and *D. searlei* can cause diseases on macadamia in Australia and South Africa (Wrona et al. 2020) and seven endophytic *Diaporthe* species were discovered on *Citrus* trees (Huang et al. 2015). As was revealed in the present study, two additional species of *Diaporthe* were proposed from the host *Smilax glabra* and *Xanthium strumarium*. This study further demonstrates that host association is not a robust character to distinguish members of *Diaporthe*.

Recently, the species classification of *Diaporthe* has become more dependent on DNA sequence-based methods rather than traditional morphological characterization. (Udayanga et al. 2014a, b, 2015; Fan et al. 2015; Gao et al. 2017; Guarnaccia and Crous 2017; Guarnaccia et al. 2018; Hyde et al. 2018, 2020; Yang et al. 2018, 2020, 2021; Long et al. 2019; Cao et al. 2022). The ITS sequence offers convincing proof for species demarcation and is recommended for identifying species boundaries in the genus *Diaporthe* (Santos and Phillips 2009, 2011; Thompson et al. 2011). However, the intraspecific variation is even greater than the interspecific variation, which makes it difficult to identify *Diaporthe* species using the ITS sequence alone (Crouch et al. 2009). Considering this, concatenation of a five-loci dataset (ITS-*tef1*-*tub2*-*cal*-*his3*) was recommended as the best combination for species identification within the genus (Udayanga et al. 2014; Fan et al. 2018; Yang et al. 2018; Guo et al. 2020).

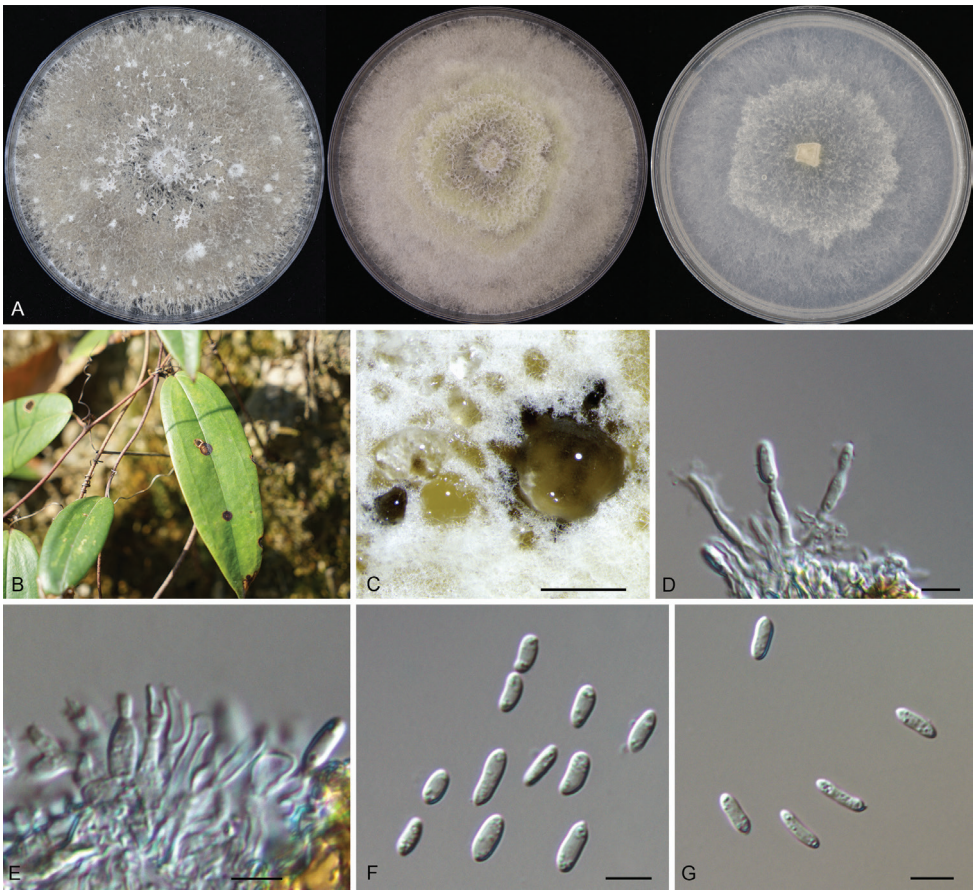

Figure 4. Morphology of *Diaporthe smilacicola* **A** colonies on PDA, MEA and SNA at 25 °C after 2 weeks **B** leaf spots on the host surface **C** conidiomata formed on the PDA **D, E** conidiogenous cells with attached alpha conidia **F–G** alpha conidia. Scale bars: 200 μm (**C**); 10 μm (**D–G**).

Two phylograms resulted from the present study also support the feasibility of the five loci data to separate species of *Diaporthe*.

The two newly introducing species could potentially be pathogens, because they were isolated from diseased plant tissues, and their pathogenicity should be evaluated in further studies. And, it is necessary to evaluate the effects of environmental conditions, such as temperature, pH, and carbon sources, on mycelium growth and pathogenicity.

Acknowledgements

This research was funded by Fundamental Research Funds for the Central Non-profit Research Institution of Chinese Academy of Forestry (grant CAFYBB2018ZB001), and National Microbial Resource Center of the Ministry of Science and Technology of the People's Republic of China (grant NMRC-2021-7).

References

Bai Q, Zhai LF, Chen XR, Hong N, Xu WX, Wang GP (2015) Biological and molecular characterization of five *Phomopsis* species associated with pear shoot canker in China. Plant Disease 99(12): 1704–1712. https://doi.org/10.1094/PDIS-03-15-0259-RE

Caio P, Bruno F, Carlos AP, Robert B (2021) *Diaporthe rosiphthora* sp. nov.: Yet another rose dieback fungus. Crop Protection (Guildford, Surrey) 139: 105365. https://doi.org/10.1016/j.cropro.2020.105365

Cao L, Luo D, Lin W, Yang Q, Deng X (2022) Four new species of *Diaporthe* (Diaporthaceae, Diaporthales) from forest plants in China. MycoKeys 91: 25–47. https://doi.org/10.3897/mycokeys.91.84970

Carbone I, Kohn LM (1999) A Method for designing primer sets for speciation studies in filamentous Ascomycetes. Mycologia 91(3): 553–556. https://doi.org/10.1080/00275514.1999.12061051

Chaisiri C, Liu X, Lin Y, Fu Y, Zhu F, Luo C (2021) Phylogenetic and haplotype network analyses of *Diaporthe eres* species in China based on sequences of multiple loci. Biology (Basel) 10(3): 179. https://doi.org/10.3390/biology10030179

Crouch JA, Clarke BB, Hillman BI (2009) What is the value of ITS sequence data in *Colletotrichum* systematics and species diagnosis? A case study using the falcate-spored graminicolous *Colletotrichum* group. Mycologia 101(5): 648–656. https://doi.org/10.3852/08-231

Crous PW (2005) Impact of molecular phylogenetics on the taxonomy and diagnostics of fungi. Bulletin OEPP. EPPO Bulletin. European and Mediterranean Plant Protection Organisation 35(1): 47–51. https://doi.org/10.1111/j.1365-2338.2005.00811.x

Crous PW, Groenewald JZ, Risède JM, Simoneau P, Hywel-Jones NL (2004) *Calonectria* species and their *Cylindrocladium* anamorphs: Species with sphaeropedunculate vesicles. Studies in Mycology 50: 415–430.

Dissanayake AJ, Phillips AJL, Hyde KD, Yan JY, Li XH (2017) The current status of species in *Diaporthe*. Mycosphere 8(5): 1106–1156. https://doi.org/10.5943/mycosphere/8/5/5

Dissanayake AJ, Chen YY, Liu JK (2020) Unravelling *Diaporthe* species associated with woody hosts from karst formations (Guizhou) in China. Journal of Fungi (Basel, Switzerland) 6(4): 251. https://doi.org/10.3390/jof6040251

Doyle JJ, Doyle JL (1990) Isolation of plant DNA from fresh tissue. Focus (San Francisco, Calif.) 12: 13–15.

Du Z, Fan XL, Hyde KD, Yang Q, Liang YM, Tian CM (2016) Phylogeny and morphology reveal two new species of *Diaporthe* from *Betula* spp. in China. Phytotaxa 269(2): 90–102. https://doi.org/10.11646/phytotaxa.269.2.2

Fan XL, Hyde KD, Udayanga D, Wu XY, Tian CM (2015) *Diaporthe rostrata*, a novel ascomycete from *Juglans mandshurica* associated with walnut dieback. Mycological Progress 14(10): 1–8. https://doi.org/10.1007/s11557-015-1104-5

Fan XL, Yang Q, Bezerra JDP, Alvarez LV, Tian CM (2018) *Diaporthe* from walnut tree (*Juglans regia*) in China, with insight of *Diaporthe eres* complex. Mycological Progress 17(7): 841–853. https://doi.org/10.1007/s11557-018-1395-4

Farr DF, Castlebury LA, Rossman AY (2002a) Morphological and molecular characterization of *Phomopsis vaccinii* and additional isolates of *Phomopsis* from blueberry and cranberry in the eastern United States. Mycologia 94(3): 494–504. https://doi.org/10.1080/15572536.2003.11833214

Farr DF, Castlebury LA, Rossman AY, Putnam ML (2002b) A new species of *Phomopsis* causing twig dieback of *Vaccinium vitisidaea* (lingonberry). Mycological Research 106(6): 745–752. https://doi.org/10.1017/S095375620200583X

Gao YH, Sun W, Su YY, Cai L (2013) Three new species of *Phomopsis* in Gutianshan nature reserve in China. Mycological Progress 13(1): 111–121. https://doi.org/10.1007/s11557-013-0898-2

Gao YH, Liu F, Duan W, Crous PW, Cai L (2017) *Diaporthe* is paraphyletic. IMA Fungus 8(1): 153–187. https://doi.org/10.5598/imafungus.2017.08.01.11

Glass NL, Donaldson GC (1995) Development of primer sets designed for use with the PCR to amplify conserved genes from filamentous ascomycetes. Applied and Environmental Microbiology 61(4): 1323–1330. https://doi.org/10.1128/aem.61.4.1323-1330.1995

Gomes RR, Glienke C, Videira SIR, Lombard L, Groenewald JZ, Crous PW (2013) *Diaporthe*: A genus of endophytic, saprobic and plant pathogenic fungi. Persoonia 31(1): 1–41. https://doi.org/10.3767/003158513X666844

Guarnaccia V, Crous PW (2017) Emerging citrus diseases in Europe caused by species of *Diaporthe*. IMA Fungus 8(2): 317–334. https://doi.org/10.5598/imafungus.2017.08.02.07

Guarnaccia V, Groenewald JZ, Woodhall J, Armengol J, Cinelli T, Eichmeier A, Ezra D, Fontaine F, Gramaje D, Gutierrez-Aguirregabiria A, Kaliterna J, Kiss L, Larignon P, Luque J, Mugnai L, Naor V, Raposo R, Sándor E, Váczy KZ, Crous PW (2018) *Diaporthe* diversity and pathogenicity revealed from a broad survey of grapevine diseases in Europe. Persoonia 40(1): 135–153. https://doi.org/10.3767/persoonia.2018.40.06

Guarnaccia V, Martino I, Tabone G, Brondino L, Gullino ML (2020) Fungal pathogens associated with stem blight and dieback of blueberry in northern Italy. Phytopathologia Mediterranea 59(2): 229–245. https://doi.org/10.14601/Phyto-11278

Guo YS, Crous PW, Bai Q, Fu M, Yang MM, Wang XH, Du YM, Hong N, Xu WX, Wang GP (2020) High diversity of *Diaporthe* species associated with pear shoot canker in China. Persoonia 45(1): 132–162. https://doi.org/10.3767/persoonia.2020.45.05

Harrison AL (1935) The perfect stage of *Phomopsis stewartii* on Cosmos. Mycologia 27(5): 521–526. https://doi.org/10.1080/00275514.1935.12017096

Hilário S, Amaral IA, Gonçalves MF, Lopes A, Santos L, Alves A (2020) *Diaporthe* species associated with twig blight and dieback of *Vaccinium corymbosum* in Portugal, with description of four new species. Mycologia 112(2): 293–308. https://doi.org/10.1080/00275514.2019.1698926

Huang F, Udayanga D, Wang X, Hou X, Mei X, Fu Y, Li H (2015) Endophytic *Diaporthe* associated with *Citrus*: A phylogenetic reassessment with seven new species from China. Fungal Biology 119(5): 331–347. https://doi.org/10.1016/j.funbio.2015.02.006

Huang ST, Xia JW, Zhang XG, Sun WX (2021) Morphological and phylogenetic analyses reveal three new species of *Diaporthe* from Yunnan, China. MycoKeys 78: 49–77. https://doi.org/10.3897/mycokeys.78.60878

Hyde KD, Chaiwan N, Norphanphoun C, Boonmee S, Camporesi E, Chethana KWT, Dayarathne MC, de Silva IN, Dissanayake AJ, Ekanayaka AH (2018) Mycosphere notes 169–224. Mycosphere 9(2): 271–430. https://doi.org/10.5943/mycosphere/9/2/8

Hyde KD, Dong Y, Phookamsak R, Jeewon R, Bhat DJ, Gareth Jones EB, Liu NG, Abeywickrama PD, Mapook A, Wei D (2020) Fungal diversity notes 1151–1276: Taxonomic and phylogenetic contributions on genera and species of fungal taxa. Fungal Diversity 100(1): 1–273. https://doi.org/10.1007/s13225-020-00439-5

Jiang N, Fan XL, Tian CM (2021a) Identification and characterization of leaf-inhabiting fungi from *Castanea* plantations in China. Journal of Fungi (Basel, Switzerland) 7(1): 64. https://doi.org/10.3390/jof7010064

Jiang N, Voglmayr H, Piao CG, Li Y (2021b) Two new species of *Diaporthe* (Diaporthaceae, Diaporthales) associated with tree cankers in the Netherlands. MycoKeys 85: 31–56. https://doi.org/10.3897/mycokeys.85.73107

Katoh K, Toh H (2010) Parallelization of the MAFFT multiple sequence alignment program. Bioinformatics 26(15): 1899–1900. https://doi.org/10.1093/bioinformatics/btq224

Kumar S, Stecher G, Tamura K (2016) MEGA7: Molecular evolutionary genetics analysis version 7.0 for bigger datasets. Molecular Biology and Evolution 33(7): 1870–1874. https://doi.org/10.1093/molbev/msw054

Long H, Zhang Q, Hao YY, Shao XQ, Wei XX, Hyde KD, Wang Y, Zhao DG (2019) *Diaporthe* species in south-western China. MycoKeys 57: 113–127. https://doi.org/10.3897/mycokeys.57.35448

Miller MA, Pfeiffer W, Schwartz T (2012) The CIPRES science gateway: enabling high-impact science for phylogenetics researchers with limited resources. Proceedings of the 1st Conference of the Extreme Science and Engineering Discovery Environment. Bridging from the extreme to the campus and beyond. Association for Computing Machinery, USA, 8 pp. https://doi.org/10.1145/2335755.2335836

Nitschke T (1870) Pyrenomycetes Germanici (2nd edn.). Eduard T rewendt, Breslau, 161–320.

Norphanphoun C, Gentekaki E, Hongsanan S, Jayawardena R, Senanayake C, Manawasinghe I, Abeywickrama P, Bhunjun CS, Hyde KD (2022) *Diaporthe*: Formalizing species-group concepts. Mycosphere 13(1): 752–819. https://doi.org/10.5943/mycosphere/13/1/9

O'Donnell K, Cigelnik E (1997) Two divergent intragenomic rDNA ITS2 types within a monophyletic lineage of the fungus *Fusarium* are nonorthologous. Molecular Phylogenetics and Evolution 7(1): 103–116. https://doi.org/10.1006/mpev.1996.0376

Petrović K, Riccioni L, Đorđević V, Balešević-Tubić S, Miladinović J, Ćeran M, Rajković D (2018) *Diaporthe pseudolongicolla*: The new pathogen on soybean seed in Serbia. Ratarstvo i Povrtarstvo 55(2): 103–109. https://doi.org/10.5937/ratpov55-18582

Ronquist F, Huelsenbeck JP (2003) MrBayes 3: Bayesian phylogenetic inference under mixed models. Bioinformatics 19(12): 1572–1574. https://doi.org/10.1093/bioinformatics/btg180

Rossman AY, Farr DF, Castlebury LA (2007) A review of the phylogeny and biology of the *Diaporthales*. Mycoscience 48(3): 135–144. https://doi.org/10.1007/S10267-007-0347-7

Rossman AY, Adams GC, Cannon PF, Castlebury LA, Crous PW, Gryzenhout M, Jaklitsch WM, Mejia LC, Stoykov D, Udayanga D, Voglmayr H, Walker DM (2015) Recommendations of generic names in *Diaporthales* competing for protection or use. IMA Fungus 6(1): 145–154. https://doi.org/10.5598/imafungus.2015.06.01.09

Santos JM, Phillips AJL (2009) Resolving the complex of *Diaporthe* (*Phomopsis*) species occurring on *Foeniculum vulgare* in Portugal. Fungal Diversity 34(11): 111–125.

Santos JM, Correia VG, Phillips AJL (2010) Primers for mating-type diagnosis in *Diaporthe* and *Phomopsis*, their use in teleomorph induction in vitro and biological species definition. Fungal Biology 114(2–3): 255–270. https://doi.org/10.1016/j.funbio.2010.01.007

Santos JM, Vrandečić K, Ćosić J, Duvnjak T, Phillips AJL (2011) Resolving the *Diaporthe* species occurring on soybean in Croatia. Persoonia 27(1): 9–19. https://doi.org/10.3767/003158511X603719

Senanayake IC, Crous PW, Groenewald JZ, Maharachchikumbura SSN, Jeewon R, Phillips AJL, Bhat DJ, Perera RH, Li QR, Li WJ, Tangthirasunun N, Norphanphoun C, Karunarathna SC, Camporesi E, Manawasighe IS, Al-Sadi AM, Hyde KD (2017) Families of *Diaporthales* based on morphological and phylogenetic evidence. Studies in Mycology 86(1): 217–296. https://doi.org/10.1016/j.simyco.2017.07.003

Senanayake IC, Jeewon R, Chomnunti P, Wanasinghe DN, Norphanphoun C, Karunarathna A, Pem D, Perera RH, Camporesi E, McKenzie EHC, Hyde KD, Karunarathna SC (2018) Taxonomic circumscription of *Diaporthales* based on multigene phylogeny and morphology. Fungal Diversity 93(1): 241–443. https://doi.org/10.1007/s13225-018-0410-z

Stamatakis A (2014) RAxML version 8: A tool for phylogenetic analysis and post-analysis of large phylogenies. Bioinformatics 30(9): 312–1313. https://doi.org/10.1093/bioinformatics/btu033

Sun W, Huang S, Xia J, Zhang X, Li Z (2021) Morphological and molecular identification of *Diaporthe* species in south-western China, with description of eight new species. MycoKeys 77: 65–95. https://doi.org/10.3897/mycokeys.77.59852

Thompson SM, Tan YP, Young AJ, Neate SM, Aitken EAB, Shivas RG (2011) Stem cankers on sunflower (*Helianthus annuus*) in Australia reveal a complex of pathogenic *Diaporthe* (*Phomopsis*) species. Persoonia 27(1): 80–89. https://doi.org/10.3767/003158511X617110

Thompson SM, Tan YP, Neate SM, Grams RM, Shivas RG, Lindbeck K, Aitken EAB (2018) *Diaporthe novem* isolated from sunflower (*Helianthus annuus*) and other crop and weed hosts in Australia. European Journal of Plant Pathology 152(3): 823–831. https://doi.org/10.1007/s10658-018-1515-7

Udayanga D, Liu X, McKenzie EH, Chukeatirote E, Bahkali AH, Hyde KD (2011) The genus *Phomopsis*: Biology, applications, species concepts and names of common phytopathogens. Fungal Diversity 50(1): 189–225. https://doi.org/10.1007/s13225-011-0126-9

Udayanga D, Liu X, Crous PW, McKenzie EH, Chukeatirote E, Chukeatirote E, Hyde KD (2012a) A multi-locus phylogenetic evaluation of *Diaporthe* (*Phomopsis*). Fungal Diversity 56(1): 157–171. https://doi.org/10.1007/s13225-012-0190-9

Udayanga D, Liu X, McKenzie EH, Chukeatirote E, Hyde KD (2012b) Multi-locus phylogeny reveals three new species of *Diaporthe* from Thailand. Cryptogamie. Mycologie 33(3): 295–309. https://doi.org/10.7872/crym.v33.iss3.2012.295

Udayanga D, Castlebury LA, Rossman AY, Chukeatirote E, Hyde KD (2014) Insights into the genus *Diaporthe*: Phylogenetic species delimitation in the *D. eres* species complex. Fungal Diversity 67(1): 203–229. https://doi.org/10.1007/s13225-014-0297-2

Udayanga D, Castlebury LA, Rossman AY, Hyde KD (2014a) Species limits in *Diaporthe*: Molecular re-assessment of *D. citri*, *D. cytosporella*, *D. foeniculina* and *D. rudis*. Persoonia 32(1): 83–101. https://doi.org/10.3767/003158514X679984

Udayanga D, Castlebury LA, Rossman AY, Chukeatirote E, Hyde KD (2014b) Insights into the genus *Diaporthe*: Phylogenetic species delimitation in the *D. eres* species complex. Fungal Diversity 67(1): 203–229. https://doi.org/10.1007/s13225-014-0297-2

Udayanga D, Castlebury LA, Rossman AY, Chukeatirote E, Hyde KD (2015) The *Diaporthe sojae* species complex: Phylogenetic re-assessment of pathogens associated with soybean, cucurbits and other field crops. Fungal Biology 119(5): 383–407. https://doi.org/10.1016/j.funbio.2014.10.009

van der Aa HA, Noordeloos ME, de Gruyter J (1990) Species concepts in some larger genera of the *Coelomycetes*. Studies in Mycology 32: 3–19.

van Rensburg JCJ, Lamprecht SC, Groenewald JZ, Castlebury LA, Crous PW (2006) Characterization of *Phomopsis* spp. associated with dieback of rooibos (*Aspalathus linearis*) in South Africa. Studies in Mycology 55: 65–74. https://doi.org/10.3114/sim.55.1.65

Vrandecic K, Cosic J, Jurkovic D, Riccioni L, Duvnjak T (2007) First report of *Phomopsis longicolla* on cocklebur (*Xanthium strumarium*) in Croatia. Plant Disease 91(12): 1687–1687. https://doi.org/10.1094/PDIS-91-12-1687B

Vrandecic K, Jurkovic D, Riccioni L, Cosic J, Duvnjak T (2010) *Xanthium italicum*, *Xanthium strumarium* and *Arctium lappa* as new hosts for *Diaporthe helianthi*. Mycopathologia 170(1): 51–60. https://doi.org/10.1007/s11046-010-9289-2

Vrandecic K, Jurkovic D, Cosic J, Postic J, Riccioni L (2011) First report of cane blight on blackberry caused by *Diaporthe eres* in Croatia. Plant Disease 95(5): 612–612. https://doi.org/10.1094/PDIS-11-10-0860

White TJ, Bruns T, Lee S, Taylor J (1990) Amplification and direct sequencing of fungal ribosomal RNA genes for phylogenetics. PCR Protocols: A Guide to Methods and Applications 18: 315–322. https://doi.org/10.1016/B978-0-12-372180-8.50042-1

Wrona CJ, Mohankumar V, Schoeman MH, Tan YP, Shivas RG, Jeff-Ego OS, Akinsanmi OA (2020) *Phomopsis* husk rot of macadamia in Australia and South Africa caused by novel *Diaporthe* species. Plant Pathology 69(5): 911–921. https://doi.org/10.1111/ppa.13170

Yang Q, Fan XL, Guarnaccia V, Tian CM (2018) High diversity of *Diaporthe* species associated with dieback diseases in China, with twelve new species described. MycoKeys 39: 97–149. https://doi.org/10.3897/mycokeys.39.26914

Yang Q, Jiang N, Tian CM (2020) Three new *Diaporthe* species from Shaanxi Province, China. MycoKeys 67: 1–18. https://doi.org/10.3897/mycokeys.67.49483

Yang Q, Jiang N, Tian CM (2021) New species and records of *Diaporthe* from Jiangxi Province, China. MycoKeys 77: 41–64. https://doi.org/10.3897/mycokeys.77.59999

Zhang QM, Yu CL, Li GF, Wang CX (2018) First report of *Diaporthe eres* causing twig canker on *Zizyphus jujuba* (Jujube) in China. Plant Disease 102(7): 1458. https://doi.org/10.1094/PDIS-12-17-1910-PDN